Control of Systems Subject to Constraints

Thesis by

Mayuresh V. Kothare

In Partial Fulfillment of the Requirements

for the Degree of

Doctor of Philosophy

California Institute of Technology

Division of Chemistry and Chemical Engineering

Pasadena, California

1997

(Submitted March 17, 1997)

Acknowledgements

A number of people have contributed to the formulation and development of the material in this thesis. First and foremost among them is my thesis supervisor, Manfred Morari. My interactions with Manfred have been very fulfilling and immensely satisfying. His continuous criticism, and a prodding and inquisitive style of work were only one part of this interaction, and probably contributed most directly to the thesis. But at a different level, the personal interaction, and the tremendous support and encouragement that he provided, especially during the move from Caltech to ETH, were about as critical in keeping me going in my work. For all these, I wish to thank him.

I would like to acknowledge several people with whom I have had the pleasure of working during the past few years: Ragu Balakrishnan, Pascale Bendotti, Peter Campo, Clement-Marc Falinower, Oliver Kaiser, Bernard Mettler, Carl Nett, Vesna Nevistić, Rolf Pfiffner and Alex Zheng. I would particularly like to acknowledge Ragu Balakrishnan, who was instrumental in stimulating my interest in the area of convex optimization and Linear Matrix Inequalities. The discussions with Ragu were most fruitful in shaping numerous ideas and concepts which went into the making of this thesis.

I am grateful to the faculty at Caltech for inculcating a spirit of research among the students and in general, for creating a scholarly environment at Caltech: John Brady, Jay Bailey, Mark Davis, George Gavalas, Zheng Gang Wang (all in Chemical Engineering), Jim Beck, John Doyle, Richard Murray (affiliated to Control and Dynamical Systems). A special thanks to Karl Åström, who served on my candidacy committee during his stay at Caltech in 1992-93, and who, by coincidence, was also present for my thesis defense.

During the course of my graduate studies, both at Caltech and later at ETH, the most pleasurable moments were those spent with colleagues and other graduate

students. From Caltech, I would like to acknowledge Nikos Bekiaris, Richard Braatz, Vassily Hatzimanikatis, Tyler Holcombe, Iftikhar Huq, George Meski, Simone de Oliveira, Cris Radu, Carl Rhodes, Matthew Tyler, Alex Zheng. A particularly special thanks to Simone, for her warmth, care and affection and her sense of camaraderie throughout the graduate years. From ETH, I would like to acknowledge Alessandro Astolfi, David Farrugio, Markus Kottman, Janusz Milek. A special thanks to Janusz for being a great friend and companion during difficult times in Zürich.

The secretarial staff at Caltech deserve a special mention, especially Kathy (Lewis) Bubash, Patricia New and the late Adria MacMillan, for providing superb administrative support. The administrative staff at ETH also deserve to be mentioned for handling the very difficult Swiss formalities and paperwork for foreigners: Danielle Couson, Esther Hagenow, June Hörmann, Brigitte von Känel.

Financial support for the research objectives pursued in this thesis came primarily from two sources: the U.S. National Science Foundation and the Swiss Federal Institute of Technology, Zürich, and is gratefully acknowledged.

Finally, I would like to acknowledge the continuous encouragement provided by my mother. But for her moral support and blessings, things would have been different.

Abstract

Every operating control system must deal with constraints. On the one hand, the range and rate of change of the *input* or manipulated variable is limited by the physical nature of the actuator (saturation limits). On the other hand, process state variables or *outputs* (pressures, temperatures, voltages) may not be allowed to exceed certain bounds arising from equipment limitation, safety considerations, or environmental regulations.

A rich theory exists for designing controllers – both linear ($\mathcal{H}_2/\mathcal{H}_\infty$, LQG, LTR, pole-placement) and nonlinear (nonlinear $\mathcal{H}_\infty$ control, feedback linearization, sliding mode control, gain scheduling). However, none of these popular and fashionable controller design techniques account for the presence of input or output constraints. Although occasionally these constraints may be neglected, in general, they lead to design and operating problems unless they are accounted for properly.

In traditional control practice, overrides or mode selection schemes are used to deal with output constraints: they switch between a "bank" of controllers, each of which is designed to achieve a specific objective. In both cases (saturation limit and mode selection), a control *input nonlinearity* is introduced into the operating system.

Despite its significance, the study of the constrained control problem has received far less attention than the traditional unconstrained (linear and nonlinear) control theory. With few exceptions, most of the controller design techniques for constrained systems are by-and-large ad-hoc, with very little guarantees of stability, performance and robustness to plant model uncertainty.

The objective of this thesis is to take a broad approach towards the constrained control problem. One part of the thesis is devoted to the development of a systematic and unifying theory for studying the so-called Anti-Windup Bumpless Transfer (AWBT) problem. The other part aims towards the development of a general novel approach for the synthesis of a robust model predictive control (MPC) algorithm.

Contents

List of Figures

List of Tables

Chapter 1 Introduction

In an aggressive global competitive environment, there is an ever increasing customer expectation for consistent high quality products. At the same time, environmental regulation agencies have been imposing stricter safety limits and tighter restrictions on emission of pollutants. Moreover, safety considerations have also led to the design of smaller storage capacities to diminish the risk of major chemical leakages. In order to meet these numerous stringent limits on product specifications and effluent concentrations, while at the same time maintaining a profitable enterprise through reduced energy and raw material costs, industrial processes have been forced to evolve over the last two decades into highly integrated and complex systems. As a result, the associated control problems have in turn become more difficult and challenging.

Traditional control techniques based on single-loop decentralized controller designs have been successful in resolving only a small sub-set of these problems. None of them can address *all* the control issues involved in this complex situation, thus stemming the need for more advanced and sophisticated control techniques. One particular problem which is by and large neglected in this complex scenario is that of dealing with *constraints*, both *input* or *manipulated variable* constraints (we will discuss these in a moment) and the aforementioned *output* or *state variable* constraints. The focus of this thesis is on addressing the general controller design problem in the presence of constraints.

1.1 Motivation

All real world control systems must deal with constraints. Consider Figure 1.1 which shows a typical control system. The process (e.g., a chemical reactor) is described by an uncertain, generally nonlinear model, with output variable y (e.g., temperature, pressure, concentration, etc.), manipulated variable u (e.g., flow rate), and is subject

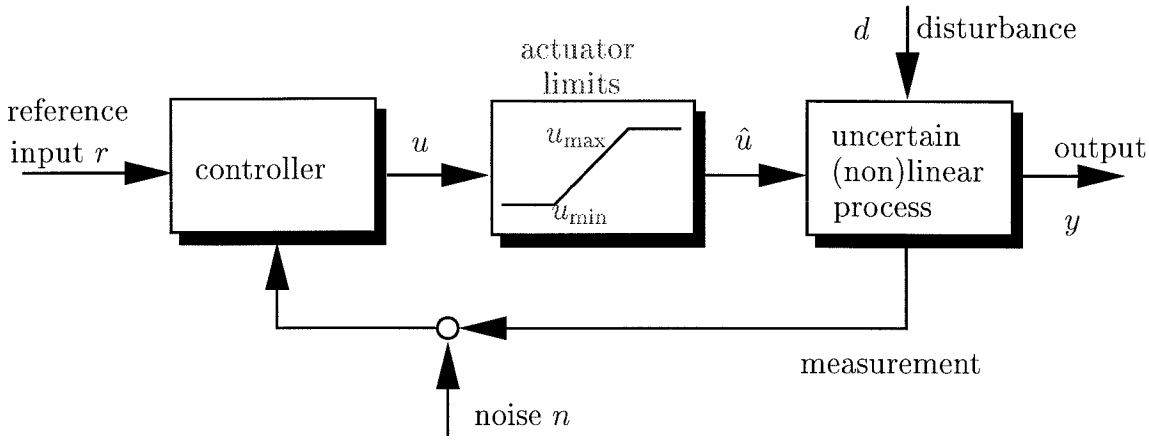

Figure 1.1: The general constrained control problem.

to a disturbance d (e.g., fluctuation of feed-stock flow rate, composition, etc.) and a measurement or sensor noise n.

On the one hand, the range of the manipulated variable u is limited to lie in a restricted range $[u_{\min}, u_{\max}]$ (consider a scalar input u for simplicity) due to the physical nature of the actuator (e.g., finite capacity of a valve, pump, compressor, etc.). For the same reason, sometimes even the rate of change of u is limited.

On the other hand, the process output y may be required to lie between prespecified limits of the reference value r, these limits arising, as we discussed before, due to stringent product specifications, safety limits, or environmental regulations. The goal of the controller is to satisfy the specifications on the plant output y, in the presence of

- plant model uncertainty;
- external disturbance d;
- measurement noise n; and
- actuator limits or saturation constraints on u.

It is safe to say that a fairly rich theory exists for designing controllers – both linear (e.g., PI/PID, LQG, LTR, $\mathcal{H}_2/\mathcal{H}_\infty$, pole placement, etc.) and nonlinear (e.g., non-

linear $\mathcal{H}_\infty$, feedback linearization, sliding mode control, gain scheduling, etc.). It is also safe to say that the effect of plant model uncertainty on controller performance has been reasonably well-understood in the context of linear systems, and attempts are being made to develop similar understanding for nonlinear systems. However, *none* of these popular controller design techniques account for the presence of input and output constraints. Although occassionally these constraints can be neglected, in general, they lead to design and operating problems in the final controller implementation unless they are accounted for properly.

For example, it is well-known that strictly unstable systems cannot be globally stabilized with constraints on the control signal [125]. A classic example of the detrimental effect of neglecting constraints comes from the nuclear industry, namely, the Chernobyl unit 4 nuclear power plant disaster in 1986. One of the causes of this mishap was attributed to the fact that the speed at which the control rods could be moved in and out of the nuclear reactor core was limited. When the reaction started accelerating, the controller tried to push the rods into the core as fast as it could to slow down the reaction. But due to the limited speed of the control rod movement, this controller action was not fast enough, and eventually led to an uncontrolled runaway reaction [123].

Although such a dramatic example is harder to find in the chemical industry, there are examples of chemical plants which handle hazardous materials and which need to operate safely and within limits. The 1984 Bhopal tragedy in India caused by the release of the highly toxic gas methyl isocyanate (MIC) from the Union Carbide Plant in Bhopal attests to this statement.

An argument against studying the effect of actuator constraints on controller design and performance is that one can always over-design the process so that physical limitations do not limit our controller performance. While true in principle, it is far from being practical to build in the extra capacity in the system, knowing very well that it will likely be used infrequently. The costs for such over design are far from being justified and typically, economically feasible processes do tend to operate at constraint boundaries.

This being the case, the constrained control problem achieves an even greater significance. Not surprisingly, there has been quite some activity in this area in recent years. For example, in a plenary lecture at the 1992 American Control Conference in Chicago, Professor Elmer Gilbert from the Department of Aerospace Engineering, University of Michigan, very clearly outlined the various issues involved in controlling *linear systems* with "point-wise-in-time constraints" [56]. Similarly, in two recent plenary addresses [96, 97], Professor David Mayne from the University of California, Davis/Imperial College, London elucidated numerous open issues in controlling *nonlinear* systems with constraints, with particular emphasis on predictive control. Additionally, the entire August 1995 issue of the *International Journal of Robust and Nonlinear Control* was devoted exclusively to the problem of controlling linear systems with saturating actuators, and a fairly extensive bibliography [16] of existing literature in this area was compiled by the guest editors of this issue. One more issue of the *International Journal of Robust and Nonlinear Control* is being planned on this topic [124].

1.2 Background and Literature Review

The existing approaches to addressing the constrained control problem can be broadly divided into two categories, based on the model used to describe the plant:

- those using *linear* plant models;
- those using *nonlinear* plant models.

1.2.1 Constrained Control of Linear Systems

The techniques using linear plant models can in turn be divided into two categories:

- Model Predictive Control (MPC);
- Anti-Windup Bumpless Transfer (AWBT) Control

It would be appropriate to include an additional category of techniques dealing with nonlinear stabilization of constrained linear systems [122, 125, 127], but this area is beyond the scope of this thesis and will not be explored further.

1.2.1.1 Model Predictive Control

Model Predictive Control (MPC), also known as Moving Horizon Control (MHC) or Receding Horizon Control (RHC), (see [52] for an introduction and survey) is a popular technique for the control of "slow" dynamical systems, such as those encountered in chemical process control. At each sampling time, MPC solves a trajectory optimization problem (typically, a linear or quadratic program) to compute optimal control inputs over a fixed future time "horizon", using a plant model to predict future plant outputs. Although more than one control move is generally calculated, only the first one is implemented. At the next sampling time, the optimization problem is reformulated with the horizon shifted forward by one time step and solved utilizing the new measurement information obtained from the system.

The main advantage of MPC, as also the reason for its immense popularity in the process industries, is its ability to explicitly handle constraints on both the manipulated (input) and the controlled (output) variables. However, due to the on-line optimization involved, the application of MPC is restricted to "slow" processes which allow the on-line computation to be completed between two sampling instances. From a conceptual point of view, the implicit definition of the MPC control law through a quadratic program, which explicitly incorporates input and output constraints, makes the analysis of its properties, such as stability and robustness, very difficult.

This motivated a flurry of research activity in the area of stability analysis of MPC algorithms. It was only a few years ago that the first useful results on nominal stability of MPC were published by Rawlings and Muske [114] using the idea of an infinite prediction horizon in the MPC algorithm. Subsequently, and in parallel to these developments, several other studies on nominal stability of MPC were carried out [12, 128, 142] to further explore this topic. Although further refinements in this area continue to appear in the literature (see [144]), by-and-large, the issue of nominal

stability of MPC appears to be a well-understood topic.

However, issues of robustness, and in particular, MPC design in the presence of plant-model uncertainty have been addressed to a much lesser extent. Early work on robustness *analysis* of MPC by Garcia and Morari [49, 50, 51] focused on the *unconstrained* implementation of MPC in the framework of internal model control (IMC). Zafiriou [136] and Zafiriou and Marchal [137] used the contraction properties of MPC to develop necessary/sufficient conditions for robust stability of *constrained* MPC. Genceli and Nikolaou [53] analyzed robustness properties of l_1 norm MPC algorithms for single-input single-output (SISO) finite impulse response (FIR) systems. More recently, Polak and Yang [111, 112] introduced the idea of a "contraction constraint" in their MPC algorithm to guarantee robust stability. This "contraction constraint" idea and variations based on it have subsequently been exploited by numerous other researchers [8, 37, 144] to further explore the robust stability properties of MPC.

Robust MPC *synthesis*, i.e., the explicit incorporation of realistic plant model uncertainty information in the MPC problem formulation, has been the focus of research in the MPC community in recent years. Relevant references in this area include the "min-max" robust MPC algorithms of Campo and Morari [26], Allwright and Papavasiliou [2] and Zheng and Morari [145]. The work reported in these references pertains to FIR plants. Robust MPC synthesis using "contraction constraint" ideas has been reported in [144] and eventually applied to FIR plants. As we will see in Chapter 8, we will develop a fairly general and novel robust MPC algorithm which is not restricted to FIR plants but is applicable to a much larger class of uncertain plants.

1.2.1.2 Anti-Windup Bumpless Transfer Control

In traditional control practice, overrides or mode selection schemes have been used to deal with output constraints: They switch between a "bank" of linear controllers, each of which is designed to achieve a specific objective. However, in resolving the output constraint problem, we have introduced a *switching* or *override* nonlinearity at the plant input, thereby creating a new problem to be addressed.

The input nonlinearities, introduced both due to saturation limits, as discussed in §1.1, and overrides or mode selection schemes as discussed above, in an otherwise linear system, are handled by the so-called **Anti-Windup Bumpless Transfer (AWBT)** techniques. The basic philosophy of AWBT control techniques is the following:

Design first the linear controller ignoring control input nonlinearities. Then add anti-windup compensation to minimize the adverse effects of any control input nonlinearities on closed-loop performance.

Compared to MPC, AWBT compensation schemes of this type provide a simpler, computationally cheaper alternative for modifying or "retro-fitting" existing unconstrained linear controllers to account for input nonlinearities (saturation and mode switching). This has probably been the main motivation for a number of somewhat ad-hoc and problem-specific anti-windup schemes that have been reported in the literature.

Windup problems were originally encountered in an industrial context when using PI/PID controllers for controlling linear systems with control input nonlinearities. One of the earliest attempts to overcome windup in PID controllers was the work by Fertik and Ross [46], which is now popularly known as anti-reset windup. However, it was recognized later that integrator windup is only a special case of a more general problem. As pointed out by Doyle *et al.* [43], any controller with slow or unstable modes will experience windup problems when implemented on a system with actuator constraints.

This motivated a more general intepretation of windup as any inconsistency between the controller output and the states of the controller when, for example, the control signal saturates. Based on this general interpretation, numerous other researchers proposed anti-windup techniques, each tailored towards addressing a particular issue involved in windup. Such techniques include the "conditioning technique" of Hanus and co-workers [62, 63, 64], the observer-based approach of Åström and co-workers [6, 7], which was further explored by Walgama and Sternby [132]. An alternative interpretation of the conditioning technique of Hanus *et al.* was attempted by Campo

and Morari [27]. Extensions of the conditioning technique can be found in [131]. A more complex and involved technique for anti-windup compensation was proposed by Kapasouris *et al.* [69, 70, 71].

While successful in addressing numerous specific windup related issues, the aforementioned techniques rely on ad-hoc spurts of engineering ingenuity. What is clearly missing is an attempt to formalize the general philosophy of AWBT and advance a more systematic AWBT theory. As we will see in Chapter 4, we will present a framework which allows us to achieve just this objective.

It is important to recognize that merely adding AWBT compensation of the type discussed above does not automatically guarantee closed-loop stability of the resulting nonlinear system (remember that we have input nonlinearities even though the remaining system may be linear). Numerous researchers attempted to develop criteria for analyzing stability of various AWBT compensation techniques.

One of the first attempts in this direction was the application of the scalar Popov and Circle criteria by Glattfelder *et al.* [57, 58, 59] to analyze stability properties of anti-reset windup control systems. The multivariable Circle Criterion was used by Kapasouris and Athans [69] to analyze the multivariable anti-reset windup scheme which they proposed. Attempts to use the small gain theorem for the same purpose were reported in [6, 27, 28, 43] and the use of describing function analysis was reported in [6].

We see that several seemingly diverse techniques and seemingly unrelated theoretical tools have been employed to address the issue of closed-loop stability of specific AWBT compensated control systems. A sense of generality to grasp the larger picture seems to be missing. We will show in Chapter 6 how we can develop general tools for analyzing AWBT stability using concepts from absolute stability and multiplier theory.

Despite these encouraging developments in unifying AWBT schemes (see Chapter 4) and in generalizing AWBT analysis techniques (see Chapter 6), very few systematic AWBT *design* techniques have been reported at present, although several heuristic methods or "tuning" rules are readily available.

The simplest case of tuning the anti-reset windup controller for PI/PID controllers can be found in Åström and Hägglund [5]. The conditioning technique of Hanus *et al.* [62, 63] is applicable to biproper linear controllers but suffers from the drawback that it does not have any additional degrees of freedom to "tune" or improve AWBT performance. Extension of the conditioning technique to multivariable systems with a more detailed consideration of issues such as directionality compensation was carried out by Campo and Morari [27], based on ideas of directionality compensation originally proposed by Doyle *et al.* [43].

More systematic anti-windup synthesis techniques can be found in Park and Choi [109], Tyan and Bernstein [129] and Kapoor *et al.* [73]. Again, most of these techniques lack generality and some of them are far too complicated to be useful in practice. Moreover, none of them allow consideration of different performance criteria, thereby lacking the ability to provide insight into the inevitable trade-offs involved in AWBT designs. In Chapter 7, we will develop a framework which allows incorporation of numerous appropriately defined performance criteria in the AWBT synthesis problem.

1.2.2 Constrained Control of Nonlinear Systems

Perhaps the only controller design techniques for nonlinear plants which can take into account constraints fall under the general category of model predictive control. These in turn can be broadly divided into:

- those using the nonlinear plant model as the *prediction* model in MPC. In general, this approach results in an on-line nonlinear optimization problem which can be computationally cumbersome. The highly complex and nonlinear nature of the on-line optimization problem makes any analysis of the control system very difficult.

- those using a local linearization of the nonlinear plant model as the *prediction* model, and then applying linear MPC techniques [37, 38]. This approach results in a quadratic program to be solved on-line.

- those using feedback linearization to *linearize* the nonlinear system and then applying MPC techniques to the feedback-linearized plant [40, 106]. The computational issues of this technique, though partially addressed in [106], still remain to be fully explored. Similarly, the stability properties have been analyzed only under idealized conditions.

It is worth mentioning that feedback linearization in conjunction with an anti-windup scheme applicable to stable IMC controllers (see Chapter 3) has been applied by Doyle III [44] and Kendi and Doyle III [74] to handle input saturation constraints for nonlinear systems.

The discussion of the constrained control problem for nonlinear systems is beyond the scope of this thesis and will not be continued further.

1.3 Thesis Overview

The thesis is organized as follows: In Chapter 2, we introduce the anti-windup bumpless transfer (AWBT) problem and summarize several existing techniques to achieve AWBT compensation. This chapter serves to illustrate the essential two-step design approach of AWBT and motivates the need for a more general framework required for this problem. Chapter 3 discusses an anti-windup scheme for controllers implemented in the IMC framework. This anti-windup IMC implementation has already found application in addressing the nonlinear constrained control problem and this extension is also discussed in this chapter.

Chapter 4 is devoted to the development of a truly general AWBT framework. This framework captures the essential feature of existing AWBT schemes, namely, the two-step controller design paradigm. The generality of the framework introduced in Chapter 4 allows us to unify all the existing AWBT schemes summarized in Chapter 2. These special cases of the general framework are illustrated in this chapter.

In Chapter 5, we momentarily digress from the main theme and summarize essential technical machinery related to linear matrix inequalities (LMIs). The emphasis is

only on those aspects of LMIs which are relevant to this thesis. After this brief digression, we return again to the main theme, in Chapter 6, where we address the problem of analyzing the stability of AWBT schemes. Based on concepts derived from the absolute stability problem, a general framework for systematically studying AWBT stability is developed. The analysis framework allows consideration of any multivariable linear AWBT scheme subject to multivariable control input nonlinearities such as saturation, relay, dead-zone, hysterisis, switching/override/logic-based nonlinearities and combinations thereof. In particular, we show in this chapter that a number of previously reported attempts to analyze stability of AWBT control schemes, using such well-known and seemingly diverse techniques such as the Popov, Circle and Off-Axis Circle criteria, the optimally scaled small-gain theorem (generalized μ upper bounds) and describing functions can all be generalized within the framework of this paper.

In Chapter 7, we address the AWBT synthesis problem. We first show that the classical two-step AWBT synthesis problem can be reduced to a static output feedback synthesis problem which is computationally difficult to solve. Next, we consider two alternatives – dynamic AWBT compensation and one-step AWBT compensation – to overcome the problem associated with the static output feedback synthesis problem. We then define suitable AWBT objectives and outline promising approaches for its solution based on recently developed techniques on multi-objective optimization.

Chapter 8 presents a novel and complete framework for robust MPC synthesis based on LMIs. The technique discussed in this chapter allows incorporation of a fairly broad and general class of plant uncertainty information in the MPC problem formulation. Using standard LMI-based techniques, the problem of minimizing an upper bound on the "worst-case" objective function, subject to constraints on the plant input and plant output, is reduced to a convex LMI-based optimization. Moreover, it is shown that the feasible receding horizon state-feedback control law robustly stabilizes the set of uncertain plants under consideration. Several extensions, such as constant set-point tracking for LTI plants, disturbance rejection, robust trajectory tracking, extension to the output feedback case with an appropriate observer design

and extesion to handle plant delays are also discussed within this framework.

Chapter 9 presents a case study of applying an extension of standard MPC techniques to linear parameter varying (LPV) systems. The example under consideration is the problem of controlling the water level in the steam generator of a nuclear power plant.

Finally, in Chapter 10, we present conclusions of the thesis, with a summary of the contributions of the thesis and an outline of the numerous areas of research that are motivated by the results of this thesis.

1.4 Notation

The notation used in the thesis is fairly standard. $\Re$ is the set of real numbers. For a matrix A, A^T denotes its transpose, A^* denotes its complex conjugate transpose, A^{-1} denotes its inverse (if it exists), A^{-*} denotes the inverse of A^* (if it exists). The matrix inequality $A > B$ ($A \geq B$) means that A and B are square Hermitian matrices and $A - B$ is positive (semi-)definite.

$\mathcal{L}_2$ is the Hilbert space of m-vector valued signals defined on $(-\infty, \infty)$, with scalar product $\langle x|y\rangle = \int_{-\infty}^{\infty} x(t)^* y(t)\, dt$ and such that $\|x\|_2 \stackrel{\Delta}{=} \langle x|x\rangle^{\frac{1}{2}} < \infty \; \forall \; x \in \mathcal{L}_2$. $\mathcal{L}_{2e}$ is the extended Hilbert space of m-vector valued signals u such that $u_T \in \mathcal{L}_2$, where

$$u_T(t) \;=\; \begin{cases} u(t) & \text{if } t \leq T \\ 0 & \text{if } t > T. \end{cases}$$

The same symbol is used to denote a time-domain signal (or the impulse response of an LTI system) and its Laplace transform. The distinction should be clear from the context.

For $u \in \Re^n$,

$$\text{sat}(u) = \begin{cases} \text{sat}(u_1) \\ \vdots \\ \text{sat}(u_n) \end{cases}, \quad \text{where} \quad \text{sat}(u_i) = \begin{cases} u_i^{max} & u_i > u_i^{max} \\ u_i & u_i^{min} \le u_i \le u_i^{max} \\ u_i^{min} & u_i < u_i^{min} \end{cases}$$

denotes the usual input saturation function. For $x \in \Re^n$,

$$|x(t)|_1 = \sum_{i=1}^{n} |x_i(t)|$$

denotes the 1-norm.

A transfer function matrix in terms of state-space data is denoted

$$G(s) = C(sI - A)^{-1}B + D \triangleq \left[\begin{array}{c|c} A & B \\ \hline C & D \end{array}\right].$$

For simplicity of notation, $f \circ G(s)x$ refers to the operation of convolving the impulse response of $G(s)$ with x and then applying the operator f. Similar interpretation can be given to $G(s) \circ fx$. With some abuse of notation, we will denote the adjoint of an LTI operator $G(s)$ by $G(-s)^T$. Thus, with the usual rules of an adjoint operator

$$\langle x | G(s)y \rangle = \langle G(-s)^T x | y \rangle.$$

If $G(s)$ is causal, stable, then its adjoint is considered to be anti-causal, stable.

$\mathcal{H}_2$ and $\mathcal{H}_\infty$ are the Hardy spaces of matrix-valued functions with analytic continuations into the right half-plane, and which are respectively, square integrable and bounded on the imaginary axis. The $\mathcal{H}_2$ and $\mathcal{H}_\infty$ norms are defined in the frequency domain for a stable transfer matrix $G(s)$ as

$$\|G\|_{\mathcal{H}_2} \triangleq \left(\frac{1}{2\pi}\int_{-\infty}^{\infty} \text{trace}[G(j\omega)^* G(j\omega)]\, d\omega\right)^{\frac{1}{2}}, \quad \|G\|_{\mathcal{H}_\infty} \triangleq \sup_{\omega}\ \sigma_{\max}[G(j\omega)],$$

where $\sigma_{\max}[G(j\omega)]$ refers to the maximum singular value of $G(j\omega)$.

Chapter 2 Anti-Windup Bumpless Transfer

Abstract

The Anti-Windup Bumpless Transfer (AWBT) problem is introduced in this chapter. Numerous existing techniques for AWBT compensation are reviewed. The emphasis is on tracing the origins of the problem and on highlighting the somewhat intuitive and problem-specific nature of the solutions available for the problem. The essential idea of a "two-step" design incorporated in AWBT compensation schemes is clearly brought out through the review. Moreover, the chapter serves to motivate the need for a more general and rigorous AWBT theory to be introduced in Chapter 4.

2.1 Introduction

All real world control systems must deal with constraints. For example, the control system must avoid unsafe operating regimes. In process control, these constraints typically appear in the form of pressure and temperature limits. In addition, physical limitations impose constraints–pumps and compressors have finite throughput capacity, surge tanks can only hold a certain volume, motors have a limited range of speed. Of special interest and common occurrence are systems with control input constraints in an otherwise linear system.

All physical systems are subject to actuator saturation. For example, a valve controlling the flow rate of the coolant to a reactor can only operate between fully open and fully closed. We will refer to such a constraint as an *input limitation.* In addition, commonly encountered control schemes must satisfy multiple objectives and hence need to operate in different control modes. Each mode has a linear controller designed to satisfy the performance objective corresponding to that mode. If the operating conditions demand a change of mode, an override or selection scheme chooses the appropriate mode and executes a mode switch. The switch between operating modes

is achieved by a selection of the plant input from among the outputs of a number of parallel controllers, each corresponding to a particular mode. We will refer to such a mode switch as a *plant input substitution* since the output of one controller is replaced by that of another.

As a result of substitutions and limitations, the actual plant input will be different from the output of the controller. When this happens, the controller output does not drive the plant and as a result, the states of the controller are wrongly updated. This effect is called *controller windup.* Since the linear controller is designed ignoring actuator nonlinearities, the adverse effect of windup caused by the presence of such nonlinearities is in the form of significant performance deterioration (as compared to the expected linear performance), large overshoots in the output and sometimes even instability [27]. Performance degradation is especially pronounced when the controller is stable with very slow dynamics and gets even worse when the controller is unstable. In addition to windup, when mode switches occur, the difference between the outputs of different controllers results in a bump discontinuity in the plant input. This in turn causes undesirable bumps in the controlled variables. What is required is a smooth transition or *bumpless transfer* between the different operating modes. We will refer to the problem of control system analysis and controller synthesis for the general class of linear time invariant (LTI) systems subject to plant input limitations and substitutions as the *anti-windup bumpless transfer* (AWBT) problem.

Windup problems were originally encountered when using PI/PID controllers for controlling linear systems with control input nonlinearities. One of the earliest attempts to overcome windup in PID controllers was the work of Fertik and Ross [46]. Their strategy has been variously referred to as *anti-reset windup*, *back calculation and tracking* and *integrator resetting.* Experimental evaluation of several digital algorithms for anti-reset windup has been reported in [76]. Extension of anti-reset windup to a general class of controllers has been reported and is commonly referred to as high gain conventional anti-windup (CAW).

It was recognized later that integrator windup is only a special case of a more general problem. As pointed out by Doyle *et al.* [43], any controller with relatively slow

or unstable modes will experience windup problems if there are actuator constraints. Windup is then interpreted as an inconsistency between the controller output and the states of the controller when, for example, the control signal saturates. The "conditioning technique" as an anti-windup and bumpless transfer scheme was originally formulated by Hanus *et al.* [62, 63], as an extension of the back calculation strategy of [46] to a general class of controllers. Åström *et al.* [7, 6] proposed that an observer be introduced into the system to estimate the states of the controller and hence restore consistency between the saturated control signal and the controller states. [132] have very clearly exposed this inherent observer property in several anti-windup schemes. Campo and Morari (1990) [27] have derived the Hanus conditioned controller as a special case of the observer-based approach. A modified Internal Model Control (IMC) implementation has recently been proposed by Zheng *et al.* (1994) [143] to improve performance in the face of actuator saturation.

We can summarize the existing approaches to solving the problem of control of LTI systems subject to control input nonlinearities as follows:
Design first the linear controller ignoring control input nonlinearities and then add anti-windup bumpless transfer (AWBT) compensation to minimize the adverse effects of any control input nonlinearities on closed loop performance.

In the following sections, several approaches to solving the AWBT problem based on the aforementioned two-step paradigm are reviewed in their light of their relevance to this thesis. Some of the schemes discussed here were originally proposed only for taking into account actuator saturation, while some allow consideration of more general actuator nonlinearities. We will use the symbol N for a general actuator nonlinearity, and the saturation block (as shown in Figure 2.1) for a saturating actuator, whichever is appropriate in the context.

2.2 Anti-Reset Windup

Anti-reset windup [27, 23] has also been referred to as *back-calculation and tracking* [6, 46] and *integrator resetting* [132]. Windup was originally observed in PI and PID

controllers designed for SISO control systems with a saturating actuator. Consider

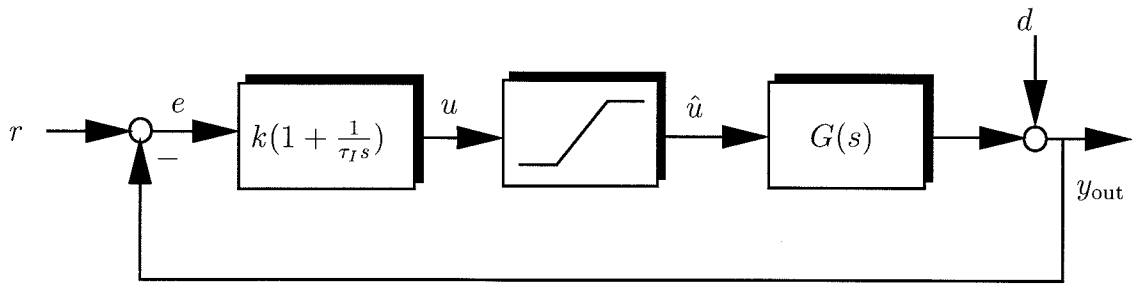

Figure 2.1: PI control of plant $G(s)$.

the output of a PI controller as shown in Figure 2.1:

$$K(s) = k(1+\frac{1}{\tau_I s}) \tag{2.1}$$

$$= \left[\begin{array}{c|c} 0 & \frac{k}{\tau_I} \\ \hline 1 & k \end{array}\right] \tag{2.2}$$

$$u = k(e+\frac{1}{\tau_I}\int_0^t e\ dt) \tag{2.3}$$

$$\hat{u} = \text{sat}(u) \tag{2.4}$$

$$= \begin{cases} u_{\min} & \text{if } u < u_{\min} \\ u & \text{if } u_{\min} \le u \le u_{\max} \\ u_{\max} & \text{if } u > u_{\max} \end{cases} \tag{2.5}$$

$$e = r - y_{\text{out}}. \tag{2.6}$$

If the error e is positive for a substantial time, the control signal gets saturated at the high limit $u_{\max}$. If the error remains positive for some time subsequent to saturation, the integrator continues to accumulate the error causing the control signal to become "more" saturated. The control signal remains saturated at this point because of the large value of the integral. It does not leave the saturation limit until the error becomes negative and remains negative for a sufficiently long time to allow the integral part to come down to a small value. The adverse effect of this integral windup is in the form of large overshoots in the output y_{out} and sometimes even

instability.

To avoid windup, an extra feedback path is provided in the controller by measuring the actuator output $\hat{u}$ and forming an error signal as the difference between the output u of the controller and the actuator output $\hat{u}$. This error signal is fed to the input of the integrator through the gain $\frac{1}{\tau_r}$. The controller equations thus modified are (refer to Figure 2.2)

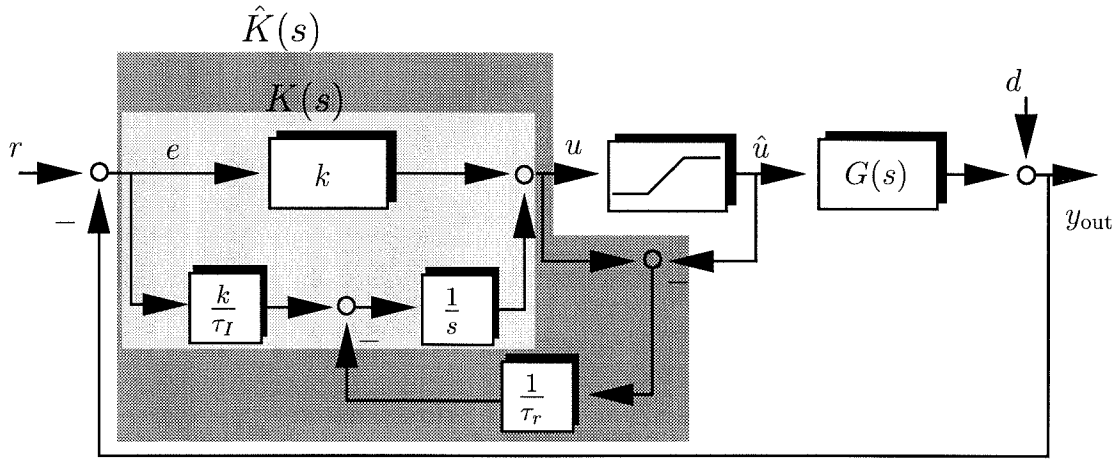

Figure 2.2: Classical anti-reset windup.

$$u = k\left[e + \frac{1}{\tau_I}\int_0^t \left(e - \frac{\tau_I}{k\tau_r}(u-\hat{u})\right)\, dt\right] \tag{2.7}$$

$$\hat{u} = \text{sat}(u) \tag{2.8}$$

$$e = r - y_{\text{out}}. \tag{2.9}$$

When the actuator saturates, the feedback signal $u-\hat{u}$ attempts to drive the error $u-\hat{u}$ to zero by recomputing the integral such that the controller output is exactly at the saturation limit. This prevents the integrator from winding up.

Rewriting equation (2.7) in the Laplace domain

$$u = \left[ke + \frac{k}{\tau_I s}e - \frac{1}{\tau_r s}(u-\hat{u})\right] \tag{2.10}$$

$$\Rightarrow u = \frac{k\tau_r(1+\tau_I s)}{\tau_I(1+\tau_r s)}e + \frac{1}{\tau_r s+1}\hat{u}. \tag{2.11}$$

Several "incremental" forms of the anti-reset windup strategy have been outlined in [132], where anti-reset windup is applied to the *increment* of the control signal rather than the control signal itself. Unfortunately, guidelines for choosing the reset-windup gain τ_r rely solely on simulations for tuning the nonlinear closed-loop performance with no sound theoretical basis.

For a PI controller, when integral action is generated as an automatic reset, Åström and Haggalund (1988) [5] suggest the implementation shown in Figure 2.3 to achieve anti-reset windup compensation. When there is no saturation, it is easy to

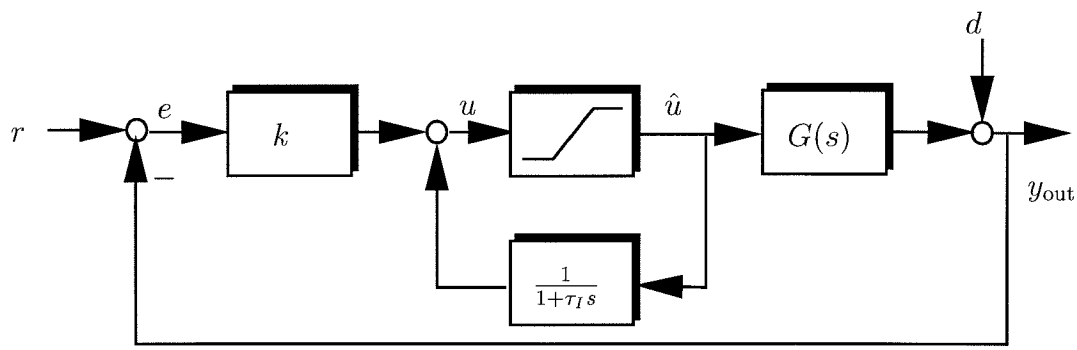

Figure 2.3: Alternate anti-reset windup implementation.

verify that this implementation results in the standard PI controller given by equations (2.1), (2.2), (2.3). In the presence of saturation, the control signal (in Laplace domain) is given by

$$u = ke + \frac{1}{1+\tau_I s}\hat{u}. \tag{2.12}$$

Comparing (2.12) with (2.11), we see that the two anti-reset windup implementations are identical when $\tau_r = \tau_I$.

2.3 Conditional Integration

The essential idea behind this approach is summarized as: *Stop integration at saturation!* Inherently a strategy for dealing with integrator windup, it prescribes that

when the control signal saturates, the integration should be stopped [132].

Åström *et al.* [6] describe how the limits on the actuator can be translated into limits on the output when using a PID controller for the error feedback case. These limits on the output constitute the "proportional band" and are such that if the instantaneous output value of the process is within these limits, then the actuator does not saturate. Conditional integration then takes the form: *Update the integral only when the process output is in the proportional band.*

One obvious disadvantage is that like the conventional anti-reset windup technique, this scheme is limited to integrator windup. Secondly, the control signal may be held in saturation indefinitely because the integrator is "locked" without being updated. This may cause severe overshoots in the process output.

The problem of a "locked integrator" can be resolved by stopping the integrator update only when the update causes the control signal to become more saturated and to allow the update when it causes the control signal to "De-saturate" [132]. Krikelis [91] has suggested the use of a pure integrator with a dead-zone nonlinearity as a feedback around it to automate the process of conditional integration in an "intelligent" way.

The basic idea of switching off the integrator can be understood from Figure 2.4. The parameters β and H are tuned appropriately to achieve the appropriate "turning-

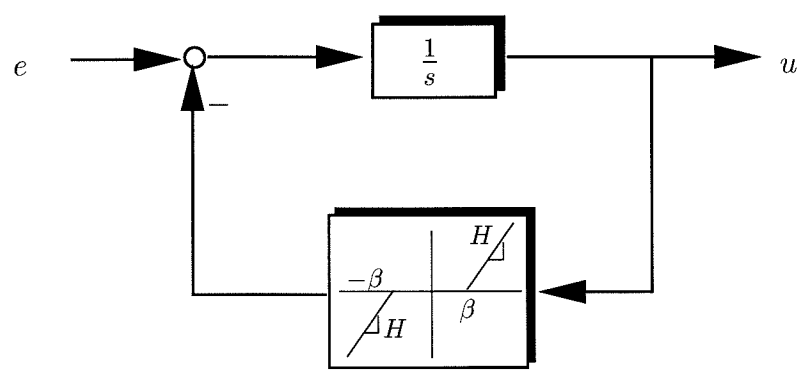

Figure 2.4: Realization of "conditional" integration.

off" of the integrator in the controller. This idea of introducing an additional dead-

zone nonlinearity into the feedback loop to achieve conditional integration has been further explored in the multivariable context by Kapasouris and Athans [69].

2.4 Conventional Anti-Windup (CAW)

High gain conventional anti-windup (CAW) [43] adopts a philosophy similar to that of anti-reset windup. Thus, in some sense CAW can be considered as a direct extension of anti-reset windup to general controllers. The implementation is shown in Figure 2.5. The AWBT compensation is provided by feeding the difference $\hat{u} - u$ through a high gain matrix X to the controller input e. Typically, $X = \alpha I$, where $\alpha >> 1$ is a scalar. Given the original linear controller $K(s)$ with state x

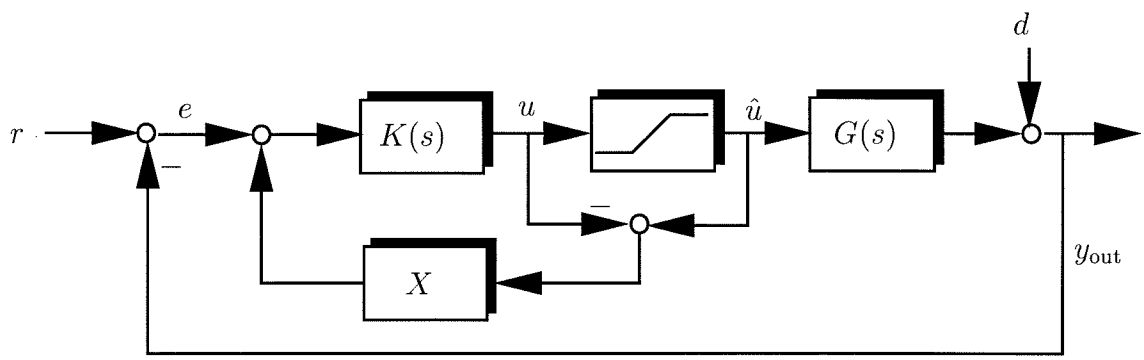

Figure 2.5: Conventional anti-windup.

$$K(s) = \left[\begin{array}{c|c} A & B \\ \hline C & D \end{array}\right] \tag{2.13}$$

the modified controller equations based on Figure 2.5 are

$$\dot{x} = Ax + B(e + X(\hat{u} - u)) \tag{2.14}$$

$$u = Cx + D(e + X(\hat{u} - u)) \tag{2.15}$$

$$\Longrightarrow u = (I + DX)^{-1}Cx + (I + DX)^{-1}De + (I + DX)^{-1}DX\hat{u}. \tag{2.16}$$

Substituting equation (2.16) into equation (2.14), we get

$$\dot{x} = (A - BX(I + DX)^{-1}C)x + (B - BX(I + DX)^{-1}D)e \quad (2.17)$$

$$+(BX - BX(I + DX)^{-1}DX)\hat{u} \quad (2.18)$$

$$= (A - BX(I + DX)^{-1}C)x + B(I + XD)^{-1}e + BX(I + DX)^{-1}\hat{u}. \quad (2.19)$$

2.5 Hanus' Conditioned Controller

The conditioning technique was originally formulated by Hanus *et al.* [62, 63] as an extension of the back calculation method proposed by Fertik and Ross (1967) [46]. In this technique, windup is interpreted as a lack of consistency between the internal states of the controller and input to the plant when there is a nonlinearity between the controller output and the control input to the plant. Consistency is restored by modifying the inputs to the controller such that if these modified inputs (the so-called "realizable references") had been applied to the controller, its output would not have been different from the control input to the plant.

Consider a simple error feedback controller as shown in Figure 2.6, with the nonlinearity N being a saturating actuator.

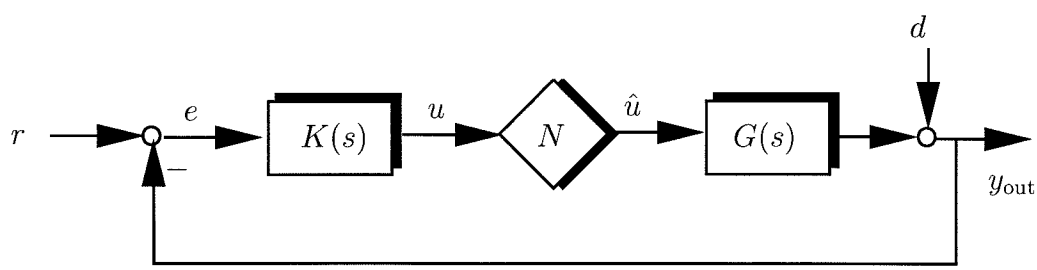

Figure 2.6: Error feedback controller with nonlinearity N.

$$\dot{x} = Ax + B(r - y_{out}) \quad (2.20)$$

$$u = Cx + D(r - y_{out}) \quad (2.21)$$

$$\hat{u} = \text{sat}(u) \quad (2.22)$$

where sat is defined in equation (2.5).

Following Hanus *et al.* (1987) [63], we can apply a realizable reference r^r to the controller such that the output of the controller is $\hat{u}$. Thus,

$$\dot{x} = Ax + B(r^r - y_{\text{out}}) \tag{2.23}$$

$$\hat{u} = Cx + D(r^r - y_{\text{out}}). \tag{2.24}$$

Based on the assumption of "present realizability" (see [63]) of the control u, we get

$$u = Cx + D(r - y_{out}) \tag{2.25}$$

for the same state x which results from equation (2.23) after application of the realizable reference r^r. Subtracting equation (2.25) from equation (2.24), we get

$$\hat{u} - u = D(r^r - r). \tag{2.26}$$

Assuming D is non-singular (i.e., the linear controller $K(s)$ is biproper with $K(\infty)$ invertible) we get

$$r^r = r + D^{-1}(\hat{u} - u). \tag{2.27}$$

Combining equations (2.22), (2.23), (2.25) and (2.27), we get

$$\dot{x} = (A - BD^{-1}C)x + BD^{-1}\hat{u} \tag{2.28}$$

$$u = Cx + D(r - y_{out}) \tag{2.29}$$

$$\hat{u} = \text{sat}(u). \tag{2.30}$$

This is the AWBT "conditioned controlled."

2.6 Generalized Conditioning Technique (GCT)

Several drawbacks of the conditioning scheme discussed in the previous section are obvious and some not-so-obvious drawbacks were recently reported [64, 131]. Firstly, the strategy fails for controllers having rank deficient D matrices [64]. Secondly, in terms of design, the strategy is "inflexible" since it modifies the linear controller without using any additional "tuning" parameters for optimizing nonlinear performance. Thirdly, it suffers from the so-called "inherent short-sightedness" problem [131] because the technique can only handle one saturation level (either the upper limit or the lower limit). Walgama *et al.* (1992) [131] have proposed two extensions to the conditioning technique to resolve these deficiencies. The first approach [131, §4] is a simple modification to the conditioned controller, where the input conditioning mechanism is improved by introducing "cautiousness" so that the change in the modified set-point at controller desaturation is made smoother.

The realizable reference r^r in equation (2.27) is modified by introducing the user-chosen parameter ρ as follows:

$$r^r = r + (D + \rho I)^{-1}(\hat{u} - u) \quad \text{where } 0 \leq \rho \leq \infty. \tag{2.31}$$

Combining equations (2.22), (2.23), (2.25) and (2.31), we get, after some simplification,

$$\dot{x} = [A - B(D + \rho I)^{-1}C]x + B\rho(D + \rho I)^{-1}(r - y_{out}) + B(D + \rho I)^{-1}\hat{u} \tag{2.32}$$

$$u = Cx + D(r - y_{out}). \tag{2.33}$$

This is the modified conditioned controller of Walgama *et al.* [131].

A second, more general modification is presented in [131, §5] where conditioning is performed on a filtered set-point signal r_f instead of the direct set-point r. We describe this approach here.

Let $F = \left[\begin{array}{c|c} A_f & B_f \\ \hline C_f & D_f \end{array}\right]$ be a stable, biproper (D_f non-singular) filter with state x_f.

Let the linear controller K be given by

$$\dot{x} = Ax + B_1 r + B_2 y_{out} \tag{2.34}$$

$$u = Cx + D_1 r + D_2 y_{out} \tag{2.35}$$

$$\text{i.e.,} \quad u = K_1 r + K_2 y_{out}. \tag{2.36}$$

$$\text{where} \quad K = [K_1 \quad K_2] = \left[\begin{array}{c|cc} A & B_1 & B_2 \\ \hline C & D_1 & D_2 \end{array}\right]. \tag{2.37}$$

Following Walgama *et al.* (1992) [131], we replace $K_1 r$ by $F r_f$ in equation (2.36). Here, r_f is the filtered reference. Thus,

$$u = F r_f + K_2 y_{out} \tag{2.38}$$

or in state space form

$$\dot{x} = Ax + B_2 y_{\text{out}} \tag{2.39}$$

$$\dot{x}_f = A_f x_f + B_f r_f \tag{2.40}$$

$$u = Cx + C_f x_f + D_f r_f + D_2 y_{\text{out}}. \tag{2.41}$$

Conditioning is now applied to this filtered reference signal r_f to give the realizable filtered reference

$$r_f^r = r_f + D_f^{-1}(\hat{u} - u). \tag{2.42}$$

Applying this conditioned reference r_f^r to the filter state equation (2.40) in exactly the same manner as described in §2.5 for the Hanus conditioned controller, we get,

$$\dot{x} = Ax + B_2 y_{out} \tag{2.43}$$

$$\dot{x}_f = (A_f - B_f D_f^{-1} C_f) x_f - B_f D_f^{-1} C x + B_f D_f^{-1} \hat{u} - B_f D_f^{-1} D_2 y_{out} \tag{2.44}$$

$$u = Cx + C_f x_f + D_2 y_{out} + D_f r_f. \tag{2.45}$$

Eliminating r_f by using the relation $Fr_f = K_1 r$, i.e., $r_f = F^{-1}K_1 r$, we get, after some simplification

$$u = \hat{K} \begin{bmatrix} r \\ y_{out} \\ \hat{u} \end{bmatrix} \tag{2.46}$$

where

$$\hat{K}(s) = \left[\begin{array}{cc|ccc} A & 0 & B_1 & B_2 & 0 \\ -B_f D_f^{-1} C & A_f - B_f D_f^{-1} C_f & -B_f D_f^{-1} D_1 & -B_f D_f^{-1} D_2 & B_f D_f^{-1} \\ \hline C & C_f & D_1 & D_2 & 0 \end{array}\right]. \tag{2.47}$$

Walgama *et al.* (1992) [131] point out that the filter F can be used to tune the transient performance of the saturated system. However, as they point out, design guidelines for F which guarantee stability and acceptable transient performance are not available.

2.7 Observer-Based Anti-Windup

As pointed out before, an interpretation of the windup problem is that the states of the controller do not correspond to the control signal being fed to the plant. This inaccuracy in the state vector of the controller is due to lack of correct estimates of the controller states in the presence of actuator nonlinearities. To obtain correct state estimates and to avoid windup, Åström *et al.* [5, 6] suggest that an observer be introduced into the controller.

Referring to Figure 2.6, let the linear controller $K(s)$ be defined by the equations

$$\dot{x} = Ax + By_m \tag{2.48}$$

$$u = Cx + Dy_m. \tag{2.49}$$

Let us assume that there is a nonlinearity N between the controller output and the

control input to the plant $P(s)$ so that the input to the plant is given by

$$\hat{u} = N(u). \tag{2.50}$$

Following Åström *et al.* [5, 6], the nonlinear observer for the controller $K(s)$ (assuming (C,A) detectable) is defined by

$$\dot{\hat{x}} = A\hat{x} + By_m + L(\hat{u} - C\hat{x} - Dy_m) \tag{2.51}$$

$$u = C\hat{x} + Dy_m \tag{2.52}$$

$$\hat{u} = N(u) \tag{2.53}$$

where $\hat{x}$ is an estimate of the controller state and L is the observer gain. Instead of having a separate controller and a separate observer, both are integrated into one scheme to form the AWBT compensator. Thus, the observer comes into the controller structure only in the presence of the actuator nonlinearity ($N \not\equiv I$) and does not affect the linear controller ($N \equiv I$).

Walgama and Sternby [132] have exploited this inherent observer property in several AWBT schemes to generalize them. Despite the significant generalization offered by this approach, no theoretically rigorous guidelines were provided in the original reference of Åström *et al.* [5, 6] to enable design of L. Recently, Kapoor *et al.* [73] carried out an investigation of the design of a stabilizing observer gain L. Park and Choi [109] extended the basic idea of the observer structure in AWBT by allowing L to have linear dynamics.

2.8 Internal Model Control (IMC)

The internal model control (IMC) structure [101, pages 44–45] was never intended to be an anti-windup scheme. Nonetheless, as pointed out in [27, 43, 101, 131], it has potential for application to the anti-windup problem, for the case where the system is open loop stable. The AWBT application of IMC has been studied by Cohen *et al.*

[35] and Debelle [39].

Figure 2.7 shows the IMC structure with an actuator nonlinearity. If the controller is implemented in the IMC configuration, actuator constraints do not cause any stability problems provided the constrained control signal is sent to both the plant and the model. Under the assumption that there is no plant-model mismatch ($G = \tilde{G}$), it is easy to show that the IMC structure remains effectively open loop and stability is guaranteed by the stability of the plant G and the IMC controller Q. Stability of G and Q is in any case imposed by linear design and hence stability of the nonlinear system is assured. Thus the IMC structure offers the opportunity of implementing

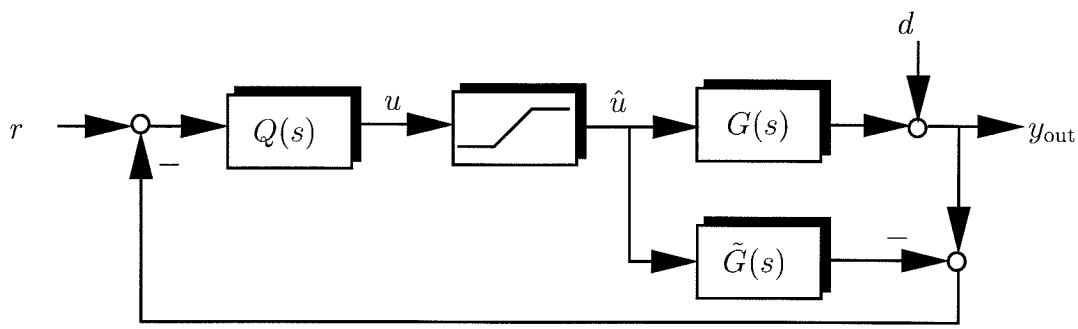

Figure 2.7: The IMC structure.

complex (possibly nonlinear) control algorithms without generating complex stability issues, provided there is no plant-model mismatch.

For the sake of generality, we will discuss the two degree of freedom IMC implementation shown in Figure 2.8. The IMC implementation of Figure 2.7 is just a special case with $Q_1(s) = Q_2(s)$. Stability of the linear system requires that $Q_1(s)$, $Q_2(s)$ and $\tilde{G}(s) = G(s)$ be stable.

In the presence of saturation, the control signal is given by (see Figure 2.8)

$$u = Q_1 r - Q_2 y_{\text{out}} + Q_2 \tilde{G} \hat{u}. \tag{2.54}$$

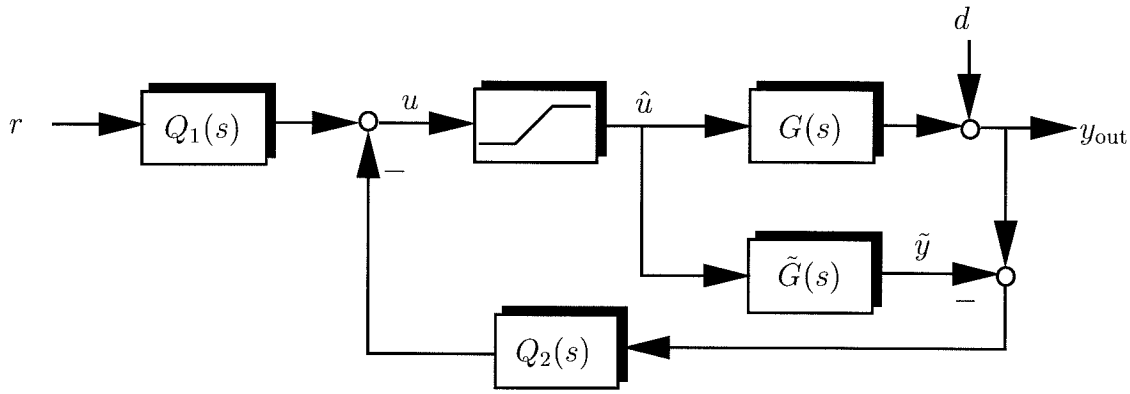

Figure 2.8: Two degree of freedom IMC structure.

Since $y_{\text{out}} = d + G\hat{u}$ and assuming no plant-model mismatch ($G \equiv \tilde{G}$), (2.54) becomes

$$u = Q_1 r - Q_2 d \tag{2.55}$$

and thus, the system is effectively open-loop and with Q_1 and Q_2 stable, closed-loop stability is guaranteed for a stable plant $G(s)$, even in the presence of input constraints.

Unfortunately, the cost to be paid for global stability of the IMC implementation is in the form of somewhat "sluggish" performance. This is because the controller output is independent of the plant output in both the linear and nonlinear regimes. While this does not matter in the linear regime, its implication in the nonlinear regime is that the controller is unaware of the effect of its actions on the output, resulting in some sluggishness. This effect is most pronounced when the IMC controller has fast dynamics which are "chopped off" by the saturation. Moreover, unless the IMC controller is designed to optimize nonlinear performance, it will not give satisfactory performance for the saturating system.

In Chapter 3, we will discuss an anti-windup structure for IMC for optimizing performance in the face of saturation.

2.9 The Extended Kalman Filter

The last scheme we consider here is an AWBT implementation applicable to observer-based linear compensators. This implementation is developed to maintain valid state estimates in the observer independent of any nonlinearities between the controller output and the plant input.

Let the plant $G(s)$ be described by the state-space equations

$$\dot{x} = Ax + B_1 r + B_2 d + B_3 u \tag{2.56}$$

$$z = C_1 x + D_{11} r + D_{12} d + D_{13} u \tag{2.57}$$

$$y_1 = C_3 x + D_{31} r + D_{32} d \tag{2.58}$$

where r is the set-point to the plant, d is an external unmeasured disturbance, u is the control input and y_1 is the measurement provided to the controller. In other words, the plant $G(s)$ has a state-space realization

$$G(s) = \left[\begin{array}{c|ccc} A & B_1 & B_2 & B_3 \\ \hline C_1 & D_{11} & D_{12} & D_{13} \\ 0 & I & 0 & 0 \\ C_3 & D_{31} & D_{32} & 0 \end{array}\right]. \tag{2.59}$$

Implicit in this realization is the assumption that the command r is available to the controller without noise and that the loop formed with the controller is well-posed.

Let $K(s)$ be the standard observer/state-feedback controller with state $\hat{x}$, whose state-space equations can be described by

$$\dot{\hat{x}} = A\hat{x} + B_1 r + B_3 u + L(y_1 - C_3\hat{x} - D_{31} r) \tag{2.60}$$

$$u = -F\hat{x}, \tag{2.61}$$

i.e.,

$$K(s) = \left[\begin{array}{c|cc} A - B_3F - LC_3 & B_1 - LD_{31} & L \\ \hline -F & 0 & 0 \end{array}\right] \tag{2.62}$$

where L is the observer gain and F is the state feedback gain. The state estimation error $e \triangleq x - \hat{x}$ satisfies the relation

$$\dot{e} = (A - LC_3)e + (B_2 - LD_{32})d. \tag{2.63}$$

In the presence of nonlinearity N between the controller output and the plant input, we have

$$\hat{u} = N(u) \neq u = -F\hat{x}.$$

It is easy to verify that in this case, the state estimation error e satisfies

$$\dot{e} = (A - LC_3)e + (B_2 - LD_{32})d + B_3(\hat{u} - u) \tag{2.64}$$

Thus, the observer in (2.62) will give poor estimates of the true plant state because of the term $\hat{u}-u$ driving the estimation error. This is because equation (2.62) assumes that $\hat{u} = u = -F\hat{x}$, which is not the case in the presence of the nonlinearity N. Hence, this will result in controller windup.

To provide anti-windup compensation, the observer equations must be modified so that the state estimator is based on the actual input $\hat{u}$ to the plant. Thus, the modified observer/state-feedback compensator is given by

$$\dot{\hat{x}} = A\hat{x} + B_1r + B_3\hat{u} + L(y_1 - C_3\hat{x} - D_{31}r) \tag{2.65}$$

$$= (A - LC_3)\hat{x} + (B_1 - LD_{31})r + B_3\hat{u} + Ly_1 \tag{2.66}$$

$$u = -F\hat{x}. \tag{2.67}$$

We refer to this AWBT scheme as an extended Kalman filter implementation since $\hat{u}$ is provided as an input to the observer either by direct measurement or by using a

nonlinear model of the input nonlinearity N acting on u. In this case, the estimation error e satisfies the relation (2.63), as in the linear case, restoring consistent state estimates.

It is worth mentioning that the classical separation principle of the observer/state feedback controller is lost with this implementation, in the presence of input nonlinearities. Thus, even though $A - LC_3$ and $A - B_3F$ may have eigenvalues in the open left half plane, the overall closed loop nonlinear system need not be asymptotically stable, and examples can be constructed to demonstrate this.

2.10 Conclusions

In this chapter, we presented a fairly extensive and detailed review of existing techniques for AWBT compensation. One particular AWBT technique, applicable to controllers implemented in the IMC framework, will be discussed in the next chapter. All these schemes adopt the two-step design paradigm discussed at the beginning of the chapter, i.e., as a first step, a linear controller is designed ignoring the presence of input nonlinearities, and then as a second step, some anti-windup compensation is added to modify or "retro-fit" the linear controller design to alleviate the effects of input nonlinearities.

As should be clear from the review, many of these schemes perform well for the particular situation that they have been designed for. However, what is lacking is an attempt to formalize these techniques and advance a general AWBT analysis and synthesis theory. In Chapter 4, we will discuss a general framework which will allow us to put the AWBT problem on a firm theoretical footing.

Chapter 3 Anti-Windup Design for Internal Model Control

Abstract

In this chapter, we consider linear control design for systems with input magnitude saturation, in the framework of Internal Model Control (IMC). An anti-windup scheme which optimizes nonlinear performance, applicable to MIMO systems, is developed. Several examples, including an ill-conditioned plant, show that the scheme provides graceful degradation of performance. The attractive features of this scheme are its simplicity and effectiveness.

3.1 Introduction

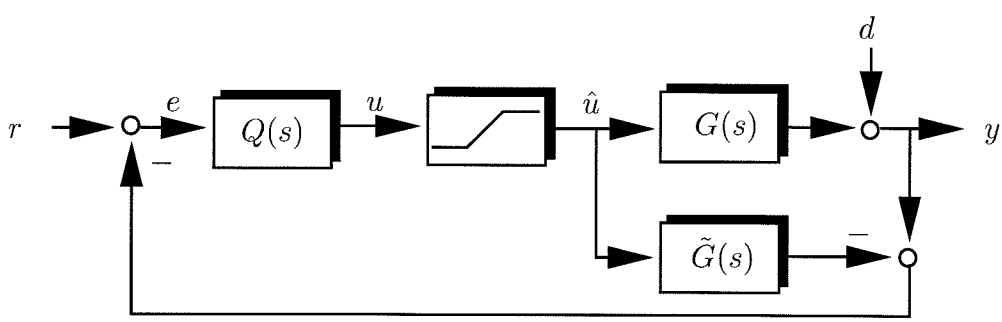

Figure 3.1: The IMC interconnection.

The Internal Model Control (IMC) [101] structure is a special case of the Youla parameterization of all stabilizing controllers for a given process. For open-loop stable processes, the IMC structure conveniently gives a nominally stable, essentially open-loop implementation, which has several attractive properties as outlined in [52].

Figure 3.1 shows a standard IMC interconnection. G is the plant and $\tilde{G}$ is a model of the plant. Q is the so-called IMC controller [101]. The equivalence of the IMC

interconnection shown in Figure 3.1 with the classic feedback control interconnection can be found in [101].

Provided there is no plant-model mismatch ($G = \tilde{G}$), global closed-loop stability is equivalent to stability of G and Q. We had discussed this in §2.8. Thus the IMC structure offers the opportunity of implementing complex (possibly nonlinear) control algorithms without generating complex stability issues even in the presence of plant input constraints, provided there is no plant-model mismatch.

However, in the presence of actuator constraints, nominal IMC performance can suffer significantly. This is because due to the absence of any feedback in the nominal case, the IMC controller is entirely unaware of the effect of its action. In particular, it does not know if and when the manipulated variable u saturates. This effect is most pronounced when the IMC controller has fast dynamics which are chopped off by the saturation. Unless the IMC controller is designed to optimize nonlinear performance, it will not give satisfactory performance for the saturating system. The focus of this chapter is on identifying this nonlinear performance objective and optimizing it by an appropriate modification of the IMC implementation.

3.2 Problem Formulation

Consider the IMC structure as shown in Figure 3.1. We will assume that the plant is a linear time invariant and stable square system with n inputs and n outputs. G, $\tilde{G}$, and Q denote the plant, the model of the plant, and the IMC controller, respectively. They are n by n transfer matrices. Define

$$y'(t) = (G * \hat{u})(t) + d(t) = \int_0^t G(t-\tau)\hat{u}(\tau)d\tau + d(t). \tag{3.1}$$

Thus y' corresponds to the output of the constrained system. Because of the saturation constraints, $y'(t)$ necessarily differs from $y(t)$, the output of the unconstrained system. In general, we would like to keep y' as close to y as possible. Mathematically, we would like to solve the following optimization problem instantaneously at each

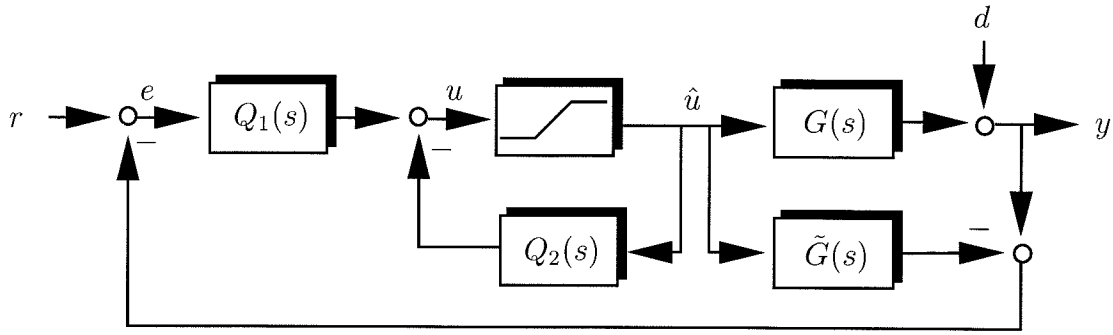

Figure 3.2: Modified IMC structure.

time t:

$$\min_{\hat{u}} |(f * y)(t) - (f * y')(t)|_1 = \min_{\hat{u}} |(fGQ * e)(t) - (fG * \hat{u})(t)|_1 \qquad (3.2)$$

where f is a filter such that fG is biproper. If G is strictly proper, then $\hat{u}$ does not affect y' instantaneously and the minimization is meaningless. Since our ultimate goal is to minimize $|y(t) - y'(t)|_1$, f must be diagonal in order not to introduce any change in the output direction.

The minimization is carried out continuously for $t \geq 0$. It is important to realize that this instantaneous minimization differs from the minimization over a horizon. For the conventional IMC structure displayed in Figure 3.1, $\hat{u}(t) = \text{sat}(u(t)) = \text{sat}(\int_0^t Qe(\tau)d\tau)$ is completely determined for any given $e(t)$. Thus, in general, the conventional IMC implementation does not solve optimization problem (3.2) which optimizes the performance for the constrained system. In the next section, we will show that a modified IMC structure actually solves the optimization problem (3.2) instantaneously.

3.3 Anti-Windup Design for IMC

Figure 3.2 shows the modified IMC structure where $Q = (I + Q_2)^{-1}Q_1$. Assume that

Q is biproper.[1] We have

$$u(s) = Q_1 e(s) - Q_2 \hat{u}(s) = Q_1 e(s) - (Q_1 Q^{-1} - I)\hat{u}(s). \tag{3.3}$$

Here zero initial condition is assumed. This is without loss of generality since Q is stable and nonzero initial conditions can be incorporated into $e(t)$. In the time domain,

$$u(t) - \hat{u}(t) = (Q_1 * e)(t) - (Q_1 Q^{-1} * \hat{u})(t). \tag{3.4}$$

The following lemma states how f should be chosen such that the modified IMC structure shown in Figure 3.2 solves the optimization problem (3.2).

Lemma 3.1 *Suppose that Q is biproper and that $G = \tilde{G}$. If $fG|_{s=\infty}$ is a diagonal nonsingular matrix with finite elements and $Q_1 = fGQ$, then $\hat{u}(t)$ resulting from the modified IMC implementation (Figure 3.2) is the solution of optimization problem (3.2). Furthermore, if $g = Df$ where D is a diagonal constant matrix, then the closed-loop responses with f and g are identical.*

Proof. $Q_1 = fGQ \Rightarrow u(t) - \hat{u}(t) = (fGQ * e)(t) - (fG * \hat{u})(t) = (f * y)(t) - (f * y')(t) \equiv y_f(t) - y'_f(t)$. We have

$$u_i(t) - \hat{u}_i(t) = y_{f_i}(t) - y'_{f_i}(t), \quad i = 1, 2, \cdots, n. \tag{3.5}$$

Since $fG|_{s=\infty}$ is diagonal, $\hat{u}_j, j \neq i$, do not affect y'_{f_i} instantaneously. Equations (3.5) can be solved independently for each $\hat{u}_i(t)$. Consider the first input, i.e., $i = 1$. When no saturation occurs at $t = t_1$, $\hat{u}_1(t_1) = u_1(t_1) = \text{sat}(u_1(t_1))$ and $|y_{f_1}(t_1) - y'_{f_1}(t_1)| = 0$ is minimized. Suppose that saturation occurs at $t = t_2$, i.e., $u_1(t_2) > u_1^{max}$ or $u_1(t_2) < u_1^{min}$, we want to show that $\hat{u}_1(t_2) = \text{sat}(u_1(t_2))$ also minimizes $|y_{f_1}(t_2) - y'_{f_1}(t_2)|$. Since $\hat{u}_1(t_2)$ affects $y'_{f_1}(t_2)$ linearly and $\hat{u}_j(t_2), j = 2, 3, \cdots, n$, do not affect $y'_{f_1}(t_2)$, $|y_{f_1}(t_2) - y'_{f_1}(t_2)|$ is a convex function of $\hat{u}_1(t_2)$ only. If $\hat{u}_1(t_2) = u_1(t_2)$ for which

[1] Q is biproper if both Q and Q^{-1} are proper.

$|y_{f_1}(t_2) - y'_{f_1}(t_2)| = 0$ is not feasible, i.e., $u_1(t_2) > u_1^{max}$ or $u_1(t_2) < u_1^{min}$, then the optimal solution which minimizes $|y_{f_1}(t_2) - y'_{f_1}(t_2)|$ must occur at the boundary, i.e., $\hat{u}_1(t_2) = \text{sat}(u_1(t_2))$. Therefore, choosing $\hat{u}_1(t) = \text{sat}(u_1(t))$ minimizes $|y_{f_1}(t) - y'_{f_1}(t)|$ for each $t \geq 0$. Since $|y_{f_i}(t) - y'_{f_i}(t)|$ is minimized for each i, $|y_f(t) - y'_f(t)|_1$ is minimized.

If $g = Df$, (3.5) becomes

$$u_i(t) - \hat{u}_i(t) = D_{ii}[y_{f_i}(t) - y'_{f_i}(t)], \quad i = 1, 2, \cdots, n \tag{3.6}$$

where $D = \text{diag}\{D_{11}, \cdots, D_{nn}\}$.

Before saturation occurs, the system is unconstrained and $\hat{u}(t) = u(t)$ does not depend on D. Assume that the system saturates for input 1 at $t = t_1$, then $\hat{u}_1(t_1) = u_1^{max}$ or $\hat{u}_1(t_1) = u_1^{min}$. As long as the right-hand side of (3.5) does not become zero for $i = 1$, input 1 stays saturated and $\hat{u}_1(t)$ is constant during this period. Input 1 becomes unsaturated only if the right-hand side of (3.5) becomes zero for $i = 1$ which is not a function of D_{11}. Therefore, the system comes out of saturation at the same time regardless of what D_{11} is. Similar arguments can be used when more than one input saturates. Therefore, the closed-loop responses for f and g are identical. ■

Remark 3.1 *If $fG|_{s=\infty}$ is not diagonal, then $y'_{f_i}(t)$ may also be affected by $\hat{u}_j(t), j \neq i$, instantaneously. The convexity argument would not work since $|y_{f_i}(t) - y'_{f_i}(t)|$ is also affected by $\hat{u}_j(t), j \neq i$.*

Remark 3.2 *f must be diagonal in order not to introduce any change in the output direction. However, f for which $fG|_{s=\infty}$ is diagonal may not be diagonal. To get around this problem, we can design a diagonal f for $\tilde{G}$ such that $f\tilde{G}|_{s=\infty}$ is diagonal. $\tilde{G}$ can be chosen arbitrarily close to G. Q_2 must be strictly proper to be implementable. This can be achieved by choosing f appropriately.*

Remark 3.3 *Q is usually minimum phase and always stable. If Q is minimum phase and Q_1 non-minimum phase, then $(I + Q_2)^{-1}$ must be unstable. Therefore, Q_1 must*

be minimum phase and stable to guarantee internal stability of the closed-loop system. f must be chosen such that fGQ is both minimum phase and stable.

Remark 3.4 *For the modified IMC structure, the input is kept saturated for an optimal amount of time until $|y_f(t) - y'_f(t)|$ becomes zero. Thus, in general, the performance is greatly improved when f is appropriately chosen.*

Different controller factorizations can be obtained by choosing f differently. We discuss two special cases here.

Case 1: $f = G^{-1}$. The optimization problem (3.2) becomes $\min_{\hat{u}} |u(t) - \hat{u}(t)|_1$. The solution corresponds to the conventional IMC structure which "chops off" the control input resulting in performance deterioration. However, stability of the closed-loop system is guaranteed.

Case 2: f **is such that** Q_1 **is a constant matrix.** The optimization becomes $\min_{\hat{u}} |Q_1[e(t) - e'(t)]|_1$, where $e'(t) = (Q^{-1} * \hat{u})(t)$. This factorization corresponds to the Model State Feedback proposed by Coulibaly *et al.* (1992) for SISO systems. The same factorization has also been proposed recently by Goodwin *et al.* (1993) where Q_1 is chosen to be $Q(\infty)$. Thus, these are special cases of the factorization we present.

The performance in this case is greatly improved, but stability of the closed-loop system is not guaranteed. If the dynamics of GQ are slow, however, minimizing the weighted controller input error $(e(t) - e'(t))$ may not be a good way to optimize the nonlinear performance. After the system comes out of the nonlinear region, the controller takes no action to compensate for the effect of the error, $e(t) - e'(t)$, introduced during the saturation.

In Case 1 f was chosen to guarantee stability while f was chosen to enhance performance in Case 2. Therefore, f can generally be tuned to trade off performance and stability of the constrained system. It should be pointed out that f in Case 2 was not an extreme choice.

3.4 Classical Feedback Structure

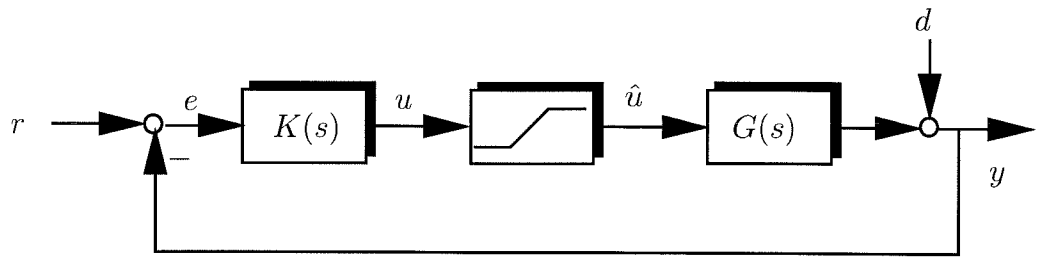

Figure 3.3: Classical feedback structure.

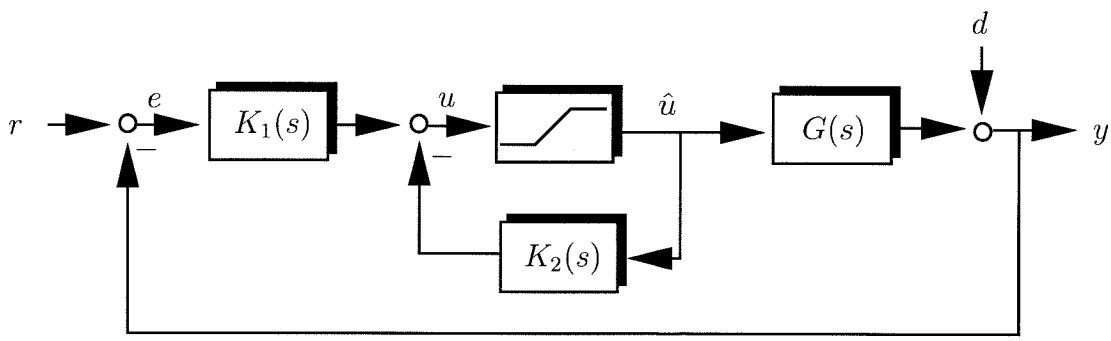

Figure 3.4: Classical feedback structure with anti-windup.

For stable unconstrained systems, the IMC structure shown in Figure 3.1 and the classical feedback structure shown in Figure 3.3 are equivalent. The results for the modified IMC structure can be extended directly to the classical feedback structure to obtain the anti-windup structure shown in Figure 3.4. The controllers K_1 and K_2 are defined as follows:

$$K_1 = Q_1 \tag{3.7}$$

$$K_2(s) = Q_2 - Q_1\tilde{G}. \tag{3.8}$$

Hanus *et al.* [63, 62] suggested the following

$$K_1 = K(\infty) \tag{3.9}$$

$$K_2(s) = K_1 K^{-1}(s) - I \tag{3.10}$$

where $K = Q(I - \tilde{G}Q)^{-1}$. This factorization corresponds to $f = K_1 Q^{-1} G^{-1}$. Therefore, Hanus' conditioning technique minimizes $|K_1[e(t) - e'(t)]|_1$.

3.5 Extension to Nonlinear Systems

The anti-windup IMC implementation which we introduced in §3.3 has been extended to nonlinear systems with appropriate modifications by Doyle III [44] and Kendi and Doyle III [74]. We briefly discuss this extension here for completeness and to bring out the relevance of the anti-windup IMC implementation proposed in this chapter.

Consider a control-affine nonlinear system described by the following state-space equations:

$$\dot{x} = f(x) + g(x)u \tag{3.11}$$

$$y = h(x). \tag{3.12}$$

The relative degree r [68] for this system at the point x_0 is defined as the integer r which satisfies:

$$L_g L_f^{i-1} h(x) = 0, \quad \forall\ i < r \tag{3.13}$$

$$L_g L_f^{r-1} h(x) \neq 0, \tag{3.14}$$

for all x in some neighborhood of x_0. Here, $L_g f$ refer to the usual Lie derivative $\sum_{i=1}^{n} \frac{\partial f}{\partial x} g_i$ as described in [68].

For this system, an input-output linearizing controller is given by [68]

$$u = \alpha(x) + (-\lambda_0 y - \lambda_1 \dot{y} - \cdots - \lambda_{n-1} y^{(n-1)} + v)\beta(x) \quad (3.15)$$

$$\text{where } \alpha(x) = \frac{-L_f^r h(x)}{L_g L_f^{r-1} h(x)}, \quad \beta(x) = \frac{1}{L_g L_f^{r-1} h(x)}. \quad (3.16)$$

Thus, for the unconstrained system, it is easy to verify that the mapping from the new input variable v to the output y is linear:

$$\frac{y}{v} = \frac{1}{\lambda_0 + \lambda_1 s + \cdots + \lambda_{n-1} s^{n-1} + s^n}. \quad (3.17)$$

However, in the presence of constraints on u, the new input variable v has to be appropriately constrained for this approach to be applicable. Referring to (3.15), which can be expressed as

$$u = f_1(x(t)) + f_2(x(t))v \quad (3.15')$$

with f_1 and f_2 appropriately defined, we see that the saturation constraint on u

$$u_{\min} \leq u \leq u_{\max}$$

translates to a constraint on x and v as follows, using (3.15) above:

$$u_{\min} \leq f_1(x(t)) + f_2(x(t))v \leq u_{\max}. \quad (3.18)$$

Assuming, without loss of generality, $f_2 > 0$ (see [44, 74] for a justification), we can explicitly solve for equivalent bounds on v, which for the SISO case are the following:

$$v_{\min}(x(t)) \leq v \leq v_{\max}(x(t)) \quad (3.19)$$

$$\text{where } v_{\min}(x(t)) = \frac{u_{\min} - f_1(x(t))}{f_2(x(t))}$$
$$v_{\max}(x(t)) = \frac{u_{\max} - f_1(x(t))}{f_2(x(t))}.$$

As long as the constraints on v are satisfied, u remains within its constraints and the input-output linearization remains valid. This scheme is illustrated in Figure 3.5.

Now, an IMC controller for the resulting input-output linearized system can be designed, and then the anti-windup IMC implementation proposed in this chapter can be applied to it. Note here that the only difference in this case is that the input nonlinearity acting on the new input variable v is not a static saturation nonlinearity, but in fact is a state-dependent nonlinearity, as we saw in (3.19).

3.6 Examples

In this section, several examples are given to demonstrate the effectiveness of the proposed method.

Example 3.1 Consider the following plant:

$$G(s) = \frac{2}{100s+1}. \tag{3.20}$$

The IMC controller designed for a step input is

$$Q(s) = \frac{100s+1}{2(20s+1)}. \tag{3.21}$$

Case 1. Choosing $f(s) = 2.5(20s+1)$ gives [2]

$$\begin{aligned} Q_1 &= 2.5 \\ Q_2(s) &= \frac{4}{100s+1}. \end{aligned}$$

Case 2. Choosing $f(s) = 50(s+1)$ gives

$$\begin{aligned} Q_1(s) &= \frac{50(s+1)}{20s+1} \\ Q_2(s) &= \frac{99}{100s+1}. \end{aligned}$$

[2]The constant 2.5 is such that $Q_2(s)$ is strictly proper.

The input is constrained between the saturation limits ± 1.

The responses to a unit step disturbance with the conventional IMC and the modified IMC implementations are shown in Figures 3.6 and 3.7 along with the unconstrained responses. The figures illustrate the sluggish performance of the conventional IMC implementation in the presence of constraints, when the closed loop dynamics are much faster than those of the open loop. For the conventional IMC implementation, the saturation effectively "chops off" the control input resulting in performance deterioration.

The modified IMC implementation keeps the control signal saturated for an optimum length of time as discussed in §3.3 resulting in improved performance. f in Case 1 corresponds to minimizing $|e(t) - e'(t)|$ while f in Case 2 corresponds approximately to minimizing $|y(t) - y'(t)|$. The control input in Case 2 stays saturated until $y(t) \approx y'(t)$ while the control input in Case 1 stays saturated until $e(t) = e'(t)$. In Case 1, the difference between $y(t)$ and $y'(t)$ resulting from the difference between $e(t)$ and $e'(t)$ during the saturation is not compensated as can be seen in Figure 3.6.

Example 3.2 This example is taken from Doyle *et al.* [43] where the conventional anti-windup method did not result in a stable closed loop system. The plant is a fourth order lag-lead butterworth:

$$G(s) = 0.2 \left(\frac{s^2 + 2\xi_1\omega_1 s + \omega_1^2}{s^2 + 2\xi_1\omega_2 s + \omega_2^2} \right) \left(\frac{s^2 + 2\xi_2\omega_1 s + \omega_1^2}{s^2 + 2\xi_2\omega_2 s + \omega_2^2} \right) \tag{3.22}$$

where $\omega_1 = 0.2115, \omega_2 = 0.0473, \xi_1 = 0.3827$ and $\xi_2 = 0.9239$.

The IMC controller is

$$Q(s) = \frac{s+1}{(16s+1)G(s)}. \tag{3.23}$$

Choosing $f(s) = \frac{5(16s+1)}{16(s+1)}$ gives

$$\begin{aligned} Q_1 &= \frac{5}{16} \\ Q_2(s) &= \frac{5}{16Q(s)} - 1. \end{aligned}$$

The input is constrained between the saturation limits ± 1. Figure 3.8 shows the responses for a disturbance input with step of magnitude of 5 at time $t = 0$ and a switch to -5 at $t = 4$. The performance improvement over the conventional IMC implementation is significant. Furthermore, the off-axis criterion (Cho and Narendra [31]) can be used to show that the closed-loop system is globally asymptotically stable with the anti-windup IMC implementation.

Example 3.3 Consider the following plant:

$$G(s) = \frac{10}{100s+1} \begin{bmatrix} 4 & -5 \\ -3 & 4 \end{bmatrix}. \tag{3.24}$$

Both inputs are constrained between the saturation limits ± 1. A set-point change of $[0.63\ 0.79]^T$ is applied. The IMC controller designed for a step input is

$$Q(s) = \frac{100s+1}{10(20s+1)} \begin{bmatrix} 4 & 5 \\ 3 & 4 \end{bmatrix}. \tag{3.25}$$

Two values of f , one diagonal and one non-diagonal, are chosen to see how f (diagonal or not diagonal) affects closed-loop performance.

Case 1.

$$\begin{aligned} f(s) &= 10(s+1) \begin{bmatrix} 4 & 5 \\ 3 & 4 \end{bmatrix} \\ Q_1(s) &= f(s)G(s)Q(s) \\ Q_2(s) &= f(s)G(s) - I. \end{aligned}$$

Case 2.

$$\begin{aligned} f(s) &= 2.5(s+1)I \\ \tilde{G}(s) &= \frac{10}{100s+1}\begin{bmatrix} 4 & \frac{-5}{0.1s+1} \\ \frac{-3}{0.1s+1} & 4 \end{bmatrix} \\ Q_1(s) &= f\tilde{G}(s)Q(s) \\ Q_2(s) &= f(s)\tilde{G}(s) - I. \end{aligned}$$

The responses for both cases and the conventional IMC implementation are shown in Figure 3.9. As we can see, choosing f to be a diagonal nonsingular matrix is crucial to obtain good nonlinear performance.

3.7 Conclusions

We have proposed an anti-windup scheme which optimizes the error between the constrained and the unconstrained outputs of the system. The method generalizes the Model State Feedback scheme for SISO systems proposed in Coulibaly *et al.* [36] and Hanus' conditioning technique [63, 62]. In particular, the Model State Feedback scheme corresponds to choosing f such that Q_1 is constant; Hanus' conditioning technique corresponds to choosing f such that $Q_1 = K(\infty)$; the factorization proposed by Goodwin *et al.* (1993) corresponds to choosing f such that $Q_1 = \lim_{s\to\infty} Q(s)$.

Furthermore, from our problem formulation, we can see what these methods do and what the consequences are. As shown by Example 3, the performance for $Q_1 = K(\infty)$ for MIMO systems may suffer when $K(\infty)$ is not diagonal. The examples illustrate that our scheme provides graceful degradation of performance. The attractive features of our scheme are its simplicity and effectiveness. The filter f can be tuned to trade off performance and stability of the constrained system.

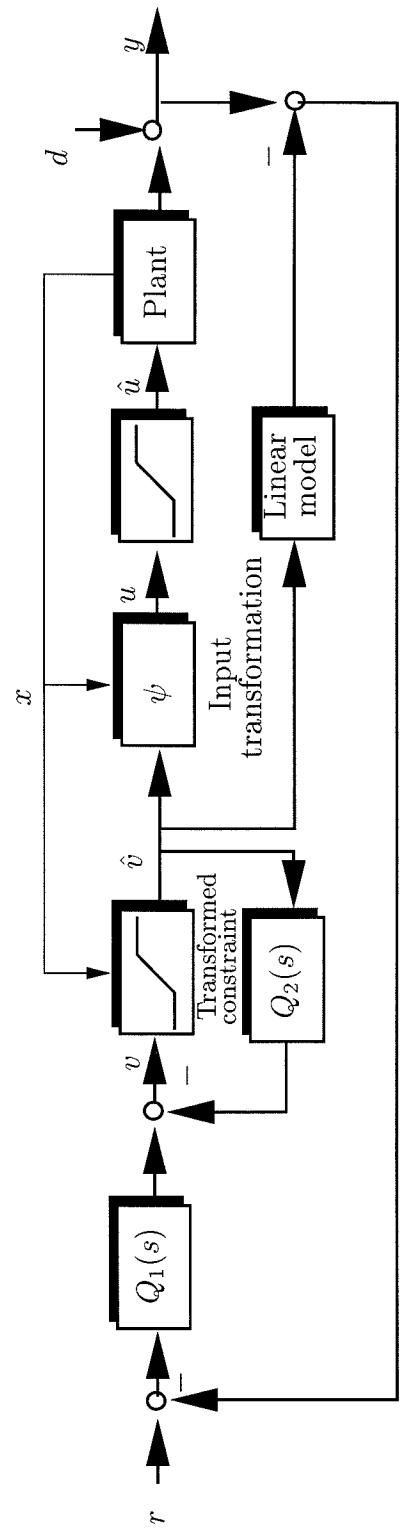

Figure 3.5: Anti-windup IMC applied to an input-output feedback linearized plant.

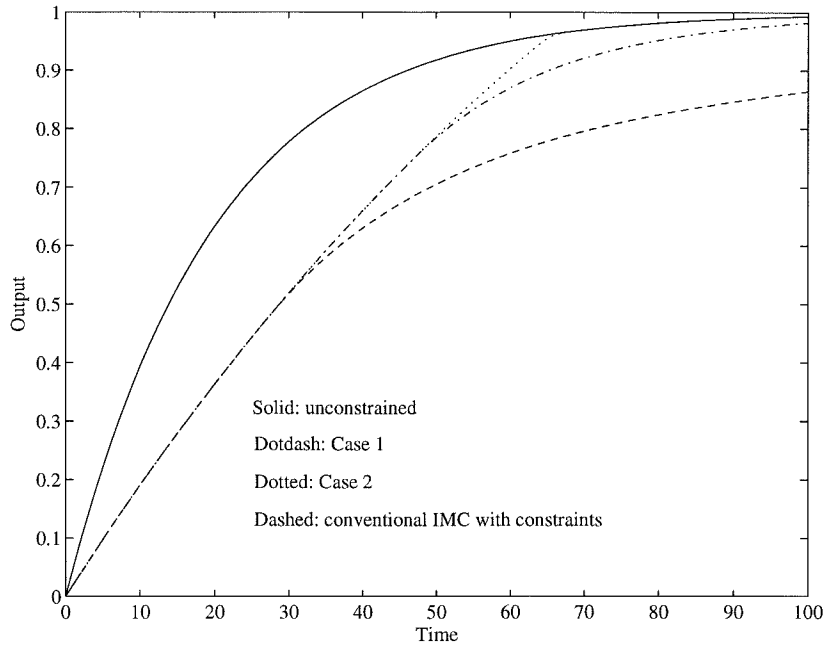

Figure 3.6: Example 1 — Plant output responses.

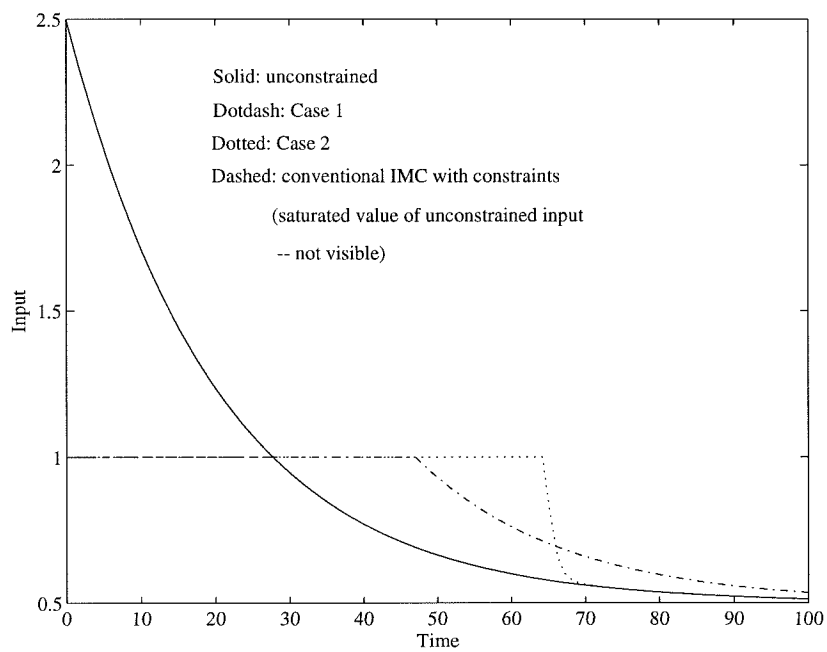

Figure 3.7: Example 1 — Controller output responses.

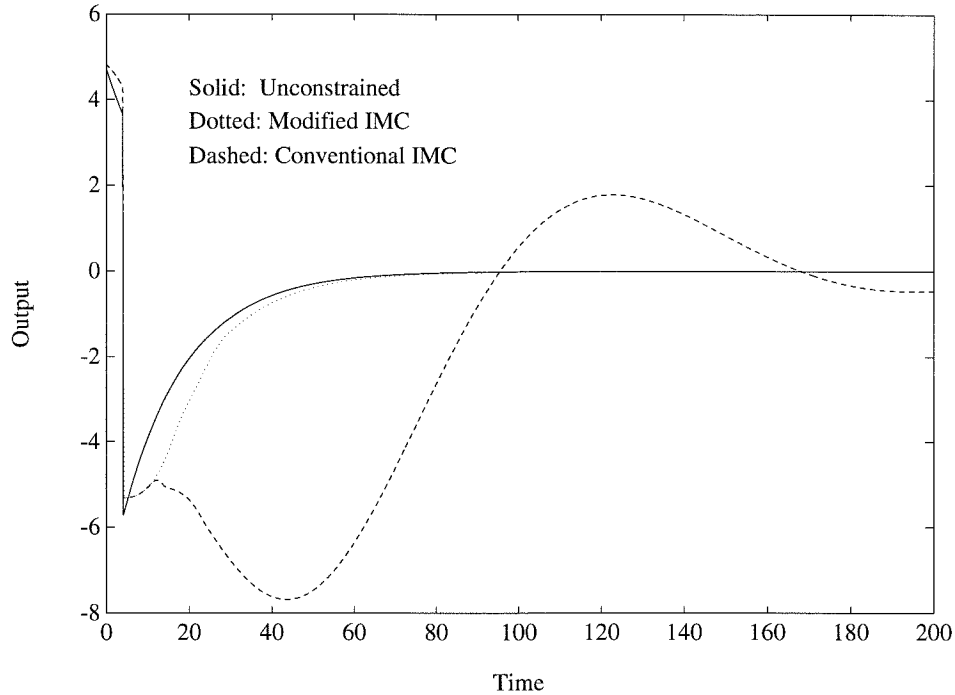

Figure 3.8: Example 2 — Plant output responses.

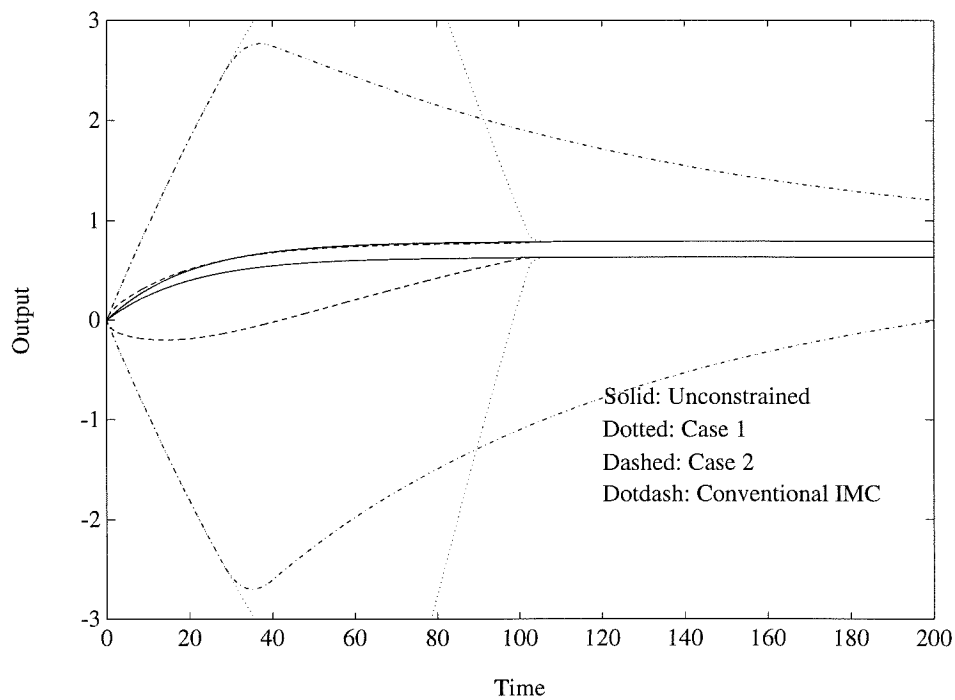

Figure 3.9: Example 3 — Plant output responses.

Chapter 4 A Unified Framework for the Study of Anti-Windup Designs

Abstract

We present a unified framework for the study of linear time-invariant (LTI) systems subject to control input nonlinearities using anti-windup bumpless transfer (AWBT) schemes. The framework is based on the following two-step design paradigm: "*Design first the linear controller ignoring control input nonlinearities and then add AWBT compensation to minimize the adverse effects of any control input nonlinearities on closed loop performance.*" The resulting AWBT compensation is applicable to multivariable controllers of arbitrary structure and order. All known LTI AWBT schemes are shown to be special cases of this framework. This unification of existing AWBT schemes under a general framework is the main result of this chapter.

4.1 Introduction

In Chapter 2 we reviewed a number of existing AWBT compensation techniques, and in Chapter 3 we discussed a particular AWBT implementation applicable to controllers implemented in the IMC framework. From both these chapters, we can summarize the existing approaches to solving the problem of control of LTI systems subject to control input nonlinearities as follows:
Design first the linear controller ignoring control input nonlinearities and then add anti-windup bumpless transfer (AWBT) compensation to minimize the adverse effects of any control input nonlinearities on closed loop performance.

While many of these schemes have been successful (at least in specific SISO situations), they are by and large intuition based and have little theoretical foundation. Specifically:

- no attempt has been made to formalize these techniques and advance a general AWBT analysis and synthesis theory;
- with the exception of a few ([43, 58, 59]), no rigorous stability analyses have been reported for anti-windup schemes in a general setting;
- the issue of robustness has been largely ignored (notable exceptions are [27, 28]);
- extension to the MIMO case has not been attempted in its entirety. As pointed out by Doyle *et al.* (1987) [43], for MIMO controllers, the saturation may cause a change in the direction of the plant input resulting in disastrous consequences;
- a major void in the existing AWBT literature is a clear exposition of the objectives (and associated engineering trade-offs) which lead to a graceful performance degradation in any reasonably general setting.

The focus of this chapter is on setting up a general framework for studying anti-windup and bumpless transfer designs. In keeping with the philosophy adopted by most of the techniques summarized in the preceding chapters, we will seek *linear* AWBT compensation for actuator nonlinearities. In particular, we will show that the generality of the framework allows unification of existing AWBT schemes as special cases of the AWBT controller parameterization introduced.

4.2 A General AWBT Framework

In the following sub-sections, the AWBT problem is formulated, the AWBT design criteria are discussed, certain admissibility criteria for AWBT are introduced and a parameterization of all admissible AWBT compensated controllers is presented. Wherever necessary, the assumptions underlying the development are clearly stated.

4.2.1 Problem Formulation

The problem that is being considered throughout the thesis can be understood with reference to Figure 4.1. In Figure 4.1, we have an idealized linear control problem

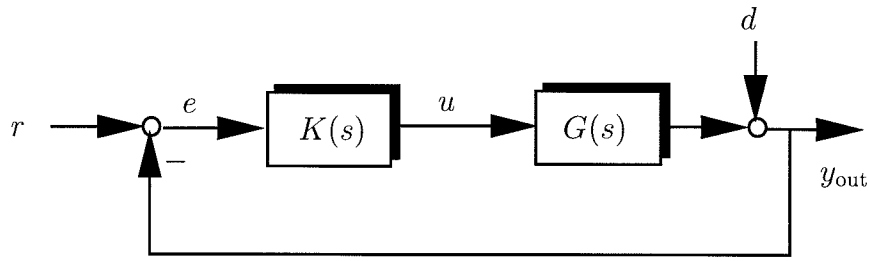

Figure 4.1: Ideal linear design–error feedback case.

where the linear plant model $G(s)$ is provided. An LTI controller $K(s)$ is designed to meet given performance specifications. These will typically be of the form, "Keep the output tracking error e small despite changes in command r and disturbance d." Alternatively, these could be specified more formally in terms of the $\mathcal{H}_2$ or $\mathcal{H}_\infty$ norm of the transfer function relating r to e.

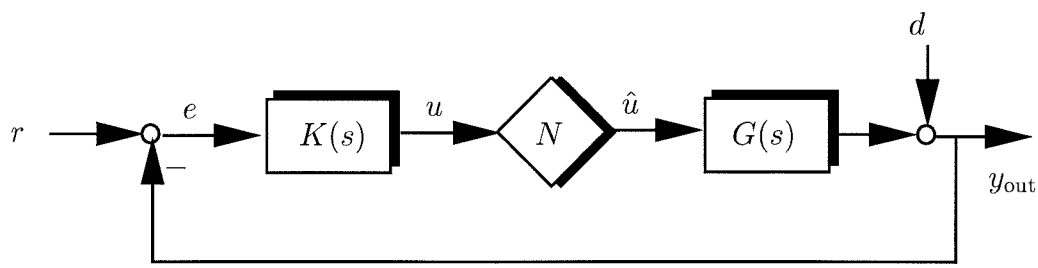

Figure 4.2: Ideal linear design with nonlinearity N–error feedback case.

As discussed in Chapter 1, due to limitations and/or substitutions, a nonlinearity N is introduced into the interconnection as shown in Figure 4.2. As a result, the actual plant input $\hat{u}$ will in general not be equal to the controller output u. This mismatch is the cause for controller windup, controller state initialization errors and a significant transient which must decay after the system returns to the linear regime. This is also the cause for degradation of performance and sometimes instability.

The AWBT problem involves the design of $\hat{K}(s)$ shown in Figure 4.3. The measured or estimated value of $\hat{u}$ provides information regarding the effect of the generic nonlinearity N and is fed back to the AWBT compensated controller $\hat{K}(s)$. The design criteria to be satisfied by $\hat{K}(s)$ are as follows:

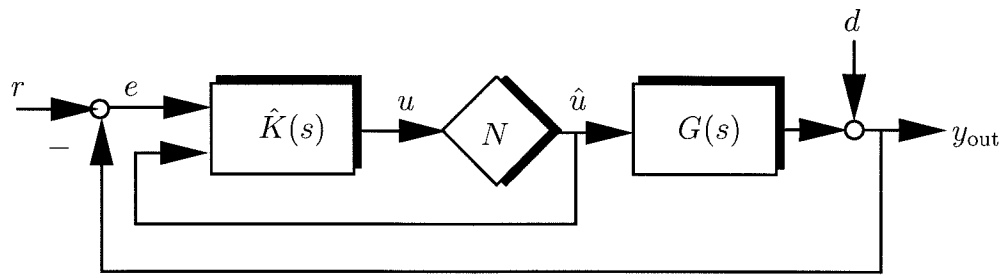

Figure 4.3: The AWBT problem–error feedback case.

1. The nonlinear closed loop system, Figure 4.3, must be stable.

2. When there are no limitations or substitutions, ($N \equiv I$), the closed loop performance of the system in Figure 4.3 should meet the specifications for the linear design in Figure 4.1. We call this the *linear performance recovery* requirement.

3. The closed loop performance of the system in Figure 4.3 should *degrade gracefully* from the linear performance of Figure 4.1 when limitations and/or substitutions occur ($N \not\equiv I$).

In order not to restrict attention to the error feedback case alone, we will consider the linear fractional transformation (LFT) shown in Figure 4.4(a) as the standard interconnection for the idealized linear design. The exogenous input w includes all signals which enter the system from its environment such as commands, disturbances and sensor noise. The input u represents the control effort applied to the plant by the controller $K(s)$. The interconnection outputs z and y_m represent the controlled output which the controller is designed to keep small (e.g., tracking error) and all measurements available to the controller (including commands, measured disturbances, measured plant inputs) respectively.

Any feed-forward/feedback interconnection of linear system elements can be brought into this general interconnection form. As an example, we consider the error feedback system of Figure 4.1. The exogenous inputs are the command r, and output disturbance d. Thus, we define $w = \begin{bmatrix} r \\ d \end{bmatrix}$. The controlled output is the tracking error,

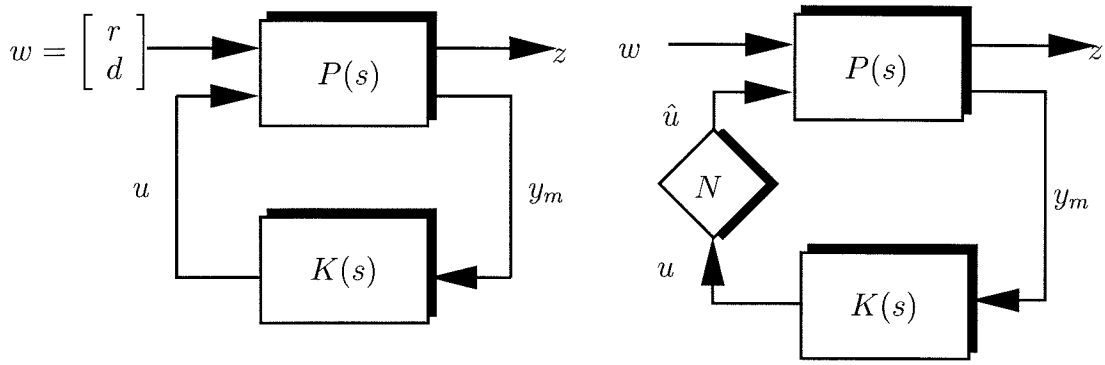

(a) without nonlinearity N (ideal case) (b) with nonlinearity N

Figure 4.4: Idealized linear design.

$e = r - y_{\text{out}}$, so we define $z = e$. The information made available to the controller, $K(s)$, is the tracking error, so $y_m = e$. The output of $K(s)$ is the plant input, u. With these definitions, the interconnection $P(s)$ is given by

$$P(s) = \begin{bmatrix} I & -I & -G(s) \\ I & -I & -G(s) \end{bmatrix}. \tag{4.1}$$

With these definitions, the input-output behavior from the exogenous input to the controlled output of the system in Figure 4.4(a) is equivalent to that in Figure 4.1.

$P(s)$ and $K(s)$ are assumed to be finite dimensional LTI systems whose state space realizations are assumed to be available. The closed loop transfer function from w to z in Figure 4.4(a) is denoted by $T_{zw}(s)$, and is given by the linear fractional transformation

$$T_{zw}(s) = P_{11} + P_{12}K(I - P_{22}K)^{-1}P_{21} \tag{4.2}$$

where

$$P(s) = \begin{bmatrix} P_{11} & P_{12} \\ P_{21} & P_{22} \end{bmatrix} \tag{4.3}$$

is partitioned according to its inputs and outputs. We assume that performance specifications are provided for the linear design and that the controller $K(s)$ meets these specifications in the absence of limitations and substitutions. For e.g., by including suitable weights in the interconnection $P(s)$, very general specification of the frequency domain characteristics of the closed loop transfer function can be specified and we assume that the linear controller is designed to meet them.

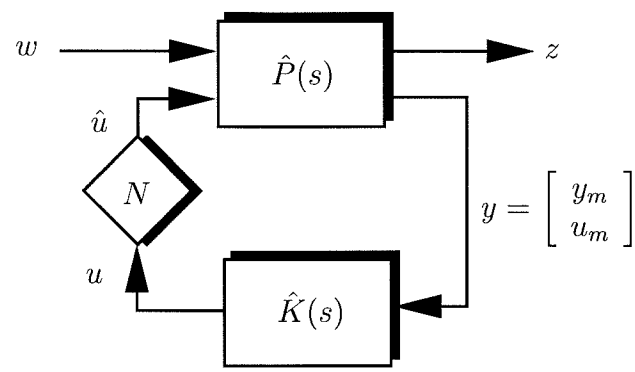

Figure 4.5: The general AWBT problem.

The general AWBT problem is based on Figure 4.5. The interconnection $\hat{P}$(s) is obtained from $P(s)$ by providing an additional output u_m. Thus,

$$\hat{P}(s) = \begin{bmatrix} P_{11} & P_{12} \\ P_{21} & P_{22} \\ P_{31} & P_{32} \end{bmatrix} \tag{4.4}$$

where

$$u_m = P_{31}w + P_{32}\hat{u}. \tag{4.5}$$

The new signal, u_m, is the measured or estimated value of the actual plant input $\hat{u}$. We allow the general relation (4.5) to account for measurement noise entering through w (i.e., $P_{31} \not\equiv 0$) and non-trivial measurement dynamics ($P_{32} \not\equiv I$). The situation where a perfect estimate of $\hat{u}$ is available corresponds to $P_{31} \equiv 0$, $P_{32} \equiv I$.

As in the error feedback example (Figure 4.3), the plant input estimate is made available to the controller $\hat{K}(s)$ as a component of the measurement vector y. Also included in Figure 4.5 is the input limitation/substitution mechanism, represented by the nonlinear block N.

Given this framework, the general AWBT problem amounts to the following: *Given the linear controller $K(s)$ which meets certain linear performance specifications, synthesize $\hat{K}(s)$ which renders the system in Figure 4.5 stable, meets our linear performance specifications when $N \equiv I$, and exhibits graceful performance degradation when $N \not\equiv I$.*

4.2.2 Decomposition of $\hat{K}$(s)

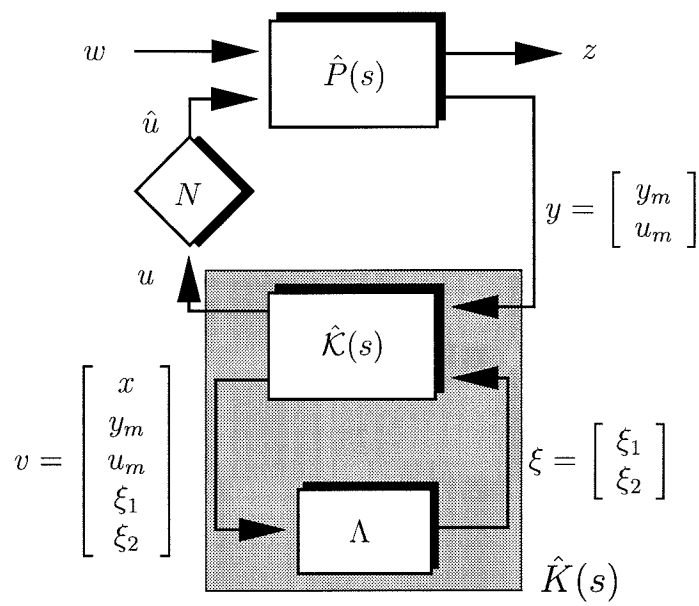

Figure 4.6: Decomposition of $\hat{K}(s)$.

Consider Figure 4.6 where we express $\hat{K}(s)$ as a feedback interconnection of an LTI block $\hat{\mathcal{K}}(s)$ and an AWBT operator Λ. This linear fractional feedback representation is quite general since at this point we allow Λ to be any, perhaps nonlinear relation. $\hat{\mathcal{K}}(s)$ contains the linear design $K(s)$.

The AWBT operator Λ uses information provided to it by $\hat{\mathcal{K}}(s)$ in the form of

the input v to generate an AWBT action denoted ξ which is fed back to $\hat{\mathcal{K}}(s)$. In order to maintain complete generality, we provide the AWBT operator, Λ, with full information in $\hat{\mathcal{K}}(s)$, including the state x of $\hat{\mathcal{K}}(s)$ and the input $\begin{bmatrix} y \\ \xi \end{bmatrix}$ to $\hat{\mathcal{K}}(s)$.

Partitioning the AWBT action as $\xi = \begin{bmatrix} \xi_1 \\ \xi_2 \end{bmatrix}$, we allow it to act on the state of $\hat{\mathcal{K}}(s)$ via ξ_1 and the output of $\hat{\mathcal{K}}(s)$ via ξ_2. This gives rise to the following realization of $\hat{\mathcal{K}}(s)$

$$\hat{\mathcal{K}}(s) = \left[\begin{array}{c|cccc} A & B & 0 & I & 0 \\ \hline C & D & 0 & 0 & I \\ I & 0 & 0 & 0 & 0 \\ 0 & I & 0 & 0 & 0 \\ 0 & 0 & I & 0 & 0 \\ 0 & 0 & 0 & I & 0 \\ 0 & 0 & 0 & 0 & I \end{array}\right] \quad \text{where} \quad K(s) = \left[\begin{array}{c|c} A & B \\ \hline C & D \end{array}\right] \quad \text{and} \quad v = \begin{bmatrix} x \\ y_m \\ u_m \\ \xi_1 \\ \xi_2 \end{bmatrix}. \tag{4.6}$$

Since the state and the input to $\hat{\mathcal{K}}(s)$ fully characterize its output, we say that Λ is provided with full information (FI). Similarly, Λ can drive both the state and the output of $\hat{\mathcal{K}}(s)$ and hence acts with full control (FC). Note that for $\Lambda = 0$, i.e., no corrective AWBT action, we have $\hat{K}(s) = \begin{bmatrix} K(s) & 0 \end{bmatrix}$ which is as expected since, in that case, we just have the original linear interconnection of Figure 4.4 but with the nonlinearity N between the output of the controller and the input to the plant.

4.2.3 Parameterization of Admissible $\hat{K}(s)$

We now impose two criteria for the admissibility of the AWBT operator Λ:

1. $\Lambda : v \to \xi$ is causal, linear, and time invariant.

2. $\forall\, t, u(t) - u_m(t) = 0 \Rightarrow \xi(t) = 0$.

The first condition ensures that the AWBT compensated controller $\hat{K}(s)$ can be realized as an LTI system. It turns out that most existing AWBT schemes satisfy this condition. Hence this condition, though restrictive, seems reasonable.

The second condition enforces the notion that we do not want the AWBT block Λ to affect the linear closed loop performance achieved by the idealized linear design $K(s)$ when there is no substitution or limitation. Strictly speaking, we would like to have $\xi(t) = 0$ whenever $u(t) - \hat{u}(t) = 0$. In general, since $\hat{u}$ is not available to Λ but only an estimate u_m is available, we cannot enforce the strict linear performance recovery requirement but instead choose to impose a more realistic but weaker condition based on the measurement u_m.

These two criteria imply that any admissible Λ must be memoryless and hence a constant matrix. The two criteria also imply that $\xi(t)$ must be linear in $u_m(t) - u(t)$. Thus,

$$\xi = \begin{bmatrix} \Lambda_1 \\ \Lambda_2 \end{bmatrix} (u_m - u) \tag{4.7}$$

$$= \begin{bmatrix} \Lambda_1 \\ \Lambda_2 \end{bmatrix} \begin{bmatrix} -C & -D & I & 0 & -I \end{bmatrix} v \tag{4.8}$$

$$= \Lambda v. \tag{4.9}$$

Incorporating the AWBT block, Λ, into $\hat{\mathcal{K}}$ we obtain the standard setup of Figure 4.5 with

$$\hat{K}(s) = [U(s) \quad I - V(s)] \tag{4.10}$$

$$\text{where } V(s) = \left[\begin{array}{c|c} A - H_1C & -H_1 \\ \hline H_2C & H_2 \end{array}\right] \tag{4.11}$$

$$U(s) = \left[\begin{array}{c|c} A - H_1C & B - H_1D \\ \hline H_2C & H_2D \end{array}\right] \tag{4.12}$$

$$H_1 = \Lambda_1(I + \Lambda_2)^{-1} \tag{4.13}$$

$$H_2 = (I + \Lambda_2)^{-1}. \tag{4.14}$$

A necessary condition for well-posedness of the AWBT feedback loop in Figure 4.6 is that $I + \Lambda_2$ must be nonsingular. Thus, H_2 must be invertible.

The blocks $U(s)$ and $V(s)$ which define the AWBT compensated controller $\hat{K}(s)$ correspond to left coprime factors of $K(s)$. It is easy to verify that

$$K(s) = V(s)^{-1}U(s) \tag{4.15}$$

for any H_1 and H_2 provided that H_2 is invertible.

If we assume that the realization of $K(s)$ is such that (C, A) is observable, then the eigenvalues of $A - H_1C$ may be arbitrarily assigned by the selection of H_1. Thus if the eigenvalues of $A - H_1C$ are chosen to be in the open left half plane, then $U(s)$, $V(s)$ and $\hat{K}(s)$ are stable. Since we will be interested in globally stable systems, we will restrict attention to the case where $\hat{P}(s)$, $U(s)$, $V(s)$ and $\hat{K}(s)$ are stable. This is because global stability of the closed loop with the actuator nonlinearity cannot be guaranteed if either $\hat{K}$ or $\hat{P}$ are unstable. For example, a mode switch from automatic to manual control will leave the loop open. If $\hat{K}$ or $\hat{P}$ are unstable, they will exhibit their unstable characteristics when the system is operating in open loop.

To demonstrate the implementation of the AWBT controller $\hat{K}(s)$, we consider the special case $P_{31} \equiv 0$, $P_{32} \equiv I$ which corresponds to $u_m \equiv \hat{u}$. The input to $\hat{K}$ is

$\begin{bmatrix} y_m \\ \hat{u} \end{bmatrix}$. Since $\hat{K}(s) = \begin{bmatrix} U(s) & I - V(s) \end{bmatrix}$, we have

$$u = U(s)y_m + (I - V(s))\hat{u}. \tag{4.16}$$

This implementation is shown in Figure 4.7. Obviously, when $N \equiv I$, we have $\hat{u} \equiv u$

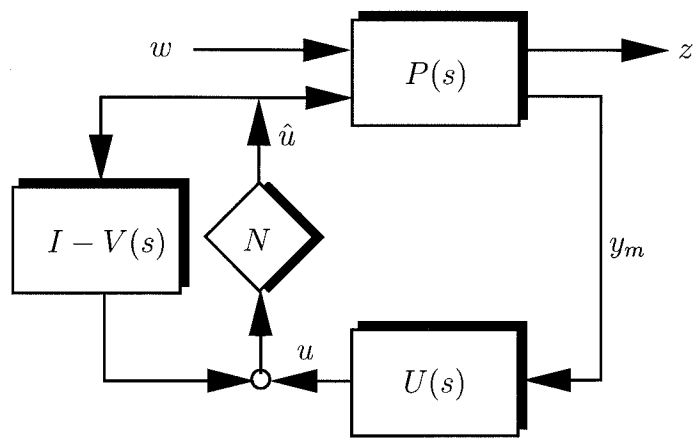

Figure 4.7: AWBT implementation with perfect measurement of $\hat{u}$.

and then, from (4.16), we have

$$\begin{aligned} u &= U(s)y_m + (I - V(s))u \\ \Rightarrow V(s)u &= U(s)y_m \\ \Rightarrow u &= V(s)^{-1}U(s)y_m \\ &= K(s)y_m. \end{aligned}$$

Thus, in this case, when $N \equiv I$, the ideal linear design is recovered exactly.

In general, however, the AWBT implementation is not equivalent to the idealized linear design, even when there are no limitations and substitutions, since $P_{31} \not\equiv 0$ and $P_{32} \not\equiv I$. To see this, we evaluate $T_{zw}(s)$ for the system in Figure 4.4 with $N \equiv I$.

$$T_{zw}(s) = P_{11} + P_{12}[I - UP_{22} - (I - V)P_{32}]^{-1}[UP_{21} + (I - V)P_{31}]. \tag{4.17}$$

Thus, performance is clearly different from the idealized linear design for which $T_{zw}(s)$ is given by (4.2)

$$\begin{aligned} T_{zw}(s) = &\ P_{11} + P_{12}K(I - P_{22}K)^{-1}P_{21} \qquad (4.2') \\ = &\ P_{11} + P_{12}(V - UP_{22})^{-1}UP_{21}. \end{aligned}$$

Of course, the two transfer functions are identical if $P_{31} \equiv 0$ and $P_{32} \equiv I$ as can be seen from (4.17) and (4.2).

4.3 Special Cases of the General Framework

In the preceding section, a fairly general and abstract framework and AWBT compensation scheme was developed. The AWBT compensated controller $\hat{K}(s)$ was decomposed into an LTI block $\hat{\mathcal{K}}(s)$ and an AWBT operator Λ. Based on certain admissibility criteria for Λ, it was shown that the only allowable Λ are constant matrices. This allowed us to parameterize all admissible AWBT compensated controllers $\hat{K}(s)$ in terms of stable left coprime factors of the initial linear controller $K(s)$. It was shown that the free parameters in the design of $\hat{K}(s)$ are two constant matrices H_1 and H_2, with the restriction that H_2 be invertible.

We will now show that the AWBT schemes which we discussed in Chapters 2 and 3 are all special cases of the framework and compensation scheme developed in the preceding section. This will enable us to unify all known (somewhat ad-hoc and problem-specific) linear AWBT compensation schemes under a general framework.

4.3.1 Anti-Reset Windup

Referring back to §2.2, consider the PI controller as shown in Figure 2.1,

$$K(s) = k(1 + \frac{1}{\tau_I s}) \qquad (2.1')$$

$$= \left[\begin{array}{c|c} 0 & \frac{k}{\tau_I} \\ \hline 1 & k \end{array}\right] \qquad (2.2')$$

whose output is given by

$$u = k(e + \frac{1}{\tau_I}\int_0^t e\ dt) \tag{2.3'}$$

$$\hat{u} = \text{sat}(u)$$

$$= \begin{cases} u_{\min} & \text{if } u < u_{\min} \\ u & \text{if } u_{\min} \le u \le u_{\max} \\ u_{\max} & \text{if } u > u_{\max} \end{cases} \tag{2.5'}$$

$$e = r - y_{\text{out}}.$$

In §2.2, we derived the controller equations modified to achieve anti-reset windup compensation based on Figure 2.2 as follows:

$$u = k\left[e + \frac{1}{\tau_I}\int_0^t \left(e - \frac{\tau_I}{k\tau_r}(u - \hat{u})\right)\ dt\right] \tag{2.7'}$$

$$\hat{u} = \text{sat}(u) \tag{2.8'}$$

$$e = r - y_{out}. \tag{2.9'}$$

Rewriting (2.7) in the Laplace domain,

$$u = \frac{k\tau_r(1 + \tau_I s)}{\tau_I(1 + \tau_r s)}e + \frac{1}{\tau_r s + 1}\hat{u}.$$

It is easy to verify that in the general framework of Figure 4.5, this corresponds to

$$w = \begin{bmatrix} r \\ d \end{bmatrix}, \quad y = \begin{bmatrix} e \\ \hat{u} \end{bmatrix}, \quad z = e$$

$$\hat{K}(s) = \begin{bmatrix} \frac{k\tau_r(1+\tau_I s)}{\tau_I(1+\tau_r s)} & \frac{1}{\tau_r s+1} \end{bmatrix}$$

$$\hat{P}(s) = \begin{bmatrix} I & -I & -G(s) \\ I & -I & -G(s) \\ 0 & 0 & I \end{bmatrix}.$$

A realization of the anti-reset windup compensator $\hat{K}(s)$ is given by

$$\hat{K}(s) = \left[\begin{array}{c|cc} -\frac{1}{\tau_r} & \frac{k}{\tau_I \tau_r}(\tau_r - \tau_I) & \frac{1}{\tau_r} \\ \hline 1 & k & 0 \end{array}\right]. \tag{4.18}$$

Comparing (4.18) with (4.10), (4.11), (4.12), we see that the anti-reset windup implementation corresponds to the choices

$$H_1 = \frac{1}{\tau_r} \tag{4.19}$$

$$H_2 = 1 \tag{4.20}$$

in the general framework of §4.2, Figure 4.5.

In §2.2, we also discussed an alternate anti-reset windup implementation (Figure 2.3). For this implementation, the control signal (in Laplace domain), modified for anti-reset windup, was given by

$$u = ke + \frac{1}{1+\tau_I s}\hat{u}. \tag{2.12'}$$

In the general framework of §4.2, Figure 4.5, this corresponds to

$$w = \begin{bmatrix} r \\ d \end{bmatrix}, \quad y = \begin{bmatrix} e \\ \hat{u} \end{bmatrix}, \quad z = e$$

$$\hat{K}(s) = \begin{bmatrix} k & \frac{1}{1+\tau_I s} \end{bmatrix} = \left[\begin{array}{c|cc} -\frac{1}{\tau_I} & 0 & \frac{1}{\tau_I} \\ \hline 1 & k & 0 \end{array}\right] \tag{4.21}$$

which is easily recognized as a special case of (4.18) for $\tau_r = \tau_I$. Thus, these seemingly different anti-reset windup schemes for PI controllers are identical for the well known heuristic choice of $\tau_r = \tau_I$. We may also note that this implementation of anti-reset windup is in the exact form shown in Figure 4.7.

4.3.2 Conventional Anti-Windup (CAW)

The implementation of the high gain conventional anti-windup (CAW) scheme is shown in Figure 2.5. The AWBT compensation is provided by feeding the difference $\hat{u} - u$ through a high gain matrix X to the controller input e. Typically, $X = \alpha I$, where $\alpha >> 1$ is a scalar. Given the original linear controller $K(s)$ with state x

$$K(s) = \left[\begin{array}{c|c} A & B \\ \hline C & D \end{array}\right]$$

we derived the modified controller equations in §2.4 based on Figure 2.5 as follows:

$$\dot{x} = (A - BX(I + DX)^{-1}C)x + B(I + XD)^{-1}e + BX(I + DX)^{-1}\hat{u} \tag{2.19'}$$

$$u = (I + DX)^{-1}Cx + (I + DX)^{-1}De + (I + DX)^{-1}DX\hat{u}. \tag{2.16'}$$

In the general framework of §4.2, Figure 4.5, this implementation corresponds to

$$w = \begin{bmatrix} r \\ d \end{bmatrix}, \quad y = \begin{bmatrix} e \\ \hat{u} \end{bmatrix}, \quad z = e$$

$$\hat{P}(s) = \begin{bmatrix} I & -I & -G(s) \\ I & -I & -G(s) \\ 0 & 0 & I \end{bmatrix} \tag{4.22}$$

$$\hat{K}(s) = \left[\begin{array}{c|cc} A - BX(I + DX)^{-1}C & B(I + XD)^{-1} & BX(I + DX)^{-1} \\ \hline (I + DX)^{-1}C & (I + DX)^{-1}D & (I + DX)^{-1}DX \end{array}\right] \tag{4.23}$$

Comparing the realization of $\hat{K}(s)$ with (4.10), (4.11), (4.12), we see that CAW corresponds to

$$H_1 = BX(I + DX)^{-1} \tag{4.24}$$

$$H_2 = (I + DX)^{-1} \tag{4.25}$$

in the general framework of §4.2, Figure 4.5.

4.3.3 Hanus' Conditioned Controller

Consider a simple error feedback controller as shown in Figure 4.2, with the nonlinearity N being a saturating actuator. For a given linear controller

$$K(s) = \left[\begin{array}{c|c} A & B \\ \hline C & D \end{array}\right],$$

we derived, in §2.5, the equations for the AWBT controller, modified using Hanus' conditioning technique. These equations are given by:

$$\dot{x} = (A - BD^{-1}C)x + BD^{-1}\hat{u} \tag{2.28'}$$

$$u = Cx + D(r - y_{out}) \tag{2.29'}$$

$$\hat{u} = \text{sat}(u). \tag{2.30'}$$

This is the AWBT "conditioned controlled." In the general framework of §4.2, Figure 4.5, we have

$$w = \begin{bmatrix} r \\ d \end{bmatrix}, \quad z = r - y_{out}, \quad y = \begin{bmatrix} r - y_{out} \\ \hat{u} \end{bmatrix}.$$

A state space realization of the AWBT controller based on the conditioned controller from equations (2.28), (2.29) is given by

$$\hat{K}(s) = \left[\begin{array}{c|cc} A - BD^{-1}C & 0 & BD^{-1} \\ \hline C & D & 0 \end{array}\right]. \tag{4.26}$$

Comparing (4.26) with (4.10), (4.11), (4.12), we see that the Hanus conditioned controller corresponds to

$$H_1 = BD^{-1} \tag{4.27}$$

$$H_2 = I \tag{4.28}$$

in the general framework of §4.2, Figure 4.5.

4.3.4 Generalized Conditioning Technique (GCT)

In §2.6, we summarized several drawbacks of the conditioning scheme discussed in the previous section. We also discussed two extensions to the conditioning technique to resolve these deficiencies.

The first approach [131, section 4] results in the following modified conditioned controller, similar in spirit to the Hanus' conditioned controller discussed in the previous section:

$$\dot{x} = [A - B(D + \rho I)^{-1}C]x + B\rho(D + \rho I)^{-1}(r - y_{out}) + B(D + \rho I)^{-1}\hat{u} \tag{2.32'}$$

$$u = Cx + D(r - y_{out}). \tag{2.33'}$$

This is the modified conditioned controller of Walgama *et al.* [131] and corresponds to

$$\hat{K}(s) = \left[\begin{array}{c|cc} A - B(D + \rho I)^{-1}C & B\rho(D + \rho I)^{-1} & B(D + \rho I)^{-1} \\ \hline C & D & 0 \end{array}\right] \tag{4.29}$$

$$H_1 = B(D + \rho I)^{-1} \tag{4.30}$$

$$H_2 = I \tag{4.31}$$

in the general framework of §4.2, Figure 4.5.

A second more general modification is presented in [131, section 5] where conditioning is performed on a filtered set-point signal r_f instead of the direct set-point r. We have already described this approach in §2.6.

The conditioned control action and the AWBT controller corresponding to this

modification are given respectively by

$$u = \hat{K} \begin{bmatrix} r \\ y_{out} \\ \hat{u} \end{bmatrix} \tag{2.46'}$$

where

$$\hat{K}(s) = \left[\begin{array}{cc|ccc} A & 0 & B_1 & B_2 & 0 \\ -B_f D_f^{-1} C & A_f - B_f D_f^{-1} C_f & -B_f D_f^{-1} D_1 & -B_f D_f^{-1} D_2 & B_f D_f^{-1} \\ \hline C & C_f & D_1 & D_2 & 0 \end{array}\right]. \tag{2.47'}$$

Writing $K(s)$ as

$$K(s) = \left[\begin{array}{c|cc} A & B_1 & B_2 \\ \hline C & D_1 & D_2 \end{array}\right] = \left[\begin{array}{cc|cc} A & 0 & B_1 & B_2 \\ 0 & A_f & 0 & 0 \\ \hline C & C_f & D_1 & D_2 \end{array}\right] \tag{4.32}$$

and comparing equation (2.47) with equations (4.10), (4.11), (4.12), we see that GCT corresponds to

$$H_1 = \begin{bmatrix} 0 \\ B_f D_f^{-1} \end{bmatrix} \tag{4.33}$$

$$H_2 = I \tag{4.34}$$

in the general framework of §4.2, Figure 4.5. Note that we have introduced stable, uncontrollable modes of F in the realization of K.

It should be pointed out here that GCT is a special case of our framework only when we augment the linear controller with the dynamics of the filter F. This means that the AWBT scheme represented by GCT is determined not only by the choices of H_1 and H_2, but also by the dynamics of the filter F which must be introduced into the linear controller.

4.3.5 Observer-Based Anti-Windup

In §2.7, we discussed that an interpretation of the windup problem is that the states of the controller do not correspond to the control signal being fed to the plant. To obtain correct state estimates and to avoid windup, Åström *et al.* [5, 6] suggest that an observer be introduced into the controller.

For a linear controller $K(s)$ defined by the equations

$$\dot{x} = Ax + By_m \tag{2.48'}$$

$$u = Cx + Dy_m \tag{2.49'}$$

we derived, in §2.7, the observer-based anti-windup modification of Åström *et al.* [5, 6] as follows:

$$\dot{x} = Ax + By_m + L(\hat{u} - Cx - Dy_m) \tag{2.51'}$$

$$u = Cx + Dy_m \tag{2.52'}$$

$$\hat{u} = N(u).$$

In the general framework of §4.2, Figure 4.5, a realization for the AWBT compensator described by (2.51), (2.52) is given by

$$\hat{K}(s) = \left[\begin{array}{c|cc} A - LC & B - LD & L \\ \hline C & D & 0 \end{array}\right]. \tag{4.35}$$

Comparing (4.35) with (4.10), (4.11), (4.12), we see that the observer-based AWBT scheme corresponds to

$$H_1 = L, \quad H_2 = I \tag{4.36}$$

in the general framework of §4.2, Figure 4.5.

4.3.6 Internal Model Control (IMC)

Figure 2.7 shows the IMC structure with an actuator nonlinearity. In §2.8, we showed that if the controller is implemented in the IMC configuration, actuator constraints do not cause any stability problems provided the constrained control signal is sent to both the plant and the model. We also showed, under the assumption that there is no plant-model mismatch ($G = \tilde{G}$), that the IMC structure remains effectively open loop and stability is guaranteed by the stability of the plant (G) and the IMC controller (Q).

For the sake of generality, we will discuss the two degree of freedom IMC implementation shown in Figure 2.8. In our general framework, the idealized linear design of §4.2, Figure 4.4, corresponding to the two degree of freedom IMC implementation is given by

$$w = \begin{bmatrix} r \\ d \end{bmatrix}, \quad z = r - y_{out}, \quad y_m = \begin{bmatrix} r \\ y_{out} \end{bmatrix}$$

$$P(s) = \begin{bmatrix} I & -I & -G(s) \\ I & 0 & 0 \\ 0 & I & G(s) \end{bmatrix} \tag{4.37}$$

$$K(s) = \begin{bmatrix} (I - Q_2\tilde{G})^{-1}Q_1 & -(I - Q_2\tilde{G})^{-1}Q_2 \end{bmatrix}. \tag{4.38}$$

In the presence of saturation, the control signal is given by (see Figure 2.8)

$$u = Q_1 r - Q_2 y_{out} + Q_2 \tilde{G} \hat{u}. \tag{4.39}$$

Thus, the two degree of freedom IMC implementation, considered as an AWBT compensation in our general framework of §4.2, Figure 4.5, corresponds to

$$w = \begin{bmatrix} r \\ d \end{bmatrix}, \quad z = r - y_{out}, \quad y = \begin{bmatrix} r \\ y_{out} \\ \hat{u} \end{bmatrix}$$

$$\hat{P}(s) = \begin{bmatrix} I & -I & -G(s) \\ I & 0 & 0 \\ 0 & I & G(s) \\ 0 & 0 & I \end{bmatrix} \tag{4.40}$$

$$\hat{K}(s) = \begin{bmatrix} Q_1 & -Q_2 & Q_2\tilde{G} \end{bmatrix}. \tag{4.41}$$

We use the following state space realizations for $\tilde{G}(s)$, $Q_1(s)$ and $Q_2(s)$.

$$Q_1(s) = \left[\begin{array}{c|c} A_1 & B_1 \\ \hline C_1 & D_1 \end{array}\right], \quad Q_2(s) = \left[\begin{array}{c|c} A_2 & B_2 \\ \hline C_2 & D_2 \end{array}\right], \quad \tilde{G}(s) = \left[\begin{array}{c|c} A_G & B_G \\ \hline C_G & D_G \end{array}\right]. \tag{4.42}$$

For simplicity, we assume $D_G = 0$, although the case $D_G \neq 0$ can also be considered but the algebra is messy. We obtain the following realizations for $K(s)$ and $\hat{K}(s)$ from (4.38), (4.41):

$$K(s) = \left[\begin{array}{ccc|cc} A_1 & 0 & 0 & B_1 & 0 \\ 0 & A_2 & B_2C_G & 0 & -B_2 \\ B_GC_1 & B_GC_2 & A_G + B_GD_2C_G & B_GD_1 & -B_GD_2 \\ \hline C_1 & C_2 & D_2C_G & D_1 & -D_2 \end{array}\right] \tag{4.43}$$

$$\hat{K}(s) = \left[\begin{array}{ccc|ccc} A_1 & 0 & 0 & B_1 & 0 & 0 \\ 0 & A_2 & B_2C_G & 0 & -B_2 & 0 \\ 0 & 0 & A_G & 0 & 0 & B_G \\ \hline C_1 & C_2 & D_2C_G & D_1 & -D_2 & 0 \end{array}\right]. \tag{4.44}$$

Comparing (4.43), (4.44) with (4.10), (4.11), (4.12), we see that the two-degree of freedom IMC implementation of $K(s)$ corresponds to

$$H_1 = \begin{bmatrix} 0 \\ 0 \\ B_G \end{bmatrix} \tag{4.45}$$

$$H_2 = I \tag{4.46}$$

in the general framework of §4.2, Figure 4.5.

4.3.7 Anti-Windup Design for IMC

In Chapter 3, we described a modified IMC structure for optimizing performance in the face of saturation. In this strategy, the IMC controller $Q(s)$ is factorized as

$$Q(s) = [I + Q_2(s)]^{-1} Q_1(s) \tag{4.47}$$

and implemented as shown in Figure 3.2. Possible choices of $Q_1(s)$ and $Q_2(s)$ were also discussed in Chapter 3.2, based on a filter parameter $f(s)$. A similar factorization for $Q(s)$ has also been reported by Goodwin *et al.* (1993) [60] but with an interpretation which is different from that reported in Chapter 3. We will only consider $Q_1(s)$ and $Q_2(s)$ as stable transfer functions without going into details of their specific choices.

Let us introduce state space realizations for $Q_1(s)$, $Q_2(s)$ and $G(s) = \tilde{G}(s)$ as follows:

$$Q_1(s) = \left[\begin{array}{c|c} A_1 & B_1 \\ \hline C_1 & D_1 \end{array}\right] \tag{4.48}$$

$$Q_2(s) = \left[\begin{array}{c|c} A_2 & B_2 \\ \hline C_2 & D_2 \end{array}\right] \tag{4.49}$$

$$\tilde{G}(s) = \left[\begin{array}{c|c} A_G & B_G \\ \hline C_G & D_G \end{array}\right]. \tag{4.50}$$

In order to simplify the algebra, we assume that $Q_2(s)$ and $G(s)$ are strictly proper, i.e., $D_2 = 0$, $D_G = 0$. The more general case where $Q_2(s)$ and $G(s)$ are not strictly proper can also be worked out, but the algebra is messy and as such does not give any additional insight into the results. Then, in terms of these realizations, the realizations of $Q(s)$ and the linear controller $K(s)$ corresponding to the IMC controller $Q(s)$ are

given below:

$$Q(s) = [I + Q_2(s)]^{-1} Q_1(s) \tag{4.51}$$

$$= \left[\begin{array}{cc|c} A_1 & 0 & B_1 \\ B_2C_1 & A_2 - B_2C_2 & B_2D_1 \\ \hline C_1 & -C_2 & D_1 \end{array}\right] \tag{4.52}$$

$$K(s) = [I - Q(s)\tilde{G}(s)]^{-1} Q(s) \tag{4.53}$$

$$= \left[\begin{array}{ccc|c} A_1 & 0 & B_1C_G & B_1 \\ B_2C_1 & A_2 - B_2C_2 & B_2D_1C_G & B_2D_1 \\ B_GC_1 & -B_GC_2 & A_G + B_GD_1C_G & B_GD_1 \\ \hline C_1 & -C_2 & D_1C_G & D_1 \end{array}\right]. \tag{4.54}$$

Referring to Figure 3.2, the control signal u is given by

$$u = Q_1[r - (y_{out} - \tilde{G}\hat{u})] - Q_2\hat{u} \tag{4.55}$$

$$= Q_1(r - y_{out}) + (Q_1\tilde{G} - Q_2)\hat{u}. \tag{4.56}$$

In the general framework of §4.2, Figure 4.5, this modified IMC implementation corresponds to

$$w = \begin{bmatrix} r \\ d \end{bmatrix}, \quad y = \begin{bmatrix} r - y_{out} \\ \hat{u} \end{bmatrix}, \quad z = r - y_{out}$$

$$\hat{P}(s) = \begin{bmatrix} I & -I & -\tilde{G}(s) \\ I & -I & -\tilde{G}(s) \\ 0 & 0 & I \end{bmatrix} \tag{4.57}$$

$$\hat{K}(s) = \begin{bmatrix} Q_1(s) & Q_1(s)\tilde{G}(s) - Q_2(s) \end{bmatrix}. \tag{4.58}$$

Comparing (4.58) with (4.10), (4.11), (4.12) we see that this implementation of IMC

corresponds to

$$U(s) = Q_1(s) = \left[\begin{array}{ccc|c} A_1 & 0 & B_1C_G & B_1 \\ 0 & A_2 & 0 & 0 \\ 0 & 0 & A_G & 0 \\ \hline C_1 & -C_2 & D_1C_G & D_1 \end{array}\right] \tag{4.59}$$

$$V(s) = I - Q_1(s)\tilde{G}(s) + Q_2(s) \tag{4.60}$$

$$= \left[\begin{array}{ccc|c} A_1 & 0 & B_1C_G & 0 \\ 0 & A_2 & 0 & -B_2 \\ 0 & 0 & A_G & -B_G \\ \hline C_1 & -C_2 & D_1C_G & I \end{array}\right]. \tag{4.61}$$

Note that we have introduced stable uncontrollable modes of $\tilde{G}(s)$ in the realization of $U(s)$. The corresponding values of H_1 and H_2 are given by

$$H_1 = \left[\begin{array}{c} 0 \\ B_2 \\ B_G \end{array}\right] \tag{4.62}$$

$$H_2 = I. \tag{4.63}$$

4.3.8 The Extended Kalman Filter

The last scheme from Chapter 2 we consider here is an AWBT implementation applicable to observer-based compensators. This implementation is developed to maintain valid state estimates in the observer independent of any nonlinearities between the controller output and the plant input.

Consider the idealized linear design of Figure 4.4 with $w = \left[\begin{array}{c} r \\ d \end{array}\right]$, $y_m = \left[\begin{array}{c} r \\ y_1 \end{array}\right]$.

The plant $P(s)$ (Figure 4.4) with the state x is described by the state-space equations

$$\dot{x} = Ax + B_1 r + B_2 d + B_3 u \tag{2.56'}$$

$$z = C_1 x + D_{11} r + D_{12} d + D_{13} u \tag{2.57'}$$

$$y_1 = C_3 x + D_{31} r + D_{32} d, \tag{2.58'}$$

i.e.,

$$P(s) = \left[\begin{array}{c|ccc} A & B_1 & B_2 & B_3 \\ \hline C_1 & D_{11} & D_{12} & D_{13} \\ 0 & I & 0 & 0 \\ C_3 & D_{31} & D_{32} & 0 \end{array}\right]. \tag{2.59'}$$

Let $K(s)$ be the standard observer/state-feedback controller with state $\hat{x}$, whose state-space equations can be described by

$$\dot{\hat{x}} = A\hat{x} + B_1 r + B_3 u + L(y_1 - C_3 \hat{x} - D_{31} r) \tag{2.60'}$$

$$u = -F\hat{x}, \tag{2.61'}$$

i.e.,

$$K(s) = \left[\begin{array}{c|cc} A - B_3 F - LC_3 & B_1 - LD_{31} & L \\ \hline -F & 0 & 0 \end{array}\right] \tag{2.62'}$$

where L is the observer gain and F is the state feedback gain.

As discussed in §2.9, to provide anti-windup compensation, the observer equations must be modified so that the state estimator is based on the actual input $\hat{u}$ to the

plant. Thus, the modified observer/state-feedback compensator is given by

$$\dot{\hat{x}} = A\hat{x} + B_1 r + B_3\hat{u} + L(y_1 - C_3\hat{x} - D_{31}r) \tag{2.65'}$$

$$= (A - LC_3)\hat{x} + (B_1 - LD_{31})r + B_3\hat{u} + Ly_1 \tag{2.66'}$$

$$u = -F\hat{x}. \tag{2.67'}$$

In the general framework of §4.2, Figure 4.5, this AWBT compensated controller corresponds to

$$w = \begin{bmatrix} r \\ d \end{bmatrix}, \quad y = \begin{bmatrix} y_m \\ \hat{u} \end{bmatrix},$$

$$\hat{P}(s) = \left[\begin{array}{c|ccc} A & B_1 & B_2 & B_3 \\ \hline C_1 & D_{11} & D_{12} & D_{13} \\ 0 & I & 0 & 0 \\ C_3 & D_{31} & D_{32} & 0 \\ 0 & 0 & 0 & I \end{array}\right] \tag{4.64}$$

$$\hat{K}(s) = \left[\begin{array}{c|ccc} A - LC_3 & B_1 - LD_{31} & L & B_3 \\ \hline -F & 0 & 0 & 0 \end{array}\right] \tag{4.65}$$

$$H_1 = B_3 \tag{4.66}$$

$$H_2 = I. \tag{4.67}$$

4.4 Conclusions

In this chapter, we developed a general theoretical framework for studying AWBT control systems. The generality of the framework allowed us to consider any control system structure, including feed-forward, feedback, multiple degree of freedom, cascade and general non-square controller designs.

The theoretical development was based on the following two-step design paradigm "*Design the linear controller ignoring control input nonlinearities and then add AWBT*

compensation to minimize the adverse effects of any control input nonlinearities on closed loop performance."

This is characteristic of most AWBT schemes reported in the literature. A parameterization of all admissible AWBT compensated controllers was presented in terms of two constant matrices H_1 and H_2. This parameterization allowed us to unify all known LTI anti-windup and/or bumpless transfer schemes under a general framework. Table 4.1 summarizes the AWBT schemes which can be generalized.

Parameters	H_1	H_2
Anti-reset windup	$\frac{1}{\tau_r}$	1
Hanus conditioned controller	BD^{-1}	I
Observer-based anti-windup	L	I
Conventional anti-windup	$\alpha B(I+\alpha D)^{-1}$	$(I+\alpha D)^{-1}$
Internal Model Control (IMC)	$\begin{bmatrix} 0 & B_p^T \end{bmatrix}^T$	I
Anti-windup IMC	$\begin{bmatrix} 0 & B_2^T & B_p^T \end{bmatrix}^T$	I
Extended Kalman filter	B_p	I
Generalized Conditioning-I	$B(D+\rho I)^{-1}$	I
Generalized Conditioning-II	$\begin{bmatrix} 0 & D_f^{-T}B_f^T \end{bmatrix}^T$	I

Table 4.1: Special cases of the general framework.

We would like to comment that attempts to unify AWBT schemes have been reported in the past. Notable is the successful attempt by Walgama and Sternby (1990) [132] to identify the inherent observer property in a class of anti-windup compensators and to unify several schemes based on this observer property. Thus, unification of these schemes is in terms of a *single* parameter, the observer gain. However, no such observer property can be identified in the conventional anti-windup (CAW) scheme discussed in §2.4 when the original linear controller $K(s)$ is not strictly proper. The parameterization we present is in terms of *two* constant matrices, H_1 and H_2. This additional degree of freedom allows us to overcome the shortcoming in the observer-based unification. Thus, as shown in §4.3.2, CAW is a special case of our scheme.

Needless to say, the aim behind our development was primarily to develop a truly general theoretical framework for AWBT controller designs. The resulting AWBT

compensation scheme that we have presented and its interpretation are completely different from those reported in the literature. Specifically, the axioms and assumptions leading to our development are novel insofar as the AWBT literature is concerned. Moreover, our framework now allows us to compare and contrast various existing AWBT schemes. Thus, for example, the two seemingly different anti-reset windup strategies discussed in §2.2 and §4.3.1 can now be seen to be identical if $\tau_r = \tau_I$.

In summary, our parameterization of admissible AWBT compensators in terms of H_1 and H_2 allowed us to unify all known LTI AWBT schemes. Thus, rather than employing the older ad-hoc and problem-specific methodologies for AWBT compensation, we can now embark on the development of systematic procedures for choosing H_1 and H_2 for the synthesis of the AWBT compensator $\hat{K}(s)$. For this purpose, quantitative design criteria for AWBT must be defined. An intrinsic part of this step is the complete analysis of systems subject to control input nonlinearities. Detailed study of the AWBT analysis theory will be the focus of Chapter 6.

Chapter 5 Linear Matrix Inequalities

Abstract

In this chapter, we give a very brief overview of the basic technical machinery related to linear matrix inequalities (LMIs) and some optimization problems based on LMIs. In particular, we summarize a number of technical terms and results which will be used in the rest of the thesis. The emphasis is on only those aspects of LMI-based optimization which are relevant to this thesis. A detailed discussion of the vast literature on LMIs and problems that can be solved using LMIs is far beyond the scope of this thesis and can be found in the monograph by Boyd *et al.* [21].

5.1 Introduction

Definition 5.1 *A linear matrix inequality is a matrix inequality of the form*

$$F(x) \;=\; F_0 + \sum_{i=1}^{l} x_i F_i > 0 \tag{5.1}$$

where $x = [x_1 \; x_2 \; \ldots \; x_l]^T \in \Re^l$ *is the variable,* $F_i = F_i^T \in \Re^{n\times n}$ *are given matrices. The symbol* > 0 *means that* $F(x)$ *is positive definite, i.e.,* $u^T F(x) u > 0$ *for all non-zero* $u \in \Re^n$.

$F(x)$ is said to be affine in the decision variables $(x_1, x_2, \ldots, x_l)$. Strictly speaking, the inequality in (5.1) should therefore be referred to as an *Affine Matrix Inequality* (AMI). But the term LMI, originally coined by J. C. Willems, seems to be accepted terminology.

The LMI (5.1) is a convex constraint on x, i.e., the set $\{x \mid F(x) > 0\}$ is convex. Multiple LMIs $F^{(1)}(x) > 0, \ldots, F^{(p)}(x) > 0$ can be expressed as the single LMI

$$\mathrm{diag}(F^{(1)}(x) > 0, \ldots, F^{(p)}(x)) > 0.$$

Therefore we will make no distinction between a set of LMIs and a single LMI. When the matrices F_i are diagonal, the LMI $F(x) > 0$ is just a set of linear inequalities, thus generalizing the scalar inequalities encountered in linear or quadratic programming problems.

Matrix inequalities which are written as affine combinations of matrix variables $X_1, X_2, \ldots, X_K$ are also referred to as LMIs since these can be expressed in the form (5.1) in terms of the components of $X_1, X_2, \ldots, X_K$.

For example, consider the standard Lyapunov inequality

$$A^T P + PA < 0 \tag{5.2}$$

where $A \in \Re^{n \times n}$ is given and $P = P^T$ is the variable. For the sake of simplicity of exposition, consider the case where $A \in \Re^{2 \times 2}$. In this case, $P = P^T$ is of the form

$$P = \begin{bmatrix} x_1 & x_2 \\ x_2 & x_3 \end{bmatrix}.$$

In this case, defining

$$P_1 = \begin{bmatrix} 1 & 0 \\ 0 & 0 \end{bmatrix}, \; P_2 = \begin{bmatrix} 0 & 1 \\ 1 & 0 \end{bmatrix}, \; P_3 = \begin{bmatrix} 0 & 0 \\ 0 & 1 \end{bmatrix}$$

we can express (5.2) in the form

$$F(x) = F_1 x_1 + F_2 x_2 + F_3 x_3 > 0$$

where $F_i = -A^T P_i - P_i A, \quad i = 1, 2, 3$. However, in general, we will not write out the LMI explicitly in the form $F(x) > 0$, but instead make clear the fact that the variables are the matrices. In addition to making the notation more compact, this also leads to more efficient computing (see the discussion in [21]).

5.2 Standard LMI Problems

In this section, we list some common LMI-based problems.

5.2.1 LMI Feasibility Problems

Given an LMI $F(x) > 0$, the LMI feasibility problem is to find x_{feas} such that $F(x_{\text{feas}}) > 0$, or determine that no such x exists. For example, finding a $P = P^T > 0$ such that the Lyapunov inequality (5.2) is satisfied for a given A is a simple LMI feasibility problem.

5.2.2 Eigenvalue Problems

An eigenvalue problem (EVP) is an optimization of the following form:

$$\begin{aligned} &\min_{x,\lambda} && \lambda \\ &\text{subject to the LMI constraint} && A(x,\lambda) > 0. \end{aligned} \tag{5.3}$$

Here, $A(x, \lambda)$ is affine in (x, λ). This problem is also sometimes referred to as a "linear objective minimization subject to LMI constraints." It can be expressed equivalently in the following form:

$$\begin{aligned} &\text{minimize} && c^T x \\ &\text{subject to} && F(x) > 0. \end{aligned} \tag{5.4}$$

Here, F is a symmetric matrix that depends affinely on the optimization variable x, and c is a real vector of appropriate size. This is a convex non-smooth optimization problem. We will see examples of this problem in Chapter 8.

5.2.3 Generalized Eigenvalue Problems

A generalized eigenvalue problem (GEVP) is an optimization of the following form:

$$\begin{aligned} &\min_{x,\lambda} && \lambda \\ &\text{subject to the constraint} \\ &&& A(x,\lambda) \;>\; 0. \end{aligned}$$

Here, $A(x,\lambda)$ is affine in x for fixed λ and affine in λ for fixed x and satisfies the monotonicity condition $\lambda > \mu \Rightarrow A(x,\lambda) \geq A(x,\mu)$. This is a quasi-convex optimization problem since the objective is convex and the constraint is quasi-convex in the optimization variables (x,λ).

We refer the reader to Boyd *et al.* [21] for more details on these and other LMI-based optimization problems.

5.3 Some Standard Results

We will use the following result extensively throughout the thesis.

Lemma 5.1 (Schur Complements) *Let $Q(x) = Q(x)^T$, $R(x) = R(x)^T$, and $S(x)$ depend affinely on x. Then the LMI*

$$\begin{bmatrix} Q(x) & S(x) \\ S(x)^T & R(x) \end{bmatrix} > 0 \tag{5.5}$$

is equivalent to the matrix inequality

$$R(x) > 0,\; Q(x) - S(x)R(x)^{-1}S(x)^T > 0 \tag{5.6}$$

or equivalently,

$$Q(x) > 0,\; R(x) - S(x)^T Q(x)^{-1} S(x) > 0. \tag{5.7}$$

Proof. Follows trivially by applying the congruence transformation

$$\begin{bmatrix} I & -S(x)R(x)^{-1} \\ 0 & I \end{bmatrix}$$

to (5.5) to give (5.6), and by applying the congruence transformation

$$\begin{bmatrix} I & 0 \\ -S(x)^T Q(x)^{-1} & I \end{bmatrix}$$

to (5.5) to give (5.7). ■

Lemma 5.1 can be used to transform nonlinear convex inequalities to LMI form. For example, it is easy to verify that the well-known Ricatti inequality

$$A^T P + PA + PBR^{-1}B^T P + Q < 0$$

which is *quadratic* in the variable P can be expressed as the following equivalent *linear* matrix inequality in P by using Lemma 5.1.

$$\begin{bmatrix} -A^T P - PA - Q & PB \\ B^T P & R \end{bmatrix} > 0.$$

In Chapter 8, we will encounter the constraint that some quadratic function be negative whenever some other quadratic functions are negative. Such conditional constraints can be combined into a single, possibly conservative though often useful, condition by using the S-procedure which we discuss next.

Lemma 5.2 (S-procedure) *[21]*

(A) Let $T_0, T_1, \ldots, T_p \in \mathcal{R}^{q\times q}$ be symmetric matrices. Consider the following condition on $T_0, T_1, \ldots, T_p$:

$$z^T T_0 z \;\; > (\geq) \;\; 0 \text{ for all } 0 \neq z \in \mathcal{R}^q \text{ such that } z^T T_i z \geq 0, \;\; i = 1, 2, \ldots, p. \quad (5.8)$$

Condition (5.8) holds if $\exists\ \tau_1 \geq 0,\ \tau_2 \geq 0, \ldots, \tau_p \geq 0$ *such that*

$$T_0 - \sum_{i=1}^{p} \tau_i T_i \quad > (\geq) \quad 0.$$

(B) Let $F_0, F_1, \ldots, F_p$ *be quadratic functions of* $z \in \mathcal{R}^q$ *given by*

$$F_i(z) \quad = \quad z^T T_i z + 2u_i^T z + v_i, \quad \textit{where,} \quad T_i = T_i^T, \quad i = 0, 1, \ldots, p.$$

Consider the following condition on $F_0, F_1, \ldots, F_p$*:*

$$F_0(z) \quad > (\geq) \quad 0 \ \textit{for all}\ z \in \mathcal{R}^q \ \textit{such that}\ F_i(z) \geq 0,\ i = 1, 2, \ldots, p. \qquad (5.9)$$

Condition (5.9) holds if $\exists\ \tau_1 \geq 0,\ \tau_2 \geq 0, \ldots, \tau_p \geq 0$ *such that for all* $z \in \mathcal{R}^q$

$$F_0(z) - \sum_{i=1}^{p} \tau_i F_i(z) \quad > (\geq) \quad 0.$$

Proof. Follows trivially from the definitions of positive definite (semi-definite) matrices. ■

5.4 Significance of LMI Problems

The observation about LMI-based optimization that is most relevant to this thesis is that

LMI problems are tractable.

LMI problems can be solved in polynomial time, which means that they have low computational complexity. From a practical standpoint, there are effective and powerful algorithms for the solution of these problems, that is, algorithms that rapidly compute the global optimum, with non-heuristic stopping criteria. Thus, on exit, the algorithms can prove that the global optimum has been obtained to within some prespecified accuracy [1, 20, 105, 130]. Numerical experience shows that these algorithms

solve LMI problems with extreme efficiency.

Thus, reducing a problem to an LMI-based optimization problem can be considered to be equivalent to "solving" that problem, even though a so-called "analytic solution" to the problem may not exist. Standard software is now available, including a MATLAB toolbox [48], for solving such LMI-based optimization problems.

A number of standard problems in systems and control can be recast as convex optimization problems involving LMIs. These include:

- multi-criterion LQG/LTR;
- matrix scaling problems such as minimization of the scaled condition number;
- synthesis of multiplier for analysis of systems with unknown constant parameters ("real μ');
- problems in robust identification;
- interpolation problems involving scaling;
- standard $\mathcal{H}_2/\mathcal{H}_\infty$ output feedback controller synthesis problems;
- multi-objective output feedback controller synthesis problems.

This list is by no means complete and only serves to illustrate a few of the large number of control problems that can be recast as LMI problems. Many of these problems are summarized in [21]. However, many new results and reformulations of old results in the LMI framework continue to appear in the literature at the present time.

Chapter 6 Multiplier Theory for Stability Analysis of Anti-Windup Control Systems

Abstract

We apply the passivity theorem with appropriate choice of multipliers to develop sufficient conditions for stability of the general anti-windup bumpless transfer (AWBT) framework presented in Chapter 4. For appropriate choices of the multipliers, we show that these tests can be performed using convex optimization over linear matrix inequalities (LMIs). We show that a number of previously reported results on stability of AWBT control systems, derived from such well-known and seemingly diverse techniques as the Popov, Circle and Off-Axis Circle criteria, the optimally scaled small-gain theorem (generalized μ upper bound) and describing functions, are all special cases of the general conditions developed in this chapter. The sufficient conditions are complemented by necessary conditions for internal stability of the AWBT compensated system. Using an example, we show how these tests can be used to analyze the stability properties of a typical anti-windup control scheme.

6.1 Introduction

In Chapter 4, we presented a general AWBT framework based on the standard two-step design paradigm of AWBT. The framework established a firm theoretical basis for AWBT control. Moreover, the resulting AWBT scheme was shown to unify *all* known LTI AWBT schemes in terms of two matrix parameters, H_1, H_2. This significantly clarified the basic underlying concept of AWBT and simplified the problem of comparing and contrasting various previously reported heuristically based AWBT methodologies.

As mentioned in §1.2.1.2, it should be clear that merely providing AWBT com-

pensation of the type discussed in the preceding chapters does not automatically guarantee closed-loop stability of the system in the presence of input constraints. A necessary step in the further development of a complete AWBT theory is, therefore, the development of tools for analyzing stability of AWBT control systems with or without plant model uncertainty. Below, we summarize the existing literature in this area:

- One of the first attempts to address this problem was by Glattfelder *et al.* [57, 58, 59]. They analyzed the stability of single input single output (SISO) anti-reset windup PI controllers using the Popov and Circle criteria.

- Kapasouris and Athans (1985) [69] applied a multivariable version of the Circle Criterion to analyze stability of their multivariable nonlinear anti-reset windup scheme.

- Zheng *et al.* (1994) [143] used the Off-Axis Circle Criterion to establish stability of their anti-windup scheme for internal model control (IMC).

- Åström and Rundqwist (1989) [6] suggested the use of describing function theory in conjunction with the Circle Criterion to analyze stability of the observer-based anti-windup scheme.

- Doyle *et al.* (1987) [43] analyzed the stability of their modified anti-windup (MAW) scheme by using extensions of μ-analysis for LTI systems with structured uncertainty to nonlinear systems [42]. A similar analysis was presented by Campo *et al.* [27, 28].

One conclusion which is apparent from the preceding review is that several seemingly diverse techniques have been applied to develop stability conditions for several specific AWBT schemes. Very little work has been done on AWBT stability analysis in a reasonably general setting.

In this chapter, we will develop general tools, based on application of the passivity theorem and multiplier theory, for analyzing the stability properties of the AWBT

framework presented in Chapter 4. In particular, we will show how this general setting allows us to interpret the previously reported AWBT stability results in a single unified setting.

6.2 Background

In this section, we summarize necessary technical machinery such as the absolute stability problem, passivity theorem, multiplier theory and linear matrix inequalities (LMIs), which will be used in the later sections. The approach that we will adopt in §6.3 for AWBT stability analysis is based on concepts derived from absolute stability theory (see [41, §VI],[75]). Specifically, we will apply the passivity theorem [31, 117, 138, 139] with appropriate choice of multipliers [10, 11, 141] to develop sufficient conditions for AWBT stability.

6.2.1 Stability and Passivity

We begin by giving formal definitions of stability and passivity.

Definition 6.1 (Stability) *A causal operator* $h : \mathcal{L}_{2e} \longrightarrow \mathcal{L}_{2e}$ *is* $\mathcal{L}_2$ *stable if* $x \in \mathcal{L}_2 \Rightarrow hx \in \mathcal{L}_2$. *Furthermore, if* $\exists\ \gamma \geq 0$ *and* β *such that*

$$\|hx\|_2 \ \leq \ \gamma\|x\|_2 + \beta, \quad \forall\ x \in \mathcal{L}_2,$$

then h *is said to be finite-gain* $\mathcal{L}_2$ *stable.*

Note that stability requires the output hx to belong to the non-extended space $\mathcal{L}_2$ for all $x \in \mathcal{L}_2$. A feedback interconnection of the form shown in Figure 6.1 is $\mathcal{L}_2$ stable if all closed-loop maps from all external inputs to all internal variables are $\mathcal{L}_2$ stable. Finite-gain $\mathcal{L}_2$ stability of the interconnection can be defined similarly. Next we define the concept of passivity.

Definition 6.2 (Passivity) *[41] An operator $h : \mathcal{L}_{2e} \longrightarrow \mathcal{L}_{2e}$ is said to be strictly passive if $\exists\ \delta > 0$ and some β such that*

$$\langle x_T | (hx)_T \rangle \ \geq \ \delta \|x_T\|_2^2 + \beta, \quad \forall\ T \in \Re,\ \forall\ x \in \mathcal{L}_{2e}. \tag{6.1}$$

If $\delta \geq 0$, then h is said to be passive.

The motivation for this definition of passivity comes from network theory where circuit elements which absorb energy are called passive elements. For example, the energy absorbed by a resistance $R > 0$ with a voltage v across it and a current i through it is given by $\langle v_T | i_T \rangle = \int_0^T i(t)v(t)dt = R\int_0^T i^2(t)dt$ and hence a resistance is a strictly passive element.

If h is a causal, stable and LTI operator with transfer function $H(s)$, then it is (strictly) passive, i.e., it satisfies (6.1) if and only if there exists $\delta \geq (>)0$ such that [41, §VI]

$$H(j\omega) + H^*(j\omega) \geq 2\delta I, \quad \forall\ \omega \in \Re. \tag{6.2}$$

A matrix transfer function $H(s)$, whether stable or unstable but having no poles on the $j\omega$ axis, and satisfying (6.2) is said to be generalized (strictly) positive real [4]. The following lemma gives an equivalent condition for checking (6.2) in terms of the state-space matrices of $H(s)$.

Lemma 6.1 (Positive Real Lemma) *[4] A matrix transfer function $H(s)$ having no poles on the $j\omega$ axis, with a controllable state-space realization (A, B, C, D), satisfies (6.2) iff there exists a symmetric matrix $Q = Q^T$ such that*

$$\begin{bmatrix} QA^T + AQ & B - QC^T \\ B^T - CQ & 2\delta I - (D + D^T) \end{bmatrix} \ \leq \ 0 \tag{6.3}$$

or equivalently, iff there exists a symmetric matrix $Q = Q^T$ *such that*

$$\begin{bmatrix} A^TQ + QA & QB - C^T \\ B^TQ - C & 2\delta I - (D + D^T) \end{bmatrix} \leq 0. \tag{6.4}$$

Remark 6.1 *If* $H(s)$ *is stable, then the matrix* $Q = Q^T$ *in (6.3), (6.4) can be taken to be positive definite without loss of generality.*

Note that (6.3), (6.4) are matrix inequalities that are affine in Q and δ and are therefore Linear Matrix Inequalities (LMIs) in Q and δ. As we discussed in Chapter 5, the significance of reducing a problem to the feasibility of an LMI is that the problem can be considered as effectively solved. This is because, due to convexity of LMI-based problems, a feasible solution (if it exists) can be computed efficiently and with low computational complexity (polynomial-time) using very effective algorithms [48].

6.2.2 The Passivity Theorem

The connection between passivity and stability of the closed-loop shown in Figure 6.1 was originally addressed by Sandberg [117] and later by Zames [138, 139]. The basic question that needs to be answered in this context is the following: *Is a network consisting of passive elements necessarily stable?* We state below a general version of the passivity theorem which answers this question.

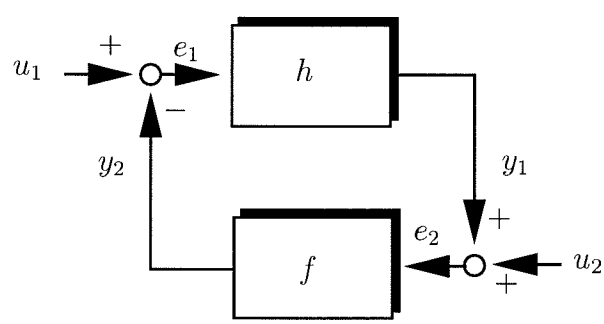

Figure 6.1: General interconnection for the passivity theorem.

Theorem 6.1 (Passivity Theorem) *Consider the feedback system shown in Figure 6.1, where the operators* $h : \mathcal{L}_{2e} \longrightarrow \mathcal{L}_{2e}$ *and* $f : \mathcal{L}_{2e} \longrightarrow \mathcal{L}_{2e}$ *are any (possibly nonlinear) causal operators. Assume that for any* $u_1, u_2 \in \mathcal{L}_2$, *there exist solutions* $e_1, e_2, y_1, y_2 \in \mathcal{L}_{2e}$. *Suppose there exist constants* $\gamma_1, \delta_1, \delta_2, \alpha_1, \beta_1, \beta_2$ *such that* $\forall\ x \in \mathcal{L}_{2e}$, $\forall\ T \in \Re$ *we have*

$$\|(hx)_T\|_2 \leq \gamma_1 \|x_T\|_2 + \alpha_1 \tag{6.5}$$

$$\langle x_T | (hx)_T \rangle \geq \delta_1 \|x_T\|_2^2 + \beta_1 \tag{6.6}$$

$$\langle x_T | (fx)_T \rangle \geq \delta_2 \|(fx)_T\|_2^2 + \beta_2. \tag{6.7}$$

If $\delta_1 + \delta_2 > 0$, *then* $u_1, u_2 \in \mathcal{L}_2 \Rightarrow\ e_1, e_2, y_1, y_2 \in \mathcal{L}_2$. *Furthermore, if* $\alpha_1, \beta_1, \beta_2$ *are zero, then the map from* (u_1, u_2) *to* (e_1, e_2, y_1, y_2) *is finite-gain* $\mathcal{L}_2$ *stable.*

Proof. See [41, 141]. ■

Note that if the operator h is $\mathcal{L}_2$ stable, then the finite gain condition (6.5) is automatically satisfied. Also, if h is strictly passive and f is passive, then conditions (6.6) and (6.7) are satisfied with $\delta_2 = 0$, $\delta_1 > 0$.

For the AWBT stability analysis problem, as we will see in §6.3, h is a fixed, stable, LTI system with transfer function $H(s)$ and f belongs to a class of sector bounded nonlinearities with a specified diagonal structure. We will be interested in developing stability conditions for the entire class of f. Such a problem is referred to as the *absolute stability* problem. Application of the passivity theorem will lead to sufficient conditions for stability which can be potentially conservative. This is because Theorem 6.1 assumes f to be any arbitrary operator satisfying (6.7), whereas, in reality, f has some additional structural properties. In this case, we can apply multiplier theory [10, 11, 141] to get less conservative conditions for stability by using this additional information about f.

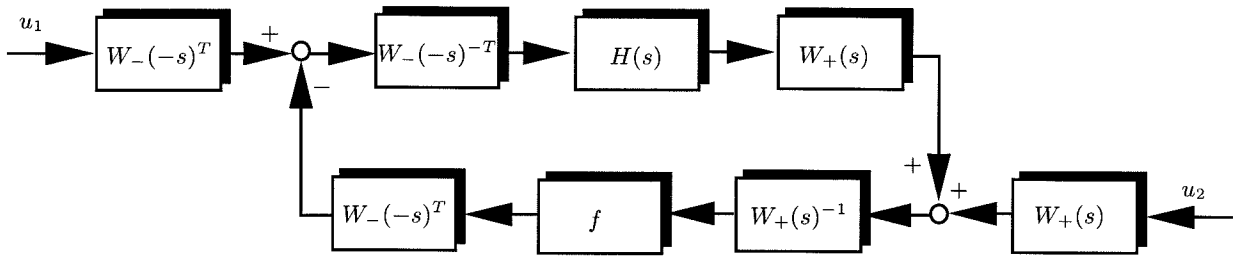

Figure 6.2: The passivity theorem with multipliers.

6.2.3 Multiplier Theory

The basic idea behind multiplier theory is that by multiplying the operators h and f by appropriately chosen *multipliers*, the product can be modified to satisfy the conditions of Theorem 6.1. Consider Figure 6.2 which is obtained from Figure 6.1 by pre- and post-multiplying $H(s)$ by $W_-(-s)^{-T}$ and $W_+(s)$ respectively, and correspondingly, pre- and post-multiplying f by $W_+(s)^{-1}$ and $W_-(-s)^T$, and the inputs u_1 and u_2 by $W_-(-s)^T$ and $W_+(s)$. If we assume that $W_+(s)$, $W_-(-s)$ are stable, proper and minimum phase with proper inverses, then the stability of the systems in Figures 6.1 and 6.2 are equivalent. Applying Theorem 6.1 then gives the following result.

Corollary 6.1 *Consider the feedback system shown in Figure 6.2. Assume that for any $u_1, u_2 \in \mathcal{L}_2$, all the signals in the system are well-defined and belong to $\mathcal{L}_{2e}$. Then, the system is $\mathcal{L}_2$ stable if*

1. *$\exists$ $W_+(s)$, $W_-(-s)$ which are stable and proper with stable and proper inverses;*
2. *$W_+(s)H(s)W_-(-s)^{-T}$ is $\mathcal{L}_2$ stable; and*
3. *$\exists$ constants $\beta_1, \beta_2, \delta_1, \delta_2$ such that $\forall\ x \in \mathcal{L}_{2e}$, $\forall\ T \in \Re$, we have*

$$\langle x_T | (\tilde{h}x)_T \rangle \geq \delta_1 \|x_T\|_2^2 + \beta_1 \tag{6.8}$$

$$\langle x_T | (\tilde{f}x)_T \rangle \geq \delta_2 \|(\tilde{f}x)_T\|_2^2 + \beta_2 \tag{6.9}$$

$$\delta_1 + \delta_2 > 0 \tag{6.10}$$

where $\tilde{h}$, $\tilde{f}$ are the operators $W_+(s)H(s)W_-(-s)^{-T}$ and $W_-(-s)^T \circ f \circ W_+(s)^{-1}$ respectively (symbol "$\circ$" denotes composition).

Remark 6.2 *In most problems of interest, as also in the AWBT analysis problem of §6.3, Corollary 6.1 is applied with $\delta_2 = 0$. This will be assumed to be the case in the rest of the chapter. In that case, using (6.2), we can conclude that conditions (6.8) and (6.10) above are equivalent to the existence of $\delta_1 > 0$ such that*

$$W_+(j\omega)H(j\omega)W_-(j\omega)^{-*} + W_-(j\omega)^{-1}H(j\omega)^*W_+(j\omega)^* \geq 2\delta_1 I, \quad \forall\, \omega \in \Re$$

$$\Longleftrightarrow \qquad W(j\omega)H(j\omega) + H(j\omega)^*W(j\omega)^* \geq \delta' I, \quad \forall\, \omega \in \Re, \text{ for some } \delta' > 0 \tag{6.11}$$

In (6.11), $W(s) = W_-(s)W_+(s)$ is commonly referred to as the *stability multiplier*. Since $W_-(-s)$ is stable, $W(s) = W_-(s)W_+(s)$ is in general unstable or, equivalently, non-causal. Note that if we are given the state-space representation of $W(s)H(s)$, then we can use Lemma 6.1 to check condition (6.11) in terms of the state-space matrices of $W(s)H(s)$.

Thus, we see that stability analysis using multipliers involves finding a multiplier $W(s)$ such that it can be factorized into $W_-(s)W_+(s)$, with $W_-(s)$, $W_+(s)$ satisfying conditions 1 and 2 of Corollary 6.1 and (6.9), and $W(s)$, $H(s)$ satisfying (6.11).

The significance of the multiplier approach to stability analysis discussed in this section is that a host of well-known, seemingly different stability analysis tests can be shown to be special cases of Corollary 6.1 for particular choices of the multiplier $W(s)$ (see [10, 11, 116]). These special cases include the Circle Criterion, the Off-Axis Circle Criterion and the Popov Criterion in the SISO case [116], and upper bounds on μ [108] for multivariable systems with structured, (mixed) real/complex and parametric uncertainties [10, 11]. Moreover, given the multiplier $W(s)$ establishing stability of the closed-loop, the corresponding quadratic Lyapunov function establishing stability for the closed-loop can be explicitly constructed [9].

With these preliminaries, we now consider the AWBT stability analysis problem.

6.3 Stability Analysis of AWBT Control Systems

Consider the AWBT compensated system of Figure 4.5, where $\hat{P}(s)$ and $\hat{K}(s)$, partitioned according to their inputs and outputs, are given respectively by (4.4) and (4.10), (4.11), (4.12) as follows:

$$\hat{P}(s) = \begin{bmatrix} P_{11} & P_{12} \\ P_{21} & P_{22} \\ P_{31} & P_{32} \end{bmatrix} \tag{4.4'}$$

$$\hat{K}(s) = [U(s) \quad I - V(s)] \tag{4.10'}$$

where

$$V(s) = \left[\begin{array}{c|c} A - H_1C & -H_1 \\ \hline H_2C & H_2 \end{array}\right] \tag{4.11'}$$

$$U(s) = \left[\begin{array}{c|c} A - H_1C & B - H_1D \\ \hline H_2C & H_2D \end{array}\right] \tag{4.12'}$$

with H_2 invertible. For simplicity, we will assume that $P_{31} \equiv 0$ in (4.4). This means that the measurement u_m of the plant input $\hat{u}$ which is provided to $\hat{K}(s)$ is given by

$$u_m = P_{32}\hat{u}. \tag{4.5'}$$

We will assume that $P_{22}(\infty) = 0$ to ensure well-posedness of the linear interconnection in Figure 4.4 (a). It is easy to verify that Figure 4.5 can be rearranged in the form

shown in Figure 6.3 with

$$\begin{aligned} M(s) &= \begin{bmatrix} (V(s)-I)P_{32}(s)-U(s)P_{22}(s) & U(s)P_{21}(s) \\ -P_{12}(s) & P_{11}(s) \end{bmatrix} \\ &= \begin{bmatrix} M_{11}(s) & M_{12}(s) \\ M_{21}(s) & M_{22}(s) \end{bmatrix}. \end{aligned} \tag{6.12}$$

N is the generic input nonlinearity which represents either component-wise actu-

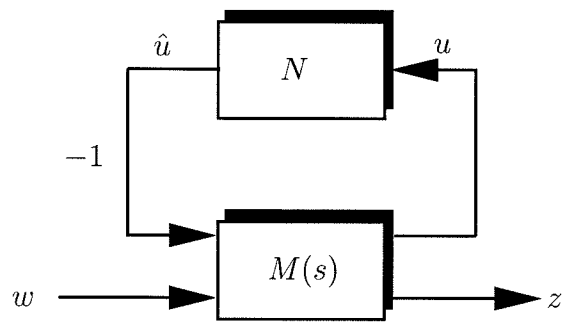

Figure 6.3: Interconnection for AWBT stability analysis.

ator saturation, relay, dead-zone, hysteresis, etc. (*input limitation*) or an override, mode selection scheme/switching logic (*input substitution*). We will assume that the $M_{11}(s) - N$ loop is well-posed. This can be ensured, for instance, by assuming that $M_{11}(\infty) + M_{11}(\infty)^T > 0$.

Exact stability analysis, i.e., development of non-conservative conditions which are both sufficient *and* necessary for stability of the system in Figure 6.3, for a given nonlinearity N (for example, saturation) is, in general, a difficult problem. On the other hand, as we will see in §6.3.1, firstly, the nonlinearity N can be assumed to be memoryless, i.e., its output at any time depends only on its input at the present time. Secondly, bounds on its input-output map (for example, sector bounds) can be easily derived. Based on these two facts, we can cover N by a class of sector bounded memoryless nonlinearities having the same structure as N. We can then apply results from absolute stability theory [41, 75] to develop sufficient conditions which guarantee stability for the entire class of N rather than N itself. This has probably been the

most common approach for analyzing AWBT stability (see for example [27, 28, 57, 58, 59, 69]), the reason being that it greatly simplifies the nonlinear analysis.

The unavoidable price paid for this simplification is conservatism since the resulting conditions ensure stability not only for N but also for all nonlinear maps with the given structure and sector bounds. In §6.3.2, we will see how we can reduce this conservatism by applying concepts from multiplier theory to incorporate additional properties of N.

6.3.1 Sector Bounds on the Nonlinearity N

In this section, we derive sector bounds for common input limitation and substitution nonlinearities. We begin by defining a sector condition on a nonlinearity.

Definition 6.3 *Let* $f : \Re^n \times \Re \longrightarrow \Re^n$ *with* $f(0,t) = 0 \ \forall \ t \geq 0$ *be a memoryless (possibly time-varying) diagonal nonlinearity* $f = diag\{f_1, \ldots, f_n\}$. *We say that* $f \in$ *sector* $[K_1, K_2]$, *with* $K_1 = diag(K_{11}, \ldots, K_{1n}), K_2 = diag(K_{21}, \ldots, K_{2n}), K_2 - K_1 > 0$ *if*

$$K_{1i}x_i^2 \leq x_i f_i(x_i, t) \leq K_{2i}x_i^2, \qquad \text{for all } x_i \in \Re, \ t \geq 0, \ i = 1, 2, \ldots, n. \quad (6.13)$$

Consider the interconnection in Figure 6.1, where h is assumed to be a fixed LTI system with transfer function $H(s)$ and f is a diagonal nonlinearity lying in the sector $[K_1, K_2]$, with K_1, K_2 as in Definition 6.3. Suppose we apply a negative feed-forward of K_1 and a positive feedback of $(K_2 - K_1)^{-1}$ to the nonlinearity f, and correspondingly, we apply a negative feedback of K_1 and a positive feed-forward of $(K_2 - K_1)^{-1}$ to $H(s)$ as shown in Figure 6.4. This is a well-known loop transformation (see [41, §VI.9]) from Figure 6.1 to the equivalent interconnection in Figure 6.4. The resulting nonlinear subsystem $\tilde{f}$ is a diagonal operator $\tilde{f} = \text{diag}\{\tilde{f}_1, \ldots, \tilde{f}_n\}$ where $\tilde{f}_i$ lies in the sector $[0, \infty]$ (see [41, §VI.9] for details) and satisfies the sector condition

$$x_i \tilde{f}_i(x_i, t) \geq 0, \ \forall \ x_i \in \Re, \ t \geq 0, i = 1, 2, \ldots, n, \quad (6.14)$$

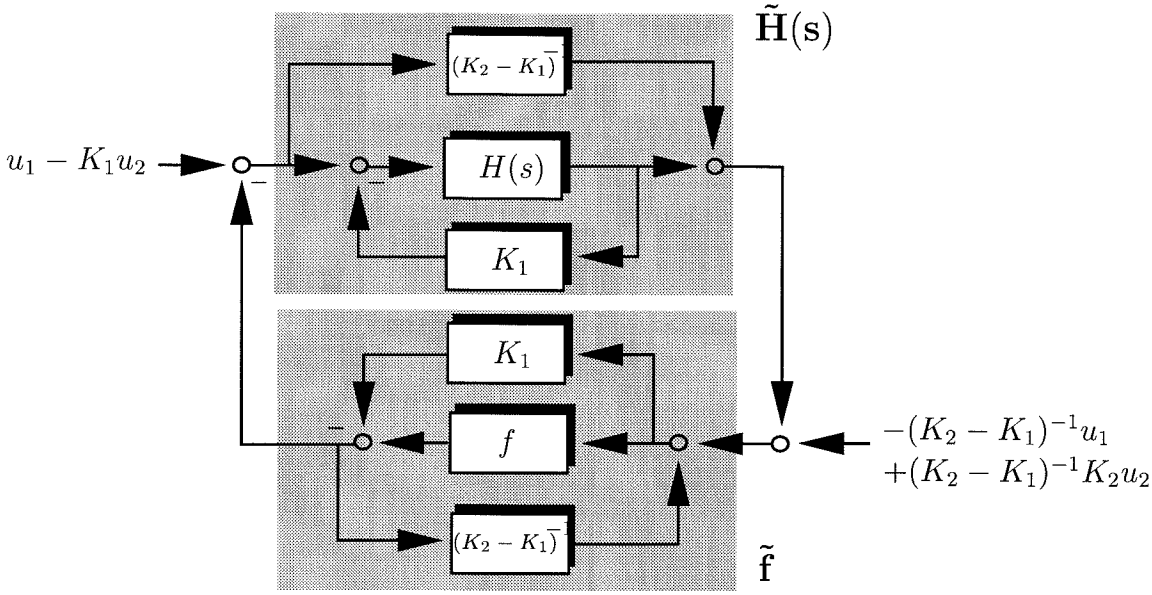

Figure 6.4: A loop transformation.

i.e., the graph of $\tilde{f}_i(x_i, t)$ vs. x_i lies in the first and third quadrants. We may note that, by definition, $\tilde{f}$ is passive and Remark 6.2 from §6.2.3 applies in this case. The linear subsystem is given by

$$\tilde{H}(s) = (K_2 - K_1)^{-1}(I + K_2 H(s))(I + K_1 H(s))^{-1}. \tag{6.15}$$

The reason for introducing this loop transformation is that, as shown in [140], applying the passivity theorem with multipliers to the transformed system in Figure 6.4 gives potentially less conservative stability conditions than those resulting from its application to the original system in Figure 6.1. We will use this loop transformation in the AWBT stability analysis problem.

6.3.1.1 Limitations

The most common example of an input limitation is actuator saturation (see Figure 6.5). Multivariable actuator saturation can be described by a memoryless, time-invariant, diagonal operator $N = \text{diag}\{N_1, \ldots, N_{n_u}\}$, where the N_i's are defined as

follows:

$$
\begin{aligned}
N_i(u_i) &= \text{sat}(u_i) \\
&= \begin{cases} u_{i,min} & \text{if } u_i < u_{i,min} \\ u_i & \text{if } u_{i,min} \le u_i \le u_{i,max} \\ u_{i,max} & \text{if } u_i > u_{i,max}. \end{cases}
\end{aligned} \tag{6.16}
$$

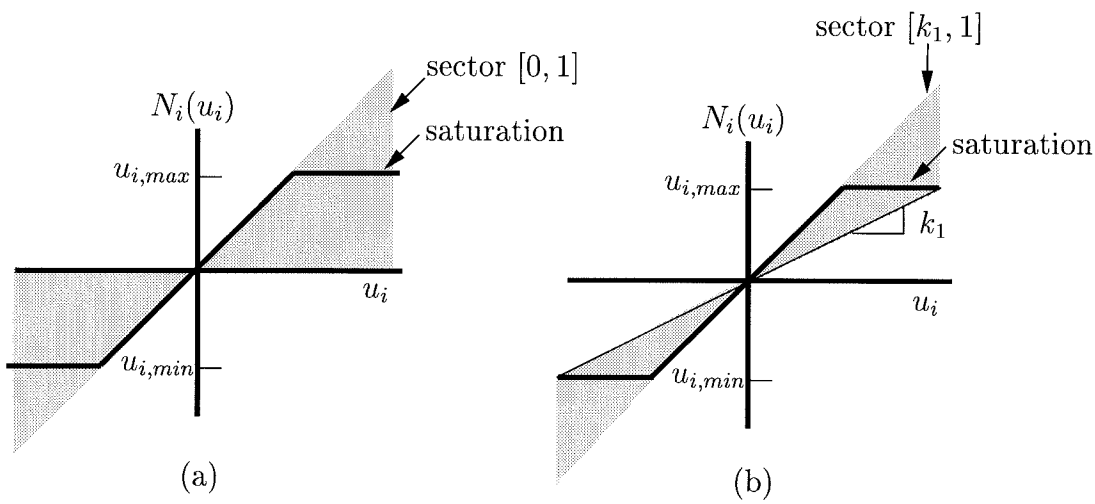

Figure 6.5: Sector bounds on the saturation nonlinearity N.

It is easy to verify that

$$0 \le u_i N_i(u_i) \le u_i^2, \quad \text{for all } u_i \in \Re$$

and hence $N \in \text{sector}[0, I]$ as shown in Figure 6.5(a). We note that both the identity operator $N = I$ and the zero operator $N = 0$ are included in the sector. However, if the controller output u_i can be bounded in magnitude, then the zero operator need not be included and we can take $K_1 \neq 0$ in (6.13). This will give a tighter sector bound for N_i as shown in Figure 6.5(b).

Other input nonlinearities such as dead-zones, relays, relays with dead-zones and hysteresis can also be covered by sectors in a similar manner. Note that except for hysteresis, all these nonlinearities are time-invariant, whereas the sector bounds include nonlinearities which are allowed to be arbitrarily time-varying.

6.3.1.2 Substitutions

Substitution mechanisms arise from the use of overrides or logic schemes which select the plant input $\hat{u}$ from among the outputs of a "bank" of controllers, each designed to achieve a different closed-loop characteristic. Commonly employed logic blocks are "min" selectors and "max" selectors which respectively select the minimum and maximum input as their output. Combinations of min-max selectors shown in Fig-

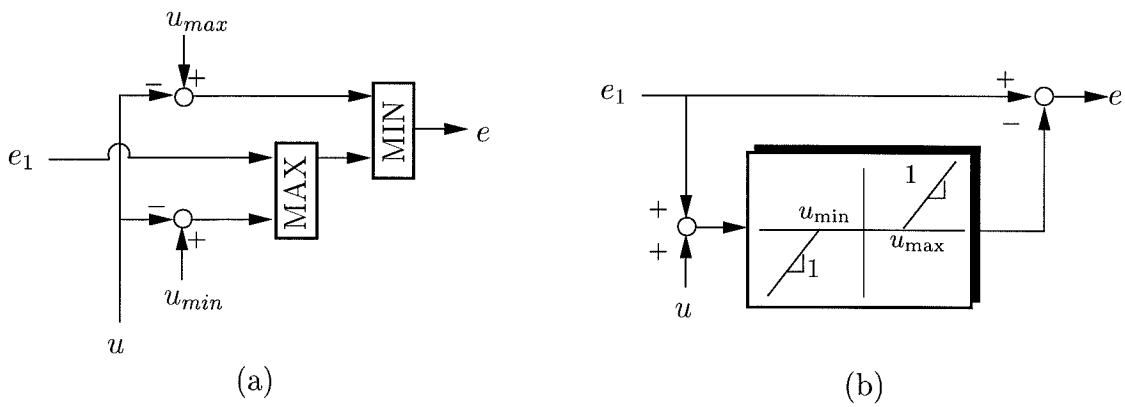

Figure 6.6: a) A combination of "min-max" selectors; b) its equivalent representation using a dead-zone nonlinearity.

ure 6.6(a) are often used to enforce upper and lower bounds on some variable, for example, u in Figure 6.6(a). It is easy to verify (see [57, 58]) that this min-max selector can be equivalently represented by using a dead-zone nonlinearity as shown in Figure 6.6(b). As discussed in §6.3.1.1, this dead-zone can then be covered by the sector $[0, 1]$.

Min and max selectors are only special cases of a "generic" selector which selects one of its inputs as its output. If we assume that the mechanism which determines which input is selected is completely unspecified or arbitrary, then the generic selector can be approximated by an arbitrarily time-varying memoryless switching nonlinearity N. For example, if the selector has two inputs u_1, u_2 and chooses one of them as

its output $\hat{u}$, then this selector can be approximated as follows:

$$\begin{aligned} \hat{u} &= N(u_1, u_2, t) \\ &= u_1 + n(t)(u_2 - u_1) \end{aligned} \tag{6.17}$$

where $n(t) \in \text{sector}[0, 1]$ is an arbitrarily time-varying memoryless parameter. $n(t) = 0$ and 1 give respectively the outputs u_1 and u_2. Selectors with more than two inputs can be modeled by decomposing them into a series of two-input selectors. The resulting multiple nonlinearities can then be arranged in a diagonal form. Sector bounds for combinations of selectors and other nonlinearities can be worked out using the same basic principles.

6.3.2 Sufficient Conditions for AWBT Stability

As discussed at the beginning of §6.3, we will derive sufficient conditions which ensure stability of the system in Figure 6.3 for all N with a given structure and sector bounds. A problem of this type was originally formulated by Lur'e [94] and is known as the *absolute stability problem.* The basic idea is to derive conditions on the linear subsystem M such that the closed loop system in Figure 6.3 is stable for all nonlinearities N belonging to a certain class. Theorem 6.1 from §6.2.2 and Corollary 6.1 from §6.2.3 form the basis of the stability results that follow.

We begin with the most general case by allowing the nonlinearity N to be arbitrarily time-varying. We then successively impose more restrictions on the nonlinearity N. Correspondingly, we modify the choice of the multiplier $W(s)$ in Corollary 6.1 to get less conservative stability conditions. In all cases, we show how the multiplier $W(s)$ establishing stability can be explicitly constructed from the feasible solution of a set of convex conditions involving LMIs.

6.3.2.1 Memoryless Time-Varying Nonlinearities

We begin by defining the set $\mathcal{N}_{TV}$ of all allowable structured nonlinearities N.

$$\begin{aligned} \mathcal{N}_{TV} \;=\; & \{N : \Re^{n_u} \times \Re \to \Re^{n_u} | N(0,t) = 0 \;\forall\; t \geq 0, \\ & N = \mathrm{diag}\{N_1, N_2, \ldots, N_{n_u}\}, N_i \in \mathrm{sector}[0,1]\}\,. \end{aligned} \tag{6.18}$$

The nonlinearities in $\mathcal{N}_{TV}$ are memoryless and are allowed to be arbitrarily time-varying. Here we consider only the sector $[0, I]$. Conditions for other sector bounds can be derived similarly. $\mathcal{N}_{TV}$ typically includes input nonlinearities such as those represented by (6.17) which model generic selectors with no pre-specified switching logic. Applying Corollary 6.1 to Figure 6.3 gives us the following result.

Theorem 6.2 (Multi-loop Circle Criterion) *The AWBT system in Figure 6.3 is $\mathcal{L}_2$ stable for all $N \in \mathcal{N}_{TV}$ if*

1. *$A - H_1 C$ has all eigenvalues in the open left-half complex plane;*
2. *$\hat{P}$ in equation (4.4) is asymptotically stable; and*
3. *$\exists\; W = diag(W_1, W_2, \ldots, W_{n_u}) \in \Re^{n_u \times n_u}$ with $W > 0$ and $\delta_1 > 0$ such that*

$$W M_{11}(j\omega) + M_{11}^*(j\omega) W + 2W \;\geq\; \delta_1 I, \quad \forall\; \omega \in \Re. \tag{6.19}$$

Furthermore, if $M_{11}(s) = \left[\begin{array}{c|c} \tilde{A} & \tilde{B} \\ \hline \tilde{C} & \tilde{D} \end{array}\right]$, then (6.19) above can be equivalently checked via the existence of a symmetric matrix $Q = Q^T > 0$, $\delta_1 > 0$ such that the following LMI in Q, W, δ_1 is satisfied

$$\left[\begin{array}{cc} \tilde{A}^T Q + Q\tilde{A} & Q\tilde{B} - \tilde{C}^T W \\ \tilde{B}^T Q - W\tilde{C} & \delta_1 I - 2W - W\tilde{D} - \tilde{D}^T W \end{array}\right] \;\leq\; 0. \tag{6.20}$$

Proof. By assumption, the loop $M_{11}(s) - N$ is well-posed. For $\mathcal{L}_2$ stability, it is enough to show that $M(s)$ is $\mathcal{L}_2$ stable and that the $M_{11}(s) - N$ loop is asymptotically stable. Condition 1 of the Theorem and (4.10), (4.11), (4.12) imply that $\hat{K}(s)$ is

asymptotically stable. Together with condition 2 above and (6.12), this implies that $M(s)$ (and hence $M_{11}(s)$) is asymptotically stable.

Next, consider the loop $M_{11}(s) - N$, where, $N \in \text{sector}[0, I]$. Applying the loop transformation of Figure 6.4, we transform the diagonal nonlinearity N to a diagonal nonlinearity $\tilde{N}$ with $\tilde{N}_i \in \text{sector}[0, \infty]$, and correspondingly, we transform $M_{11}(s)$ to $\tilde{M}_{11}(s) = M_{11}(s) + I$. Since $\tilde{N}_i \in \text{sector}[0, \infty]$, $\tilde{N}$ is passive. Corollary 6.1 can now be applied to the $\tilde{M}_{11}(s) - \tilde{N}$ loop with $H(s) = \tilde{M}_{11}(s)$, $f = \tilde{N}$.

Since $\tilde{N}$ is an arbitrarily time-varying, memoryless nonlinearity, an appropriate multiplier for this case is $W(s) = W > 0$ where $W = \text{diag}(W_1, W_2, \ldots, W_{n_u}) \in \Re^{n_u \times n_u}$, with $W_+(s) = W$, $W_-(s) = I$ (see [10, 11]). This multiplier clearly satisfies (6.9) with $\delta_2 = 0$ (see Remark 6.2) and conditions 1 and 2 of Corollary 6.1. (6.8) and (6.10) can be checked via (6.11) as follows:

$$
\begin{aligned}
& W\tilde{M}_{11}(j\omega) + \tilde{M}_{11}^*(j\omega)W \geq \delta_1 I, \quad \forall\, \omega \in \Re \\
\Leftrightarrow\ & WM_{11}(j\omega) + M_{11}^*(j\omega)W + 2W \geq \delta_1 I, \quad \forall\, \omega \in \Re
\end{aligned}
$$

which establishes (6.19).

Further, if $M_{11}(s) = \left[\begin{array}{c|c} \tilde{A} & \tilde{B} \\ \hline \tilde{C} & \tilde{D} \end{array}\right]$, then $W\tilde{M}_{11}(s) = \left[\begin{array}{c|c} \tilde{A} & \tilde{B} \\ \hline W\tilde{C} & W + W\tilde{D} \end{array}\right]$. Lemma 6.1 then establishes (6.20). ■

We may note that the stability multiplier $W(s) = W$ is directly computed once the LMI (6.20) is solved.

6.3.2.2 Memoryless Time-Invariant (Static) Nonlinearities

In the previous section, the set $\mathcal{N}_{TV}$ included arbitrarily time-varying memoryless nonlinearities. A large class of input nonlinearities such as saturation, relay, dead-zone, relay with dead-zone, etc., are memoryless and *time-invariant*, i.e., static. Almost all previously reported AWBT stability analysis results [27, 28, 43, 57, 58, 59, 69] model these static nonlinearities as time-varying to simplify the analysis problem. The resulting stability conditions, as also those obtained from Theorem 6.2, are potentially extremely conservative in such cases. This conservatism can be reduced by appro-

priately modifying the choices of $W_+(s)$ and $W_-(s)$ such that the time-invariance property of N is taken into account.

Let us define the class of memoryless time-invariant nonlinearities as follows:

$$\begin{aligned} \mathcal{N}_{TI} &= \{N : \Re^{n_u} \to \Re^{n_u} | N(0) = 0, \\ &\quad N = \text{diag}\{N_1, N_2, \ldots, N_{n_u}\}, N_i \in \text{sector}[0,1]\}. \end{aligned} \tag{6.21}$$

Using a variety of techniques, Popov (1961) [113], Zames (1966) [139] and Brockett and Willems (1965) [22] have shown that the appropriate multiplier for this case, with a scalar nonlinearity ($n_u = 1$), is $W(s) = 1 + Ws$, $W \geq 0$, with $W_+(s) = 1 + Ws$, $W_-(s) = 1$. As we will see, with a multivariable diagonal nonlinearity N belonging to the set $\mathcal{N}_{TI}$, the appropriate multiplier is the following:

$$W(s) = X + sW \quad \text{with} \quad W_+(s) = (X + sW), \quad W_-(s) = I \tag{6.22}$$

where $W = \text{diag}(W_1, W_2, \ldots, W_{n_u}) \in \Re^{n_u \times n_u}$, $X = \text{diag}(X_1, X_2, \ldots, X_{n_u}) \in \Re^{n_u \times n_u}$, $W \geq 0$, $X > 0$. Note that although $(X + sW)$ is not proper, it can be obtained as the limit

$$X + sW = \lim_{n \to \infty} \frac{1}{1 + \frac{s}{n}}(X + sW)$$

where $\frac{1}{1+\frac{s}{n}}(X + sW)$ is the appropriate proper multiplier satisfying the conditions of Corollary 6.1. We will need the following lemma to prove AWBT stability with static input nonlinearities.

Lemma 6.2 *Let $f = diag\{f_1, f_2, \ldots, f_n\}$ be a memoryless, time-invariant, diagonal nonlinearity $f : \Re^n \longrightarrow \Re^n$, with $f_i \in sector[0, \infty]$. Let $W(s) = X + sW$, $X = diag(X_1, X_2, \ldots, X_n) \in \Re^{n \times n}$, $W = diag(W_1, W_2, \ldots, W_n) \in \Re^{n \times n}$ with $W \geq 0$, $X > 0$. Then $f \circ W(s)^{-1}$ is passive.*

Proof. The proof is a multivariable extension of the proof of Lemma 2 in [139]. Since $f_i \in \text{sector}[0, \infty]$, f is passive, i.e., it satisfies

$$\langle x_T | (fx)_T \rangle \geq 0, \ \forall \ x \in \Re^n, \ T \geq 0.$$

We need to show that $f \circ W(s)^{-1}$ is passive, i.e., that it satisfies

$$\langle x_T | (f \circ W(s)^{-1} x)_T \rangle \geq 0, \ \forall \ x \in \Re^n, \ T \geq 0.$$

Now,

$$\begin{aligned}
\langle x_T | (f \circ W(s)^{-1} x)_T \rangle &= \langle (W(s)y)_T | (fy)_T \rangle \quad \text{(substituting } y = W(s)^{-1}x\text{)} \\
&= \int_0^T (Xy(t) + W\dot{y}(t))^T f(y(t)) \, dt \\
&= \int_0^T y(t)^T X f(y(t)) \, dt + \int_0^T \dot{y}(t)^T W f(y(t)) \, dt \\
&\geq \int_0^{y(t)} f(y(t))^T W \, dy \geq 0.
\end{aligned}$$

The last two inequalities follow from the fact that f is diagonal, i.e., $f = \text{diag}\{f_1, \ldots, f_n\}$ with $f_i \in \text{sector}[0, \infty]$ and $W \geq 0$, $X > 0$ are diagonal matrices. ■

The following theorem, a multivariable extension of the classical scalar Popov criterion, states conditions for AWBT stability with static input nonlinearities.

Theorem 6.3 (Multivariable Popov Criterion) *The AWBT system in Figure 4.5 is $\mathcal{L}_2$ stable for all $N \in \mathcal{N}_{TI}$ if*

1. *$A - H_1 C$ has all eigenvalues in the open left-half complex plane;*

2. *$\hat{P}$ in equation (4.4) is asymptotically stable; and*

3. *$\exists \ X = diag(X_1, X_2, \ldots, X_{n_u}) \in \Re^{n_u \times n_u}$, $W = diag(W_1, W_2, \ldots, W_{n_u}) \in \Re^{n_u \times n_u}$ with $W \geq 0$, $X > 0$ and $\delta_1 > 0$ such that if $M_{11}(s) = \left[\begin{array}{c|c} \tilde{A} & \tilde{B} \\ \hline \tilde{C} & \tilde{D} \end{array}\right]$, then*

$$\begin{aligned}
&(X + j\omega W)(M_{11}(j\omega) - \tilde{D}) + (M_{11}^*(j\omega) - \tilde{D}^T)(X - j\omega W) \\
&\quad + X\tilde{D} + \tilde{D}^T X + 2X \geq \delta_1 I, \quad \forall \ \omega \in \Re.
\end{aligned} \tag{6.23}$$

Furthermore, (6.23) above can be equivalently checked via the existence of a symmetric matrix $Q = Q^T > 0$, $\delta_1 > 0$ such that the following LMI in Q, W, X, δ_1

is satisfied

$$\begin{bmatrix} \tilde{A}^T Q + Q\tilde{A} & Q\tilde{B} - \tilde{C}^T X - \tilde{A}^T \tilde{C}^T W \\ \tilde{B}^T Q - X\tilde{C} - W\tilde{C}\tilde{A} & \delta_1 I - W\tilde{C}\tilde{B} - \tilde{B}^T \tilde{C}^T W - X\tilde{D} - \tilde{D}^T X - 2X \end{bmatrix} \leq 0. \quad (6.24)$$

Proof. As in the proof of Theorem 6.2, we see that $M(s)$ is stable and the $M_{11}(s) - N$ loop is well-posed. Also, as in the proof of Theorem 6.2, the $M_{11}(s) - N$ loop can be transformed to the $\tilde{M}_{11}(s) - \tilde{N}$ loop with $\tilde{M}_{11}(s) = M_{11}(s) + I$, $\tilde{N} = \text{diag}\{\tilde{N}_1, \ldots, \tilde{N}_{n_u}\}, \tilde{N}_i \in \text{sector}[0, \infty]$ with $\tilde{N}$ passive. Corollary 6.1 can now be applied to the $\tilde{M}_{11}(s) - \tilde{N}$ loop with $H(s) = \tilde{M}_{11}(s)$, $f = \tilde{N}$, $W(s) = X + sW$, $W_+(s) = X + sW$, $W_-(s) = I$, where $W = \text{diag}(W_1, W_2, \ldots, W_{n_u}) \in \Re^{n_u \times n_u}$, $X = \text{diag}(X_1, X_2, \ldots, X_{n_u}) \in \Re^{n_u \times n_u}$, $W \geq 0$, $X > 0$.

By Lemma 6.2, $\tilde{N} \circ W(s)^{-1}$ is passive and hence (6.9) is satisfied with $\delta_2 = 0$ (see Remark 6.2). (6.8) and (6.10) can be checked via (6.11) as follows:

$$\begin{aligned} &(X + j\omega W)\tilde{M}_{11}(j\omega) + \tilde{M}_{11}^*(j\omega)(X - j\omega W) \geq \delta_1 I, \quad \forall \omega \in \Re \\ \Leftrightarrow\ &(X + j\omega W)(M_{11}(j\omega) - \tilde{D}) + (M_{11}^*(j\omega) - \tilde{D}^T)(X - j\omega W) \\ &+ X\tilde{D} + \tilde{D}^T X + 2X \geq \delta_1 I, \quad \forall\, \omega \in \Re \end{aligned}$$

which establishes (6.23). Note that the above inequality can be rigorously derived using the multiplier $W(s) = \frac{1}{1+\frac{s}{n}}(X + sW)$ and taking the limit as $n \to \infty$. Furthermore, it can be verified that

$$(X + sW)(M_{11}(s) - \tilde{D}) = \left[\begin{array}{c|c} \tilde{A} & \tilde{B} \\ \hline X\tilde{C} + W\tilde{C}\tilde{A} & W\tilde{C}\tilde{B} \end{array}\right].$$

(6.24) then follows from Lemma 6.1 and this completes the proof. ■

As in Theorem 6.2, we may note that the multiplier $W(s) = X + sW$ establishing stability is explicitly determined once we compute a feasible solution to the LMI (6.24).

6.3.2.3 Monotonic Slope-Restricted Static Nonlinearities

Several input nonlinearities, in addition to being memoryless and time-invariant, are also (odd) monotonic and/or slope-restricted. Examples include saturation, dead-zone, relay and relay with dead-zone. To the best of our knowledge, there has been no attempt to incorporate these additional properties of the input nonlinearities to get improved AWBT stability conditions. As we will see, it is possible to exploit these properties, by appropriately choosing the multiplier $W(s)$, to get less conservative stability conditions.

Definition 6.4 *Let $f : \Re^n \to \Re^n$ with $f(0) = 0$ be a static diagonal nonlinearity $f = diag\{f_1, f_2, \ldots, f_n\}$. f is said to be monotone non-decreasing if*

$$(x_{1i} - x_{2i})(f_i(x_{1i}) - f_i(x_{2i})) \geq 0, \quad \forall\ x_{1i}, x_{2i} \in \Re,\ i = 1, 2, \ldots, n, \tag{6.25}$$

and f is said to be odd monotone non-decreasing if, in addition,

$$f(-x) = -f(x), \quad \forall\ x \in \Re^n. \tag{6.26}$$

Definition 6.5 *Let $f : \Re^n \to \Re^n$ with $f(0) = 0$ be a static diagonal nonlinearity $f = diag\{f_1, f_2, \ldots, f_n\}$. f is said to be incrementally inside (or slope-restricted in) sector$[K_1, K_2]$, with $K_1 = diag(K_{11}, \ldots, K_{1n}), K_2 = diag(K_{21}, \ldots, K_{2n}), K_2 - K_1 > 0$ if*

$$K_{1i} \leq \frac{f_i(x_{1i}) - f_i(x_{2i})}{x_{1i} - x_{2i}} \leq K_{2i}, \quad \forall\ x_{1i}, x_{2i} \in \Re,\ x_{1i} \neq x_{2i}, i = 1, 2, \ldots, n. \tag{6.27}$$

It is easy to verify that the saturation nonlinearity N_i of Figure 6.5(a) satisfies (6.25) and (6.27) with $K_{1i} = 0$, $K_{2i} = 1$. Furthermore, if $u_{i,min} = -u_{i,max}$, then N_i also satisfies (6.26).

Absolute stability of the feedback interconnection in Figure 6.1, where h is a causal LTI system with transfer function $H(s)$ and f is an (odd) monotonic, slope-restricted, static scalar nonlinearity, was originally studied by Zames and Falb (1968) [141]. The

basic idea of the stability proof was to characterize the appropriate multiplier to be used in Corollary 6.1. The following theorem, a multivariable extension of the result from Zames and Falb (1968) [141], states conditions for AWBT stability with static slope-restricted (odd) monotone nonlinearities.

Theorem 6.4 *Let $w_i(t),\ i =, 1, 2, \ldots, n_u$ be the impulse response of a scalar LTI (possibly non-causal) operator on $t \in (-\infty, \infty)$ with*

$$\int_{-\infty}^{\infty} |w_i(t)|\, dt \ < \ X_i,\ X_i > 0, \quad i = 1, 2, \ldots, n_u. \tag{6.28}$$

Then the AWBT system in Figure 4.5 is $\mathcal{L}_2$ stable for all $N \in \mathcal{N}_{\mathrm{TI}}$ with N being odd monotone non-decreasing and incrementally inside sector $[0, I]$ if

1. *$A - H_1 C$ has all eigenvalues in the open left-half complex plane;*
2. *$\hat{P}$ in equation (4.4) is asymptotically stable; and*
3. *$\exists\ w_i(t)$, with Fourier transform $W_i(j\omega)$, and $X_i > 0,\ i = 1, 2, \ldots, n_u$ satisfying (6.28) such that for some $\delta_1 > 0$*

$$(X - W(j\omega))(M_{11}(j\omega) + I) + (M_{11}^*(j\omega) + I)(X - W^*(j\omega)) \geq \delta_1 I,\ \forall\ \omega \in \Re, \tag{6.29}$$

where,

$$W(j\omega) \ = \ diag(W_1(j\omega), \ldots, W_{n_u}(j\omega)),\ X = diag(X_1, \ldots, X_{n_u}) > 0. \tag{6.30}$$

If N is not odd, then in the stability conditions stated above, we require, in addition, w_i to satisfy

$$w_i(t) \geq 0,\ \forall\ t \in (-\infty, \infty). \tag{6.31}$$

Proof. The proof involves application of Corollary 6.1 with the multiplier $X - W(s)$ and is given in § 6.7 as Appendix A. It requires several intermediate results which are extensions of the scalar results from [141] to the multivariable case. ■

The AWBT stability conditions in Theorem 6.4 are not very useful since they are not constructive, i.e., it is not clear how to search for the infinite dimensional, non-causal operators $w_i(t), i = 1, \ldots, n_u$, satisfying (6.28), (6.29), (6.30) and (6.31). One alternative is to decompose $w_i(t)$ into causal and anti-causal components and then approximate each component by a finite dimensional LTI system. Such an approach and a complete solution involving LMIs has been presented in [30]. For completeness, we briefly discuss this approach here. Details can be found in [30].

Let us express $w_i(t)$ in terms of its causal and anti-causal components as $w_i(t) = w_i^+(t) + w_i^-(t)$, where

$$w_i^+(t) = \begin{cases} w_i(t) & \text{if } t \geq 0, \\ 0 & \text{if } t < 0; \end{cases} \qquad w_i^-(t) = \begin{cases} w_i(t) & \text{if } t \leq 0, \\ 0 & \text{if } t > 0. \end{cases}$$

We can now obtain finite series expansions of $w_i^+(t)$ and $w_i^-(t)$ with basis functions $e_j^+(t) = e^{-t}t^j, t \geq 0$, (zero for $t < 0$) and $e_j^-(t) = e^t t^j, t \leq 0$, (zero for $t > 0$) respectively. This leads to an m^{th} order approximation of $w_i(t)$ as follows:

$$w_i(t) = \sum_{j=0}^{m} (a_{i,j} e_j^+(t) + b_{i,j} e_j^-(t)).$$

This is equivalent to using $\frac{1}{(s+1)^j}$ and $\frac{1}{(s-1)^j}$, $j \geq 1$, as basis functions for approximating the causal and anti-causal components of $W_i(s)$ respectively. Condition (6.31), i.e., $w_i(t) \geq 0, t \in (-\infty, \infty)$ can be shown to be equivalent to (see [30])

$$\frac{\sum_{j=0}^{m} a_{i,j}(-1)^j s^{2j}}{(-s+1)^m(s+1)^m} \geq 0 \quad \text{and} \quad \frac{\sum_{j=0}^{m} b_{i,j} s^{2j}}{(-s+1)^m(s+1)^m} \geq 0, \ \forall\ s = j\omega,\ \omega \in \Re, \tag{6.32}$$

and the condition (6.28) can be expressed as

$$\sum_{j=0}^{m} (a_{i,j} + (-1)^j b_{i,j}) j! \ < \ X_i. \tag{6.33}$$

By Lemma 6.1, condition (6.32) reduces to checking that the state-space matrices of

$$\frac{\sum_{j=0}^{m} a_{i,j}(-1)^j s^{2j}}{(-s+1)^m(s+1)^m} = \left[\begin{array}{c|c} A_j^{(a)} & B_j^{(a)} \\ \hline C_j^{(a)} & D_j^{(a)} \end{array}\right] \text{ and } \frac{\sum_{j=0}^{m} b_{i,j} s^{2j}}{(-s+1)^m(s+1)^m} = \left[\begin{array}{c|c} A_j^{(b)} & B_j^{(b)} \\ \hline C_j^{(b)} & D_j^{(b)} \end{array}\right]$$

satisfy (6.4). Here, $C_j^{(a)}, D_j^{(a)}$ are affine in $a_{i,j}$ and $C_j^{(b)}, D_j^{(b)}$ are affine in $b_{i,j}$ (see [30]). Application of (6.4) leads to two matrix inequalities which are affine in $C_j^{(a)}, D_j^{(a)}$ and $C_j^{(b)}, D_j^{(b)}$, respectively, and hence are LMIs in $a_{i,j}, b_{i,j}$. Condition (6.33) is an obvious LMI in $a_{i,j}$, $b_{i,j}$, X_i.

For absolute stability, Theorem 6.4 requires that $W(j\omega)$, $M_{11}(j\omega)$ should satisfy (6.29), which is equivalent, by Lemma 6.1, to checking that the state-space matrices of $(X - W(s))(M_{11}(s) + I) = \left[\begin{array}{c|c} \tilde{A} & \tilde{B} \\ \hline \tilde{C} & \tilde{D} \end{array}\right]$ satisfy (6.4). Here, $\tilde{C}$ is affine in $a_{i,j}, b_{i,j}$ and $\tilde{D}$ is affine in X_i (see [30]). Hence the matrix inequality resulting from (6.4) is affine in $a_{i,j}, b_{i,j}, X_i$.

If we do not require $w_i(t) \geq 0, t \in (-\infty, \infty)$, which is the case when the nonlinearity N is odd, then the above procedure is a bit more involved and we refer the reader to [30] for details.

Thus, an intractable problem of finding an infinite dimensional multiplier satisfying the conditions in Theorem 6.4 is approximated by a tractable problem of finding a finite dimensional multiplier via the feasibility of a set of convex LMI conditions. It is worth mentioning that this finite dimensional solution approximates the solution to the original problem to an arbitrary accuracy, as the order m of the approximation of $w_i(t)$ tends to infinity.

6.3.3 Necessary Conditions for AWBT Stability

Since we are concerned with stability conditions for all $N \in \text{sector}[0, I]$, we immediately get the following necessary condition.

Theorem 6.5 *The AWBT system in Figure 4.5 is $\mathcal{L}_2$ stable for all $N \in \mathcal{N}_{TV}$ (or $\mathcal{N}_{TI}$) only if the AWBT controller $\hat{K}(s)$ stabilizes $\hat{P}(s)\begin{bmatrix} I & 0 \\ 0 & N \end{bmatrix}$ for all constant gain matrices $N = diag\{N_1, N_2, \ldots, N_{n_u}\} \in \Re^{n_u \times n_u}$ such that $0 \leq N \leq I$.*

Furthermore, if $\hat{P}(s) = \left[\begin{array}{c|cc} \tilde{A} & \tilde{B}_1 & \tilde{B}_2 \\ \hline \tilde{C}_1 & \tilde{D}_{11} & \tilde{D}_{12} \\ \tilde{C}_2 & \tilde{D}_{21} & \tilde{D}_{22} \\ \tilde{C}_3 & \tilde{D}_{31} & \tilde{D}_{32} \end{array}\right]$ *(actually, $\tilde{D}_{22} = 0$ since $P_{22}(\infty) = 0$, see §6.3), then the above statement is equivalent to the requirement that for every constant gain matrix $N = diag\{N_1, N_2, \ldots, N_{n_u}\} \in \Re^{n_u \times n_u}$ such that $0 \leq N \leq I$, there exists a symmetric matrix $Q = Q^T > 0$ such that the following LMI is satisfied:*

$$\mathcal{A}^T Q + Q\mathcal{A} < 0$$

$$\text{where } \mathcal{A} = \begin{bmatrix} \tilde{A} + \tilde{B}_2 N T^{-1}(H_2 D\tilde{C}_2 + (I - H_2)\tilde{C}_3) & \tilde{B}_2 N T^{-1} H_2 C \\ (B - H_1 D)\tilde{C}_2 + H_1\tilde{C}_3 + & A - H_1 C + \\ H_1\tilde{D}_{32} N T^{-1}(H_2 D\tilde{C}_2 + (I - H_2)\tilde{C}_3) & H_1\tilde{D}_{32} N T^{-1} H_2 C \end{bmatrix}, \quad (6.34)$$

with $T = I - (I - H_2)\tilde{D}_{32}N$.

Proof. Follows trivially by forming the closed-loop $\mathcal{A}$ matrix of $\hat{P}\begin{bmatrix} I & 0 \\ 0 & N \end{bmatrix}$ and $\hat{K}$ and using Lyapunov's theorem. Note that the inverse of $T = I - (I - H_2)\tilde{D}_{32}N$ is well-defined for all $0 \leq N \leq I$ since, by assumption (see §6.3), the loop formed by N is well-posed. ■

Remark 6.3 *For a SISO nonlinearity ($n_u = 1$), a similar condition was claimed to be sufficient for stability and is the well-known Aizermann's conjecture. That conjecture has since been proved false [47].*

By considering the cases $N \equiv 0$ and $N \equiv I$, we get the following corollary from Theorem 6.5.

Corollary 6.2 *The AWBT system in Figure 4.5 is $\mathcal{L}_2$ stable for all $N \in \mathcal{N}_{TV}$ (or $\mathcal{N}_{TI}$) only if*

1. *$\hat{P}(s)$ and $\hat{K}(s)$ are stable; and*

2. *$\hat{K}(s)$ stabilizes $\hat{P}(s)$.*

6.4 Generalization of Existing AWBT Analyses

In this section, we review a number of previous attempts to analyze AWBT stability, which used seemingly diverse theoretical techniques in the analysis. We show that our analysis presented in the previous section in effect generalizes these previously reported results and allows us to interpret and understand them in a single unified setting.

6.4.1 The Analysis of Glattfelder *et al.*

Glattfelder *et al.* [57, 58, 59] analyzed stability properties of anti-reset windup PI controllers. The essential idea in their work is to rearrange the system as in Figure 6.3. The graphical stability condition they use is the following SISO graphical Popov criterion:
Find a constant scalar $q \geq 0$ such that the Nyquist plot of $(1 + sq)M_{11}(s)$ lies to the right of the line $s = -1$. This is equivalent to checking that

$$Re(1 + j\omega q)M_{11}(j\omega) > -1, \quad \forall\, \omega \in \Re, \text{ for some } q \geq 0. \tag{6.35}$$

This is essentially condition (6.23) in Theorem 6.3, with $X = 1, W = q \geq 0$. The case $q = 0$ has also been considered by Glattfelder *et al.* [57, 58, 59]. In this case, the stability test they use is that the Nyquist plot of $M_{11}(s)$ should lie to the right of the line $s = -1$ (SISO graphical Circle criterion). As can be easily verified, this corresponds to checking that

$$Re\{(M_{11}(j\omega)\} > -1, \quad \forall\, \omega \in \Re, \tag{6.36}$$

which is condition (6.19) of Theorem 6.2 with $W = 1$.

Note that these graphical results are restricted to the SISO case. The conditions we derive in Theorems 6.2 and 6.3 are generalizations of these SISO graphical conditions to the MIMO case. Moreover, our conditions do not require any graphical checking, rather they require checking the feasibility of convex LMI conditions.

6.4.2 The Analysis of Doyle *et al.*

Doyle *et al.* [43] used extensions of conventional linear μ analysis to analyze stability of their modified anti-windup (MAW) scheme. Their basic idea for analysis was further explored by Campo *et al.* [27, 28] in greater detail and so we will only confine ourselves to the work of Campo *et al.* [27, 28] in the next section since the essential idea is the same for both these analyses.

6.4.3 The Analysis of Campo *et al.*

Campo *et al.* [27, 28] used the scaled-small gain theorem to develop anti-windup stability conditions. For this purpose, the AWBT control system is rearranged as in Figure 6.3. The nonlinearity N is expressed in terms of its conic sector bounds as follows:

$$N = C + \hat{N} \circ R, \tag{6.37}$$

where $C = \frac{1}{2}I$ is the cone center and $R = \frac{1}{2}I$ is the cone radius, and $\hat{N}$ is a nonlinearity in Cone$(0, I)$. Absorbing C and R in the linear block M of Figure 6.3, $M_{11}(s)$ is transformed to $-M_{11}(s)(2I + M_{11}(s))^{-1}$. Applying the small gain theorem with appropriate constant real diagonal scalings $T > 0$, the stability condition derived in Campo *et al.* [27, 28] is the following:

$$\|TM_{11}(s)(2I + M_{11}(s))^{-1}T^{-1}\|_\infty < 1. \tag{6.38}$$

This condition was then shown to be equivalent to the following (see [27])

$$T(M_{11}(j\omega)+I)T^{-1}+T^{-1}(M_{11}(j\omega)^*+I)T>0, \quad \forall\omega\in\Re. \tag{6.39}$$

The last condition is equivalent to

$$T^2M_{11}(j\omega)+(M_{11}(j\omega)^*T^2+2T^2>0, \quad \forall\omega\in\Re. \tag{6.40}$$

Defining $W=T^2$, we see that the above condition is equivalent to (6.19) in Theorem 6.2. It should be mentioned that to simplify the computation of stability condition (6.39) above, Campo *et al.* [27, 28] conservatively used complex matrices T, although the appropriate choice of the matrices T which commute with the nonlinearity $\hat{N}$ is the set of constant, diagonal, *real* matrices.

6.4.4 The Analysis of Kapasouris and Athans

Kapasouris and Athans [69] analyzed stability of their nonlinear anti-windup scheme using the MIMO Circle Criterion. Again, as before, this involves redrawing the AWBT system by isolating the linear part and the nonlinear part, which in their case consisted of the actuator nonlinearity and an additional static nonlinearity arising from the anti-windup compensation. These nonlinearities are in turn expressed in terms of their conic sector bounds, similar to equation (6.37). The stability condition is then derived by applying the small gain theorem to give the following condition (see [69] for details):

$$\sigma_{\max}[\underline{R}\ M_{11}(j\omega)(I+\underline{C}\ M_{11}(j\omega))^{-1}]\leq 1, \quad ,\forall\omega\in\Re, \tag{6.41}$$

where $M_{11}(s)$ is as in Figure 6.3, after isolating the nonlinear part of the system, $\underline{C},\underline{R}$ are, respectively, the cone center and the cone radius for the nonlinear part of the interconnection. For simplicity of exposition, we will take both of these to be $\frac{1}{2}I$. It

can now be easily checked that (6.41) is equivalent to

$$(I+\frac{1}{2}M_{11}(j\omega)^*)^{-1}\frac{1}{2}M_{11}(j\omega)^*\frac{1}{2}M_{11}(j\omega)(I+\frac{1}{2}M_{11}(j\omega))^{-1} \leq I, \quad ,\forall\omega \in \Re, \quad (6.42)$$

which on simplification gives:

$$M_{11}(j\omega)+M_{11}(j\omega)^*+2I>0, \ \forall\omega \in \Re. \quad (6.43)$$

Clearly, the above condition is the same as (6.19) of Theorem 6.2, with $W = I$. Note that the stability condition (6.41) derived by Kapasouris and Athans [69] does not take into account the diagonal structure of the nonlinearities since it chooses $W = I$.

6.4.5 The Analysis of Åström and Rundqwist

Åström and Rundqwist [6] suggested the use of describing functions in conjunction with the Circle Criterion to establish stability of anti-windup control systems. Redrawing the anti-windup control system as in Figure 6.3, we see that describing function theory predicts the existence of a limit cycle for the case of a scalar nonlinearity if the Nyquist plot of $M_{11}(s)$ crosses the interval $(-\infty,-1)$ on the real axis. Based on this observation, Åström and Rundqwist [6] suggest that a condition which will guarantee that this does not happen is that

$$Re(M_{11}(j\omega))+1>0, \quad \forall\omega \in \Re. \quad (6.44)$$

Clearly, the above condition is equivalent to

$$M_{11}(j\omega)+M_{11}(j\omega)^*+2>0, \quad \forall\omega \in \Re, \quad (6.45)$$

which is exactly condition (6.19) of Theorem 6.2 with $W = 1$.

6.4.6 The Analysis of Zheng *et al.*

A modification of the internal model control (IMC) structure to account for input constraints was presented by Zheng *et al.* [143]. This anti-windup implementation of IMC was analyzed for its stability properties, through an example, using the Off-Axis Circle Criterion. In the framework of Figure 6.3, the stability condition (scalar case) in this case is the following:

$$Re[e^{j\theta}(M_{11}(j\omega)+1)] > 0, \qquad \forall \omega \in \Re, \tag{6.46}$$

$$\Leftrightarrow \; e^{j\theta}(M_{11}(j\omega)+1) + e^{-j\theta}(M_{11}(j\omega)^*+1) > 0, \qquad \forall \omega \in \Re, \tag{6.47}$$

for some $\theta \in (-\frac{\pi}{2}, \frac{\pi}{2})$. Note that $e^{j\theta}$ can be obtained as a limiting case of the elements of the class of SISO RC and RL multipliers [139], as the number of terms in the RC/RL multipliers tends to infinity. We may also note that the RC and RL multipliers introduced in [139] are special cases of the multipliers characterized in Theorem 6.4 by equation (6.28). In this sense, condition (6.47) can be obtained from condition (6.29) of Theorem 6.4 by using these RC/RL multipliers and letting the number of terms in these multipliers tend to infinity.

6.5 Example

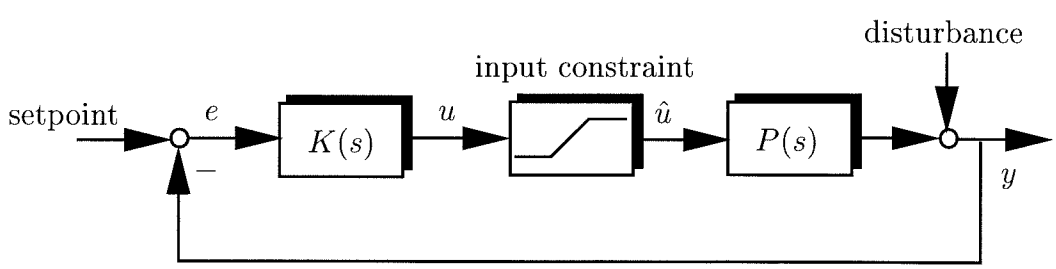

Figure 6.7: Standard feedback interconnection for the example.

The plant we consider here is a fourth order lead-lag butterworth filter taken from

Doyle *et al.* (1987) [43]:

$$P(s) = 0.2\left(\frac{s^2 + 2\xi_1\omega_1 s + \omega_1^2}{s^2 + 2\xi_1\omega_2 s + \omega_2^2}\right)\left(\frac{s^2 + 2\xi_2\omega_1 s + \omega_1^2}{s^2 + 2\xi_2\omega_2 s + \omega_2^2}\right)$$

where $\omega_1 = 0.2115, \omega_2 = 0.0473, \xi_1 = 0.3827$ and $\xi_2 = 0.9239$. The control input u to the plant is constrained to lie in the range $[-0.5, 0.5]$, i.e., (see Figure 6.7)

$$\hat{u} = \text{sat}(u) = \begin{cases} -0.5 & \text{if } u < -0.5 \\ u & \text{if } -0.5 \leq u \leq 0.5 \\ 0.5 & \text{if } u > 0.5. \end{cases}$$

In the absence of any input constraints, a PI controller which stabilizes the plant is given by

$$K(s) = k(1 + \frac{1}{\tau_I s}), \text{ with } k = 100,\ \tau_I = 10.$$

The feedback interconnection in Figure 6.7 can be redrawn in the standard form of Figure 4.5 with N in Figure 4.5 corresponding to the saturation nonlinearity in Figure 6.7.

We would like to analyze the stability properties of typical anti-windup schemes applied to this problem. Several anti-windup schemes and the anti-windup controller $\hat{K}(s)$ corresponding to Figure 4.5 are listed below (see Chapter 2 for a description of these techniques). The corresponding values of the matrix parameters H_1 and H_2 in the general AWBT framework of §4.2, as summarized in Table 4.1, are also listed.

- **Classical anti-reset windup:**

$$\hat{K}(s) = \left[\begin{array}{c|cc} -\frac{1}{\tau_r} & \frac{k}{\tau_I\tau_r}(\tau_r - \tau_I) & \frac{1}{\tau_r} \\ \hline 1 & k & 0 \end{array}\right],\ H_1 = \frac{1}{\tau_r},\ H_2 = 1,$$

  where τ_r is the so-called *reset* time constant.

- **Hanus' conditioned controller:**

$$\hat{K}(s) = \left[\begin{array}{c|cc} -\frac{1}{\tau_I} & 0 & \frac{1}{\tau_I} \\ \hline 1 & k & 0 \end{array}\right], \; H_1 = \frac{1}{\tau_I}, \; H_2 = 1.$$

- **Generalized conditioned controller:**

$$\hat{K}(s) = \left[\begin{array}{c|cc} -\frac{k}{\tau_I(k+\rho)} & \frac{k\rho}{\tau_I(k+\rho)} & \frac{k}{\tau_I(k+\rho)} \\ \hline 1 & k & 0 \end{array}\right], \; H_1 = \frac{k}{\tau_I(k+\rho)}, \; H_2 = 1,$$

  where ρ is a tuning parameter.

- **Observer-based anti-windup:**

$$\hat{K}(s) = \left[\begin{array}{c|cc} -L & \frac{k}{\tau_I} - Lk & L \\ \hline 1 & k & 0 \end{array}\right], \; H_1 = L, \; H_2 = 1,$$

  where L is the observer gain.

AWBT design for these seemingly different techniques can be considered as the single problem of choosing an appropriate H_1 (or equivalently, L in the observer-based anti-windup scheme) since a given value of H_1 corresponds to unique values of the AWBT parameters τ_r, ρ and L in these techniques. Note that the Hanus' conditioned controller has no free AWBT parameters to "tune" or optimize nonlinear performance.

Table 6.1 shows the results of applying the stability tests from Theorems 6.2, 6.3, 6.4 (using a finite series expansion of the multiplier), and the Off-Axis Circle Criterion, for various values of the single free anti-windup parameter H_1. The corresponding multipliers $X - W(s)$ establishing stability for the four cases above, using Theorem 6.4 and the finite dimensional approximation of the multiplier, as discussed in §6.3.2.3, are given respectively by

- $H_1 = 1$:

$$1.4118 - \frac{2.0237}{s+1} + \frac{0.7659}{(s+1)^2} - \frac{0.1534}{(s+1)^3} - \frac{6.072 \times 10^{-4}}{s-1} - \frac{5.9974 \times 10^{-4}}{(s-1)^2} - \frac{5.04 \times 10^{-4}}{(s-1)^3}.$$

H_1	1	10	100	10000
Theorem 2 (Circle Criterion)	inconclusive	inconclusive	inconclusive	inconclusive
Theorem 3 (Popov Criterion)	inconclusive	inconclusive	inconclusive	inconclusive
Off-Axis Circle Criterion	inconclusive	inconclusive	inconclusive	inconclusive
Theorem 4	stable	stable	stable	stable

Table 6.1: Application of various AWBT stability conditions.

- $H_1 = 10$:

$$1234.6 - \frac{183.442}{s+1} - \frac{1048.8}{(s+1)^2} - \frac{0.5927}{s-1} + \frac{0.6012}{(s-1)^2}.$$

- $H_1 = 100$:

$$19.7278 - \frac{1.2138}{s+1} - \frac{18.47}{(s+1)^2} - \frac{0.0116}{s-1} + \frac{0.0127}{(s-1)^2}.$$

- $H_1 = 10000$:

$$346.59 - \frac{18.65}{s+1} - \frac{326.97}{(s+1)^2} - \frac{0.2407}{s-1} + \frac{0.2415}{(s-1)^2}.$$

A simple Nyquist plot like the one shown in Figure 6.8(a) can be used to verify that in each case, these multipliers satisfy the frequency domain condition (6.23) of Theorem 6.4. The Nyquist plot of $M_{11}(s) + 1$ is shown in Figure 6.8(b). Comparing the two Nyquist plots, we see that by multiplying $M_{11}(s) + 1$ with the multiplier $X - W(s)$, we effectively move the Nyquist plot to the right of the imaginary axis, as required by the stability condition in Theorem 6.4.

6.6 Conclusions

In this chapter, we presented a general approach for analyzing the stability properties of AWBT control systems. The approach involved application of the passivity theorem with suitable choice of multipliers to develop sufficient conditions for stability. This AWBT stability analysis framework allowed us to consider any multivariable

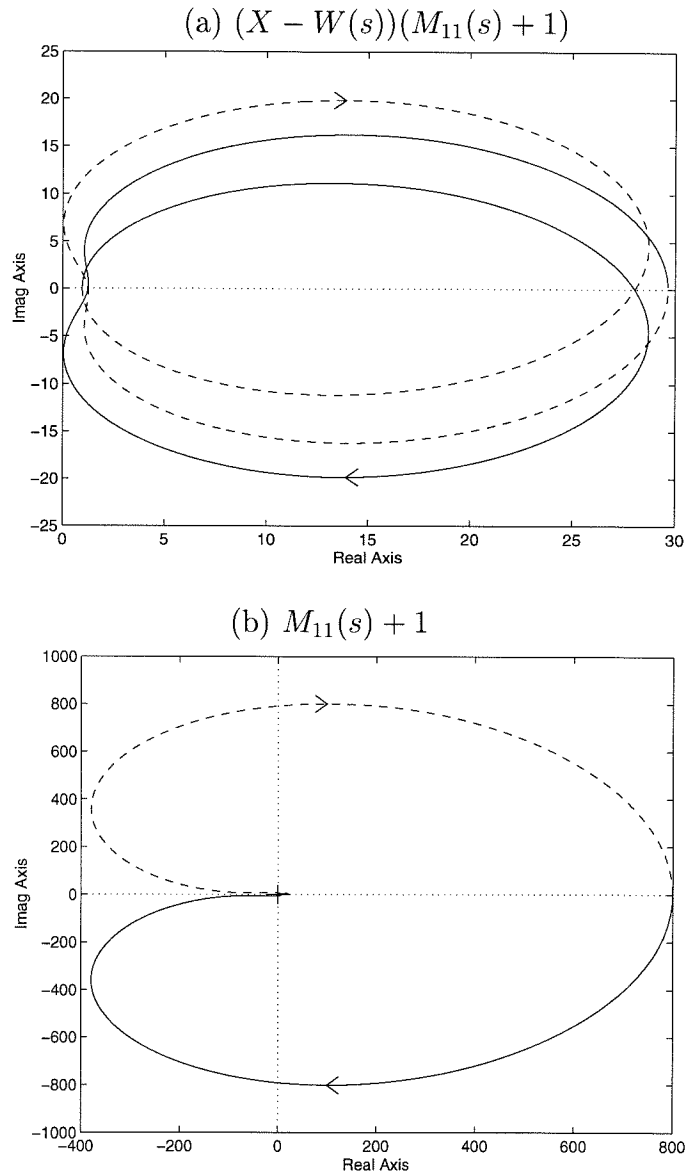

Figure 6.8: Nyquist plot of (a) $(X - W(s))(M_{11}(s) + 1)$; (b) $M_{11}(s) + 1$ for $H_1 = 1$.

linear AWBT control system subject to multivariable control input nonlinearities. In the same setting, we could deal with several classes of input nonlinearities encountered in operating control systems, such as saturation, relay, dead-zone, hysteresis, switching/override/logic-based nonlinearities and combinations thereof.

The basic premise was to cover the input nonlinearity by a class of sector bounded memoryless structured nonlinearities and then apply concepts from absolute stability

theory to develop sufficient conditions guaranteeing stability for all nonlinearities in the specified class. Indeed, this has been the predominant approach to analyzing stability properties of AWBT control system reported in the literature [27, 28, 43, 57, 58, 59, 69]. These previous attempts to analyze AWBT stability properties were based on application of seemingly diverse results and theorems to the AWBT problem. Our approach generalizes these previous attempts to analyze AWBT stability. This generalization comes from two sources:

- The AWBT framework from Chapter 4, which is central to the AWBT stability problem under consideration, unifies all known LTI AWBT schemes reported in the literature.

- The multiplier approach to stability analysis used in this chapter has been shown to be a generalization of several seemingly diverse stability analysis techniques [10, 11, 116]. Similarly, the connection between the multiplier approach and conventional Lyapunov stability analysis is also well-established [9].

Thus, Theorems 6.2 and 6.3 generalize the results from [6, 27, 28, 43, 69] and [57, 58, 59] respectively, which were derived using small-gain arguments, μ upper bounds, a version of the multi-loop Circle Criterion, describing functions and the SISO Popov Criterion. Theorem 6.4, in its general form, has never been used for analyzing AWBT stability. One particular case which it generalizes is the Off-Axis Circle Criterion which was used in [143] for analyzing stability of the anti-windup IMC scheme.

Moreover, our sufficient conditions for AWBT stability, derived under various restrictions on the input nonlinearity, can be checked easily via the feasibility of equivalent convex LMI conditions. In particular, the multiplier establishing stability can be explicitly constructed from the feasible solution to the LMIs. The necessary conditions, derived in §6.3.3, give insight into the extent of conservatism involved in the sufficient AWBT stability conditions. Extensions to account for structured plant uncertainty can be worked out in a straightforward manner by augmenting the nonlinear block N with structured, norm-bounded uncertainty blocks and using "mixed" multipliers.

The ultimate goal in studying AWBT control schemes is to develop systematic AWBT synthesis techniques for designing the AWBT matrix parameters H_1 and H_2. In Chapter 7, we will use the analysis results presented in this chapter as a starting point to study the AWBT synthesis problem.

6.7 Appendix A: Proof of Theorem 6.4

We will need several subsidiary lemmas before we can prove Theorem 6.4. Most of these lemmas are straightforward extensions of the scalar results from [141] to the multivariable case. Hence, we will only outline the proofs without going into details. We begin with a factorization lemma.

Lemma 6.3 *Let $w_i(t)$, $i =, 1, 2, \ldots, n_u$ be the impulse response of a scalar LTI (possibly non-causal) operator on $t \in (-\infty, \infty)$ satisfying (6.28) for some $X_i > 0$. Let $W_i(s)$ be its Laplace transform*

$$W_i(s) = \int_{-\infty}^{\infty} e^{-st} w_i(t)\, dt, \;\; i = 1, 2, \ldots, n_u. \tag{6.48}$$

Let $W(s) = diag(W_1(s), W_2(s), \ldots, W_{n_u}(s))$ and $X = diag(X_1, X_2, \ldots, X_{n_u}) > 0$. Then, there exist matrix transfer functions $W_+(s)$ and $W_-(-s)$ which are stable and proper with stable and proper inverses such that

$$X - W(s) = W_-(s) W_+(s). \tag{6.49}$$

Proof. From [141, Lemma 3], it follows that since $\int_{-\infty}^{\infty} |w_i(t)|\, dt < X_i$, there exist scalar transfer functions $W_{i-}(-s)$, $W_{i+}(s)$ which are stable and proper with stable and proper inverses such that

$$X_i - W_i(s) = W_{i-}(s) W_{i+}(s), \quad i = 1, 2, \ldots, n_u.$$

Choosing $W_-(s) = \text{diag}(W_{1-}(s), \ldots, W_{n_u-}(s))$, $W_+(s) = \text{diag}(W_{1+}(s), \ldots, W_{n_u+}(s))$ then establishes the lemma. ■

Lemma 6.4 *Let $w_i(t), W_i(s), W(s), X_i, X$ be as in Lemma 6.3. Let $X - W(s)$ be factorized as $W_-(s)W_+(s)$ as in Lemma 6.3. Let $N = diag\{N_1, \ldots, N_{n_u}\}$ be a static, monotone non-decreasing, passive nonlinearity. If either N_i is odd or $w_i(t) \geq 0,\ t \in \Re$, then $W_-(-s)^T \circ N \circ W_+(s)^{-1}$ is passive.*

Proof. From [141, Proposition 1], since $\int_{-\infty}^{\infty} |w_i(t)|\ dt < X_i$ and either N_i is odd or $w_i(t) \geq 0,\ t \in \Re$, we conclude that $(X_i - W_i(-s)) \circ N_i$ is passive, i.e.,

$$\begin{aligned} \langle x_{iT} | [(X_i - W_i(-s)) \circ N_i x_i]_T \rangle &\geq 0, \forall\ x_i \in \Re,\ T \geq 0 \\ \Leftrightarrow \langle x_{iT} | [W_{i+}(-s)W_{i-}(-s) \circ N_i x_i]_T \rangle &\geq 0, \forall\ x_i \in \Re,\ T \geq 0 \\ \Leftrightarrow \langle [W_{i+}(s)x_i]_T | [W_{i-}(-s) \circ N_i x_i]_T \rangle &\geq 0, \forall\ x_i \in \Re,\ T \geq 0 \end{aligned}$$

$\Leftrightarrow \langle y_{iT} | [W_{i-}(-s) \circ N_i \circ W_{i+}(s)^{-1} y_i]_T \rangle \geq 0, \forall\ y_i \in \Re,\ T \geq 0$ (substituting $y = W_{i+}(s)x_i$).

Hence $W_{i-}(-s)^T \circ N_i \circ W_{i+}(s)^{-1}$ is passive. Since $W_-(-s)^T \circ N \circ W_+(s)^{-1}$ is a diagonal operator with all its diagonal entries passive, hence it is passive. ■

Lemma 6.5 *Let $N = diag\{N_1, \ldots, N_{n_u}\}$ be a diagonal nonlinearity satisfying the conditions in Definitions 6.4 and 6.5. Suppose we apply the loop transformation of Figure 6.4 to N to get a diagonal nonlinearity $\tilde{N} = diag\{\tilde{N}_1, \ldots, \tilde{N}_{n_u}\}$ with $\tilde{N}_i \in$ sector$[0, \infty]$. Then, if N is odd and monotone non-decreasing, so is $\tilde{N}$.*

Proof. Since $N = \text{diag}\{N_1, \ldots, N_{n_u}\}$, if N is odd, monotone non-decreasing, then so are $N_i,\ i = 1, 2, \ldots, n_u$. From [141, §7], we conclude that if N_i is odd, monotone non-decreasing, then so is $\tilde{N}_i$. The lemma then follows since $\tilde{N} = \text{diag}\{\tilde{N}_1, \ldots, \tilde{N}_{n_u}\}$. ■

Proof of Theorem 6.4. As in the proofs of Theorems 6.2 and 6.3, we can show that $M(s)$ is stable and the $M_{11}(s) - N$ loop is well-posed. Also, we can transform the $M_{11}(s) - N$ loop to the $\tilde{M}_{11}(s) - \tilde{N}$ loop where $\tilde{M}_{11}(s) = M_{11}(s) + I$ and $\tilde{N} = \text{diag}\{\tilde{N}_1, \ldots, \tilde{N}_{n_u}\},\ \tilde{N}_i \in \text{sector}[0, \infty]$, with $\tilde{N}$ passive. From Lemma 6.5, we conclude that if N is odd, monotone non-decreasing and incrementally inside sector$[0, I]$, then $\tilde{N}$ is odd and monotone non-decreasing.

We can now apply Corollary 6.1 to the $\tilde{M}_{11}(s) - \tilde{N}$ loop with $H(s) = \tilde{M}_{11}(s)$ and $f = \tilde{N}$. The appropriate multiplier is $X - W(s)$, where $W(s) = \text{diag}(W_1(s), \ldots, W_{n_u}(s))$, with the impulse responses $w_i(t)$ of the scalar transfer functions $W_i(s)$ satisfying (6.28). From Lemma 6.3, we conclude that $X - W(s)$ can be factorized into $W_-(s)W_+(s)$ which satisfy conditions 1 and 2 of Corollary 6.1. By Lemma 6.4, (6.9) of Corollary 6.1 holds with $\delta_2 = 0$. (6.8) and (6.10) can be checked via (6.11) (see Remark 6.2) as follows:

$$(X - W(j\omega))(M_{11}(j\omega) + I) + (M_{11}^*(j\omega) + I)(X - W^*(j\omega)) \geq \delta_1 I, \ \forall \ \omega \in \Re$$

which establishes (6.29) and the proof is complete. ■

Chapter 7 Multivariable Anti-Windup Controller Synthesis using Multi-Objective Optimization

Abstract

We consider the problem of multivariable anti-windup bumpless transfer (AWBT) controller synthesis based on the general AWBT framework presented in Chapter 4. Numerous existing AWBT synthesis techniques are reviewed. Next, we give a completely general formulation of the AWBT controller synthesis problem and propose several possible solutions to obtain an appropriate AWBT controller. We use recent results on multi-objective controller synthesis to show how these numerous approaches can give a solution in terms of linear matrix inequalities (LMIs).

7.1 Introduction

In Chapter 4, we presented a general AWBT framework based on the classical two-step design concept of AWBT. This framework was shown to capture the essential structure inherent in existing AWBT control schemes. Not surprisingly, the resulting framework was shown to unify numerous existing LTI AWBT schemes in terms of two matrix parameters H_1 and H_2.

In Chapter 6, we addressed the problem of analyzing stability of anti-windup control schemes by applying the passivity theorem and multiplier theory to develop sufficient stability conditions. Moreover, we showed that these results generalized several previously reported attempts to analyze stability of anti-windup schemes, which were based on seemingly diverse techniques such as the Popov, Circle and Off-Axis Circle criteria [57, 69, 143], the optimally scaled small-gain theorem (with constant scalings) [6, 27, 43] and describing functions [6]. Also, the AWBT stability conditions developed in Chapter 6 were shown to be less conservative than those

reported in the literature.

Despite these developments in the area of AWBT analysis, AWBT *synthesis*, i.e., the design of suitable AWBT compensated controllers, remains an active area of research mainly because of the lack of a general satisfactory solution to the synthesis problem. Below, we summarize the existing literature on AWBT controller synthesis:

- Åström and Hägglund (1988) [5, page 10] presented heuristic guidelines for choosing the reset time-constant τ_r in anti-reset windup PI/PID controllers. A detailed study of the choice of the tuning parameters in the anti-reset windup technique was carried out by Glattfelder *et al.* [57, 58, 59], using the Circle and Popov Criteria for guaranteeing closed-loop stability.

- Hanus *et al.* (1987) [63] proposed the "conditioning" anti-windup technique and the concept of realizable references to design the "conditioned controller" applicable to linear controllers which are biproper. A similar technique was presented by Campo and Morari (1990) [27] based on a different interpretation of windup. Extension of the conditioning anti-windup technique to handle strictly proper linear controllers has been reported in [131].

- An interpretation of windup under control input nonlinearities is that the states of the controller do not correspond to the control signal being injected into the plant. To correct for this controller state error, Åström *et al.* [6, 7] suggested the use of an observer. However, they did not provide any guidelines for choosing the observer gain other than the *a posteriori* check of closed-loop stability using describing functions and hyperstability theory. An investigation of the design of this observer gain was recently carried out by Kapoor *et al.* (1995) [72].

- In the context of multivariable controllers with integral action, Kapasouris and Athans (1985) [69] used a static nonlinearity to "turn-off" the integrators during saturation, thereby preventing reset-windup.

- Kapasouris *et al.* [70, 71] presented a technique based on the use of an Error Governor (EG) to scale down the input to the controller so as to prevent actuator

saturation, thereby preventing controller windup.

- Dynamic anti-windup compensation schemes which employ a dynamic feedback component in the anti-windup compensation as opposed to a static feedback compensation have been reported by Park and Choi [109] and Teel and Kapoor [126].

Other reported anti-windup schemes include the anti-windup modification for Internal Model Control which we discussed in Chapter 3, the fixed structure one-step anti-windup controller synthesis which minimizes an LQG-type cost presented by Tyan and Bernstein (1995) [129], and a more general factorization approach with minimization of an appropriately defined $\mathcal{H}_\infty$ norm anti-windup objective presented by Miyamoto and Vinnicombe [99].

From the preceding review, we see that there are several useful schemes for AWBT compensation which work for many systems. However, many of these techniques (e.g., [5, 6, 7, 63, 131]) do not provide any guarantees of closed-loop stability and performance. Some (e.g., [70, 71]) are computationally far too complicated to be useful in practice. Moreover, none of them is general enough to allow consideration of different performance criteria, thereby providing insight into the various engineering trade-offs involved in AWBT designs.

In this chapter, we present several possible approaches to synthesizing the AWBT controller in the framework of Chapter 4. We will first show that the AWBT synthesis problem in the framework of Chapter 4 can be reduced to a multi-objective static output feedback synthesis problem. This problem is known to be hard to tackle computationally.

One possible alternative which we will discuss deviates somewhat from the classical two-step design paradigm of AWBT. Instead, it involves design of the AWBT controller in a single step. As we will show, the corresponding *linear* controller, which refers to the controller to be implemented in the absence of control input nonlinearities, can then be recovered from the AWBT controller. In this way, in a single step, we not only design the AWBT controller but also recover the ideal (in the absence

of input nonlinearities) linear controller. A second possible alternative involves using a dynamic anti-windup compensation, and this also deviates somewhat from the classical "static" compensation paradigm of AWBT.

Before we discuss the AWBT synthesis problem, we briefly review some recent results on multi-objective output feedback controller synthesis which will be used in the sequel.

7.2 Multi-Objective Output Feedback Controller Synthesis

In this section, we summarize the essential technical machinery related to output feedback controller synthesis subject to the requirement that the closed-loop system satisfies a number of objectives simultaneously. Much of the literature in this area pertains to the so-called "mixed $\mathcal{H}_2/\mathcal{H}_\infty$" problem [77, 118], though significant generalizations, incorporating numerous other objectives, have been reported recently [55, 119, 120]. Some of the results quoted here have appeared in the literature very recently and a lucid presentation of this material can be found in [119, 120].

Consider the finite dimensional LTI plant $G(s)$ in Figure 7.1, described by

$$\begin{bmatrix} z_1 \\ z_2 \\ y \end{bmatrix} = G(s) \begin{bmatrix} w_1 \\ w_2 \\ u \end{bmatrix} = \left[\begin{array}{c|ccc} A & B_1 & B_2 & B \\ \hline C_1 & D_{11} & D_{12} & E_1 \\ C_2 & D_{21} & D_{22} & E_2 \\ C & D_1 & D_2 & 0 \end{array}\right] \begin{bmatrix} w_1 \\ w_2 \\ u \end{bmatrix}. \tag{7.1}$$

Here, as usual, u is the control input, y is the measured output available to the controller, and the channels $w_i \longrightarrow z_j$ can be used to specify different performance objectives. The controller is a finite dimensional LTI system

$$u = C(s)y = \left[\begin{array}{c|c} A_c & B_c \\ \hline C_c & D_c \end{array}\right] y. \tag{7.2}$$

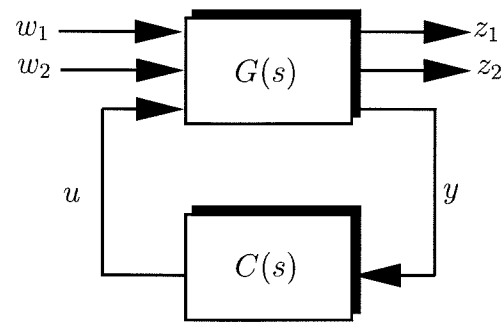

Figure 7.1: Multi-objective controller synthesis.

The closed-loop system is given by

$$\begin{bmatrix} z_1 \\ z_2 \end{bmatrix} = F_l(G(s), C(s)) \begin{bmatrix} w_1 \\ w_2 \end{bmatrix} = \begin{bmatrix} T_{11}(s) & T_{12}(s) \\ T_{21}(s) & T_{22}(s) \end{bmatrix} \begin{bmatrix} w_1 \\ w_2 \end{bmatrix}$$

$$= \left[\begin{array}{c|cc} \mathcal{A} & \mathcal{B}_1 & \mathcal{B}_2 \\ \hline \mathcal{C}_1 & \mathcal{D}_{11} & \mathcal{D}_{12} \\ \mathcal{C}_2 & \mathcal{D}_{21} & \mathcal{D}_{22} \end{array}\right] \begin{bmatrix} w_1 \\ w_2 \end{bmatrix}$$

$$= \left[\begin{array}{cc|cc} A + BD_cC & BC_c & B_1 + BD_cD_1 & B_2 + BD_cD_2 \\ B_cC & A_c & B_cD_1 & B_cD_2 \\ \hline C_1 + E_1D_cC & E_1C_c & D_{11} + E_1D_cD_1 & D_{12} + E_1D_cD_1 \\ C_2 + E_2D_cC & E_2C_c & D_{21} + E_2D_cD_2 & D_{22} + E_2D_cD_2 \end{array}\right] \begin{bmatrix} w_1 \\ w_2 \end{bmatrix} \tag{7.3}$$

where $F_l(G(s), C(s))$ is the usual *lower* LFT of $G(s)$ and $C(s)$. For the controller $C(s)$ to be stabilizing, $\mathcal{A}$ should have all its eigenvalues in the open left half-plane.

For the purpose of illustration, we consider the classical problem of minimizing, with a stabilizing controller $C(s)$, the $\mathcal{H}_2$ norm of the closed-loop transfer function $T_{11} : w_1 \longrightarrow z_1$, while at the same time ensuring that the $\mathcal{H}_\infty$ norm of the closed-loop transfer function $T_{22} : w_2 \longrightarrow z_2$ is bounded by a prespecified limit. This is the so-called two channel, mixed $\mathcal{H}_2/\mathcal{H}_\infty$ problem. Before addressing this problem, we state two well-known results which relate $\mathcal{H}_2$ and $\mathcal{H}_\infty$ norm bounds to equivalent linear

matrix inequalities (LMIs).

Lemma 7.1 (Bounded Real Lemma) *$\mathcal{A}$ is stable and $\|T_{22}(s)\|_{\mathcal{H}_\infty} = \|\mathcal{C}_2(sI - \mathcal{A})^{-1}\mathcal{B}_2 + \mathcal{D}_{22}\|_{\mathcal{H}_\infty} < \gamma$ iff there exists a real symmetric matrix $\mathcal{X} > 0$ such that the following linear matrix inequality (LMI) in $\mathcal{X}$ holds:*

$$\begin{bmatrix} \mathcal{A}^T\mathcal{X} + \mathcal{X}\mathcal{A} & \mathcal{X}\mathcal{B}_2 & \mathcal{C}_2^T \\ \mathcal{B}_2^T\mathcal{X} & -\gamma I & \mathcal{D}_{22}^T \\ \mathcal{C}_2 & \mathcal{D}_{22} & -\gamma I \end{bmatrix} < 0. \tag{7.4}$$

Proof. See [21, page 91]. ■

Lemma 7.2 *$\mathcal{A}$ is stable and $\|T_{11}(s)\|_{\mathcal{H}_2} = \|\mathcal{C}_1(sI - \mathcal{A})^{-1}\mathcal{B}_1 + \mathcal{D}_{11}\|_{\mathcal{H}_2} < \alpha$ iff $\mathcal{D}_{11} = 0$ and there exist real symmetric matrices $\mathcal{Y}$, Z such that the following LMIs in $\mathcal{Y}$ and Z hold:*

$$\begin{bmatrix} \mathcal{A}^T\mathcal{Y} + \mathcal{Y}\mathcal{A} & \mathcal{Y}\mathcal{B}_1 \\ \mathcal{B}_1^T\mathcal{Y} & -I \end{bmatrix} < 0, \quad \begin{bmatrix} \mathcal{Y} & \mathcal{C}_1^T \\ \mathcal{C}_1 & Z \end{bmatrix} > 0, \quad \text{trace}(Z) < \alpha. \tag{7.5}$$

Proof. See [21, Page 141]. ■

The mixed $\mathcal{H}_2/\mathcal{H}_\infty$ problem can now be formulated as the minimization of α such that there exists a controller $C(s)$ and the matrices $\mathcal{X}, \mathcal{Y}, Z$ satisfying (7.4) and (7.5). As discussed in [119], this is a computationally expensive problem. The alternative is to solve a modified problem by constraining $\mathcal{X}$ and $\mathcal{Y}$ to be equal, i.e.,

$$\mathcal{X} = \mathcal{Y}. \tag{7.6}$$

In this case, the minimization of α subject to (7.6) amounts to minimizing an upper bound on the original mixed $\mathcal{H}_2/\mathcal{H}_\infty$ objective. A complete solution to this problem has been presented in [119, 120]. Before stating the main result from [119, 120], we state the following result which is the basis for the solution presented in [119, 120].

Lemma 7.3 (Controller parameter transformation) *[119]. Suppose the controller $C(s)$ has the same order as the plant $G(s)$. Let the positive definite matrix $\mathcal{X}$*

in (7.4) and its inverse $\mathcal{X}^{-1}$ *be partitioned according to* $\mathcal{A}$ *as follows:*

$$\mathcal{X} = \begin{bmatrix} X & U \\ U^T & \hat{X} \end{bmatrix}, \quad \mathcal{X}^{-1} = \begin{bmatrix} Y & V \\ V^T & \hat{Y} \end{bmatrix}. \tag{7.7}$$

Define the transformed controller parameters as follows:

$$\begin{aligned} K = XBN + UB_c, \quad L = NCY + C_cV^T, \\ M = X(A - BNC)Y + KCY + XBL + UA_cV^T, \quad N = D_c. \end{aligned} \tag{7.8}$$

Then, with $\mathcal{T} = \begin{bmatrix} I & 0 \\ Y & V \end{bmatrix}$, *the following hold:*

$$\begin{aligned} \mathcal{T}\mathcal{X}\mathcal{T}^T &= \begin{bmatrix} X & I \\ I & Y \end{bmatrix}, \quad \mathcal{T}\mathcal{X}\mathcal{A}\mathcal{T}^T = \begin{bmatrix} XA + KC & M \\ A + BNC & AY + BL \end{bmatrix}, \\ \mathcal{T}\mathcal{X}\mathcal{B}_j &= \begin{bmatrix} XB_j + KD_j \\ B_j + BND_j \end{bmatrix}, \quad \mathcal{C}_j\mathcal{T}^T = \begin{bmatrix} C_j + E_jNC & C_jY + E_jL \end{bmatrix}. \end{aligned} \tag{7.9}$$

Proof. Using the partitions of $\mathcal{X}$ and $\mathcal{X}^{-1}$ from (7.7) and the fact that $\mathcal{X}\mathcal{X}^{-1} = I$, we conclude that $XY + UV^T = I$, $U^TV + \hat{X}\hat{Y} = I$, $XV + U\hat{Y} = 0$, $U^TY + \hat{X}V^T = 0$. The result then follows by direct substitution. ■

The following theorem states necessary and sufficient conditions for the existence of the solution to the modified mixed $\mathcal{H}_2/\mathcal{H}_\infty$ problem. The theorem also gives explicit formulae for computing a controller $C(s)$ achieving this optimum.

Theorem 7.1 (Scherer (1996) [119]) *Assuming that the controller* $C(s)$ *has the same order as the plant* $G(s)$, *the optimal value* α_* *of the objective function in the modified mixed* $\mathcal{H}_2/\mathcal{H}_\infty$ *control problem is given by the minimization of* α *subject to the feasibility of the following LMIs in the matrices* K, L, M, N *and the symmetric*

matrices X, Y, Z:

$$\begin{bmatrix} A^TX + XA + KC + (KC)^T & * & * \\ M^T + A + BNC & AY + YA^T + BL + (BL)^T & * \\ (XB_1 + KD_1)^T & (B_1 + BND_1)^T & -I \end{bmatrix} < 0, \quad (7.10)$$

$$\begin{bmatrix} X & * & * \\ I & Y & * \\ C_1 + E_1NC & C_1Y + E_1L & Z \end{bmatrix} > 0, \quad (7.11)$$

$$\begin{bmatrix} A^TX + XA + KC + (KC)^T & * & * & * \\ M^T + A + BNC & AY + YA^T + BL + (BL)^T & * & * \\ (XB_2 + KD_2)^T & (B_2 + BND_2)^T & -\gamma I & * \\ C_2 + E_2NC & C_2Y + E_2L & D_{22} + E_2ND_2 & -\gamma I \end{bmatrix} < 0, \quad (7.12)$$

$$\text{trace}(Z) < \alpha. \quad (7.13)$$

Moreover, if such a solution exists, then one can always determine nonsingular U and V with $UV^T = I - XY$. Then, a stabilizing controller satisfying the $\mathcal{H}_2$ and $\mathcal{H}_\infty$ norm bounds is given by the following state-space matrices:

$$\begin{aligned} A_c &= U^{-1}(M - X(A - BNC)Y - KCY - XBL)V^{-T}, \\ B_c &= U^{-1}(K - XBN), \quad C_c = (L - NCY)V^{-T}, \quad D_c = N. \end{aligned} \quad (7.14)$$

Proof. We will only sketch the essence of the proof. A detailed treatment can be found in [119]. Let $\mathcal{T}$ be defined as in Lemma 7.3. Applying a congruence transformation $\text{diag}(\mathcal{T}, I)$ to the first two inequalities in (7.5), and using (7.8) and (7.9) from Lemma 7.3, we get (7.10) and (7.11) above. Similarly, applying the congruence transformation $\text{diag}(\mathcal{T}, I, I)$ to (7.4) and again using (7.8) and (7.9) from Lemma 7.3, we get (7.12) above. This establishes necessity.

For sufficiency, note that given X, Y, K, L, M, N establishing the three LMIs (7.10), (7.11), (7.12), we can always find non-singular U and V such that $UV^T = I - XY$.

This follows from (7.11) since $I-XY$ is nonsingular. Defining $\hat{X} = U^{-1}(X-Y^{-1})U^{-T}$ ensures that $\mathcal{X}$ defined by (7.7) is positive definite and $\mathcal{X}^{-1}$ is as defined in (7.7). U, V being nonsingular, the controller transformation (7.8) can be inverted to get the controller matrices A_c, B_c, C_c, D_c as in (7.14). Furthermore, since $\mathcal{T}$ is square nonsingular, the congruence transformations $\mathrm{diag}(\mathcal{T}, I)$ and $\mathrm{diag}(\mathcal{T}, I, I)$ described in the previous paragraph can be inverted to get (7.5) from (7.10), (7.11) and (7.4) from (7.12) respectively. ■

Remark 7.1 *The proof is simple and relies on the following key idea [119]: Given matrix inequalities which contain the terms $\mathcal{X}$, $\mathcal{X}\mathcal{A}$, $\mathcal{X}\mathcal{B}_j$, $\mathcal{C}_j$ and their transposes, we only need to find appropriate congruence transformations involving $\mathcal{T}$ as defined in Lemma 7.3 so as to get matrix inequalities in $\mathcal{T}\mathcal{X}\mathcal{T}^T$, $\mathcal{T}\mathcal{X}\mathcal{A}\mathcal{T}^T$, $\mathcal{T}\mathcal{X}\mathcal{B}_j$, $\mathcal{C}_j\mathcal{T}^T$ and their transposes. Lemma 7.3 then implies that the resulting matrix inequalities are indeed linear matrix inequalities in K, L, M, N, X, Y as we saw in Theorem 7.1.*

Note that the mixed $\mathcal{H}_2/\mathcal{H}_\infty$ problem is only a particular problem we have chosen here for the purpose of illustration. Exploiting the basic idea from Remark 7.1, numerous other performance objectives can be incorporated in the same framework by defining more input and output channels w_i and z_i in Figure 7.1. For example, minimization of the $\mathcal{H}_\infty$ norm (as opposed to the $\mathcal{H}_2$ norm discussed above) of a certain channel subject to an $\mathcal{H}_\infty$ norm constraint on another channel can also be formulated in the same setting as that of Theorem 7.1. Similarly, constraints such as location of the closed-loop poles, positive realness of certain input to output channels, etc., can also be imposed within this framework. We refer the reader to [119, 120] for an excellent discussion of all the implications and extensions of the basic result stated in Theorem 7.1.

It must be stressed that Theorem 7.1 gives only a suboptimal solution to the mixed $\mathcal{H}_2/\mathcal{H}_\infty$ problem due to the restriction (7.6) which requires that the $\mathcal{H}_2$ and $\mathcal{H}_\infty$ norm specifications be expressed in terms of a *single* closed-loop Lyapunov function. As discussed in [119, 120], restrictions such as (7.6) are automatically imposed whenever an additional performance objective (e.g., positive realness of a certain input-output

channel) is incorporated in the problem. This is the inevitable price to be paid for obtaining a convex solution to the problem.

With these preliminaries, we now consider the AWBT controller synthesis problem.

7.3 General AWBT Controller Synthesis

Consider Figure 4.5 which represents the AWBT control problem. We may recall that given the linear controller $K(s)$ as in (4.6) which was designed ignoring control input nonlinearities (see Figure 4.4), any admissible AWBT controller $\hat{K}(s)$ in Figure 4.5 is parameterized by (4.10), (4.11), (4.12) in terms of the matrix parameters H_1 and H_2, with H_2 square invertible.

The classical AWBT controller synthesis problem is to design H_1, H_2 given the linear controller $K(s)$, i.e., given (A, B, C, D). With the exception of [129, 109], this has been the predominant approach to AWBT compensation [5, 6, 7, 27, 43, 63, 72, 143]. We will show next that this problem can be reduced to the synthesis of a structured static output feedback gain matrix.

7.3.1 AWBT Synthesis via Static Output Feedback

Let us assume that $\hat{P}(s)$ is partitioned as in (4.4) as follows:

$$\hat{P}(s) = \begin{bmatrix} P_{11} & P_{12} \\ P_{21} & P_{22} \\ 0 & P_{32} \end{bmatrix} \tag{4.4'}$$

where we have assumed for simplicity that $P_{31}(s) \equiv 0$ which implies that the measurement u_m of the plant input $\hat{u}$ which is provided to $\hat{K}(s)$ is given by

$$u_m = P_{32}\hat{u}. \tag{4.5'}$$

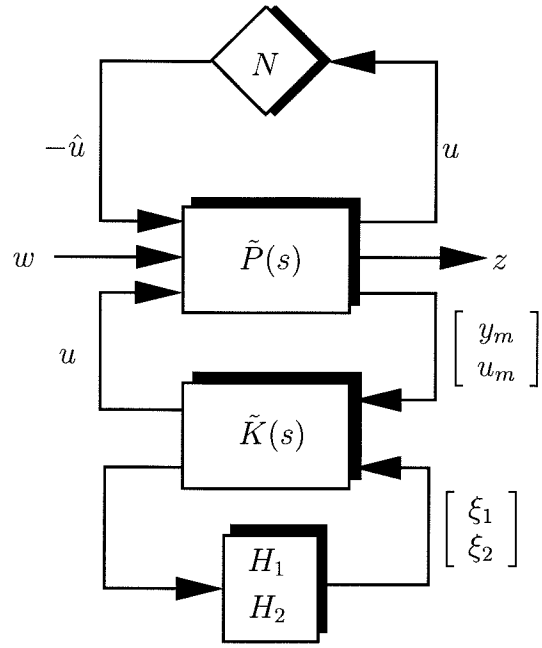

Figure 7.2: AWBT controller synthesis via static output feedback.

Then, with a realization of $\hat{K}(s)$ given by

$$\hat{K}(s) = [U(s) \quad I - V(s)] \tag{4.10'}$$

where

$$V(s) = \left[\begin{array}{c|c} A - H_1C & -H_1 \\ \hline H_2C & H_2 \end{array}\right] \tag{4.11'}$$

$$U(s) = \left[\begin{array}{c|c} A - H_1C & B - H_1D \\ \hline H_2C & H_2D \end{array}\right], \tag{4.12'}$$

the AWBT interconnection in Figure 4.5 can be redrawn in the form shown in Fig-

ure 7.2. It can be verified that $\tilde{P}(s)$ and $\tilde{K}(s)$ in Figure 7.2 are given by

$$\tilde{P}(s) = \begin{bmatrix} 0 & 0 & I \\ -P_{12}(s) & P_{11}(s) & 0 \\ -P_{22}(s) & P_{21}(s) & 0 \\ -P_{32}(s) & 0 & 0 \end{bmatrix}, \quad \tilde{K}(s) = \left[\begin{array}{c|cccc} A & B & 0 & -I & 0 \\ \hline 0 & 0 & I & 0 & I \\ C & D & -I & 0 & 0 \end{array}\right]. \tag{7.15}$$

It should be clear from Figure 7.2 that classical AWBT controller synthesis amounts to designing the static output feedback gain matrix $\begin{bmatrix} H_1 \\ H_2 \end{bmatrix}$ with H_2 square invertible, so as to satisfy certain AWBT performance objectives.

From a computational point of view, solving the general static output feedback synthesis problem even for achieving a single objective such as closed-loop stability in the presence of the nonlinearity N is a non-convex problem. Typically, the AWBT controller $\hat{K}(s)$ is required to satisfy more than one objective to give a meaningful closed-loop design. Such a multi-objective static output feedback synthesis problem is far more difficult to handle computationally (see [28] for a discussion on this point). Partial solutions to this problem can be found in Hanus *et al.* (1987) [63], Campo and Morari (1990) [27] ($H_1 = BD^{-1}$, $H_2 = I$) and in Åström *et al.* [6, 7], Kapoor *et al.* (1995) [72] ($H_1 = L$, $H_2 = I$).

For example, the matrix $\begin{bmatrix} H_1 \\ H_2 \end{bmatrix}$ can be considered as the "controller" $C(s) = \left[\begin{array}{c|c} A_c & B_c \\ \hline C_c & D_c \end{array}\right]$ in the multi-objective synthesis framework of §7.2. However, since $\begin{bmatrix} H_1 \\ H_2 \end{bmatrix}$ is required to be static, we would have to force $C(s)$ to be static by putting $C_c = 0$, $D_c = \begin{bmatrix} H_1 \\ H_2 \end{bmatrix}$, for example. In this case, the controller transformations in

Lemma 7.3 are the following:

$$\begin{aligned} K &= XBN + UB_c, \quad L = NCY, \\ M &= X(A - BNC)Y + KCY + XBL + UA_cV^T, \quad N = D_c. \end{aligned} \tag{7.8'}$$

Note that because we have lost one degree of freedom through the choice $C_c = 0$, we need to enforce the equality constraint

$$L = NCY. \tag{7.16}$$

This immediately makes the synthesis of $C(s) = \left[\begin{array}{c|c} A_c & B_c \\ \hline 0 & D_c \end{array}\right]$ a non-convex problem.

Assuming $H_2 = I$, Marcopoli and Phillips (1996) [95] have solved this problem using an iterative technique involving LMIs to obtain the matrix H_1.

7.3.2 AWBT Synthesis via Dynamic Output Feedback

One alternative to addressing the problem mentioned in the previous section is to allow H_1 and H_2 to be linear *dynamical* systems instead of static gain matrices. In this case, the results from §7.2 can be directly applied to synthesize the dynamical system $\left[\begin{array}{c} H_1(s) \\ H_2(s) \end{array}\right]$ which can be considered as the "controller" $C(s)$ in the multi-objective synthesis framework of Figure 7.1. An approach based on this idea of dynamic AWBT compensation has been reported by Park and Choi (1995) [109]. More recently, this approach has been exploited by Teel and Kapoor [126] in an attempt to come up with a more rigorous anti-windup controller design.

7.3.3 Direct One-Step AWBT Controller Synthesis

As a second alternative, suppose we consider the problem of directly synthesizing the

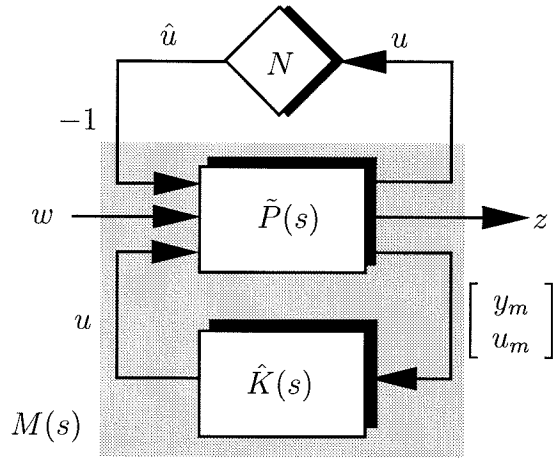

Figure 7.3: One-step direct AWBT controller synthesis for $\hat{K}(s)$.

AWBT controller

$$\hat{K}(s) = \left[\begin{array}{c|cc} A_{\hat{K}} & B_{1,\hat{K}} & B_{2,\hat{K}} \\ \hline C_{\hat{K}} & D_{1,\hat{K}} & D_{2,\hat{K}} \end{array}\right]. \tag{7.17}$$

This is contrary to the classical AWBT paradigm of first designing a linear controller ignoring input nonlinearities and then adding AWBT compensation to account for these nonlinearities. But it does simplify the AWBT controller synthesis. Now, we can design the state-space matrices of a stabilizing (in the presence of the input nonlinearity) AWBT controller $\hat{K}(s)$ satisfying a set of suitably defined objectives in the multi-objective synthesis framework of Figure 7.1.

Once the state-space matrices of $\hat{K}(s)$ are computed, we can then back-calculate A, B, C, D, H_1, H_2 from the following equations which are easily derived by comparing equations (4.10), (4.11), (4.12) with (7.17) above:

$$\begin{aligned} &H_1 = B_{2,\hat{K}}, \quad H_2 = I - D_{2,\hat{K}}, \\ &C = H_2^{-1} C_{\hat{K}}, \quad D = H_2^{-1} D_{1,\hat{K}}, \\ &B = B_{1,\hat{K}} + H_1 D, \quad A = A_{\hat{K}} + H_1 C. \end{aligned} \tag{7.18}$$

Then (A, B, C, D) is a realization of the linear unconstrained controller $K(s)$, and H_1 and H_2 provide the anti-windup compensation via the AWBT controller (4.10).

Note that the additional constraint of H_2 being invertible can be incorporated in the synthesis problem by requiring that $I - D_{2,\hat{K}}$ be invertible.

A similar one-step AWBT synthesis approach has been explored by Tyan and Bernstein (1995) [129] for the case of $H_2 = I$ and has also been suggested by Campo and Morari (1990) [27]. Although such a one-step approach lacks the simplicity of traditional two-step anti-windup designs, it seems to have some appeal for situations where the impact of input nonlinearities on closed-loop performance is particularly severe.

The analysis of Campo and Morari (1990) [27] showed that the requirements of stability and good performance in the presence of input nonlinearities impose certain restrictions on the initial unconstrained (i.e., $N \equiv I$) linear controller design. For example, an overly aggressive or poor initial linear unconstrained controller design might necessarily lead to a poor nonlinear performance in the presence of input nonlinearities, no matter what anti-windup technique is used to correct for input nonlinearities. This is analogous to the situation in linear robust control where the requirements of *robust stability* and *robust performance* in the presence of uncertainty impose restrictions on *nominal* performance. Thus, it seems reasonable to couple the initial linear controller design with the AWBT compensation to achieve the appropriate trade-offs.

Although this is indeed a one-step synthesis approach, we still retain the inherent *structure* underlying the AWBT controller, namely that given by (4.10), (4.11), (4.12). For this one-step approach to be justifiable and meaningful in the anti-windup context, it is important to be able to incorporate, in the controller design, desirable linear unconstrained (i.e., $N \equiv I$) performance criteria as well as nonlinear stability/good performance requirements in the presence of input nonlinearities. We will see in the subsequent discussion how such multiple objectives can be specified in this one-step AWBT problem formulation using the results summarized in §7.2.

7.4 Objectives for AWBT Controller Synthesis

We will first define objectives that need to be satisfied by the AWBT controller such as nonlinear stability [85, 86], linear performance recovery, and good nonlinear performance. We will then show how we can design the state-space matrices of a stabilizing (in the presence of the input nonlinearity) AWBT controller $\hat{K}(s)$ satisfying these requirements, using the results from §7.2. The important feature of the problem formulation is that several AWBT objectives can be incorporated in the design of the AWBT controller $\hat{K}$. In particular, a desired linear performance, which corresponds to $N \equiv I$ can be enforced on the AWBT controller design.

7.4.1 Stability

Our primary concern is to maintain closed-loop stability of the AWBT system (Figure 4.5) in the face of the input nonlinearity N. It is well-known that the presence of the nonlinearity N can destabilize an otherwise stable linear system. In the case of a saturation nonlinearity, a typical instability mechanism could be that the plant input remains "stuck" at the constraint value or limit cycles across the linear regime between the upper and lower constraint values. In the case of mode-switching nonlinearities, instability can result in the form of an indefinite switching between the various operating modes. It is precisely these stability problems which have motivated the various attempts to analyze the AWBT systems for their stability properties.

A detailed discussion of the various issues related to stability of AWBT systems has been addressed in Chapter 6. Here, we will only state the main results which will be used to quantify the nonlinear stability requirement.

Theorem 7.2 *Suppose the diagonal nonlinearity N lies in the sector $[0, I]$, i.e.,*

$$0 \leq u_i N_i(u_i, t) \leq u_i^2, \quad \forall\ i = 1, \ldots, n_u, \quad \forall\ u \in \mathcal{R}^{n_u}.$$

Let $M_{11}(s)$ denote the transfer function relating $-\hat{u}$ to u in Figure 7.2. Then, the closed-loop in Figure 4.5 is stable for all N lying in the sector $[0, I]$ if

1. *$A - H_1C$ has all eigenvalues in the open left-half complex plane;*

2. *$\hat{P}$ in equation (4.4) is asymptotically stable; and*

3. *there exists an appropriate "stability multiplier" $W(s)$ such that*

$$W(j\omega)(M_{11}(j\omega) + I) + (M_{11}^*(j\omega) + I)W^*(j\omega) \geq \delta I, \quad \delta > 0, \quad \forall\, \omega \in \mathcal{R}. \tag{7.19}$$

where the choice of the multiplier $W(s)$ depends on the properties of the nonlinearity N, as discussed in Chapter 6.

The following theorem from Chapter 6 states a necessary condition for AWBT stability.

Theorem 7.3 ([85, 86]) *The AWBT system in Figure 4.5 is $\mathcal{L}_2$ stable for all $N \in$ sector$[0, I]$ only if the AWBT controller $\hat{K}(s)$ stabilizes $\hat{P}(s)\begin{bmatrix} I & 0 \\ 0 & N \end{bmatrix}$ for all constant gain matrices $N = diag\{N_1, N_2, \ldots, N_{n_u}\} \in \mathcal{R}^{n_u}$ such that*

$$0 \leq N \leq I.$$

7.4.2 Recovery of Linear Performance

An obvious requirement of any AWBT design is that it leaves the original linear performance specifications intact in the event that $N \equiv I$. This is the essence of the whole AWBT two-step design philosophy which requires that the AWBT controller $\hat{K}(s)$ should provide compensation only when $N \not\equiv I$ and that it should recover the original linear performance when $N \equiv I$.

Suppose now that $u_m \equiv \hat{u}$, i.e., the exact value of the plant input $\hat{u}$ is available to the AWBT controller $\hat{K}(s)$. This corresponds to the case $P_{32}(s) \equiv I$, i.e. no measurement dynamics. Then it is easy to verify that with $N \equiv I$, the closed-loop transfer functions from w to z are identical in Figure 4.1 and Figure 4.5 and the original linear performance is recovered identically.

However, the assumption that $u_m \equiv \hat{u}$, or equivalently, $P_{32}(s) \equiv I$ is unrealistic. We therefore need to take special care in ensuring that the linear performance specification is indeed recovered with the AWBT controller when $N \equiv I$. This can be made precise as follows. Suppose the original linear controller design (Figure 4.1) achieves the following linear performance objective in terms of the closed-loop map T_{zw}

$$\|T_{zw}\|_{\mathcal{H}_2 \text{ or } \mathcal{H}_\infty} \leq \alpha. \tag{7.20}$$

Let $T_{zw,NL}$ represent the closed-loop transfer function relating w and z in Figure 7.2 when $N \equiv I$. Then, the AWBT design of Figure 7.2 is said to recover the original linear performance if

$$\|T_{zw,NL}\|_{\mathcal{H}_2 \text{ or } \mathcal{H}_\infty} \leq \alpha. \tag{7.21}$$

This definition of linear performance recovery directly extends to the cases with the dynamic AWBT synthesis and the one-step direct AWBT synthesis approaches discussed in §7.3.2 and §7.3.3.

7.4.3 Optimization of AWBT Performance

The issue of an appropriate choice of the objective function to quantify "good" AWBT performance has been an area of interest in numerous recent references [29, 95, 99, 109, 126]. We saw one possible choice in Chapter 3, where we used the 1−norm of the instantaneous difference between the outputs of the constrained ($N \not\equiv I$) and the unconstrained ($N \equiv I$) systems as an anti-windup objective function. Similar objectives using the $\mathcal{L}_2$ norms of this difference vector have been proposed in [29, 109].

We will define AWBT performance in terms of the minimization of the induced $\mathcal{L}_2$ gain between the exogenous input w and the output z. Denoting the mapping from w to z by T_{zw}, we require that the induced $\mathcal{L}_2$ gain between w and z be less than 1 for all nonlinearities N lying in the sector $[0, I]$. This is equivalent to checking that the interconnection shown in Figure 7.4 is stable for all unstructured Δ_p which

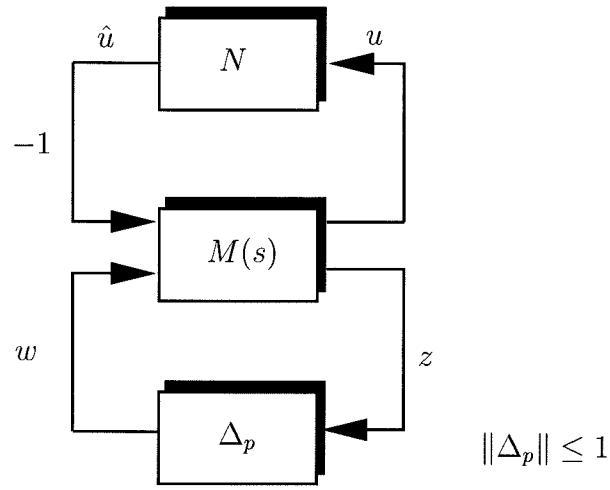

Figure 7.4: Interconnection for AWBT performance analysis.

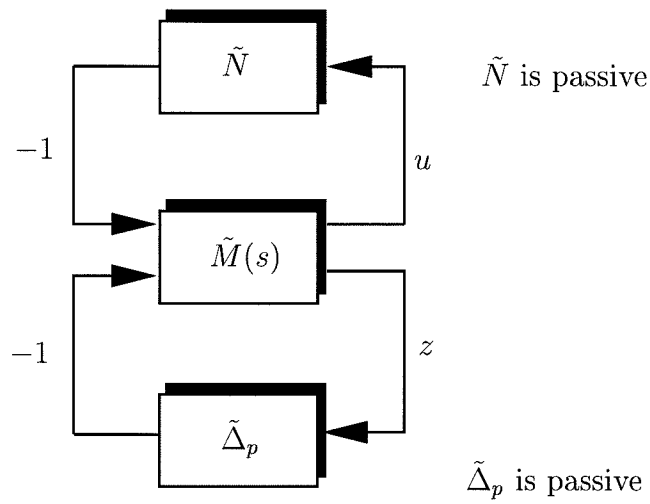

Figure 7.5: Interconnection for AWBT performance analysis in the passivity framework.

are norm bounded by 1. Applying the loop transformation discussed in Chapter 6, we can transform the interconnection in Figure 7.4 to that in Figure 7.5. Then, performance requirement is equivalent to checking the stability of the interconnection in Figure 7.5. We state the performance requirement in the following theorem.

Theorem 7.4 *The induced $\mathcal{L}_2$ gain between w and z is less than 1 for all input nonlinearities N lying in the sector $[0, I]$ if*

1. *$A - H_1C$ has all eigenvalues in the open left-half complex plane;*

2. *$\hat{P}$ in equation (4.4) is asymptotically stable; and*

3. *there exists an appropriate "stability multiplier" $W(s)$ such that*

$$\begin{bmatrix} W(j\omega) & 0 \\ 0 & I \end{bmatrix} \begin{bmatrix} \tilde{M}_{11}(j\omega) & \tilde{M}_{12}(j\omega) \\ \tilde{M}_{21}(j\omega) & \tilde{M}_{22}(j\omega) \end{bmatrix} \quad \textit{is generalized strictly positive real.} \tag{7.22}$$

The choice of the multiplier $W(j\omega)$ depends on the properties of the nonlinearity N, as discussed in Chapter 6.

7.5 AWBT Controller Synthesis

The three performance requirements described in the previous section need to be incorporated in the multi-objective controller synthesis framework of §7.2 to design the AWBT controller $\hat{K}(s)$. From a conceptual point of view, this is most feasible for the case where H_1, H_2 are allowed to be dynamical systems or in the one-step AWBT synthesis approach of §7.3.3. There is, however, an iteration involved due the multiplier $W(s)$. In this case, one would iterate between the search for the multiplier $W(s)$ which establishes the condition in Theorem 7.4 and the search for the AWBT compensation.

7.6 Conclusions

In this chapter, we addressed the AWBT controller synthesis problem. We showed that the classical two-step AWBT synthesis problem leads to a static output feedback synthesis problem which is computationally difficult to solve. Two alternatives involving use of dynamic AWBT compensation and a one-step AWBT design were outlined. Background material on multi-objective output feedback controller synthesis was presented. Objectives for obtaining "good" AWBT controllers were defined.

A promising outline for the design of the AWBT controller $\hat{K}$ was presented.

Chapter 8 Robust Constrained Model Predictive Control using Linear Matrix Inequalities

Abstract

The primary disadvantage of current design techniques for model predictive control (MPC) is their inability to deal *explicitly* with plant model uncertainty. In this chapter, we present a new approach for robust MPC synthesis which allows explicit incorporation of the description of plant uncertainty in the problem formulation. The uncertainty is expressed both in the time and frequency domains. The goal is to design, at each time step, a state-feedback control law which minimizes a "worst-case" infinite horizon objective function, subject to constraints on the control input and plant output. Using standard techniques, the problem of minimizing an upper bound on the "worst-case" objective function, subject to input and output constraints, is reduced to a convex optimization involving linear matrix inequalities (LMIs). It is shown that the feasible receding horizon state-feedback control design robustly stabilizes the set of uncertain plants. Several extensions, such as consideration of the output feedback case, application to systems with time-delays, problems involving constant set-point tracking, trajectory tracking and disturbance rejection, which follow naturally from our formulation, are discussed. The controller design is illustrated with two examples.

8.1 Introduction

Model Predictive Control (MPC), also known as Moving Horizon Control (MHC) or Receding Horizon Control (RHC), is a popular technique for the control of slow dynamical systems, such as those encountered in chemical process control in the petrochemical, pulp and paper industries, and in gas pipeline control. At every time

instant, MPC requires the on-line solution of an optimization problem to compute optimal control inputs over a fixed number of future time instants, known as the "time horizon." Although more than one control move is generally calculated, only the first one is implemented. At the next sampling time, the optimization problem is reformulated and solved with new measurements obtained from the system. The on-line optimization can be typically reduced to either a linear program or a quadratic program.

Using MPC, it is possible to handle inequality constraints on the manipulated and controlled variables in a systematic manner during the design and implementation of the controller. Moreover, several process models as well as many performance criteria of significance to the process industries can be handled using MPC. A fairly complete discussion of several design techniques based on MPC and their relative merits and demerits can be found in the review article by Garcia et al. (1989) [52].

Perhaps the principal shortcoming of existing MPC-based control techniques is their inability to *explicitly* incorporate plant model uncertainty. Thus, nearly all known formulations of MPC minimize, on-line, a *nominal* objective function, using a single linear time-invariant (LTI) model to predict the future plant behavior. Feedback, in the form of plant measurement at the next sampling time, is expected to account for plant model uncertainty. Needless to say, such control systems which provide "optimal" performance for a particular model may perform very poorly when implemented on a physical system which is not exactly described by the model (for example, see [145]).

Similarly, the extensive amount of literature on stability analysis of MPC algorithms [33, 34, 49, 102, 114, 128, 137, 136, 142] is by and large restricted to the nominal case, with no plant-model mismatch; the issue of the behavior of MPC algorithms in the face of uncertainty, i.e., "robustness," has been addressed to a much lesser extent. Broadly, the existing literature on robustness in MPC can be summarized as follows:

- *Analysis of robustness properties of MPC.* Garcia and Morari [49, 50, 51] have analyzed the robustness of unconstrained MPC in the framework of internal model control (IMC) and have developed tuning guidelines for the IMC filter

to guarantee robust stability. Zafiriou (1990) [136] and Zafiriou and Marchal (1991) [137] have used the contraction properties of MPC to develop necessary/sufficient conditions for robust stability of MPC with input and output constraints. Given upper and lower bounds on the impulse response coefficients of a single-input-single-output (SISO) plant with Finite Impulse Responses (FIR), Genceli and Nikolaou (1993) [53] have presented robustness analysis of constrained ℓ_1-norm MPC algorithms. Polak and Yang (1993) [111, 112] have analyzed robust stability of their MHC algorithm for continuous-time linear systems with variable sampling times by using a "contraction" constraint on the state. This "contraction" constraint idea has been further explored in [37, 144]. A review of stability analysis using the so-called "end-point constraints" can be found in [8].

- *MPC with explicit uncertainty description.* The basic philosophy of MPC-based design algorithms which explicitly account for plant uncertainty [2, 26, 145] is the following:

  > *Modify the on-line constrained minimization problem to a min-max problem, i.e., minimization of the worst-case value of the objective function, where the worst-case is taken over the set of uncertain plants.*

  Based on this concept, Campo and Morari (1987) [26], Allwright and Papavasiliou (1992) [2] and Zheng and Morari (1993) [145] have presented robust MPC schemes for SISO FIR plants, given uncertainty bounds on the impulse response coefficients. For certain choices of the objective function, the on-line problem is shown to be reducible to a linear program.

  One of the problems with this linear programming approach is that to simplify the on-line computational complexity, one must choose simplistic, albeit unrealistic model uncertainty descriptions, for example, fewer FIR coefficients. Secondly, this approach cannot be extended to unstable systems.

  Robust MPC algorithms using "contraction constraints" and "end-point con-

straints" can be found in [37, 111, 112, 144] and [8] respectively.

From the preceding review, we see that there has been progress in the *analysis* of robustness properties of MPC. But *robust synthesis*, i.e., the explicit incorporation of realistic plant uncertainty description in the problem formulation, has been addressed only in a restrictive framework for FIR models. There is a need for computationally inexpensive techniques for robust MPC synthesis which are suitable for on-line implementation and which allow incorporation of a broad class of model uncertainty descriptions.

In this chapter, we present one such MPC-based technique for the control of plants with uncertain models. This technique is motivated by recent developments in the theory and application (to control) of optimization involving Linear Matrix Inequalities (LMIs) [21]. There are two reasons why LMI optimization is relevant to MPC. Firstly, as we discussed in Chapter 5, LMI-based optimization problems can be solved in polynomial-time, often in times comparable to that required for the evaluation of an analytical solution for a similar problem. Thus, LMI optimization can be implemented on-line. Secondly, it is possible to recast much of existing robust control theory in the framework of LMIs.

The implication is that we can devise an MPC scheme where at each time instant, an LMI optimization problem (as opposed to a conventional linear or quadratic program) is solved, which incorporates input and output constraints and a description of the plant uncertainty and guarantees certain robustness properties.

8.2 Background

In this section, we discuss background material such as models of systems with uncertainties, which will be considered in the sequel. We also give a brief overview of MPC. Fairly good tutorials on MPC can be found in numerous recent references [37, 100, 114, 144]. The essential technical machinery which we will use from the area of LMIs has already been summarized in Chapter 5.

8.2.1 Models for Uncertain Systems

We present two paradigms for robust control which arise from two different modeling and identification procedures. The first is a "multi-model" paradigm, and the second is the more popular "linear system with a feedback uncertainty" robust control model. Underlying both these paradigms is a linear time-varying (LTV) system

$$\begin{aligned} x(k+1) &= A(k)x(k) + B(k)u(k), \\ y(k) &= Cx(k), \\ [A(k) \quad B(k)] &\in \Omega, \end{aligned} \tag{8.1}$$

where $u(k) \in \mathcal{R}^{n_u}$ is the control input, $x(k) \in \mathcal{R}^{n_x}$ is the state of the plant and $y(k) \in \mathcal{R}^{n_y}$ is the plant output, and Ω is some prespecified set.

(a) Polytopic or multi-model paradigm

For polytopic systems, the set Ω is the polytope

$$\Omega = \mathrm{Co}\{[A_1 \ B_1], [A_2 \ B_2], \ldots, [A_L \ B_L]\}, \tag{8.2}$$

where Co refers to the convex hull. In other words, if $[A \ B] \in \Omega$, then for some nonnegative $\lambda_1, \lambda_2, \ldots, \lambda_L$ summing to one, we have

$$[A \ B] = \sum_{i=1}^{L} \lambda_i [A_i \ B_i]. \tag{8.3}$$

$L = 1$ corresponds to the nominal LTI system.

Polytopic system models can be developed as follows. Suppose that for the (possibly nonlinear) system under consideration, we have input/output data sets at different operating points, or at different times. From each data set, we develop a number of linear models (for simplicity, we assume that the various linear models involve the same state vector). Then, it is reasonable to assume that any analysis and design methods for the polytopic system (8.1), (8.2) with vertices given by the linear models

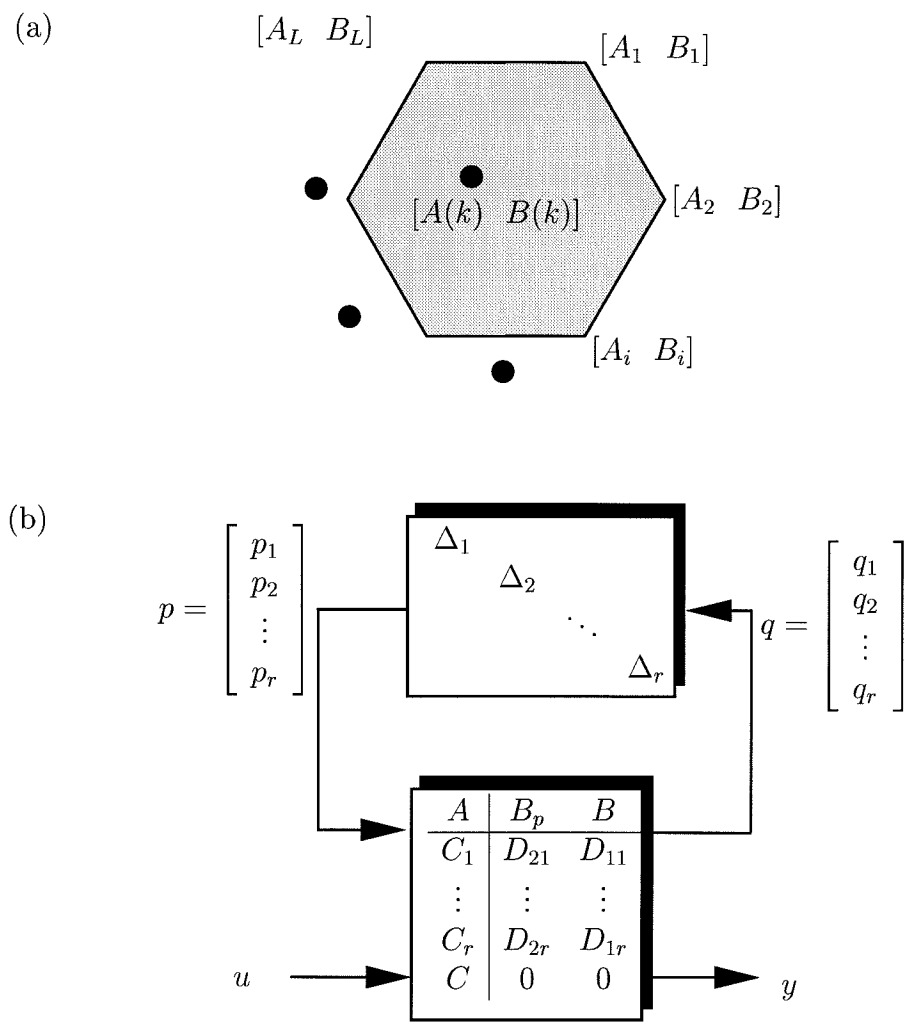

Figure 8.1: (a) Graphical representation of polytopic uncertainty; (b) Structured uncertainty.

will apply to the real system.

Alternatively, suppose the Jacobian $\begin{bmatrix} \frac{\partial f}{\partial x} & \frac{\partial f}{\partial u} \end{bmatrix}$ of a nonlinear discrete time-varying system $x(k+1) = f(x(k), u(k), k)$ is known to lie in the polytope Ω. Then it can be shown that every trajectory (x, u) of the original nonlinear system is also a trajectory of (8.1) for some LTV system in Ω [93]. Thus, the original nonlinear system can be approximated (possibly conservatively) by a polytopic uncertain LTV system.

Similarly, it can be shown that bounds on impulse response coefficients of SISO FIR plants, as discussed in [2, 26, 145], can be translated to a polytopic uncertainty

description on the state-space matrices. Thus, this polytopic uncertainty description is suitable for several problems of engineering significance.

(b) Structured feedback uncertainty

A second, more common paradigm for robust control consists of an LTI system with uncertainties or perturbations appearing in the feedback loop (see Figure 8.1(b)):

$$\begin{aligned} x(k+1) &= Ax(k) + Bu(k) + B_p p(k), \\ y(k) &= Cx(k), \\ q(k) &= C_q x(k) + D_{qu} u(k), \\ p(k) &= (\Delta q)(k). \end{aligned} \tag{8.4}$$

The operator Δ is block diagonal:

$$\Delta = \begin{bmatrix} \Delta_1 & & & \\ & \Delta_2 & & \\ & & \ddots & \\ & & & \Delta_r \end{bmatrix} \tag{8.5}$$

with $\Delta_i : \mathcal{R}^{n_i} \longrightarrow \mathcal{R}^{n_i}$. Δ can represent either a memoryless time-varying matrix with $\|\Delta_i(k)\|_2 \equiv \bar{\sigma}(\Delta_i(k)) \leq 1, \quad i = 1, 2, \ldots, r, \quad k \geq 0$; or a convolution operator (for e.g., a stable LTI dynamical system) with the operator norm induced by the truncated ℓ_2-norm less than 1, i.e.,

$$\sum_{j=0}^{k} p_i(j)^T p_i(j) \leq \sum_{j=0}^{k} q_i(j)^T q_i(j), \; i = 1, \ldots, r, \quad \forall k \geq 0. \tag{8.6}$$

Each Δ_i is assumed to be either a *repeated scalar* block or a *full* block [108] and models a number of factors, such as nonlinearities, dynamics or parameters, that are unknown, unmodeled or neglected. A number of control systems with uncertainties can be recast in this framework [108]. For ease of reference, we will refer to such systems as systems with structured uncertainty. Note that in this case, the uncertainty

set Ω is defined by (8.4) and (8.5).

When Δ_i is a stable LTI dynamical system, the quadratic sum constraint (8.6) is equivalent to the following frequency domain specification on the z-transform $\hat{\Delta}_i(z)$

$$\|\hat{\Delta}_i\|_{\mathcal{H}_\infty} \equiv \sup_{\theta\in[0,2\pi)} \bar{\sigma}(\hat{\Delta}_i(e^{j\theta})) \leq 1.$$

Thus, the structured uncertainty description is allowed to contain both LTI and LTV blocks, with frequency domain and time-domain constraints respectively. We will, however, only consider the LTV case since the results we obtain are identical for the general mixed uncertainty case, with one exception, as pointed out in §8.3.2.2. The details can be found in [21, Sec. 8.2] and will be omitted here for brevity. For the LTV case, it is easy to show through routine algebraic manipulations that system (8.4) corresponds to system (8.1) with

$$\Omega = \left\{ \begin{bmatrix} A + B_p\Delta C_q & B + B_p\Delta D_{qu} \end{bmatrix} : \Delta \text{ satisfies (8.5) with } \bar{\sigma}(\Delta_i) \leq 1 \right\} \quad (8.7)$$

$\Delta \equiv 0,\ p(k) \equiv 0,\ k \geq 0$, corresponds to the nominal LTI system.

The issue of whether to model a system as a polytopic system or a system with structured uncertainty depends on a number of factors, such as the underlying physical model of the system, available model identification and validation techniques, etc. For example, nonlinear systems can be modeled either as polytopic systems or as systems with structured perturbations. We will not concern ourselves with such issues here; instead we will assume that one of the two models discussed thus far is available.

8.2.2 Model Predictive Control

MPC is an open-loop control design procedure. Its general structure is shown in Figure 8.2. At sampling time k, represented by the origin of the axes in Figure 8.3, a plant measurement $\hat{y}(k)$ of the output y is obtained, as shown in Figure 8.2. An estimator uses this measurement and knowledge of the plant input $u(k)$ at the current

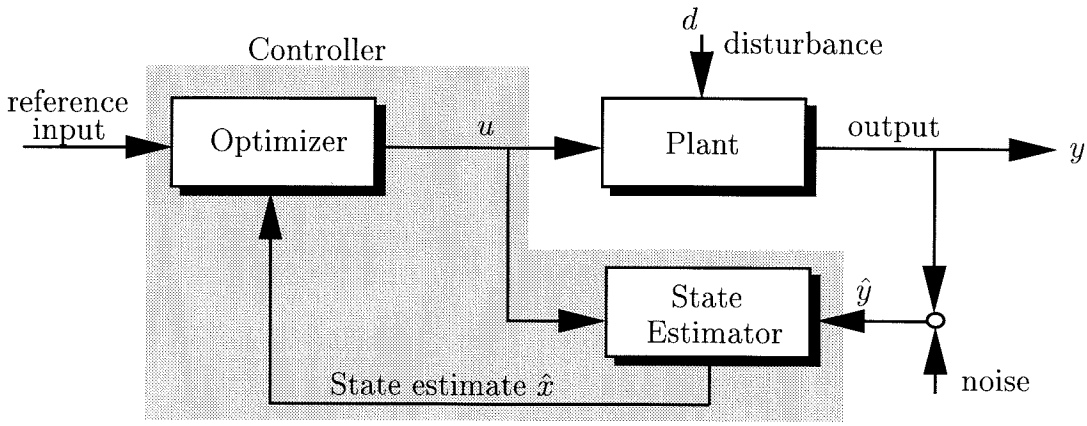

Figure 8.2: Basic feedback structure of MPC.

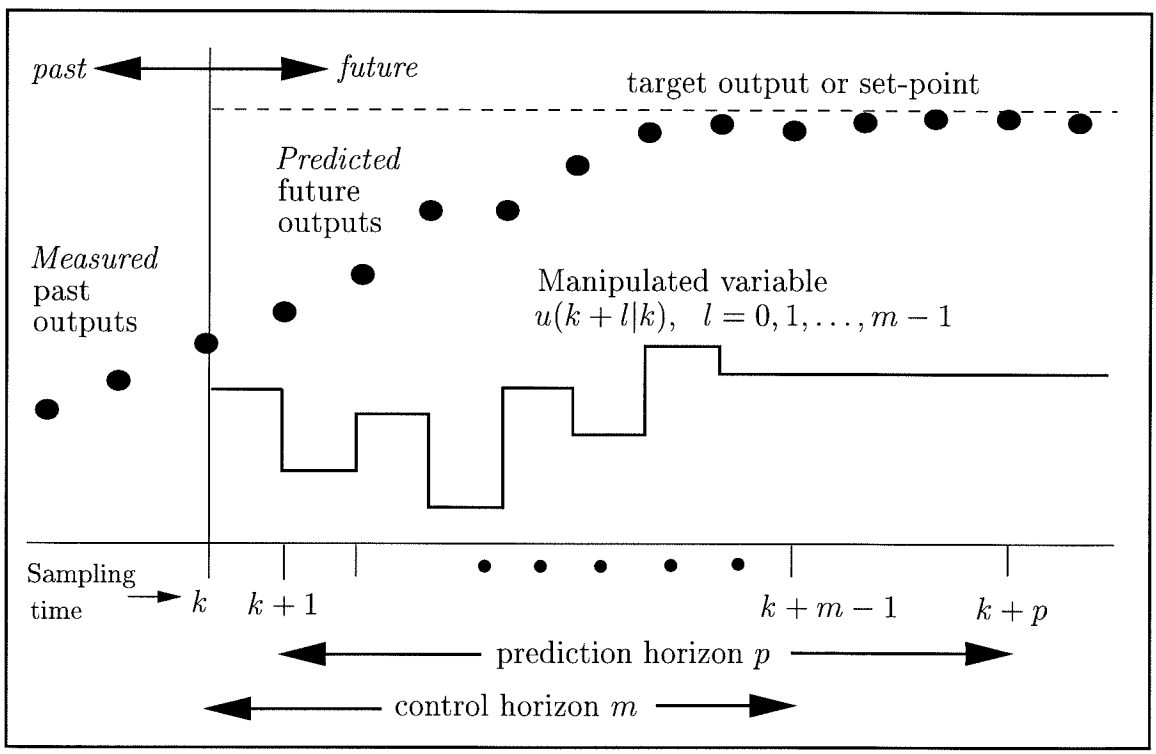

Figure 8.3: Basic philosophy of MPC.

sampling time k to obtain an estimate $\hat{x}(k)$ of the plant state x. This state estimate $\hat{x}(k)$ and a model of the plant can be used to predict the future states and outputs $x(k+i|k), y(k+i|k),\ i = 1, \ldots, p$ of the system over a future time-horizon called the *output* or *prediction* horizon p (see Figure 8.3), when the manipulated input

$u(k+i|k), i = 0, 1, \ldots, m-1$ is changed over some future time-horizon called the *input* or *control* horizon m.

The task of the MPC optimizer is to compute a sequence of m control moves $u(k+i|k), i = 0, 1, \ldots, m-1$ such that the predicted output follows a specified target or set-point in a desirable manner (see Figure 8.3). The optimizer can take into account inequality constraints on the inputs and outputs arising from the particular process. The MPC optimizer computes this desirable sequence of control inputs by minimizing an objective function $J_p(k)$, appropriately defined over the output horizon p as follows:

$$\min_{u(k+i|k), i=0,1,\ldots,m-1} J_p(k), \tag{8.8}$$

subject to constraints on the control input $u(k+i|k), i = 0, 1, \ldots, m-1$ and possibly also on the state $x(k+i|k), i = 0, 1, \ldots, p$ and the output $y(k+i|k), i = 1, 2, \ldots, p$. Here

$x(k+i|k)$, $y(k+i|k)$: state and output respectively, at time $k+i$, predicted based on the measurements at time k; $x(k|k)$ and $y(k|k)$ refer respectively to the state and output measured at time k.

$u(k+i|k)$: control move at time $k+i$, computed by the optimization problem (8.8) at time k; $u(k|k)$ is the control move to be implemented at time k.

p : *output* or *prediction* horizon

m : *input* or *control* horizon.

It is assumed that the control action is not changed after time $k+m-1$, i.e., $u(k+i|k) = u(k+m-1|k),\ i \geq m$. Alternatively, for state regulation problems, $u(k+i|k) = 0, i \geq m$. Although more than one optimal control input is computed, only the first computed control move $u(k|k)$ is implemented. At the next sampling time $k+1$, new measurements $\hat{y}(k+1)$ are obtained from the plant and a new estimate $\hat{x}(k+1)$ of the plant state $x(k+1)$ is obtained from the estimator. Now, predictions of the plant state and output $x(k+1+i|k+1), y(k+1+i|k),\ i = 1, \ldots, p$ can be

computed over a shifted prediction horizon $k+1+1$ to $k+1+p$, and the above optimization is solved again using these predictions to recompute m optimal control moves $u(k+1+i|k+1), i=0,1,\ldots,m-1$.

Thus, both the control horizon m and the prediction horizon p *move* or *recede* ahead by one step as time moves ahead by one step. This is the reason why MPC is also sometimes referred to as Receding Horizon Control (RHC) or Moving Horizon Control (MHC). The purpose of taking new measurements at each time step is to compensate for unmeasured disturbances and model inaccuracy both of which cause the system output to be different from the one predicted by the model. We assume that exact measurement of the state of the system is available at each sampling time k, i.e.,

$$x(k|k) = x(k). \tag{8.9}$$

Several choices of the objective function $J_p(k)$ in the optimization (8.8) have been reported [52, 53, 102, 137] and have been compared in [25]. In this chapter, we consider the following quadratic objective:

$$J_p(k) = \sum_{i=0}^{p} \left(x(k+i|k)^T Q_1 x(k+i|k) + u(k+i|k)^T R u(k+i|k) \right), \tag{8.10}$$

where $Q_1 > 0$ and $R > 0$ are symmetric weighting matrices. In particular, we will consider the case $p = \infty$ which is referred to as the infinite horizon MPC (IH-MPC). Finite horizon control laws have been known to have poor nominal stability properties [18, 114]. Nominal stability of finite horizon MPC requires imposition of a terminal state constraint ($x(k+i|k) = 0, i = m$) and/or use of the contraction mapping principle [136, 137] to tune Q_1, R, m and p for stability. But the terminal state constraint is somewhat artificial since only the first control move is implemented. Thus, in the closed loop, the states actually approach zero only asymptotically. Also, the computation of the contraction condition [136, 137] at all possible combinations of active constraints at the optimum of the on-line optimization can be extremely

time consuming, and as such, this issue remains unaddressed.

On the other hand, infinite horizon control laws have been shown to guarantee nominal stability [102, 114]. We therefore believe that rather than using the above methods to "tune" the parameters for stability, it is preferable to adopt the infinite horizon approach to guarantee at least nominal stability.

In this chapter, we consider Euclidean norm bounds and component-wise peak bounds on the input $u(k+i|k)$, given respectively as

$$\|u(k+i|k)\|_2 \leq u_{\max}, \quad k,\ i \geq 0, \tag{8.11}$$

and

$$|u_j(k+i|k)| \leq u_{j,\max}, \quad k,\ i \geq 0, \quad j = 1, 2, \ldots, n_u. \tag{8.12}$$

Similarly, for the output, we consider the Euclidean norm constraint and component-wise peak bounds on $y(k+i|k)$, given respectively as

$$\|y(k+i|k)\|_2 \leq y_{\max}, \quad k \geq 0,\ i \geq 1, \tag{8.13}$$

and

$$|y_j(k+i|k)| \leq y_{j,\max}, \quad k \geq 0,\ i \geq 1,\ j = 1, 2, \ldots, n_y. \tag{8.14}$$

Note that the output constraints have been imposed strictly over the future horizon (i.e., $i \geq 1$) and not at the current time (i.e, $i = 0$). This is because the current output cannot be influenced by the current or future control action and hence imposing any constraints on y at the current time is meaningless. Note also that (8.13) and (8.14) specify "worst-case" output constraints. In other words, (8.13) and (8.14) must be satisfied for any time-varying plant in Ω used as a model for predicting the output.

Remark 8.1 Constraints on the input are typically *hard* constraints, since they represent limitations on process equipment (such as valve saturation) and as such cannot

be relaxed or *softened*. Constraints on the output, on the other hand, are often performance goals; it is usually only required to make $y_{\max}$ and $y_{i,\max}$ as small as possible, subject to the input constraints.

8.3 Model Predictive Control using Linear Matrix Inequalities

In this section, we discuss the problem formulation for robust MPC. In particular, we modify the minimization of the *nominal* objective function, discussed in §8.2.2, to a minimization of the *worst-case* objective function. Following the motivation in §8.2.2, we consider the IH-MPC problem. We begin with the robust IH-MPC problem without input and output constraints and reduce it to a linear objective minimization problem subject to LMI constraints. We then incorporate input and output constraints. Finally, we show that the feasible receding horizon state-feedback control law robustly stabilizes the set of uncertain plants Ω.

8.3.1 Robust Unconstrained IH-MPC

The system is described by (8.1) with the associated uncertainty set Ω (either (8.2) or (8.7)). Analogous to the familiar approach from linear robust control, we replace the minimization, at each sampling time k, of the nominal performance objective (given in (8.8)), by the minimization of a *robust* performance objective as follows:

$$\min_{u(k+i|k),i=0,1,\ldots,m} \quad \max_{[A(k+i)\ B(k+i)]\in\Omega,\ i\geq 0} J_\infty(k),$$

$$\text{where } J_\infty(k) = \sum_{i=0}^{\infty} \left(x(k+i|k)^T Q_1 x(k+i|k) + u(k+i|k)^T R u(k+i|k)\right). \tag{8.15}$$

This is a "min-max" problem. The maximization is over the set Ω and corresponds to choosing that time-varying plant $[A(k+i)\ B(k+i)] \in \Omega,\ i \geq 0$ which, if used as a "model" for predictions, would lead to the largest or "worst-case" value of $J_\infty(k)$ among all plants in Ω. This worst-case value is minimized over present and future

control moves $u(k+i|k), i = 0, 1, \ldots, m$.

This min-max problem, though convex for finite m, is not computationally tractable, and as such has not been addressed in the MPC literature. We address problem (8.15) by first deriving an upper bound on the robust performance objective. We then minimize this upper bound with a constant state feedback control law $u(k+i|k) = Fx(k+i|k),\ i \geq 0$.

Derivation of the upper bound

Consider a quadratic function $V(x) = x^T Px,\ P > 0$ of the state $x(k|k) = x(k)$ (see (8.9)) of the system (8.1) with $V(0) = 0$. At sampling time k, suppose V satisfies the following inequality for all $x(k+i|k),\ u(k+i|k),\ i \geq 0$ satisfying (8.1), and for any $[A(k+i)\ B(k+i)] \in \Omega,\ i \geq 0$:

$$\begin{aligned} &V(x(k+i+1|k)) - V(x(k+i|k)) \\ &\quad \leq -\left(x(k+i|k)^T Q_1 x(k+i|k) + u(k+i|k)^T R u(k+i|k)\right). \end{aligned} \tag{8.16}$$

For the robust performance objective function to be finite, we must have $x(\infty|k) = 0$ and hence, $V(x(\infty|k)) = 0$. Summing (8.16) from $i = 0$ to $i = \infty$, we get

$$-V(x(k|k)) \leq -J_\infty(k).$$

Thus,

$$\max_{[A(k+i)\ B(k+i)] \in \Omega,\, i \geq 0} J_\infty(k) \leq V(x(k|k)). \tag{8.17}$$

This gives an upper bound on the robust performance objective. Thus, the goal of our robust MPC algorithm has been redefined to synthesize, at each time step k, a constant state-feedback control law $u(k+i|k) = Fx(k+i|k)$ to minimize this upper bound $V(x(k|k))$. As is standard in MPC, only the first computed input $u(k|k) = Fx(k|k)$ is implemented. At the next sampling time, the state $x(k+1)$ is

measured and the optimization is repeated to recompute F. The following theorem gives us conditions for the existence of the appropriate $P > 0$ satisfying (8.16) and the corresponding state feedback matrix F.

Theorem 8.1 *Let $x(k) = x(k|k)$ be the state of the uncertain system (8.1) measured at sampling time k. Assume that there are no constraints on the control input and plant output.*

(A) *Suppose the uncertainty set Ω is defined by a polytope as in (8.2). Then, the state feedback matrix F in the control law $u(k+i|k) = Fx(k+i|k), i \geq 0$ which minimizes the upper bound $V(x(k|k))$ on the robust performance objective function at sampling time k is given by*

$$F = YQ^{-1}, \tag{8.18}$$

where $Q > 0$ and Y are obtained from the solution (if it exists) to the following linear objective minimization problem (this problem is of the same form as problem (5.4)):

$$\min_{\gamma,\, Q,\, Y} \quad \gamma \tag{8.19}$$

subject to

$$\begin{bmatrix} 1 & x(k|k)^T \\ x(k|k) & Q \end{bmatrix} \geq 0 \tag{8.20}$$

and

$$\begin{bmatrix} Q & QA_j^T + Y^T B_j^T & QQ_1^{\frac{1}{2}} & Y^T R^{\frac{1}{2}} \\ A_jQ + B_jY & Q & 0 & 0 \\ Q_1^{\frac{1}{2}}Q & 0 & \gamma I & 0 \\ R^{\frac{1}{2}}Y & 0 & 0 & \gamma I \end{bmatrix} \geq 0, \quad j = 1, 2, \ldots, L. \tag{8.21}$$

The corresponding value of $P > 0$ in (8.16) is given by $P = \gamma Q^{-1}$.

(B) *Suppose the uncertainty set Ω is defined by a structured norm-bounded perturbation Δ as in (8.7). In this case, F and $P > 0$ are given by*

$$F = YQ^{-1}, \quad P = \gamma Q^{-1}, \tag{8.22}$$

where $Q > 0$, γ and Y are obtained from the solution (if it exists) to the following linear objective minimization problem with variables γ, Q, Y and Λ:

$$\min_{\gamma,\, Q,\, Y,\, \Lambda} \quad \gamma \tag{8.23}$$

subject to

$$\begin{bmatrix} 1 & x(k|k)^T \\ x(k|k) & Q \end{bmatrix} \geq 0, \tag{8.24}$$

and

$$\begin{bmatrix} Q & Y^T R^{\frac{1}{2}} & QQ_1^{\frac{1}{2}} & QC_q^T + Y^T D_{qu}^T & QA^T + Y^T B^T \\ R^{\frac{1}{2}} Y & \gamma I & 0 & 0 & 0 \\ Q_1^{\frac{1}{2}} Q & 0 & \gamma I & 0 & 0 \\ C_q Q + D_{qu} Y & 0 & 0 & \Lambda & 0 \\ AQ + BY & 0 & 0 & 0 & Q - B_p \Lambda B_p^T \end{bmatrix} \geq 0 \tag{8.25}$$

where

$$\Lambda = \begin{bmatrix} \lambda_1 I_{n_1} & & & \\ & \lambda_2 I_{n_2} & & \\ & & \ddots & \\ & & & \lambda_r I_{n_r} \end{bmatrix} > 0. \tag{8.26}$$

Proof. The proof is given in §8.7 in the form of Appendix A. ■

Remark 8.2 Part (A) of Theorem 1 can be derived from the results in [17] for quadratic stabilization of uncertain polytopic continuous-time systems and their ex-

tension to the discrete-time case [54]. Part (B) can be derived using the same basic techniques in conjunction with the $\mathcal{S}$-procedure (see [134] and the references therein).

Remark 8.3 Strictly speaking, the variables in the above optimization should be denoted by Q_k, F_k, Y_k, etc., to emphasize that they are computed at time k. For notational convenience, we omit the subscript here and in the next section. We will, however, briefly utilize this notation in the robust stability proof (Theorem 8.3). Closed loop stability of the receding horizon state-feedback control law given in Theorem 8.1 will be established in §8.3.2.

Remark 8.4 For the nominal case, ($L = 1$ or $\Delta(k) \equiv 0, p(k) \equiv 0,\ k \geq 0$), we recover the standard discrete-time Linear Quadratic Regulator (LQR) solution (Kwakernaak and Sivan (1972) [92]). This is stated in the following corollary.

Corollary 8.1 (Discrete-time LQR) *Suppose there is no model uncertainty ($L = 1$ and $\Delta(k) \equiv 0, p(k) \equiv 0,\ k \geq 0$, respectively for the polytopic and structured uncertainties) and no input and output constraints. Then, the optimal receding horizon state-feedback control law resulting from the solution in Theorem 8.1 at each time k is identical to the static state-feedback control law $u(k) = F_{LQR}x(k)$ obtained from the standard discrete-time linear quadratic regulator (LQR) problem, i.e.,*

$$F_{LQR} = -(R + B^T P_{LQR} B)^{-1} B^T P_{LQR} A \tag{8.27}$$

where $P_{LQR} > 0$ is the unique positive definite solution of the following steady state Ricatti equation:

$$A^T P_{LQR} A - P_{LQR} - A^T P_{LQR} B (B^T P_{LQR} B + R)^{-1} B^T P_{LQR} A + Q_1 = 0 \tag{8.28}$$

Moreover, the optimum value of the discrete-time LQR objective

$$x(0)^T P_{LQR} x(0) = \min_u \sum_{i=0}^{\infty} [x(i)^T Q_1 x(i) + u(i)^T R u(i)] \tag{8.29}$$

is the same as the optimum value of the objective $V(x(0))$ obtained from Theorem 8.1 at sampling time $k = 0$.

Proof. The nominal case corresponds to $L = 1$ and $\Delta(k) \equiv 0,\ p(k) \equiv 0,\ k \geq 0$ respectively for the polytopic and structured uncertainties. The state space matrices $[A \quad B]$ in equation (8.1) are constant. In this case, both equations (8.58) and (8.60) reduce to

$$(A + BF)^T P(A + BF) - P + F^T RF + Q_1 \leq 0. \tag{8.30}$$

It can be verified that $P_{LQR} > 0$ and F_{LQR} obtained from equations (8.27) and (8.28) satisfy equation (8.30) as an equality. Hence, $P_{LQR} > 0$ and F_{LQR} are feasible solutions for the linear objective minimization problem in Theorem 8.1. Next, consider any other feasible $P > 0,\ F$ satisfying (8.30). Since $Q_1 > 0,\ R > 0$, we know from Lyapunov's theorem that $(A + BF)$ is a stable matrix with eigenvalues in the unit disk. Using equations (8.27), (8.28) and after some simplification, we get

$$(A + BF)^T (P - P_{LQR})(A + BF) - (P - P_{LQR}) \ \leq \ -W^T W \leq 0$$

where, $W = (R + B^T P_{LQR} B)^{-\frac{1}{2}} B^T P_{LQR} A + (R + B^T P_{LQR} B)^{\frac{1}{2}} F$. Since $(A + BF)$ is stable, from Lyapunov's theorem, this implies that $P - P_{LQR} \geq 0$. Thus, at any time k,

$$x(k|k)^T P_{LQR} x(k|k) \ \leq \ x(k|k)^T P x(k|k).$$

Hence, at any time k, among all P and F which are feasible for the linear objective minimization problem in Theorem 8.1, P_{LQR} and F_{LQR} are optimal since P_{LQR} gives the smallest value of the upper bound $V(x(k|k) = x(k|k)^T P x(k|k)^T$ which is the objective to be minimized in Theorem 8.1. Equation (8.29) then follows and this completes the proof. ■

Remark 8.5 The previous remark establishes that for the nominal case, the feedback matrix F computed from Theorem 8.1 is constant, independent of the state of the system. However, in the presence of uncertainty, even without constraints on the control input or plant output, F can show strong dependence on the state of the system. In such cases, using a receding horizon approach and recomputing F at each sampling time shows significant improvement in performance as opposed to using a static state feedback control law. This is one of the key ideas in this chapter and is illustrated with the following simple example.

Consider the polytopic system (8.1), Ω being defined by (8.2) with

$$A_1 = \begin{bmatrix} 0.9347 & 0.5194 \\ 0.3835 & 0.8310 \end{bmatrix}, \quad A_2 = \begin{bmatrix} 0.0591 & 0.2641 \\ 1.7971 & 0.8717 \end{bmatrix}, \quad B = \begin{bmatrix} -1.4462 \\ -0.7012 \end{bmatrix}.$$

Figure 8.4 (a) shows the initial state response of a time-varying system in the set Ω, using the receding horizon control law of Theorem 8.1 ($Q_1 = 1, R = 1$). Also included is the static state-feedback control law from Theorem 8.1, where the feedback matrix F is not recomputed at each time k. The response with the receding horizon controller is about five times faster. Figure 8.4 (b) shows the norm of F as a function of time for the two schemes and thus explains the significantly better performance of the receding horizon scheme.

Remark 8.6 Traditionally, feedback in the form of plant measurement at each sampling time k is interpreted as accounting for model uncertainty and unmeasured disturbances (see §8.2.2). In our robust MPC setting, this feedback can now be reinterpreted as potentially reducing the conservatism in our worst-case MPC synthesis by recomputing F using new plant measurements.

Remark 8.7 The speed of the closed-loop response can be influenced by specifying a minimum decay rate on the state x ($\|x(k)\| \leq c\rho^k \|x(0)\|$, $0 < \rho < 1$) as follows:

$$x(k+i+1|k)^T P x(k+i+1|k) \leq \rho^2 x(k+i|k)^T P x(k+i|k), \quad i \geq 0 \quad (8.31)$$

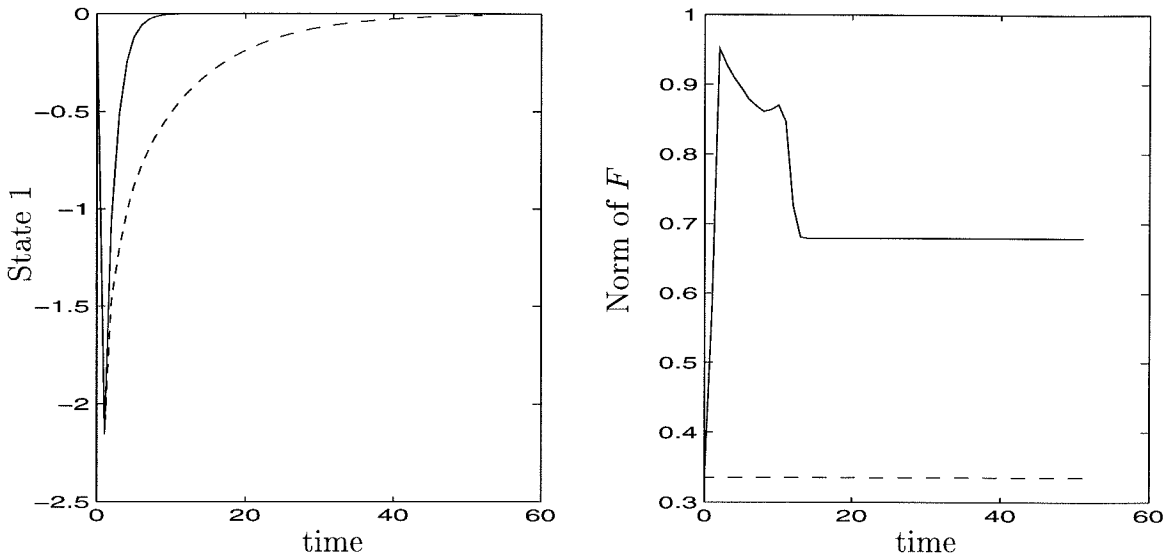

(a) (b)

Figure 8.4: (a) Unconstrained closed-loop responses and (b) norm of the feedback matrix F; solid: using receding horizon state-feedback; dash: using robust static state-feedback.

for any $[A(k+i)\ B(k+i)] \in \Omega,\ i \geq 0$. This implies that

$$\|x(k+i+1|k)\| \leq \left[\frac{\bar{\sigma}(P)}{\underline{\sigma}(P)}\right]^{\frac{1}{2}} \rho \|x(k+i|k)\|, \quad i \geq 0.$$

Following the steps in the proof of Theorem 8.1, it can be shown that requirement (8.31) reduces to the following LMIs for the two uncertainty descriptions:

Polytopic uncertainty

$$\begin{bmatrix} \rho^2 Q & (A_i Q + B_i Y)^T \\ A_i Q + B_i Y & Q \end{bmatrix} \geq 0, \quad i = 1, \ldots, L \tag{8.32}$$

$$\begin{bmatrix} \rho^2 Q & (C_q Q + D_{qu} Y)^T & (AQ + BY)^T \\ C_q Q + D_{qu} Y & \Lambda & 0 \\ AQ + BY & 0 & Q - B_p \Lambda B_p^T \end{bmatrix} \geq 0 \qquad (8.33)$$

where $\Lambda > 0$ is of the form (8.26).

Thus, an additional tuning parameter $\rho \in (0, 1)$ is introduced in the MPC algorithm to influence the speed of the closed-loop response. Note that with $\rho = 1$, the above two LMIs are trivially satisfied if (8.21) and (8.25) are satisfied.

8.3.2 Robust Constrained IH-MPC

In the previous section, we formulated the robust MPC problem without input and output constraints, and derived an upper bound on the robust performance objective. In this section, we show how input and output constraints can be incorporated as LMI constraints in the robust MPC problem. As a first step, we need to establish the following lemma which will also be required to prove robust stability.

Lemma 8.1 (Invariant ellipsoid) *Consider the system (8.1) with the associated uncertainty set Ω.*

(A) *Let Ω be a polytope described by (8.2). At sampling time k, suppose there exist $Q > 0$, γ and $Y = FQ$ such that (8.21) holds. Also suppose that $u(k+i|k) = Fx(k+i|k)$, $i \geq 0$.*

Then if

$$x(k|k)^T Q^{-1} x(k|k) \leq 1 \text{ (or equivalently, } x(k|k)^T P x(k|k) \leq \gamma \text{ with } P = \gamma Q^{-1}),$$

then

$$\max_{[A(k+j)\ B(k+j)] \in \Omega,\, j \geq 0} x(k+i|k)^T Q^{-1} x(k+i|k) < 1, \quad i \geq 1, \qquad (8.34)$$

or equivalently,

$$\max_{[A(k+j)\ B(k+j)]\in\Omega,\, j\geq 0} x(k+i|k)^T P x(k+i|k) < \gamma,\ i \geq 1. \tag{8.35}$$

Thus, $\mathcal{E} = \{z|z^T Q^{-1} z \leq 1\} = \{z|z^T P z \leq \gamma\}$ *is an invariant ellipsoid for the predicted states of the uncertain system.*

(B) *Let* Ω *be described by (8.7) in terms of a structured* Δ *block as in (8.5). At sampling time* k*, suppose there exist* $Q > 0$*,* γ*,* $Y = FQ$ *and* $\Lambda > 0$ *such that (8.25) and (8.26) hold. If* $u(k+i|k) = Fx(k+i|k)$*,* $i \geq 0$*, then the result in* **(A)** *holds as well for this case.*

Remark 8.8 The maximization in (8.34) and (8.35) is over the set Ω of time-varying models that can be used for prediction of the future states of the system. This maximization leads to the "worst-case" value of $x(k+i|k)^T Q^{-1} x(k+i|k)$ (equivalently, $x(k+i|k)^T P x(k+i|k)$) at every instant of time $k+i$, $i \geq 1$.

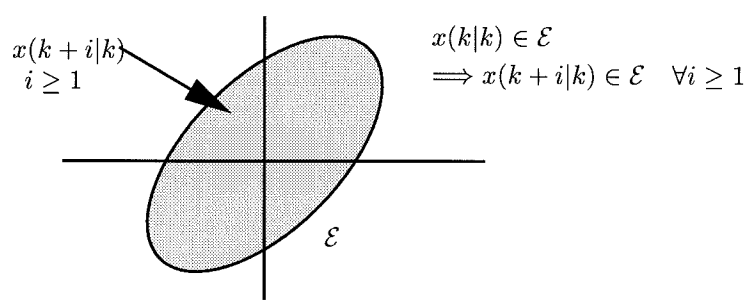

Figure 8.5: Graphical representation of the state-invariant ellipsoid $\mathcal{E}$ in two dimensions.

Proof. The proof is given in §8.8 in the form of Appendix B. ■

8.3.2.1 Input Constraints

Physical limitations inherent in process equipment invariably impose *hard* constraints on the manipulated variable $u(k)$. In this section, we show how limits on the control

signal can be incorporated into our robust MPC algorithm as *sufficient* LMI constraints. The basic idea of the discussion that follows can be found in Boyd et al. (1994) [21] in the context of continuous time systems. We present it here to clarify its application in our (discrete-time) robust MPC setting and also for completeness of exposition. We will assume for the rest of this section that the postulates of Lemma 8.1 are satisfied so that $\mathcal{E}$ is an invariant ellipsoid for the predicted states of the uncertain system.

At sampling time k, consider the Euclidean norm constraint (8.11):

$$\|u(k+i|k)\|_2 \leq u_{\max}, \quad i \geq 0. \tag{8.11'}$$

The constraint is imposed on the present and the entire horizon of future manipulated variables, although only the first control move $u(k|k) = u(k)$ is implemented. Following [21], we have

$$\begin{aligned} \max_{i\geq 0} \|u(k+i|k)\|_2^2 &= \max_{i\geq 0} \|YQ^{-1}x(k+i|k)\|_2^2 \\ &\leq \max_{z\in\mathcal{E}} \|YQ^{-1}z\|_2^2 \\ &= \lambda_{\max}(Q^{-\frac{1}{2}}Y^TYQ^{-\frac{1}{2}}). \end{aligned}$$

Using Lemma 5.1 from Chapter 5, we see that $\|u(k+i|k)\|_2^2 \leq u_{\max}^2$, $i \geq 0$ if

$$\begin{bmatrix} u_{\max}^2 I & Y \\ Y^T & Q \end{bmatrix} \geq 0. \tag{8.36}$$

This is an LMI in Y and Q.

Similarly, let us consider peak bounds on each component of $u(k+i|k)$ at sampling time k (8.12):

$$|u_j(k+i|k)| \leq u_{j,\max}, \quad i \geq 0, \ j = 1, 2, \ldots, n_u. \tag{8.12'}$$

Now,

$$\begin{aligned}
\max_{i\geq 0} |u_j(k+i|k)|^2 &= \max_{i\geq 0} |\left(YQ^{-1}x(k+i|k)\right)_j|^2 \\
&\leq \max_{z\in\mathcal{E}} |\left(YQ^{-1}z\right)_j|^2 \\
&\leq \|\left(YQ^{-\frac{1}{2}}\right)_j\|_2^2 \quad \text{(using the Cauchy Schwarz inequality)} \\
&= \left(YQ^{-1}Y^T\right)_{jj}.
\end{aligned}$$

Thus, the existence of a symmetric matrix X such that

$$\begin{bmatrix} X & Y \\ Y^T & Q \end{bmatrix} \geq 0, \quad \text{with} \quad X_{jj} \leq u_{j,\max}^2, \quad j = 1, 2, \ldots, n_u, \tag{8.37}$$

guarantees that $|u_j(k+i|k)| \leq u_{j,\max}, \quad i \geq 0, \quad j = 1, 2, \ldots, n_u$. These are LMIs in X, Y and Q. Note that (8.37) is a slight generalization of the result derived in [21].

Remark 8.9 Inequalities (8.36) and (8.37) represent sufficient LMI constraints which guarantee that the specified constraints on the manipulated variables are satisfied. In practice, these constraints have been found to be not too conservative, at least in the nominal case.

8.3.2.2 Output Constraints

Performance specifications impose constraints on the process output $y(k)$. As in §8.3.2.1, we derive sufficient LMI constraints for both the uncertainty descriptions which guarantee that the output constraints are satisfied.

At sampling time k, consider the Euclidean norm constraint (8.13):

$$\max_{[A(k+j)\ B(k+j)]\in\Omega,\, j\geq 0} \|y(k+i|k)\|_2 \leq y_{\max}, \quad i \geq 1. \tag{8.13'}$$

As discussed in §8.2.2, this is a worst-case constraint over the set Ω and is imposed strictly over the future prediction horizon ($i \geq 1$).

Polytopic uncertainty

In this case, Ω is given by (8.2). As shown in §8.9 in Appendix C, if

$$\begin{bmatrix} Q & (A_jQ + B_jY)^TC^T \\ C(A_jQ + B_jY) & y_{\max}^2 I \end{bmatrix} \geq 0, \quad j = 1, 2, \ldots, L, \tag{8.38}$$

then

$$\max_{[A(k+j)\ B(k+j)]\in\Omega,\ j\geq 0} \|y(k+i|k)\|_2 \leq y_{\max}, \quad i \geq 1.$$

Condition (8.38) represents a set of LMIs in Y and $Q > 0$.

Structured uncertainty

In this case, Ω is described by (8.4), (8.5) in terms of a structured Δ block. As shown in §8.9 in Appendix C, if

$$\begin{bmatrix} y_{\max}^2 Q & (C_qQ + D_{qu}Y)^T & (AQ + BY)^TC^T \\ C_qQ + D_{qu}Y & T^{-1} & 0 \\ C(AQ + BY) & 0 & I - CB_pT^{-1}B_p^TC^T \end{bmatrix} \geq 0 \tag{8.39}$$

with

$$T = \begin{bmatrix} t_1 I_{n_1} & & & \\ & t_2 I_{n_2} & & \\ & & \ddots & \\ & & & t_r I_{n_r} \end{bmatrix} > 0,$$

then

$$\max_{[A(k+j)\ B(k+j)]\in\Omega,\ j\geq 0} \|y(k+i|k)\|_2 \leq y_{\max}, \quad i \geq 1.$$

Condition (8.39) is an LMI in $Y, Q > 0$ and $T^{-1} > 0$.

In a similar manner, component-wise peak bounds on the output (see (8.14)) can be translated to sufficient LMI constraints. The development is identical to the preceding development for the Euclidean norm constraint if we replace C by C_l and

T by T_l, $l = 1, 2, \ldots, n_y$ in (8.38), (8.39), where

$$y(k) = \begin{bmatrix} y_1(k) \\ y_2(k) \\ \vdots \\ y_{n_y}(k) \end{bmatrix} = Cx(k) = \begin{bmatrix} C_1 \\ C_2 \\ \vdots \\ C_{n_y} \end{bmatrix} x(k).$$

T_l is in general different for each $l = 1, 2, \ldots, n_y$.

Note that for the case with mixed Δ blocks, we can satisfy the output constraint over the current and future horizon $\max_{i \geq 0} \|y(k+i|k)\|_2 \leq y_{\max}$ and not over the (strict) future horizon ($i \geq 1$) as in (8.13). The corresponding LMI is derived as follows:

$$\begin{aligned} \max_{i \geq 0} \|Cx(k+i|k)\|_2^2 &\leq \max_{z \in \mathcal{E}} \|Cz\|_2^2 \\ &= \lambda_{\max}(Q^{\frac{1}{2}} C^T C Q^{\frac{1}{2}}) \end{aligned}$$

Thus, $CQC^T \leq y_{\max}^2 I \Longrightarrow \|y(k+i|k)\|_2 \leq y_{\max}$, $i \geq 0$. For component-wise peak bounds on the output, we replace C by C_l, $l = 1, \ldots, n_y$.

8.3.2.3 Robust Stability

We are now ready to state the main theorem for robust MPC synthesis with input and output constraints and establish robust stability of the closed-loop.

Theorem 8.2 *Let $x(k) = x(k|k)$ be the state of the uncertain system (8.1) measured at sampling time k.*

(A) *Suppose the uncertainty set Ω is defined by a polytope as in (8.2). Then, the state feedback matrix F in the control law $u(k+i|k) = Fx(k+i|k), i \geq 0$, which minimizes the upper bound $V(x(k|k))$ on the robust performance objective function at sampling time k and satisfies a set of specified input and output constraints is given by*

$$F = YQ^{-1},$$

where $Q > 0$ and Y are obtained from the solution (if it exists) to the following linear objective minimization problem:

$$\min \{\gamma \mid \gamma,\ Q,\ Y \text{ and variables in the LMIs for input and output constraints}\},$$

subject to (8.20), (8.21), either (8.36) or (8.37), depending on the input constraint to be imposed, and (8.38) with either C and T, or C_l and T_l, $l = 1, 2, \ldots, n_y$, depending on the output constraint to be imposed. The corresponding $P > 0$ satisfying (8.16) *is given by $P = \gamma Q^{-1}$.*

(B) *Suppose the uncertainty set Ω is defined by (8.7) in terms a structured perturbation Δ as in (8.5). In this case, F and P are given by*

$$F = YQ^{-1}, \quad P = \gamma Q^{-1},$$

where $Q > 0$, γ and Y are obtained from the solution (if it exists) to the following linear objective minimization problem:

$$\min \{\gamma \mid \gamma, Q, Y, \Lambda \text{ and variables in the LMIs for input and output constraints}\}$$

subject to (8.24), (8.25), (8.26), either (8.36) or (8.37) depending on the input constraint to be imposed, and (8.39) with either C and T, or C_l and T_l, $l = 1, 2, \ldots, n_y$, depending on the output constraint to be imposed.

Proof. From Lemma 8.1, we know that (8.21) and (8.24), (8.25) imply respectively for the polytopic and structured uncertainties, that $\mathcal{E}$ is an invariant ellipsoid for the predicted states of the uncertain system (8.1). Hence, the arguments in §8.3.2.1 and §8.3.2.2 used to translate input and output constraints to sufficient LMI constraints hold true. The rest of the proof is similar to that of Theorem 8.1. ■

In order to prove robust stability of the closed loop, we need to establish the following lemma.

Lemma 8.2 (Feasibility) *Any feasible solution of the optimization in Theorem 8.2 at time k is also feasible for all times $t > k$. Thus, if the optimization problem in Theorem 8.2 is feasible at time k, then it is feasible for all times $t > k$.*

Proof. Let us assume that the optimization problem in Theorem 8.2 is feasible at sampling time k. The only LMI in the problem which depends explicitly on the measured state $x(k|k) = x(k)$ of the system is the following:

$$\begin{bmatrix} 1 & x(k|k)^T \\ x(k|k) & Q \end{bmatrix} \geq 0.$$

Thus, to prove the lemma, we need only prove that this LMI is feasible for all future measured states $x(k+i|k+i) = x(k+i), i \geq 1$.

Now, feasibility of the problem at time k implies satisfaction of (8.21) and (8.24), (8.25), which, using Lemma 8.1, in turn imply respectively for the two uncertainty descriptions that (8.34) is satisfied. Thus, for any $[A(k+i) \;\; B(k+i)] \in \Omega, i \geq 0$ (where Ω is the corresponding uncertainty set), we must have

$$x(k+i|k)^T Q^{-1} x(k+i|k) < 1, \quad i \geq 1.$$

Since the state measured at $k+1$, that is, $x(k+1|k+1) = x(k+1)$, equals $(A(k) + B(k)F)\, x(k|k)$ for some $[A(k) \;\; B(k)] \in \Omega$, it must also satisfy this inequality, i.e.,

$$x(k+1|k+1)^T Q^{-1} x(k+1|k+1) < 1,$$

or

$$\begin{bmatrix} 1 & x(k+1|k+1)^T \\ x(k+1|k+1) & Q \end{bmatrix} > 0 \text{ (using Lemma 5.1 from Chapter 5).}$$

Thus, the feasible solution of the optimization problem at time k is also feasible at time $k+1$. Hence, the optimization is feasible at time $k+1$. This argument can be continued for time $k+2, k+3, \ldots$ to complete the proof. ■

Theorem 8.3 (Robust stability) *The feasible receding horizon state feedback control law obtained from Theorem 8.2 robustly asymptotically stabilizes the closed loop system.*

Proof. In what follows, we will refer to the uncertainty set as Ω since the proof is identical for the two uncertainty descriptions.

To prove asymptotic stability, we will establish that $V(x(k|k)) = x(k|k)^T P_k x(k|k)$, where $P_k > 0$ is obtained from the *optimal* solution at time k, is a strictly decreasing Lyapunov function for the closed-loop.

First, let us assume that the optimization in Theorem 8.2 is feasible at time $k = 0$. Lemma 8.2 then ensures feasibility of the problem at all times $k > 0$. The optimization being convex, therefore, has a unique minimum and a corresponding optimal solution (γ, Q, Y) at each time $k \geq 0$.

Next, we note from Lemma 8.2 that γ, $Q > 0$, Y (or equivalently, γ, $F = YQ^{-1}$, $P = \gamma Q^{-1} > 0$) obtained from the optimal solution at time k are feasible (of course, not necessarily optimal) at time $k+1$. Denoting the values of P obtained from the optimal solutions at time k and $k+1$ respectively by P_k and P_{k+1} (see Remark 8.3), we must have

$$x(k+1|k+1)^T P_{k+1} x(k+1|k+1) \leq x(k+1|k+1)^T P_k x(k+1|k+1). \quad (8.40)$$

This is because P_{k+1} is optimal whereas P_k is only feasible at time $k+1$.

And lastly, we know from Lemma 8.1 that if $u(k+i|k) = F_k x(k+i|k)$, $i \geq 0$ (F_k is obtained from the optimal solution at time k), then for any $[A(k) \;\; B(k)] \in \Omega$, we must have

$$x(k+1|k)^T P_k x(k+1|k) < x(k|k)^T P_k x(k|k), \quad (x(k|k) \neq 0) \qquad (8.41)$$

(see (8.64) with $i = 0$).

Since the measured state $x(k+1|k+1) = x(k+1)$ equals $(A(k) + B(k)F_k)\, x(k|k)$ for some $[A(k) \;\; B(k)] \in \Omega$, it must also satisfy inequality (8.41). Combining this with

inequality (8.40) we conclude that

$$x(k+1|k+1)^T P_{k+1} x(k+1|k+1) < x(k|k)^T P_k x(k|k), \quad (x(k|k) \neq 0).$$

Thus, $x(k|k)^T P_k x(k|k)$ is a strictly decreasing Lyapunov function for the closed-loop, which is bounded below by a positive definite function of $x(k|k)$ (see (8.17)). We therefore conclude that $x(k) \to 0$ as $k \to \infty$. ■

Remark 8.10 The proof of Theorem 8.1 (the unconstrained case) is identical to the preceding proof if we recognize that Theorem 8.1 is only a special case of Theorem 8.2 without the LMIs corresponding to input and output constraints.

8.4 Extensions

The presentation up to this point was restricted to the infinite horizon regulator with state feedback and a zero target. In this section, we extend the preceding development to several standard problems encountered in practice.

8.4.1 Reference Trajectory Tracking

In optimal tracking problems, the system output is required to track a reference trajectory $y_r(k) = C_r x_r(k)$ where the reference states x_r are computed from the following equation

$$x_r(k+1) = A_r x_r(k), \quad x_r(0) = x_{r0}.$$

The choice of $J_\infty(k)$ for the robust trajectory tracking objective in the optimization (8.15) is the following

$$J_\infty(k) = \sum_{i=0}^{\infty} \Big((Cx(k+i|k) - C_r x_r(k+i))^T Q_1 (Cx(k+i|k) - C_r x_r(k+i)) + u(k+i|k)^T R u(k+i|k) \Big), \quad Q_1 > 0, \; R > 0.$$

As discussed in [92], the plant dynamics can be augmented by the reference trajectory dynamics to reduce the robust reference trajectory tracking problem (with input and output constraints) to the standard form as in §8.3. Due to space limitations, we will omit these details.

8.4.2 Constant Set-Point Tracking

For uncertain linear *time-invariant* systems, the desired equilibrium state may be a constant point $x_s,\ u_s$ (called the *set-point*) in state-space, different from the origin. Consider (8.1) which we will now assume to represent an uncertain LTI system, i.e., $[A\ \ B] \in \Omega$ are *constant* unknown matrices. Suppose that the system output y is required to track the target vector y_t by moving the system to the set-point x_s, u_s where

$$x_s = Ax_s + Bu_s, \quad y_t = Cx_s.$$

We assume that $x_s,\ u_s,\ y_t$ are feasible, i.e., they satisfy the imposed constraints. The choice of $J_\infty(k)$ for the robust set-point tracking objective in the optimization (8.15) is the following:

$$\begin{aligned} J_\infty(k) = \sum_{i=0}^{\infty} \Big(& (Cx(k+i|k) - Cx_s)^T Q_1 \left(Cx(k+i|k) - Cx_s\right) \\ & + (u(k+i|k) - u_s)^T R (u(k+i|k) - u_s) \Big), \quad Q_1 > 0,\ R > 0. \end{aligned} \tag{8.42}$$

As discussed in [92], we can define a shifted state $\tilde{x}(k) = x(k) - x_s$, a shifted input $\tilde{u}(k) = u(k) - u_s$ and a shifted output $\tilde{y}(k) = y(k) - y_t$ to reduce the problem to the standard form as in §8.3. Component-wise peak bounds on the control signal u can be translated to constraints on $\tilde{u}$ as follows:

$$|u_j| \leq |u_{j,\max}| \iff |\tilde{u}_j + u_{s,j}| \leq u_{j,\max} \iff -u_{j,\max} - u_{s,j} \leq \tilde{u}_j \leq u_{j,\max} - u_{s,j}$$

Constraints on the transient deviation of $y(k)$ from the steady state value y_t, i.e., $\tilde{y}(k)$ can be incorporated in a similar manner.

8.4.3 Disturbance Rejection

In all practical applications, some disturbance invariably enters the system and hence it is meaningful to study its effect on the closed-loop response. Let an unknown disturbance $e(k)$, having the property $\lim_{k\to\infty} e(k) = 0$, enter the system (8.1) as follows:

$$\begin{aligned} x(k+1) &= A(k)x(k) + B(k)u(k) + e(k) \\ y(k) &= Cx(k) \\ [A(k)\ \ B(k)] &\in \Omega. \end{aligned} \tag{8.43}$$

A simple example of such a disturbance is any energy bounded signal ($\sum_{i=0}^{\infty} e(i)^T e(i) < \infty$). Assuming that the state of the system $x(k)$ is measurable, we would like to solve the optimization problem (8.15). We will assume that the predicted states of the system satisfy the following equation

$$\begin{aligned} x(k+i+1|k) &= A(k+i)x(k+i|k) + B(k+i)u(k+i|k) \\ [A(k+i)\ \ B(k+i)] &\in \Omega. \end{aligned} \tag{8.44}$$

As in §8.3, we can derive an upper bound on the robust performance objective (8.15). The problem of minimizing this upper bound with a state-feedback control law $u(k+i|k) = Fx(k+i|k)$, $i > 0$, at the same time satisfying constraints on the control input and plant output, can then be reduced to a linear objective minimization as in Theorem 8.2. The following theorem establishes stability of the closed-loop for the system (8.43) with this receding horizon control law, in the presence of the disturbance $e(k)$.

Theorem 8.4 *Let $x(k) = x(k|k)$ be the state of the system (8.43) measured at sampling time k and let the predicted states of the system satisfy (8.44). Then, assuming feasibility at each sampling time $k \geq 0$, the receding horizon state feedback control law obtained from Theorem 2 robustly asymptotically stabilizes the system (8.43) in the presence of any asymptotically vanishing disturbance $e(k)$.*

Proof. It is easy to show that for sufficiently large time $k > 0$, $V(x(k|k)) = x(k|k)^T P x(k|k)$, where $P > 0$ is obtained from the optimal solution at time k, is a strictly decreasing Lyapunov function for the closed-loop. Due to lack of space, we will skip these details. ■

8.4.4 Systems with Delays

Consider the following uncertain discrete-time linear time-varying system with delay elements, described by the following equations:

$$\begin{aligned} x(k+1) &= A_0(k)x(k) + \sum_{i=1}^{m} A_i(k)x(k-\tau_i) + B(k)u(k-\tau), \\ y(k) &= Cx(k) \\ \text{with} &\quad [A_0(k) \;\; A_1(k) \ldots A_m(k) \;\; B(k)] \in \Omega. \end{aligned} \tag{8.45}$$

We will assume, without loss of generality, that the delays in the system satisfy $0 < \tau < \tau_1 < \cdots < \tau_m$. At sampling time $k \geq \tau$, we would like to design a state-feedback control law $u(k+i-\tau|k) = Fx(k+i-\tau|k), i \geq 0$, to minimize the following modified infinite horizon robust performance objective

$$\max_{[A(k+i) \;\; B(k+i)] \in \Omega, \; i \geq 0} J_\infty(k), \tag{8.46}$$

where

$$J_\infty(k) = \sum_{i=0}^{\infty} \left(x(k+i|k)^T Q_1 x(k+i|k) + u(k+i-\tau|k)^T R u(k+i-\tau|k) \right),$$

subject to input and output constraints. Defining an augmented state

$$w(k) = \left[x(k)^T \; x(k-1)^T \ldots x(k-\tau)^T \ldots x(k-\tau_1)^T \ldots x(k-\tau_m)^T \right]^T$$

which is assumed to be measurable at each time $k \geq \tau$, we can derive an upper bound on the robust performance objective (8.46) as in §8.3. The problem of minimizing this

upper bound with the state-feedback control law $u(k+i-\tau|k) = Fx(k+i-\tau|k), k \geq \tau, i \geq 0$, subject to constraints on the control input and plant output, can then be reduced to a linear objective minimization as in Theorem 8.2. These details can be worked out in a straightforward manner and will be omitted here.

Note, however, that the appropriate choice of the function $V(w(k))$, satisfying an inequality of the form (8.16), is the following:

$$\begin{aligned} V(w(k)) &= x(k)^T P_0 x(k) + \sum_{i=1}^{\tau} x(k-i)^T P_\tau x(k-i) + \sum_{i=\tau+1}^{\tau_1} x(k-i)^T P_{\tau_1} x(k-i) \\ &\quad + \cdots + \sum_{i=\tau_{m-1}+1}^{\tau_m} x(k)^T P_{\tau_m} x(k) \quad = \quad w(k)^T P w(k) \end{aligned}$$

where P is appropriately defined in terms of $P_0, P_\tau, P_{\tau_1} \ldots, P_{\tau_m}$. The motivation for this modified choice of V comes from [45] where such a V is defined for continuous time systems with delays, and is referred to as a Modified Lyapunov-Krasovskii (MLK) functional.

8.4.5 The Output Feedback Case

Throughout the development in this chapter, we made the assumption (8.9) that the state of the system is measurable at each sampling time k, i.e.,

$$x(k|k) = x(k). \tag{8.9'}$$

Relaxing this assumption to obtain a stabilizing output feedback MPC controller even in the nominal case is not straightforward. This is because, due to the input and/or output constraints, the closed-loop system may be nonlinear and therefore we cannot apply the classical Separation Principle to prove stability of the closed-loop system. A discussion of the nominal output feedback case can be found in [146].

Here, for the uncertain case, we will only consider the case where the system is linear parameter varying, with the system parameters measurable at each sampling time. Thus, for the polytopic system (8.2), (8.3), we will assume that the co-ordinates

$\lambda_i(k),\ i = 1, \ldots, L$, which define the state-space matrices $[A(k)\ B(k)]$ as functions of the polytope vertices $[A_i\ B_i]$, are measurable at each sampling time k. And for the system with structured feedback "uncertainty" described by (8.7), we will assume that $\Delta_i(k),\ i = 1, \ldots, r$ are measurable at each sampling time k.

The estimated system state $\hat{x}$ and estimated system output $\hat{y}$ are obtained from the following standard observer equations:

$$\begin{aligned} \hat{x}(k|k) &= A(k-1)\hat{x}(k-1|k-1) + B(k-1)u(k-1) \\ &\quad + L(y(k) - \hat{y}(k|k-1)) \qquad (8.47) \\ \hat{x}(k+i+1|k) &= A(k+i)x(k+i|k) + B(k+i)u(k+i),\quad i \geq 0 \qquad (8.48) \\ \hat{y}(k+i|k) &= C\hat{x}(k+i|k),\ i \geq 0 \qquad (8.49) \end{aligned}$$

where L is the observer gain. Note that (8.48) is the prediction equation which does not contain any correction term for the observation error. Combining the system equation (8.1) with the observer equations (8.47), (8.48), (8.49), we get

$$\begin{aligned} e(k+1) &= (I - LC)A(k)e(k) \\ \text{where } e(k) &= x(k) - \hat{x}(k|k) \end{aligned} \qquad (8.50)$$

which in turn implies that (8.47) can be rewritten as

$$\hat{x}(k|k) = \hat{x}(k|k-1) + LCA(k)e(k-1). \qquad (8.51)$$

The "worst-case" objective function to be minimized is now based on the observer state $\hat{x}$:

$$\min_{u(k+i|k),i=0,1,\ldots,m} \quad \max_{[A(k+i)\ B(k+i)]\in\Omega,\ i\geq 0} J_\infty(k),$$

$$\text{where } J_\infty(k) = \sum_{i=0}^{\infty} \left(\hat{x}(k+i|k)^T Q_1 \hat{x}(k+i|k) + u(k+i|k)^T R u(k+i|k)\right). \qquad (8.52)$$

We seek to minimize this objective function by synthesizing the control law $u(k+$

$i|k) = F\hat{x}(k+i|k),\ i \geq 0$. Since the prediction equations for the estimator state are essentially the same as the prediction equations with state-feedback, except that the system is now replaced by the estimator state, we can design this state-feedback matrix F using the same result as in Theorem 8.1. Constraints on the future computed inputs $u(k+i|k)$ and the future predicted outputs $\hat{y}(k+i|k)$ can all be incorporated in the same manner as in the state-feedback case.

The observer gain L is designed to robustly stabilize the dynamics of the estimation error e, given by (8.50). For the case of polytopic uncertainty, such an observer gain is given by

$$L = P^{-1}Y \tag{8.53}$$

where Y and $P = P^T > 0$ are the solutions of the following LMIs

$$\begin{bmatrix} P & PA_j + YCA_j \\ A_j^T P + A^T C^T A_j & P \end{bmatrix} \geq 0, \quad j = 1, 2, \ldots, L. \tag{8.54}$$

For the case of structured uncertainty, the corresponding observer gain is given by

$$L = P^{-1}Y \tag{8.55}$$

where Y and $P = P^T > 0$ are the solutions of the following LMIs

$$\begin{bmatrix} P - C_q^T \Lambda C_q & 0 & A^T P - A^T C^T Y^T \\ 0 & \Lambda & B_P^T (P - C^T Y^T) \\ PA - YCA & (P - YC)B_p & P \end{bmatrix} \geq 0 \tag{8.56}$$

with

$$\Lambda = \begin{bmatrix} \lambda_1 I_{n_1} & & & \\ & \lambda_2 I_{n_2} & & \\ & & \ddots & \\ & & & \lambda_r I_{n_r} \end{bmatrix} > 0. \tag{8.57}$$

We now have the following theorem which establishes stability of the closed loop with this output feedback robust MPC controller.

Theorem 8.5 *Assume that the estimator state update equation is given by* (8.47) *and the estimator state prediction equations are given* (8.48) *and* (8.49). *Suppose the control law is given by* $u(k+i|k) = F\hat{x}(k+i|k)$, *where* F *is obtained as in Theorem 8.1, with the system state* $x(k|k)$ *replaced by the updated estimator state* $\hat{x}(k|k)$ *at each sampling time* k. *Moreover, assume that the observer gain* L *in the state estimator update equation* (8.47) *is given by either* (8.53), (8.54) *or* (8.55), (8.56), (8.57) *depending on the plant uncertainty model. Then, assuming feasibility of the LMI-based optimization which computes* F *at each sampling time* $k \geq 0$, *the closed-loop system is robustly asymptotically stable.*

Proof. The proof follows along the same lines as the proof of Theorem 8.4 for the case of rejection of an asymptotically decaying disturbance. ■

8.5 Numerical Examples

In this section, we present two examples which illustrate the implementation of the proposed robust MPC algorithm. The examples also serve to highlight some of the theoretical results in the chapter. For both these examples, the software LMI Control Toolbox [48][1] in the MATLAB environment was used to compute the solution of the linear objective minimization problem.

[1]We would like to thank Pascal Gahinet for providing an initial version of the LMI-Lab software.

No attempt was made to optimize the computation time. Also, it should be noted that the times required for computation of the closed-loop responses, as indicated at the end of each example, only reflect the state-of-the-art of LMI solvers. While these solvers are significantly faster than classical convex optimization algorithms, research in LMI optimization is still very active and substantial speed-ups can be expected in the future.

8.5.1 Example 1

The first example is a classical angular positioning system adapted from [92]. The system (see Figure 8.6) consists of a rotating antenna at the origin of the plane, driven by an electric motor. The control problem is to use the input voltage to the motor (u volts) to rotate the antenna so that it always points in the direction of a moving object in the plane.

We assume that the angular positions of the antenna and the moving object (θ and θ_r radians respectively) and the angular velocity of the antenna ($\dot{\theta}$ rad/sec) are measurable. The motion of the antenna can be described by the following discrete-time

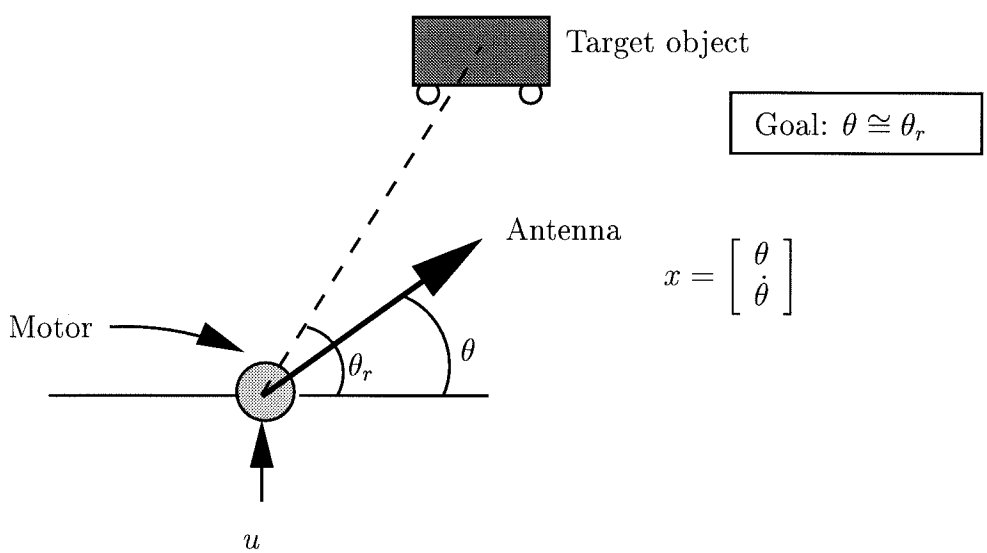

Figure 8.6: Angular positioning system.

equations obtained from their continuous-time counterparts by discretization, using

a sampling time of 0.1 sec and Euler's first-order approximation for the derivative

$$\begin{aligned} x(k+1) &= \begin{bmatrix} \theta(k+1) \\ \dot{\theta}(k+1) \end{bmatrix} = \begin{bmatrix} 1 & 0.1 \\ 0 & 1-0.1\alpha(k) \end{bmatrix} x(k) + \begin{bmatrix} 0 \\ 0.1\kappa \end{bmatrix} u(k) \\ &\triangleq A(k)x(k) + Bu(k) \\ y(k) &= [1 \;\; 0]\, x(k) \triangleq Cx(k) \end{aligned}$$

$\kappa = 0.787$ rad/(volts sec^2), $0.1 \text{ sec}^{-1} \leq \alpha(k) \leq 10 \text{ sec}^{-1}$.

The parameter $\alpha(k)$ is proportional to the coefficient of viscous friction in the rotating parts of the antenna and is assumed to be arbitrarily time-varying in the indicated range of variation. Since $0.1 \leq \alpha(k) \leq 10$, we conclude that $A(k) \in \Omega = \text{Co}\{A_1,\ A_2\}$, where

$$A_1 = \begin{bmatrix} 1 & 0.1 \\ 0 & 0.99 \end{bmatrix}, \quad \text{and} \quad A_2 = \begin{bmatrix} 1 & 0.1 \\ 0 & 0 \end{bmatrix}.$$

Thus, the uncertainty set Ω is a polytope, as in (8.2). Alternatively, if we define

$$\delta(k) = \frac{\alpha(k) - 5.05}{4.95},\ A = \begin{bmatrix} 1 & 0.1 \\ 0 & 0.495 \end{bmatrix},\ B_p = \begin{bmatrix} 0 \\ -0.1 \end{bmatrix},\ C_q = [0 \;\; 4.95],\ D_{qu} = 0$$

then $\delta(k)$ is time-varying and norm-bounded with $|\delta(k)| \leq 1,\ k \geq 0$. The uncertainty can then be described as in (8.4) with

$$\Omega = \{[A + B_p \delta C_q] : |\delta| \leq 1\}.$$

Given an initially disturbed state $x(k)$, the robust IH-MPC optimization to be solved at each time k is the following:

$$\min_{u(k+i|k)=Fx(k+i|k),\ i\geq 0} \max_{A(k+i)\in\Omega,\ i\geq 0} \left(J_\infty(k) = \sum_{i=0}^{\infty} \left(y(k+i|k)^2 + Ru(k+i|k)^2 \right) \right),$$

$R = 0.00002$

subject to $|u(k+i|k)| \leq 2$ volts, $\quad i \geq 0$.

No existing MPC synthesis technique can address this robust synthesis problem. If

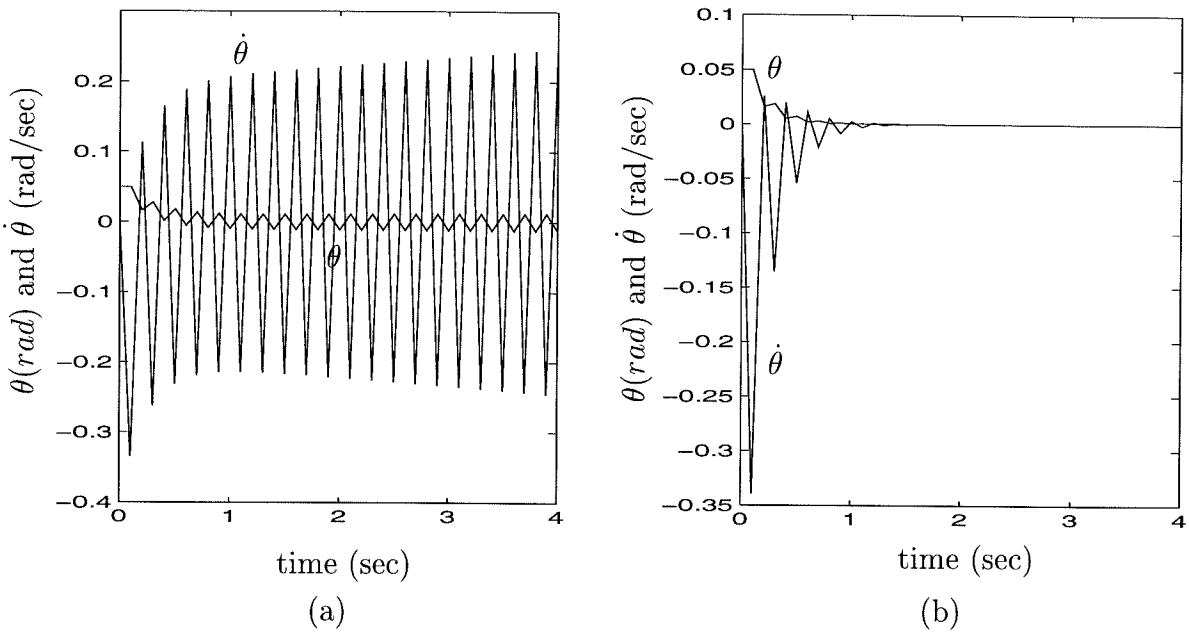

Figure 8.7: Unconstrained closed-loop responses for nominal plant ($\alpha(k) \equiv 9$ sec^{-1}); (a) using nominal MPC with $\alpha(k) \equiv 1$ sec^{-1}; (b) using robust LMI-based MPC.

the problem is formulated without *explicitly* taking into account plant uncertainty, the output response could be unstable. Figure 8.7(a) shows the closed-loop response of the system corresponding to $\alpha(k) \equiv 9$ sec^{-1}, given an initial state of $x(0) = \begin{bmatrix} 0.05 \\ 0 \end{bmatrix}$. The control law is generated by minimizing a *nominal* unconstrained infinite horizon objective function using a *nominal* model corresponding to $\alpha(k) \equiv \alpha_{\text{nom}} \equiv 1$ sec^{-1}. The response is unstable.

Note that the optimization is feasible at each time $k \geq 0$ and hence the controller cannot diagnose the unstable response via infeasibility, even though the horizon is infinite (see [114]). This is not surprising and shows that the prevalent notion

feedback in the form of plant measurements at each time step k is expected to compensate for unmeasured disturbances and model uncertainty

is only an ad-hoc fix in MPC for model uncertainty without any guarantees of robust stability.

Figure 8.7(b) shows the response using the control law derived from Theorem 8.1.

Notice that the response is stable and the performance is very good. Figure 8.8(a)

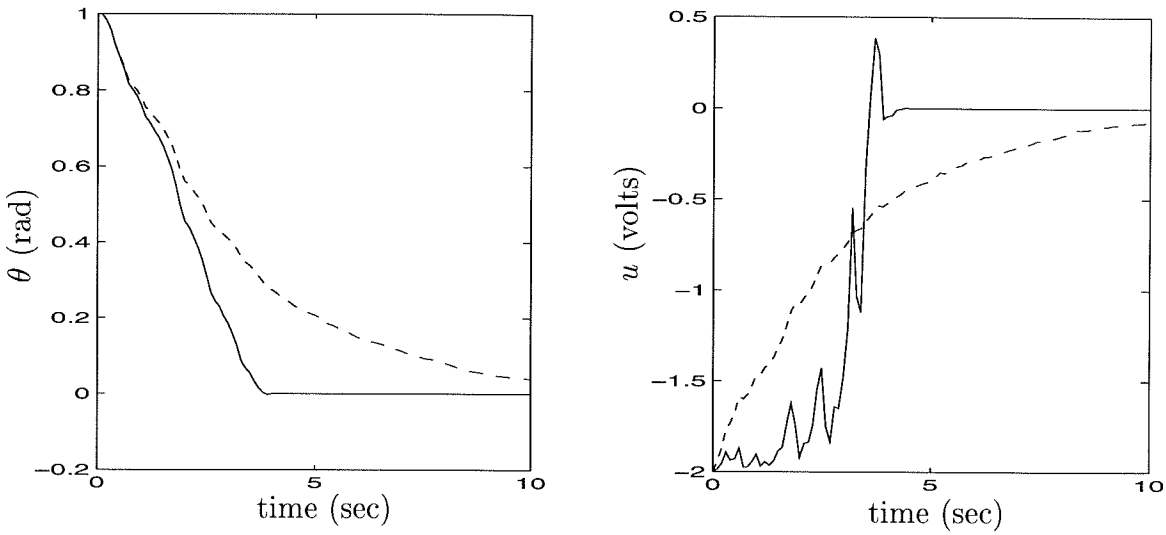

Figure 8.8: Closed-loop responses for the time-varying system with input constraint; solid: using robust receding horizon state-feedback; dash: using robust static state-feedback.

shows the closed-loop response of the system when $\alpha(k)$ is randomly time-varying between 0.1 and 10 sec^{-1}. The corresponding control signal is given in Figure 8.8(b). A control constraint of $|u(k)| \leq 2$ volts is imposed. The control law is synthesized according to Theorem 8.2.

We see that the control signal stays close to the constraint boundary up to time $k \approx 3$ sec, thus shedding light on Remark 8.9. Also included in Figure 8.8 are the response and control signal using a *static* state-feedback control law, where the feedback matrix F computed from Theorem 8.2 at time $k = 0$ is kept constant for all times $k > 0$, i.e., it is not recomputed at each time k. The response is about four times slower than the response with the receding horizon state-feedback control law.

This sluggishness can be understood if we consider Figure 8.9 which shows the norm of F as a function of time for the receding horizon controller and for the static state-feedback controller. To meet the constraint $|u(k)| = |Fx(k)| \leq 2$ volts for small k, F must be "small" since $x(k)$ is large for small k. But as $x(k)$ approaches 0, F

can be made larger while still meeting the input constraint. This "optimal" use of the control constraint is possible only if F is recomputed at each time k, as in the receding horizon controller. The static state-feedback controller does not recompute F at each time $k \geq 0$ and hence shows a sluggish (though stable) response.

For the computations, the solution at time k was used as an initial guess for solving the optimization at time $k+1$. The total times required to compute the closed-loop responses in Figure 8.7 (b) (40 samples) and Figure 8.8 (100 samples) were about 27 and 77 seconds respectively (or equivalently, 0.68 and 0.77 seconds per sample), on a SUN SPARCstation 20, using MATLAB code. The actual CPU times were about 18 and 52 seconds (i.e., 0.45 and 0.52 seconds per sample) respectively. In both cases, nearly 95% of the time was required to solve the LMI optimization at each sampling time.

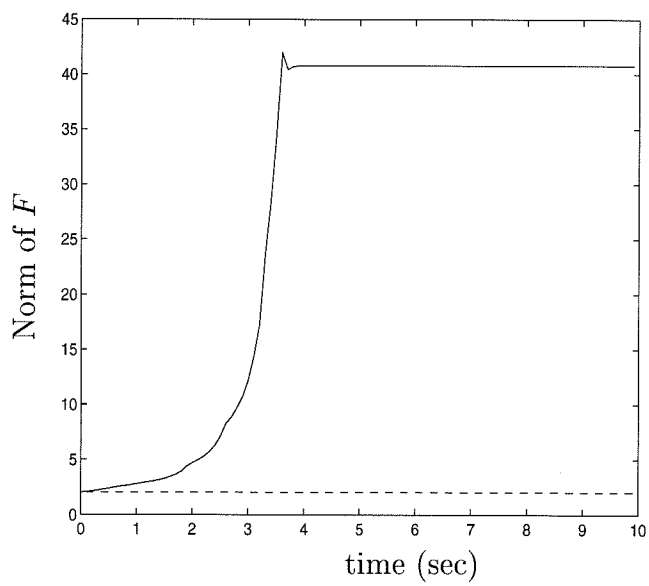

Figure 8.9: Norm of the feedback matrix F as a function of time; solid: using robust receding horizon state-feedback; dash: using robust static state-feedback.

8.5.2 Example 2

The second example is adapted from Problem 4 of the benchmark problems described

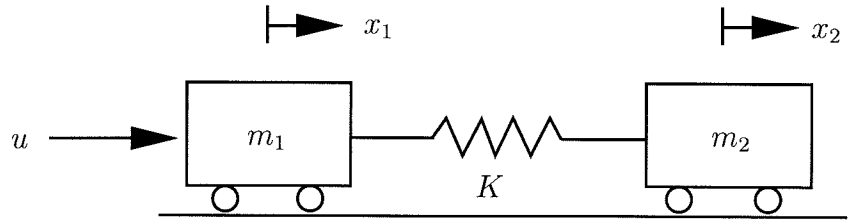

Figure 8.10: Coupled spring-mass system.

in [133]. The system consists of a two-mass-spring system shown in Figure 8.10. Using Euler's first-order approximation for the derivative and a sampling time of 0.1 sec, the following discrete-time state-space equations are obtained by discretizing the continuous-time equations of the system (see [133])

$$\begin{bmatrix} x_1(k+1) \\ x_2(k+1) \\ x_3(k+1) \\ x_4(k+1) \end{bmatrix} = \begin{bmatrix} 1 & 0 & 0.1 & 0 \\ 0 & 1 & 0 & 0.1 \\ -\frac{0.1K}{m_1} & \frac{0.1K}{m_1} & 1 & 0 \\ \frac{0.1K}{m_2} & -\frac{0.1K}{m_2} & 0 & 1 \end{bmatrix} \begin{bmatrix} x_1(k) \\ x_2(k) \\ x_3(k) \\ x_4(k) \end{bmatrix} + \begin{bmatrix} 0 \\ 0 \\ \frac{0.1}{m_1} \\ 0 \end{bmatrix} u(k)$$

$$y(k) = x_2(k).$$

Here, x_1 and x_2 are the positions of body 1 and 2, and x_3 and x_4 are their velocities respectively. m_1 and m_2 are the masses of the two bodies and K is the spring constant. For the nominal system, $m_1 = m_2 = K = 1$ with appropriate units. The control force u acts on m_1.

The performance specifications are defined in Problem 4 of [133] as follows: Design a feedback/feed-forward controller for a unit-step output command tracking problem for the output y with the following properties:

1. A control input constraint of $|u| \leq 1$ must be satisfied.

2. Settling time and overshoot are to be minimized.

3. Performance and stability robustness with respect to m_1, m_2, K are to be maximized.

We will assume for this problem that exact measurement of the state of the system, that is, $[x_1\ x_2\ x_3\ x_4]^T$ is available. We will also assume that the masses m_1 and m_2 are constant equal to 1, and that K is an uncertain constant in the range $K_{\min} \leq K \leq K_{\max}$. The uncertainty in K is modeled as in (8.4) by defining

$$\delta = \frac{K - K_{\text{nom}}}{K_{\text{dev}}},\ A = \begin{bmatrix} 1 & 0 & 0.1 & 0 \\ 0 & 1 & 0 & 0.1 \\ -0.1K_{\text{nom}} & 0.1K_{\text{nom}} & 1 & 0 \\ 0.1K_{\text{nom}} & -0.1K_{\text{nom}} & 0 & 1 \end{bmatrix},\ B_p = \begin{bmatrix} 0 \\ 0 \\ -0.1 \\ 0.1 \end{bmatrix},$$

$$C_q = [K_{\text{dev}}\ \ -K_{\text{dev}}\ 0\ 0],\ D_{qu} = 0$$

where $K_{\text{nom}} = \frac{K_{\max} + K_{\min}}{2}$, $K_{\text{dev}} = \frac{K_{\max} - K_{\min}}{2}$.

For unit-step output tracking of y, we must have at steady state $x_{1s} = x_{2s} = 1$, $x_{3s} = x_{4s} = 0$, $u_s = 0$. As in §8.4.2, we can shift the origin to the steady state. The problem we would like to solve at each sampling time k is the following:

$$\min_{u(k+i|k) = Fx(k+i|k),\ i \geq 0} \ \max_{A(k+i) \in \Omega,\ i \geq 0} J_\infty(k)$$

subject to $|u(k+i|k)| \leq 1,\ i \geq 0$. Here, $J_\infty(k)$ is given by (8.42) with $Q_1 = I$, $R = 1$. Figure 8.11 shows the output and control signal as functions of time, as the spring constant K (assumed to be constant but unknown) is varied between $K_{\min} = 0.5$ and $K_{\max} = 10$. The control law is synthesized using Theorem 8.2. An input constraint of $|u| \leq 1$ is imposed. The output tracks the set-point to within 10% in about 25 sec for all values of K. Also, the worst-case overshoot (corresponding to $K = K_{\min} = 0.5$) is about 0.2. It was found that asymptotic tracking is achievable in a range as large as $0.01 \leq K \leq 100$. The response in that case was, as expected, much more sluggish than that in Figure 8.11.

The total time required to compute the closed-loop response in Figure 8.11 (500 samples) for each fixed value of the spring constant K was about 438 seconds (about 0.87 seconds per sample) on a SUN SPARCstation 20, using MATLAB code. The CPU time was about 330 seconds (about 0.66 seconds per sample). Of these times,

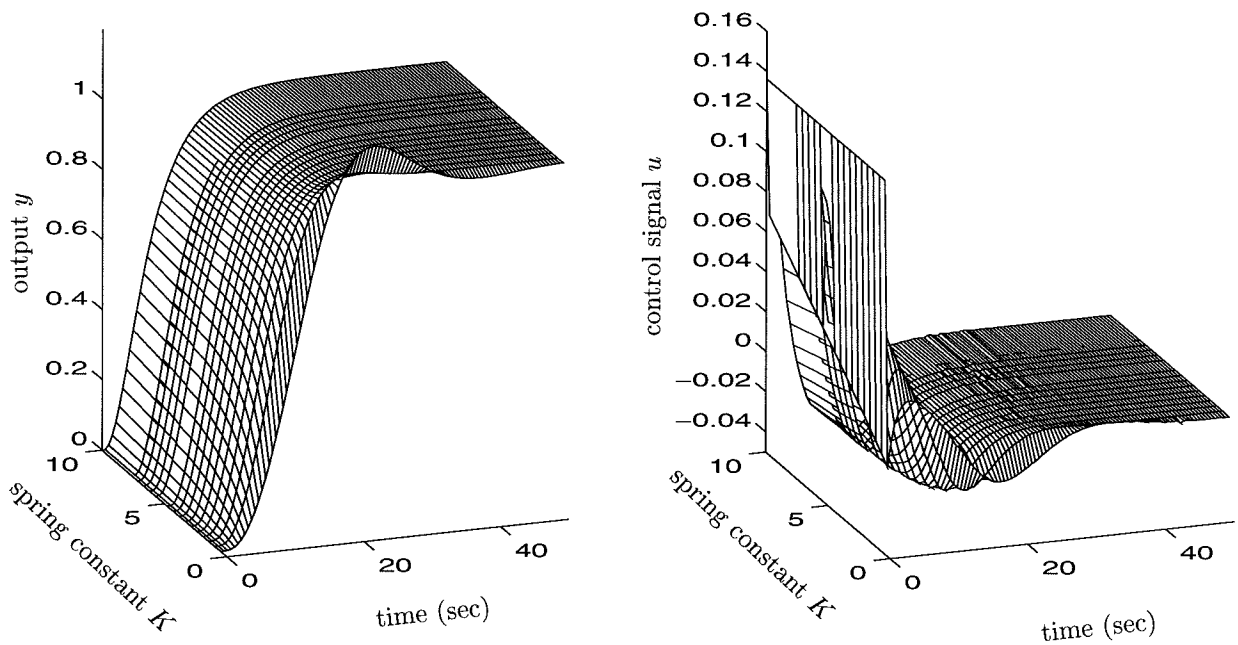

Figure 8.11: Position of body 2 and the control signal as functions of time for varying values of the spring constant.

nearly 94% was required to solve the LMI optimization at each sampling time.

8.6 Conclusions

Model Predictive Control (MPC) has gained wide acceptance as a control technique in the process industries. From a theoretical standpoint, the stability properties of nominal MPC have been studied in great detail in the past 7-8 years. Similarly, the analysis of robustness properties of MPC has also received significant attention in the MPC literature. However, robust synthesis for MPC has been addressed only in a restrictive sense for uncertain FIR models.

In this chapter, we have described a new and complete theory for robust MPC synthesis for two classes of very general and commonly encountered uncertainty descriptions. The on-line optimization involves solution of an LMI-based linear objective minimization. The resulting time-varying state-feedback control law minimizes, at each time-step, an upper bound on the robust performance objective, subject to

input and output constraints. Several extensions such as constant set-point tracking, reference trajectory tracking, disturbance rejection, application to systems with time delays and the output feedback case with an appropriate observer design complete the theoretical development. Two examples serve to illustrate application of the control technique.

8.7 Appendix A: Proof of Theorem 1

Minimization of $V(x(k|k)) = x(k|k)^T P x(k|k),\ P > 0$ is equivalent to

$$\begin{aligned} & \min_{\gamma,P} && \gamma \\ \text{subject to} \quad & x(k|k)^T P x(k|k) && \leq \ \gamma. \end{aligned}$$

Defining $Q = \gamma P^{-1} > 0$ and using Lemma 5.1 from Chapter 5, this is equivalent to

$$\begin{aligned} & \min_{\gamma,Q} && \gamma \\ \text{subject to} \quad & \begin{bmatrix} 1 & x(k|k)^T \\ x(k|k) & Q \end{bmatrix} && \geq \ 0, \end{aligned}$$

which establishes (8.19), (8.20), (8.23) and (8.24). It remains to prove (8.18), (8.21), (8.22), (8.25) and (8.26). We will prove these by considering **(A)** and **(B)** separately.

(A) The quadratic function V is required to satisfy (8.16). Substituting $u(k+i|k) = Fx(k+i|k),\ i \geq 0$ and the state space (8.1), inequality (8.16) becomes:

$$\begin{aligned} x(k+i|k)^T \big(& (A(k+i) + B(k+i)F)^T P (A(k+i) + B(k+i)F) - P \\ & + F^T R F + Q_1 \big) x(k+i|k) \ \leq \ 0. \end{aligned}$$

This is satisfied for all $i \geq 0$ if

$$(A(k+i)+B(k+i)F)^T P(A(k+i)+B(k+i)F) - P \\ +F^T RF + Q_1 \leq 0. \tag{8.58}$$

Substituting $P = \gamma Q^{-1}, Q > 0,\ Y = FQ$, pre- and post-multiplying by Q (which leaves the inequality unaffected), and using Lemma 5.1 from Chapter 5, we see that this is equivalent to

$$\begin{bmatrix} Q & QA(k+i)^T + Y^T B(k+i)^T & QQ_1^{\frac{1}{2}} & Y^T R^{\frac{1}{2}} \\ A(k+i)Q + B(k+i)Y & Q & 0 & 0 \\ Q_1^{\frac{1}{2}} Q & 0 & \gamma I & 0 \\ R^{\frac{1}{2}} Y & 0 & 0 & \gamma I \end{bmatrix} \geq 0. \tag{8.59}$$

Inequality (8.59) is affine in $[A(k+i)\ \ B(k+i)]$. Hence, it is satisfied for all

$$[A(k+i)\ \ B(k+i)] \in \Omega = \mathrm{Co}\{[A_1\ B_1], [A_2\ B_2], \ldots, [A_L\ B_L]\}$$

if and only if there exist $Q > 0$, $Y = FQ$ and γ such that

$$\begin{bmatrix} Q & QA_j^T + Y^T B_j^T & QQ_1^{\frac{1}{2}} & Y^T R^{\frac{1}{2}} \\ A_j Q + B_j Y & Q & 0 & 0 \\ Q_1^{\frac{1}{2}} Q & 0 & \gamma I & 0 \\ R^{\frac{1}{2}} Y & 0 & 0 & \gamma I \end{bmatrix} \geq 0, \quad j = 1, 2, \ldots, L.$$

The feedback matrix is then given by $F = YQ^{-1}$. This establishes (8.18) and (8.21).

(B) Let Ω be described by (8.4) in terms of a structured uncertainty block Δ as in (8.5). As in **(A)**, we substitute $u(k+i|k) = Fx(k+i|k),\ i \geq 0$ and the state space

equations (8.4) in (8.16) to get

$$\begin{bmatrix} x(k+i|k) \\ p(k+i|k) \end{bmatrix}^T \begin{bmatrix} (A+BF)^T P(A+BF) - P & (A+BF)^T P B_p \\ +F^T R F + Q_1 & \\ B_p^T P(A+BF) & B_p^T P B_p \end{bmatrix} \times \begin{bmatrix} x(k+i|k) \\ p(k+i|k) \end{bmatrix} \leq 0, \tag{8.60}$$

with

$$\begin{aligned} p_j(k+i|k)^T p_j(k+i|k) \leq x(k+i|k)^T (C_{q,j} + D_{qu,j}F)^T \\ \times (C_{q,j} + D_{qu,j}F) x(k+i|k), j = 1, 2, \ldots, r. \end{aligned} \tag{8.61}$$

Using the $\mathcal{S}$ procedure described in Lemma 5.2 of Chapter 5, it is easy to see that (8.60) and (8.61) are satisfied if $\exists\ \lambda_1', \lambda_2', \ldots, \lambda_r' > 0$ such that

$$\begin{bmatrix} (A+BF)^T P(A+BF) - P + F^T R F & (A+BF)^T P B_p \\ +Q_1 + (C_q + D_{qu}F)^T \Lambda' (C_q + D_{qu}F) & \\ B_p^T P(A+BF) & B_p^T P B_p - \Lambda' \end{bmatrix} \leq 0, \tag{8.62}$$

$$\text{where} \quad \Lambda' = \begin{bmatrix} \lambda_1' I_{n_1} & & & \\ & \lambda_2' I_{n_2} & & \\ & & \ddots & \\ & & & \lambda_r' I_{n_r} \end{bmatrix} > 0. \tag{8.63}$$

Substituting $P = \gamma Q^{-1}$ with $Q > 0$, using Lemma 5.1 from Chapter 5 and after some straightforward manipulations, we see that this is equivalent to the existence of

$Q > 0,\ Y = FQ,\ \Lambda' > 0$ such that

$$\begin{bmatrix} Q & Y^T R^{\frac{1}{2}} & QQ_1^{\frac{1}{2}} & QC_q^T + Y^T D_{qu}^T & QA^T + Y^T B^T \\ R^{\frac{1}{2}} Y & \gamma I & 0 & 0 & 0 \\ Q_1^{\frac{1}{2}} Q & 0 & \gamma I & 0 & 0 \\ C_q Q + D_{qu} Y & 0 & 0 & \gamma \Lambda'^{-1} & 0 \\ AQ + BY & 0 & 0 & 0 & Q - B_p \gamma \Lambda'^{-1} B_p^T \end{bmatrix} \geq 0.$$

Defining $\Lambda = \gamma \Lambda'^{-1} > 0$ and $\lambda_i = \gamma \lambda_i'^{-1} > 0,\ i = 1, 2, \ldots, r$ then gives (8.22), (8.25) and (8.26) and the proof is complete. ■

8.8 Appendix B: Proof of Lemma 1

(A) From the proof of Theorem 8.1, Part **(A)**, we know that

$$(8.21) \Longleftrightarrow (8.59) \Longleftrightarrow (8.58) \Longrightarrow (8.16).$$

Thus,

$$\begin{aligned} & x(k+i+1|k)^T P x(k+i+1|k) - x(k+i|k)^T P x(k+i|k) \\ \leq\ & -x(k+i|k)^T Q_1 x(k+i|k) - u(k+i|k)^T R u(k+i|k) \\ <\ & 0 \quad \text{since } Q_1 > 0. \end{aligned}$$

Therefore,

$$\begin{aligned} & x(k+i+1|k)^T P x(k+i+1|k) < x(k+i|k)^T P x(k+i|k), \\ & \qquad i \geq 0, \quad (x(k+i|k) \neq 0). \end{aligned} \tag{8.64}$$

Thus, if $x(k|k)^T P x(k|k) \leq \gamma$, then $x(k+1|k)^T P x(k+1|k) < \gamma$. This argument can be continued for $x(k+2|k), x(k+3|k), \ldots$ and this completes the proof. ■

(B) From the proof of Theorem 8.1, Part **(B)**, we know that:

$$(8.25),\ (8.26) \Longleftrightarrow (8.62),\ (8.63) \Longrightarrow (8.60),\ (8.61) \Longleftrightarrow (8.16).$$

Arguments identical to case **(A)** then establish the result. ■

8.9 Appendix C: Output Constraints as LMIs

As in §8.3.2.1, we will assume that the postulates of Lemma 8.1 are satisfied so that $\mathcal{E}$ is an invariant ellipsoid for the predicted states of the uncertain system (8.1).

Polytopic uncertainty

For any plant $[A(k+j) \;\; B(k+j)] \in \Omega, \; j \geq 0$, we have

$$\begin{aligned}
\max_{i\geq 1} \|y(k+i|k)\|_2 &= \max_{i\geq 0} \|C\left(A(k+i)+B(k+i)F\right)x(k+i|k)\|_2 \\
&\leq \max_{z\in\mathcal{E}} \|C\left(A(k+i)+B(k+i)F\right)z\|_2, \; i\geq 0 \\
&= \bar{\sigma}\left[C\left(A(k+i)+B(k+i)F\right)Q^{\frac{1}{2}}\right], \; i\geq 0.
\end{aligned}$$

Thus, $\|y(k+i|k)\|_2 \leq y_{\max}, \; i \geq 1$ for any $[A(k+j) \;\; B(k+j)] \in \Omega, \; j \geq 0$ if

$$\bar{\sigma}\left[C\left(A(k+i)+B(k+i)F\right)Q^{\frac{1}{2}}\right] \leq y_{\max}, \quad i\geq 0,$$

or $Q^{\frac{1}{2}}(A(k+i)+B(k+i)F)^T C^T C(A(k+i)+B(k+i)F)Q^{\frac{1}{2}} \leq y_{\max}^2 I, \quad i\geq 0,$

which, in turn, is equivalent to

$$\begin{bmatrix} Q & (A(k+i)Q+B(k+i)Y)^T C^T \\ C(A(k+i)Q+B(k+i)Y) & y_{\max}^2 I \end{bmatrix} \geq 0, \; i\geq 0$$

(multiplying on the left and right by $Q^{\frac{1}{2}}$ and using Lemma 5.1 from Chapter 5).

Since the last inequality is affine in $[A(k+i) \;\; B(k+i)]$, it is satisfied for all

$$[A(k+i) \;\; B(k+i)] \in \Omega = \mathrm{Co}\{[A_1 \;\; B_1], [A_2 \;\; B_2], \ldots, [A_L \;\; B_L]\}$$

if and only if

$$\begin{bmatrix} Q & (A_jQ + B_jY)^TC^T \\ C(A_jQ + B_jY) & y_{\max}^2 I \end{bmatrix} \geq 0, \quad j = 1, 2, \ldots, L.$$

This establishes (8.38).

Structured uncertainty

For any admissible $\Delta(k+i),\ i \geq 0$, we have

$$\begin{aligned} \max_{i\geq 1} \|y(k+i|k)\|_2 &= \max_{i\geq 0} \|C(A+BF)x(k+i|k) + CB_p p(k+i|k)\|_2 \\ &\leq \max_{z\in\mathcal{E}} \|C(A+BF)z + CB_p p(k+i|k)\|_2,\ i \geq 0 \\ &= \max_{z^Tz\leq 1} \|C(A+BF)Q^{\frac{1}{2}}z + CB_p p(k+i|k)\|_2,\ i \geq 0. \end{aligned}$$

We want $\|C(A+BF)Q^{\frac{1}{2}}z + CB_p p(k+i|k)\|_2 \leq y_{\max},\ i \geq 0$ for all $p(k+i|k), z$ satisfying

$$p_j(k+i|k)^T p_j(k+i|k) \leq z^T Q^{\frac{1}{2}}(C_{q,j} + D_{qu,j}F)^T(C_{q,j} + D_{qu,j}F)Q^{\frac{1}{2}}z, \quad j = 1, 2, \ldots, r$$

and $z^Tz \leq 1$. This is satisfied if $\exists\ t_1, t_2, \ldots, t_r, t_{r+1} > 0$ such that for all $z, p(k+i|k)$

$$\begin{bmatrix} z \\ p(k+i|k) \end{bmatrix}^T \begin{bmatrix} Q^{\frac{1}{2}}(A+BF)^TC^TC(A+BF)Q^{\frac{1}{2}} & \\ +Q^{\frac{1}{2}}(C_q + D_{qu}F)^TT(C_q + D_{qu}F)Q^{\frac{1}{2}} & Q^{\frac{1}{2}}(A+BF)^TC^TCB_p \\ -t_{r+1}I & \\ B_p^TC^TC(A+BF)Q^{\frac{1}{2}} & B_p^TC^TCB_p - T \end{bmatrix}$$
$$\times \begin{bmatrix} z \\ p(k+i|k) \end{bmatrix} \leq y_{\max}^2 - t_{r+1},\ i \geq 0,$$

where

$$T = \begin{bmatrix} t_1 I_{n_1} & & & \\ & t_2 I_{n_2} & & \\ & & \ddots & \\ & & & t_r I_{n_r} \end{bmatrix} > 0.$$

Without loss of generality, we can choose $t_{r+1} = y_{\max}^2$. Then, the last inequality is satisfied for all $z, p(k+i|k)$ if

$$\begin{bmatrix} Q^{\frac{1}{2}}(A+BF)^T C^T C(A+BF)Q^{\frac{1}{2}} & Q^{\frac{1}{2}}(A+BF)^T C^T C B_p \\ +Q^{\frac{1}{2}}(C_q + D_{qu}F)^T T(C_q + D_{qu}F)Q^{\frac{1}{2}} - y_{\max}^2 I & \\ B_p^T C^T C(A+BF)Q^{\frac{1}{2}} & B_p^T C^T C B_p - T \end{bmatrix} \leq 0,$$

or equivalently,
$$\begin{bmatrix} y_{\max}^2 Q & (C_q Q + D_{qu}Y)^T & (AQ+BY)^T C^T \\ C_q Q + D_{qu}Y & T^{-1} & 0 \\ C(AQ+BY) & 0 & I - CB_p T^{-1} B_p^T C^T \end{bmatrix} \geq 0$$

(using Lemma 5.1 from Chapter 5 and after some simplification). This establishes (8.39).

Chapter 9 Level Control in the Steam Generator of a Nuclear Power Plant – Case Study

Abstract

Poor control of the steam generator water level in the secondary circuit of a nuclear power plant can lead to frequent reactor shutdowns. Such shutdowns are caused by violation of safety limits on the water level and are common at low operating power where the plant exhibits strong non-minimum phase characteristics and flow measurements are unreliable. There is, therefore, a need to systematically investigate the problem of controlling the water level in the steam generator in order to prevent costly reactor shutdowns. This chapter presents a general framework for addressing all aspects of this problem using model predictive control techniques.

9.1 Introduction

Nuclear fission reaction provides about 76% of the energy required for electrical power generation in France[1]. Economic feasibility of a nuclear power plant requires smooth and uninterrupted plant operation in the face of varying electrical power demand. Unplanned shutdowns or reactor trips initiated due to conservative safety considerations, which in turn are necessitated by poor control, are particularly expensive and must be minimized.

Several studies [65, 98, 110] investigating the causes of reactor trips have shown that the feed-water system in the nuclear reactor is a major contributor to plant unavailability. Up to 13% of all reactor trips in France in 1983 [110] were attributed to steam generator control problems.

[1]Electricité de France (EDF) home page http://www.edf.fr

9.1.1 Factors Leading to Poor Control

The difficulties in designing an effective level control system for the steam generator (SG) arise from a number of factors:

- *Non-minimum-phase (NMP) characteristics of the plant.* The plant exhibits strong inverse response behavior, particularly at low operating power due to the so-called "swell and shrink" effects. This NMP characteristic limits the achievable controller bandwidth.

- *Nonlinear plant characteristics.* The plant dynamics are highly nonlinear. This is reflected by the fact that the linearized plant model shows significant variation with operating power.

- *Sensor measurements.* At low powers, the flow measurement sensors are known to be unreliable and this precludes effective use of feed-forward control.

- *Constraints.* The feed-water system can only deliver a limited throughput of water to the SG. This imposes a *hard* limitation on the available control action, and thus on the available controller bandwidth. Moreover, input constraints can lead to the classical controller windup problem [81] which causes degradation of system performance and sometimes even instability if not accounted for in the controller design.

9.1.2 Previous Work

Various approaches that address one or more of the above issues in the design of the level controller have been reported in the literature.

- Irving *et al.* [67] presented a linear parameter varying model to describe the SG dynamics over the entire operating power range and proposed a model reference adaptive PID level controller.

  The Irving model and modifications based on it have probably been the most widely accepted SG models for use in controller design.

- The Irving model [67] was used by Choi *et al.* (1989) [32] to design a PI-like locally stabilizing controller. The same model was used by Kim *et al.* (1993) [78] to design a local model-based PI controller to offset the inverse response of the SG.

- A more general LQG/LTR-based controller design, using local linearization of a nonlinear validated model of the SG was presented by Menon and Parlos (1992) [98]. The local linear controllers were then "gain-scheduled" to cover the entire operating range.

- Na (1995) [103], Na and No (1992) [104] addressed the issue of unreliable flow measurements at low power by designing an adaptive observer to simultaneously estimate the flow errors and the parameters of the steam generator model at low power. These estimates were then used to estimate the unmeasurable water level and design a control action by minimizing a quadratic cost.

- A robust $\mathcal{H}_2$ level controller design was studied by Ambos *et al.* (1996) [3] and a robust $\mathcal{H}_\infty$ level controller was proposed by Bendotti *et al.* (1997) [14].

Level control systems based on fuzzy logic have been reported in numerous references. These are beyond the scope of this study and will, therefore, not be considered here.

From the preceding review, we see a preponderance of PI-like controllers in functional SGs. Some attempts have been made to design general controllers, e.g., $\mathcal{H}_2/\mathcal{H}_\infty$ and LQG/LTR, which are not restricted to PI/PID structures. However, with the exception of [98], all the level controller designs summarized above only handle the problem around a local operating point, with no clear understanding of how to address the global level control problem over the entire operating power range. Issues such as hard constraints on the control inputs (feed-water flow-rate), (soft) constraints on outputs (limits on water level), stability and robustness to unmodeled dynamics and parametric uncertainty are only handled indirectly and in an ad-hoc fashion after the controller has been designed.

A detailed evaluation of all these issues at the design stage of the controller can lead to a greater confidence in the controller design, resulting in a relaxation of the safety margins and as a consequence, a reduction in the frequency of reactor trips.

9.1.3 Model Predictive Control

With the advent of the current generation of high-speed computers, it is now conceivable that more advanced control strategies, not limited to PI/PID, can be applied in a realistic setting. Model Predictive Control (MPC), also known as Moving Horizon Control (MHC) or Receding Horizon Control (RHC), is one such controller design technique which has gained wide acceptance in process control applications in the petrochemical, pulp and paper industries, and in gas pipeline control (see [52]). As we saw in Chapter 8, MPC is probably the only methodology currently available which can explicitly handle constraints on the manipulated and output variables systematically during the design and implementation of the controller. Several process models as well as many performance criteria of significance to the process industries can be handled using MPC.

In this chapter, we apply MPC techniques to develop a general framework for systematically addressing the various issues in the SG level control problem.

9.2 Plant Description

The nuclear reactor under consideration is a pressurized water reactor (PWR) (see Figure 9.1). PWRs are currently in use in most French nuclear power plants.

The PWR can be divided into two sub-systems:

- The *steam supply system* composed of the nuclear reactor, the reactor coolant system and the steam generator (SG). The thermal energy released by the fission reaction in the nuclear reactor is transferred by the reactor coolant, which is pressurized water, from the reactor vessel to the steam generator in a closed loop. This loop is referred to as the *primary loop* or *primary circuit.*

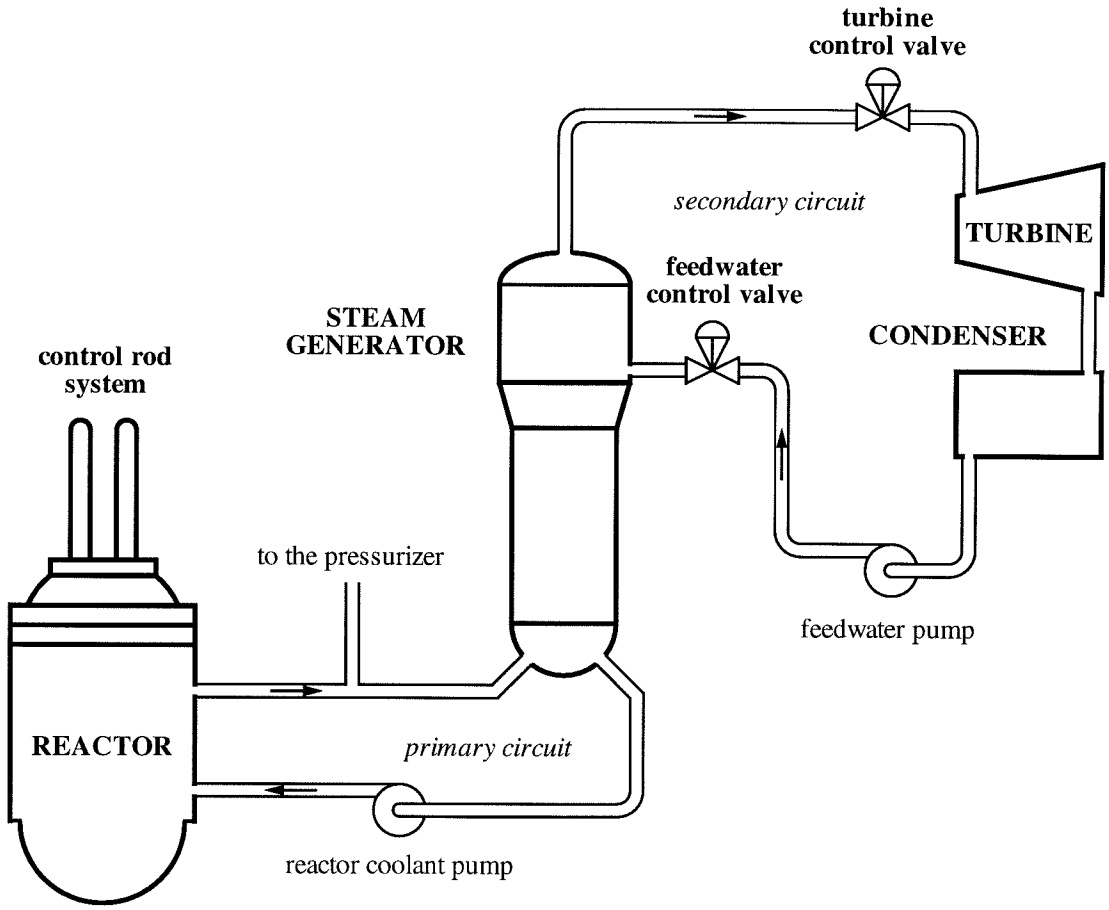

Figure 9.1: Layout of a pressurized water reactor (PWR).

- The *power conversion system* composed of the steam turbine, the electric generator and the condenser. This is a closed circuit and is also commonly referred to as the *secondary loop* or *secondary circuit.*

The primary circuit reactor coolant exchanges heat with the water in the SG. Thus, the water fed to the steam generator is vaporized, then released within the turbine where it expands and produces mechanical work. This mechanical work is transformed into electrical power by the electric generator. The steam leaving the turbines is condensed to liquid state in the condensers and fed back to the SG.

A changing electrical power demand causes a change in the steam demanded by the turbine, thereby requiring a change in the feed-water flow-rate to the SG and also a change in the thermal energy produced in the nuclear reactor. The rate of nuclear

reaction is regulated by the two control rod systems as shown in Figure 9.1. The rods capture neutrons, slowing down the nuclear reaction; withdrawing them increases the reaction, lowering them into the reactor slows down the reaction.

Our goal in this chapter is to study the use of the feed-water flow-rate as a manipulated variable to maintain the SG water level within allowable limits, in the face of the changing steam demand resulting from a change in the electrical power demand. We will assume that the primary side temperature is appropriately maintained at its reference value by the primary circuit control rod system. The identification and controller design issues for the primary circuit can be found elsewhere [13, 15, 19].

9.2.1 The U-Tube Steam Generator (UTSG)

The steam generator is the principal interface for exchange of heat between the primary circuit and the secondary circuit. It is a tubular evaporator of the natural circulation type (see Figure 9.2). We will briefly describe its operation. A detailed discussion of its operation can be found, for example, in [66].

The heat exchange region of the steam generator consists of a number of equivalent inverted vertical U-tubes, hence the name UTSG. The reactor coolant enters the UTSG at the bottom. It moves within the U-tubes upwards and then downwards, transferring heat through the tube wall to the secondary fluid before exiting at the bottom of the UTSG.

The secondary fluid, the feed-water, enters the UTSG through a torical distributor, located in the upper downcomer. It flows down to the lower downcomer through the space between the tube bundle wrapper and the SG shell. It enters the secondary side of the tube bundle in its lower part. As the secondary fluid heats up due to heat exchanged with the primary fluid, it flows upwards. It reaches saturation temperature, starts boiling and turns into a two-phase fluid. The two-phase mixture successively moves up through the separator/riser section, where steam is separated from water, and then through the dryers, which ensure that the exiting steam is essentially dry (steam quality of at least 99.75% by mass). The separated saturated

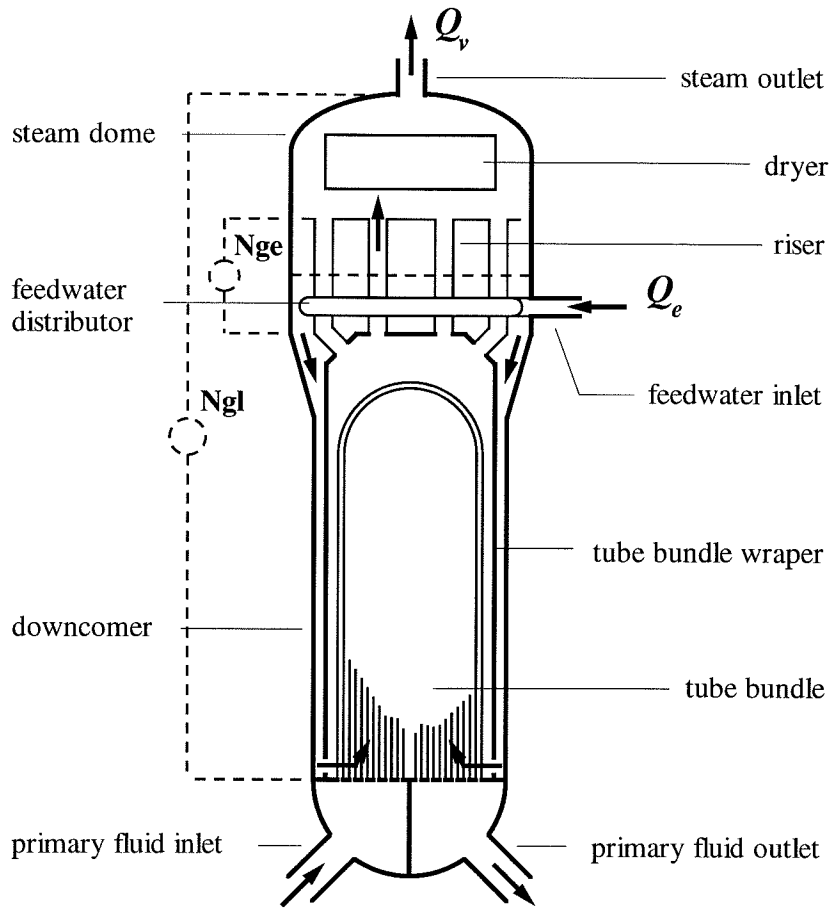

Figure 9.2: Schematic of a steam generator.

water is recirculated back to the downcomer.

9.2.2 Sensors and Actuators in the UTSG

Due to the complex two-phase nature of the steam-water interface in the tube bundle of the UTSG, the water level in the downcomer is not a well-defined quantity. Two types of water level measurements are provided, as shown in Figure 9.2, each reflecting a different level concept. The narrow range level N_{ge} is based on the pressure difference measured between two points close to the water level and gives the mixture level. The wide range level N_{gl} is based on the pressure difference measured between the two extremities of the steam generator (steam dome and bottom of the downcomer)

and gives the "collapsed liquid level" which reflects the mass of water in the steam generator.

The steam and feed-water flow-rates are also available as measurements. However, at low powers ($< 15 - 20\%$) and during startup, the flow sensors are known to be unreliable.

The actuator used to command the feed-water flow-rate consists of a main valve and a bypass valve. Such a setting is used to increase the precision of the actuator at low flow-rates. The bypass valve has about $\frac{1}{6}^{\text{th}}$ the capacity of the main valve.

9.2.3 Water Level "Swell and Shrink" Effects

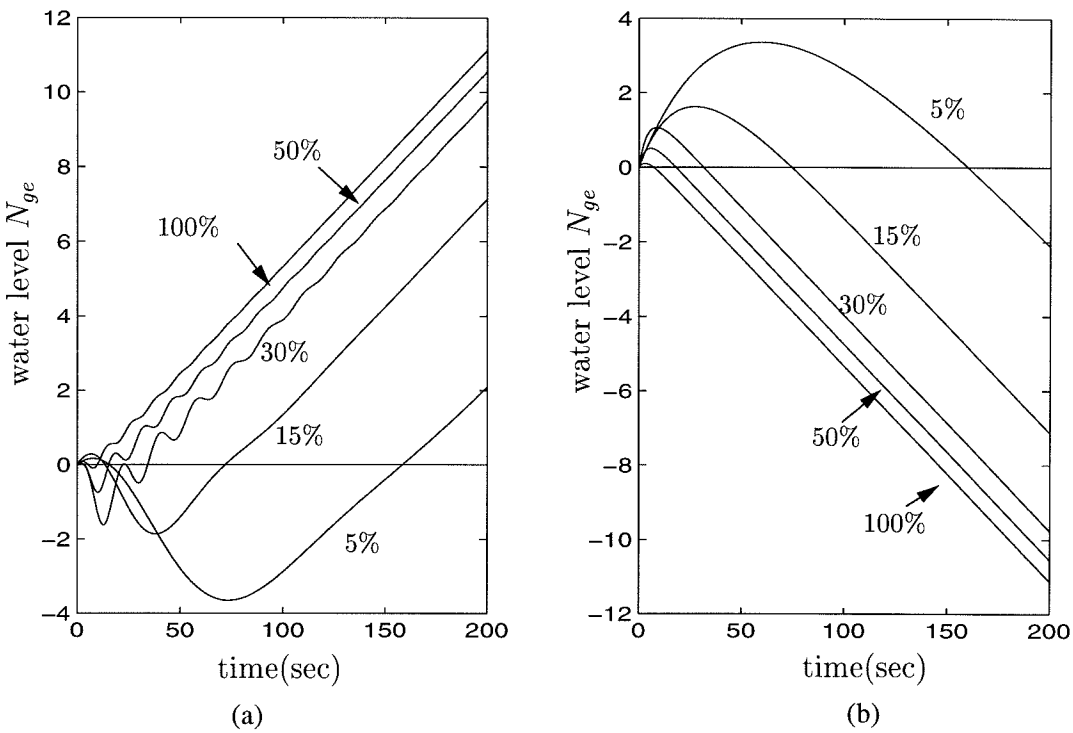

Figure 9.3: Responses of the water level at different operating powers (indicated by %) to (a) a step in feed-water flow-rate; (b) a step in steam flow-rate.

The ultimate change in the water level in the steam generator is governed by the balance between the flow-rates of exiting steam and the incoming feed-water. However, the transient behavior of the water level in the steam generator is dominated by the thermodynamic properties of the two-phase mixture present in the tube bundle

region and exhibits an inverse response behavior caused by the so-called "swell and shrink" phenomena.

When the steam flow-rate is increased, the steam pressure in the steam dome decreases, and the two-phase fluid in the tube bundle expands, causing the water level to rise initially (swell) instead of falling as should be expected from the mass balance. A decrease in steam flow-rate leads to an opposite effect of collapse of the steam bubbles in the two-phase fluid caused by an increase in the pressure in the steam dome. The water in the downcomer then flows to occupy this space, thereby leading to an initial counterintuitive lowering of the water level (shrink).

Similarly, when the feed-water flow-rate is increased, the cold feed-water which enters the bottom of the tube bundle region causes the steam bubbles to collapse. This causes a decrease in the volume occupied by the two-phase mixture. The water in the downcomer fills this empty region causing a drop in the water level (shrinking). When the feed-water flow-rate is decreased, the opposite phenomenon of swelling occurs.

Figure 9.3 shows responses of the water level to steps in feed-water and steam flow-rates at different operating powers. For generating the responses, we have used the power dependent linear parameter varying model identified by Irving *et al.* (1980) [67]. The inverse response behavior of the water level is immediately apparent in both the responses. It is more severe at low power and is observed only in the narrow range level N_{ge} and not in the wide range level N_{gl} (not shown here) since N_{gl} directly reflects the mass of water in the steam generator, as we discussed in §9.2.2.

The changing steam generator dynamics and the inverse response behavior significantly complicate the design of an effective water level control system.

9.3 Steam Generator Modeling

The controller design and the resulting controller performance on the actual plant are both strongly dependent on the accuracy of the mathematical model used to describe the plant. However, a highly accurate model is generally also highly complex and nonlinear, and therefore, rarely suitable for use in controller design. Development

of detailed models for the UTSG using basic principles can be found, for example in [66, 135]. Such theoretical models use fundamental conservation equations for mass, energy, momentum and volume and basic thermodynamic principles. These models are typically used prior to plant licensing for simulating realistic accident conditions [66], for operator training [135] and to validate controller performance prior to implementation on the real plant [98].

For the purpose of controller design, the model should be simple and at the same time relatively accurate in describing the principal dynamics of the UTSG. Linearized models have the advantage that they can be used to design controllers by applying any of a number of well-established controller design techniques.

We will discuss two models which are relevant to this chapter.

9.3.1 The Model of Irving *et al.* (1980)

A linear model which has been widely used in steam generator modeling for control purposes is the parameter-dependent transfer function model identified by Irving *et al.* (1980) [67] from experimental measurements of the steam generator responses to steps in the feed-water and steam flow-rates.

Let y_1 and y_2 be the narrow and wide range water levels N_{ge} and N_{gl} respectively, from §9.2.2. Let u and d be the feed-water and steam flow-rates. Then, the transfer functions relating the inputs u and d to the water levels y_1 and y_2 are given by [67]

$$\begin{aligned} y_1(s) &= \left(\frac{G_1}{s} - \frac{G_2}{1+\tau_2 s}\right)(u(s) - d(s)) \\ &\qquad + \frac{G_3 s}{\tau_1^{-2} + 4\pi^2 T^{-2} + 2\tau_1^{-1} s + s^2} u(s) \qquad (9.1) \\ &= \left(\frac{G_1 - (G_2 - G_1\tau_2)s}{s(1+\tau_2 s)}\right)(u(s) - d(s)) \\ &\qquad + \frac{G_3 s}{\tau_1^{-2} + 4\pi^2 T^{-2} + 2\tau_1^{-1} s + s^2} u(s) \qquad (9.2) \\ y_2(s) &= \frac{G_1}{s}(u(s) - d(s)). \qquad (9.3) \end{aligned}$$

Each term in equation (9.1) has a physical interpretation as explained below:

- $\frac{G_1}{s}$, where $G_1 > 0$, is the *mass capacity effect* of the steam generator. It essentially integrates the flow difference $u(s) - d(s)$ to calculate the change in water level.

- $-\frac{G_2}{1+\tau_2 s}$, where $G_2, \tau_2 > 0$, is the *thermal negative effect* caused by the "swell and shrink" effects as explained in §9.2.3.

- $\frac{G_3 s}{\tau_1^{-2}+4\pi^2 T^{-2}+2\tau_1^{-1}s+s^2}$, where $G_3, \tau_1, T > 0$ is the *mechanical oscillation effect* caused by the direct addition of feed-water to the steam generator. This quantity appears only in response to a feed-water flow-rate change. It decays rapidly after a small multiple of the damping time constant τ_1.

An equivalent state-space representation of (9.1) and (9.3) is the following:

$$\begin{aligned}
\dot{x}(t) &= \begin{bmatrix} 0 & 0 & 0 & 0 \\ 0 & -\frac{1}{\tau_2} & 0 & 0 \\ 0 & 0 & -\frac{2}{\tau_1} & 1 \\ 0 & 0 & -(\frac{1}{\tau_1^2}+\frac{4\pi^2}{T^2}) & 0 \end{bmatrix} x(t) + \begin{bmatrix} G_1 \\ -G_2 \\ G_3 \\ 0 \end{bmatrix} u(t) + \begin{bmatrix} -G_1 \\ G_2 \\ 0 \\ 0 \end{bmatrix} d(t) \\
y(t) &= \begin{bmatrix} y_1(t) \\ y_2(t) \end{bmatrix} = \begin{bmatrix} 1 & 1 & 1 & 0 \\ 1 & 0 & 0 & 0 \end{bmatrix} x(t).
\end{aligned} \tag{9.4}$$

From (9.2), we see that if $G_2 - G_1\tau_2 > 0$, then the transfer function from u and d to y is non-minimum phase. From the responses shown in Figure 9.3, we see that the dynamics of the UTSG change with operating power. This is reflected in the above model by allowing the parameters $G_1, G_2, G_3, \tau_1, \tau_2, T$ to be dependent on operating power. This parameter dependence has been characterized in [67], where the values of these parameters at different operating powers have been identified. These values are summarized in Table 9.1.

9.3.2 The Model Provided by Electricité de France

The model which will be used in this study for the purpose of controller design is a simple 4^{th} order model. This model is currently being used for control studies in

Power (%)	5	15	30	50	100
G_1	0.058	0.058	0.058	0.058	0.058
G_2	9.63	4.46	1.83	1.05	0.47
G_3	0.181	0.226	0.31	0.215	0.105
τ_1	41.9	26.3	43.4	34.8	28.6
τ_2	48.4	21.5	4.5	3.6	3.4
T	119.6	60.5	17.7	14.2	11.7

Table 9.1: Steam generator model parameter variation (Irving et al. (1980)).

the Research and Development Division of Electricité de France (EDF). The model is built together out of transfer function equations which are derived from simple dynamical considerations. We briefly describe the steps which are used to arrive at the model description.

The narrow range level N_{ge} is assumed to be governed by the flow balance of the incoming water and the outgoing steam-water mass across the tube bundle region of the steam generator. This balance for the narrow range water level N_{ge} can be described by the following transfer function:

$$N_{ge} = \frac{1}{T_n s}(Q_{ef} - Q_{GV}) \tag{9.5}$$

where Q_{ef} is the flow-rate of the incoming water in the tube bundle and Q_{GV} is the equivalent steam-water mixture flow-rate exiting the tube bundle region.

The incoming water flow-rate Q_{ef} in the tube bundle region is related to the fresh feed-water flow-rate by two simple first order lags as follows:

$$Q_{ef} = \frac{1}{(1+\tau s)(1+T_h s)} Q_e. \tag{9.6}$$

where the lag $\frac{1}{1+\tau s}$ accounts for the feed-water valve dynamics and $\frac{1}{1+T_h s}$ accounts for the water mass transportation dynamics. In this equation, it is also possible to include a higher order term to account for water mass oscillations which can be induced by the large water flow-rates involved. However, this term is ignored in the model currently in use at EDF. A non-minimum phase term can also be added to account for the

feed-water system inverse response behavior. This too has been ignored in the model of EDF. In §9.6.3, we will see the effect of adding a non-minimum phase term to the feed-water system dynamics.

The exiting steam-water mass Q_{GV} from the tube bundle region is related to the turbine steam demand Q_v by a simple first order lag $\frac{1}{1+T_g s}$. In addition, a non-minimum phase term $1 - F_g T_g s$ is also incorporated to account for the two-phase swell and shrink effects. Thus,

$$Q_{GV} = \frac{1 - F_g T_g s}{1 + T_g s} Q_v. \tag{9.7}$$

Combining (9.5), (9.6), (9.7), we get the following equation relating the narrow range water level N_{ge} to the feed-water flow-rate Q_e and the steam demand Q_v:

$$N_{ge}(s) = \frac{1}{T_n s}\left(\frac{Q_e(s)}{(1+\tau s)(1+T_h s)} - \frac{1 - F_g T_g s}{1 + T_g s} Q(s)\right). \tag{9.8}$$

The wide range water level N_{gl}, being representative of the overall water mass in the steam generator, is given simply by the integral equation

$$N_{gl} = \frac{1}{T_{int} s}(Q_e - Q_v). \tag{9.9}$$

Denoting the water levels by $y_1 = N_{ge}$ and $y_2 = N_{gl}$ and the steam and feed-water flow-rates by $d = Q_v$ and $u = Q_e$, we can rewrite (9.8), (9.9) in the following equivalent state-space form:

$$\dot{x}(t) = \begin{bmatrix} 0 & 0 & 0 & \frac{1}{T_n} \\ 0 & -\frac{1}{T_h} & 0 & -\frac{1}{T_n} \\ 0 & 0 & -\frac{1}{T_g} & 0 \\ 0 & 0 & 0 & -\frac{1}{\tau} \end{bmatrix} x(t) + \begin{bmatrix} 0 \\ 0 \\ 0 \\ \frac{1}{\tau} \end{bmatrix} u(t) + \begin{bmatrix} -\frac{1}{T_n} \\ 0 \\ \frac{1+F_g}{T_n} \\ 0 \end{bmatrix} d(t) \tag{9.10}$$

$$y(t) = \begin{bmatrix} y_1(t) \\ y_2(t) \end{bmatrix} = \begin{bmatrix} 1 & 1 & 1 & 0 \\ \frac{T_n}{T_{int}} & 0 & 0 & 0 \end{bmatrix} x(t). \tag{9.11}$$

The parameters T_n, F_g, T_h, τ are functions of the operating power and have been identified by EDF from experimental data. These parameter values are summarized in Table 9.2. Note that $T_g = 10$ sec and $T_{int} = 140$ sec are constants and do not vary with operating power. Figure 9.4 shows water level responses of the EDF model

Power θ (%)	3.2	4.1	9.5	24.2	30	50	100
T_n	36	56	63	44	40	40	40
F_g	13	18	10	4	4	4	4
T_h	170	56	30	10	8	5	5
τ	10	10	10	30	30	30	30

Table 9.2: Variation of the steam generator model parameters over the power range.

to steps in the feed-water and steam flow-rates at different operating powers. As expected, the response to a step in the feed-water flow-rate does not show an inverse response since this was never model-led, although the response to a step in steam flow-rate exhibits non-minimum phase characteristics.

9.4 Steam Generator Level Control

Underlying the basic objective of water level control in the steam generator, there are three different issues which have individual motivation.

Control of the water level in the downcomer If the water level in the downcomer reaches too high a level, the steam separator and dryer do not function properly and excessive moisture is carried in the exiting steam, increasing erosion of the turbine blades. Furthermore, high moisture content in the exiting steam also reduces turbine efficiency. Too low a level leads to insufficient cooling of the primary fluid. Beside the direct link with the downcomer water mass, the water level is strongly related to the water/steam mixture in the tube bundle. Hence it will be referred to as the mixture level. It is well represented by the mean of the narrow range level measurement N_{ge} (see Figure 9.2).

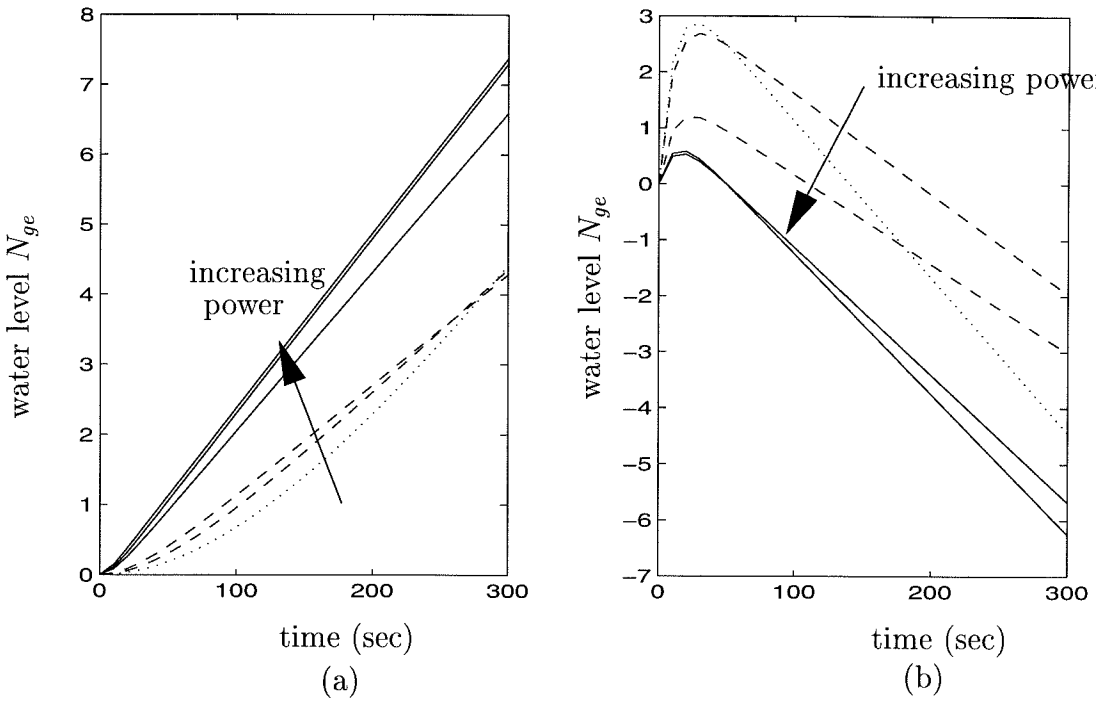

Figure 9.4: Responses of the water level at different operating powers to (a) a step in feed-water flow-rate; (b) a step in steam flow-rate.

Control of the water mass in the steam generator The water mass of the steam generator is relevant for the coolability of the primary circuit. When the steam demand is increased due to an increase in the demand of power, the feed-water has to be increased to maintain the water mass at the correct set-point. The water level corresponding to this water mass set-point is referred to as the collapsed water level and is represented by the mean of the wide range water level measurement N_{gl} (see Figure 9.2).

Prevention of instabilities of the water columns The last issue is related to the dynamical behavior of the water level. Because of the large mass of water and the large flows involved in the steam generator operation, it is important to have a smooth operation and in particular to avoid fast transients and persistent oscillations. Such oscillations are detrimental to the steam generator operation since they may lead to cracking and denting of the steam generator tubes.

9.4.1 Water Level Set-Points and Alarm Limits

The three objectives mentioned above are achieved by specifying appropriate set-points for the narrow and wide range water levels. These set-points are functions of the operating power and are shown in Figure 9.5. Figure 9.5(a) also shows the high level and low level alarm limits for N_{ge}. Violation of these pre-specified upper and lower limits on the allowable deviations of the water level N_{ge} from these set-points results in an alarm and, subsequently, an automatic reactor trip. An excellent discussion on the setting up of alarm limits and initiation and execution of reactor trips can be found in Schneider and Boyd (1985) [121], based on their experience at the Point Lepreu plant of the New Brunswick Electric Power Commission, using steam generators developed by Babcock & Wilcox Canada.

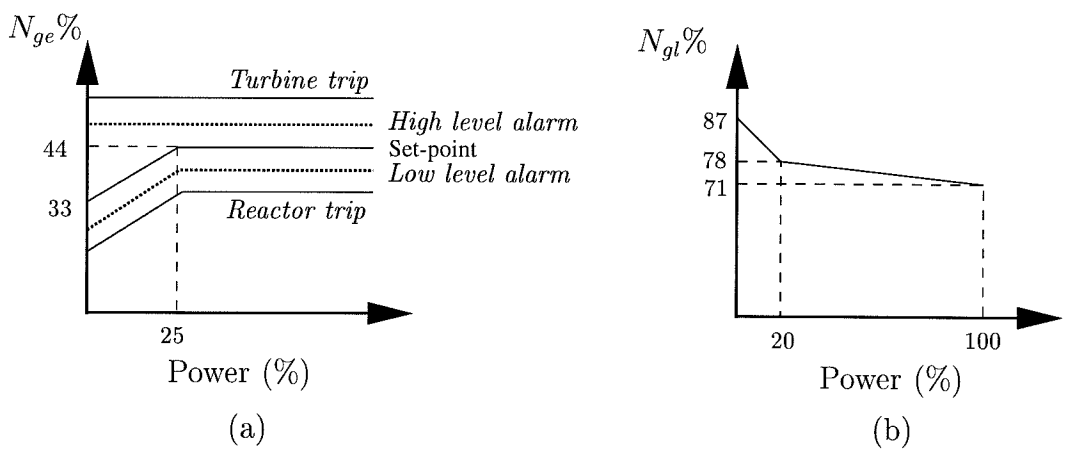

Figure 9.5: Normalized set-points for (a) N_{ge}, with high and low level alarm limits; (b) N_{gl}.

9.4.2 General Control Strategy

The general control strategy consists in achieving all the three objectives by maintaining the narrow range and wide range water levels within limits of their set-points. This can be accomplished by concentrating the control effort on the single controlled variable: the narrow range water level N_{ge}. In fact, since there is only one manipulated variable – the feed-water flow-rate – only one of the two water levels can be

independently controlled with zero steady-state offset. The narrow range water level N_{ge}, being a more critical variable, is chosen to be the controlled variable. Nonetheless, with this strategy, as we will see, good control of N_{gl} is also achieved.

Either of the model equations (9.1) or (9.8), which relate the feed-water and steam flow-rates u and d to the narrow range water level $y_1 = N_{ge}$, can be rewritten as follows:

$$y_1(s) = P(s,\theta)u(s) + P_d(s,\theta)d(s) \tag{9.12}$$

with P and P_d appropriately defined. Here, θ represents the operating power, which determines the values of the various parameters in the transfer functions $P(s)$ and $P_d(s)$, as described in §9.3.1 and §9.3.2. The corresponding state-space models (9.4) or (9.10), (9.11) can be rewritten as follows:

$$\begin{aligned} \dot{x}(t) &= A(\theta)x(t) + B(\theta)u(t) + B_d(\theta)d(t) \\ y_1(t) &= Cx(t). \end{aligned} \tag{9.13}$$

Thus we see that the change in the steam demanded from the UTSG can be considered as a disturbance d to the plant. The control problem is to reject the effect of this disturbance on the UTSG narrow range water level N_{ge}, by using the feed-water flow-rate u as the manipulated variable (see Figure 9.6). We immediately

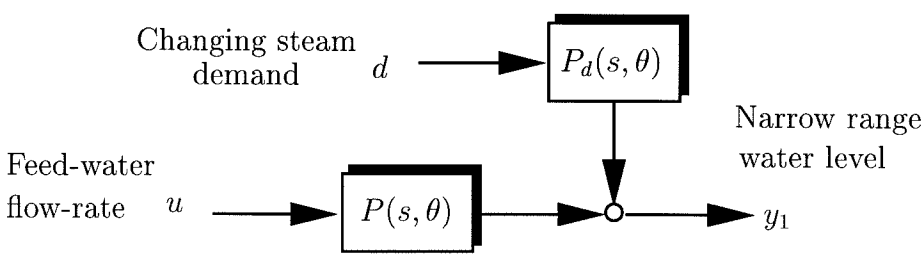

Figure 9.6: Disturbance rejection for a linear parameter varying system.

see that this is a disturbance rejection problem for a linear parameter varying (LPV) system since P and P_d are dependent on the operating power θ.

Since the feed-water system can only deliver a finite flow-rate, the manipulated variable u is constrained. With normalized variables, this is equivalent to

$$0\% \leq u(t) \leq 100\%. \tag{9.14}$$

The lower limit of 0% arises from the fact that we cannot withdraw water from the steam generator and thus the feed-water flow-rate cannot be negative. As we will see, model predictive control (MPC) provides an ideal framework for systematically accounting for input constraints.

9.5 UTSG Level Control using MPC

A number of factors make MPC particularly suitable for the UTSG level control problem:

- *Hard actuator constraints.* We saw in §9.4.2 that the manipulated variable, the feed-water flow-rate, is constrained. At present, MPC is the only control technique which can handle such *hard* inequality actuator constraints in a systematic manner during the design and implementation of the controller.

- *Soft level constraints.* The water level alarm limits discussed in §9.4.1 are generally referred to as *soft constraints* on the output variable N_{ge} since they can be relaxed somewhat depending on how much of a safety margin is required. Again, as with the actuator constraints, such *soft* constraints can conceptually be incorporated directly in the MPC formulation as inequality constraints on N_{ge} (see §8.2.2). Quite often though, incorporation of output constraints leads to infeasibility of the on-line optimization. For this reason, we did not consider them directly in the simulation study in §9.6.

- *Feed-forward control.* MPC allows incorporation of feed-forward control action through the use of measured disturbances in the control law computation.

Moreover, MPC is probably the only control technique which can incorporate *all* the above features.

In §8.2.2, we reviewed the basic structure of MPC and its implementation. For an LTI system described in discrete-time by

$$\begin{aligned} x(k+1) &= Ax(k) + Bu(k) + B_d d(k) + n_1(k) \\ y(k) &= Cx(k) + n_2(k) \end{aligned} \tag{9.15}$$

with $x(k) \in \Re^{n_x}$ denoting the state of the system at sampling time k, $u(k) \in \Re^{n_u}$ the control input, $y(k) \in \Re^{n_y}$ the controlled output, $d(k) \in \Re^{n_d}$ an external measured disturbance, $n_1(k) \in \Re^{n_x}$ is the state excitation noise and $n_2(k) \in \Re^{n_y}$ is the measurement noise, the model used for prediction of the future outputs is given by

$$\begin{aligned} x(k|k-1) &= Ax(k-1|k-1) + Bu(k-1|k-1) \\ y(k|k-1) &= Cx(k|k-1). \end{aligned} \tag{9.16}$$

This equation assumes that $d(k)$ is an unmeasured disturbance, hence it does not appear in the prediction equations. The case where a measured disturbance is used for feed-forward control can also be considered. Prediction for more than one step ahead is obtained by applying the above equations recursively.

Correspondingly, the state estimator, which is used to update the plant state and correct for measurement noise, is given by

$$\hat{x}(k) = x(k|k) = x(k|k-1) + K(\hat{y}(k) - y(k|k-1)) \tag{9.17}$$

where K is the optimal Kalman filter gain determined from the solution of a discrete-time Riccati equation [92] as follows:

$$\begin{aligned} &K = QC^T(CQC^T + V)^{-1}, \quad \text{where, } Q > 0 \text{ solves} \\ &Q - AQA^T + AQC^T(CQC^T + V)^{-1}CQA^T - W = 0. \end{aligned} \tag{9.18}$$

Here, W is the covariance matrix of the state excitation white noise n_1, and $V > 0$ is the covariance matrix of the output measurement white noise n_2 affecting the output y. It is assumed that n_1 and n_2 are uncorrelated.

The typical optimization problem which is solved by the MPC optimizer is the one defined in Chapter 8 (see also notation defined in Chapter 8):

$$\min_{u(k+i|k),i=0,1,\ldots,m-1} J_p(k), \tag{8.8'}$$

subject to constraints on the control input $u(k+i|k), i = 0, 1, \ldots, m-1$ and possibly also on the state $x(k+i|k), i = 0, 1, \ldots, p$ and the output $y(k+i|k), i = 1, 2, \ldots, p$. A typical objective function which is considered is the following (compare with (8.10))

$$\begin{aligned} J_p(k) = &\sum_{i=1}^{p} (r - y(k+i|k))^T \Gamma_y (r - y(k+i|k)) + \sum_{i=0}^{m-1} u(k+i|k)^T \Gamma_u u(k+i|k) \\ &+ \sum_{i=0}^{m-1} \Delta u(k+i|k)^T \Gamma_{\Delta u} \Delta u(k+i|k). \end{aligned} \tag{9.19}$$

where

r = set-point for y,

$\Delta u(k+i|k) = u(k+i|k) - u(k+i-1|k)$,

$\Gamma_y, \Gamma_u, \Gamma_{\Delta u} \geq 0$ are weighting matrices.

In general, the weights Γ_y, $\Gamma_u, \Gamma_{\Delta u}$ and the set-point r can all be allowed to vary over the prediction horizon p.

We immediately see that in this formulation, MPC is limited to linear time-invariant processes or nonlinear processes in a restricted operating region where they can be approximated reasonably by a linear time-invariant model. In applications such as the UTSG level control problem, the range of operation goes beyond the limits of the neighborhood where such a linear approximation is reasonable. This is especially true for the UTSG problem since, as we saw in §9.2.3, the open-loop dynamics of the process change significantly with the operating power. Therefore, for the global UTSG level control problem over the entire range of operating powers, such an approach using a single linear time-invariant model for MPC design would

almost certainly jeopardize performance.

The aforementioned problem is common to all linear model-based controllers such as $\mathcal{H}_2/\mathcal{H}_\infty$ control, for example. For linear controllers, a common solution to this problem is to design local linear controllers at different points in the operating regime and then apply *gain scheduling* techniques [61, 107, 115] to *schedule* these controllers to obtain a globally applicable controller.

For MPC, a natural solution to the global control problem would be to identify the operating point at each sampling time and use the plant model corresponding to this operating point as the *prediction* model or the *internal* model in the MPC computation. We will explore this extension of MPC and its application to the UTSG level control problem.

9.5.1 The Concept of a Varying Model in MPC

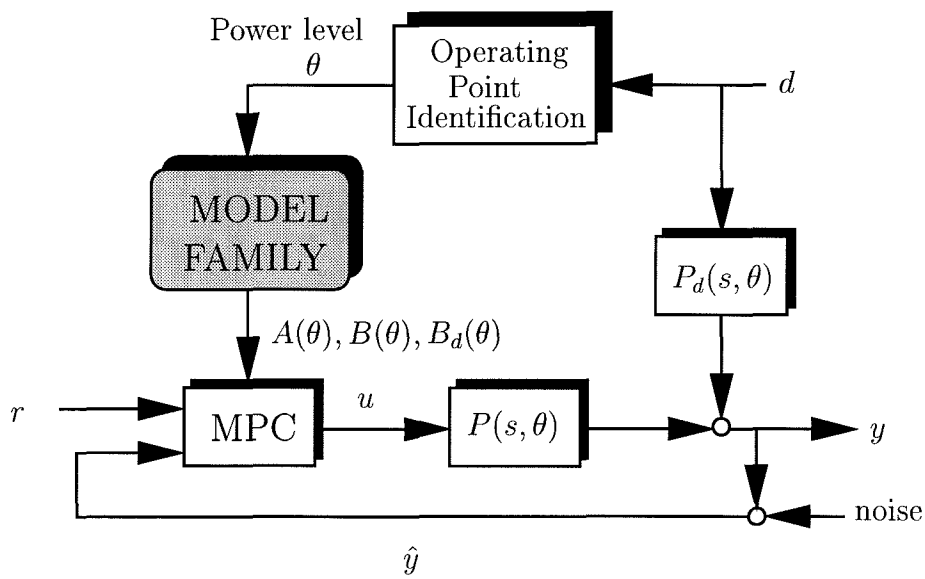

Figure 9.7: Model varying MPC for UTSG level control.

In MPC, a model is used to predict future outputs of the plant, and a sequence of present and future control moves is computed such that the predicted future outputs show a desirable response. It should be intuitively clear, therefore, that the accuracy of the future predictions is critical for obtaining the truly optimal control sequence

at each sampling time.

For the UTSG level control problem, the plant can be described reasonably well by a model which is structurally the same over the entire operating range, i.e., linear with the same number of states, but the model parameters depend on the operating power. As we saw in §9.4.2, it can be represented as follows:

$$\begin{aligned} \dot{x}(t) &= A(\theta)x(t) + B(\theta)u(t) + B_d(\theta)d(t) \\ y(t) &= Cx(t) \end{aligned} \tag{9.13'}$$

which after discretization with an appropriate sampling time and after adding fictitious state and measurement noise terms, can be represented as follows:

$$\begin{aligned} x(k+1) &= \bar{A}(\theta)x(k) + \bar{B}(\theta)u(k) + \bar{B}_d(\theta)d(t) + n_1(k) \\ y(k) &= Cx(k) + n_2(k). \end{aligned} \tag{9.20}$$

Assuming that we do not have a priori knowledge of how the power is going to vary in the future, the best prediction model that we can use at each sampling time is the model corresponding to the operating point at that sampling time. The operating point at each sampling time can in turn be identified by using the steam flow measurement or, for low powers where steam flow measurements are unreliable, directly from a knowledge of the demanded electric power. Generally, in the absence of steam flow measurements, the temperature difference between the incoming and exiting streams of the primary fluid is used to determine the steam generator operating point [98].

Application of this model-varying MPC to the UTSG level control problem then involves the following steps (see Figure 9.7):

Step 1 At sampling time k, identify the operating power level $\theta(k)$ at the current time k using the measured value of the steam demand $d(k)$.

Step 2 Choose the appropriate model $A(\theta(k))$, $B(\theta(k)), B_d(\theta(k))$ (or equivalently, the discretized model $\bar{A}(\theta(k)), \bar{B}(\theta(k)), \bar{B}_d(\theta(k))$) for the plant corresponding to this operating power level.

Step 3 Obtain new plant measurements $\hat{y}(k)$ and estimate the state $\hat{x}(k) = x(k|k)$ of the plant using the MPC estimator with the model chosen in **Step 2**.

Step 4 Solve the MPC optimization problem using the state estimate $\hat{x}(k)$ and the *fixed* model from **Step 2** as the prediction model.

Step 5 Implement the first computed control move $u(k|k)$.

Step 6 $k = k + 1$. Go to **Step 1**.

In **Step 2**, it is implicitly assumed that the functional dependence of the model $A(\theta)$, $B(\theta)$ on θ is known in the form of a continuous function. In other words, it is assumed that the model parameters $(G_1, G_2, \tau_1, \tau_2, T)$ for the Irving model (9.4) or (T_h, T_n, F_g, τ) for the EDF model (9.10), (9.11) can be expressed as a continuous function of the operating power θ. There are several reasons why this may not be a reasonable assumption:

- A continuous functional dependence of the model parameters on the operating power is rarely available in practice. Typically, as we saw in §9.3.1 and §9.3.2, the values of the operating parameters at *discrete* power levels are known from experimental data.

- The steam flow-rate measurement d is susceptible to measurement noise, and as a result, the operating power θ identified from the steam flow measurement is also subject to this noise. This would mean that in **Step 2** of the algorithm described above, if we assume a continuous dependence of the model parameters on θ, there would be unnecessary switching of the prediction model in the MPC computation. This is highly undesirable since it can lead to "chattering" of the control signal.

The alternative is to sub-divide the operating power range into sub-ranges and use a single model within each sub-range as the prediction model in MPC. This would result in a "family" of linear models, and the switch in **Step 2** of the algorithm above will occur depending on which sub-range the system is currently operating. This

eliminates unnecessary model switching and also ensures that the discrete model "family" can be realistically obtained from identification experiments at a discrete set of operating points. An additional advantage is that within each sub-range, the designed parameters of MPC can be tuned so as to get the best possible performance within that sub-range, independent of the MPC parameters chosen in the other sub-ranges.

9.5.2 Sub-Division of the Operating Power Range

The operating range sub-division is the basis of our model varying MPC concept. A number of different approaches can be used to arrive at a suitable sub-division of the operating power range. The simplest approach might involve a sub-division of the power range $0 - 100\%$ into equal sub-ranges, each of which covers, for example, 5% of the operating power, starting from 0%.

While this may be a simple technique, it may not reflect the non-uniform variation in the dynamics of the plant with operating power. For example, in the EDF model which we discussed in §9.3.2, the parameters T_h, T_n, F_g, τ (see Table 9.2) have been observed to show very little variation in the power range $50 - 100\%$, whereas they show significant variation in the low power range $3 - 24\%$. Clearly, in this case, the sub-ranges have to be much more closely spaced in the low power range than in the high power range.

What should be equal for the sub-ranges is not the power range they cover, but the *model error* they admit, assuming that a single model is used to represent all plants within the sub-range. We present one approach to arriving at a reasonable solution to this problem which ensures that an appropriately defined *model error* is equal for these sub-ranges. Alternative approaches addressing this problem can be found, for example, in [98].

9.5.2.1 Definition of Model Error

We define the model error for a sub-range of power $[\theta_1, \theta_2]$, $\theta_1 \leq \theta_2$ in terms of the model transfer functions $P(s, \theta_1)$ and $P(s, \theta_2)$ as follows:

$$e_{[\theta_1,\theta_2]} \triangleq \left\| \frac{P(s,\theta_2) - P(s,\theta_1)}{P(s,\theta_1)} \right\|_{\mathcal{H}_\infty}. \tag{9.21}$$

This definition of the model error is motivated by standard definitions for model uncertainty bounds which can be found, for example, in [101, 147]. Note that more general definitions for the model error, using frequency dependent weights, can also be considered but we restrict ourselves to this simple choice. Also, the choice of the *nominal* model for a given sub-range $[\theta_1, \theta_2]$, $\theta_1 \leq \theta_2$ is subjective, and one could, for example, choose the mid-point of the range $[\theta_1, \theta_2]$ as the nominal point and the model $P(s, \theta)$ corresponding to the mid-point as the nominal model. For this study, we chose the lower point θ_1 and the corresponding model $P(s, \theta_1)$ as the nominal model for the range $[\theta_1, \theta_2]$. We found that the final performance was not very sensitive to this choice.

In the sub-division procedure to be discussed next, we will show how we can divide the operating power range into sub-ranges of power such that the model error defined by (9.21) achieves the same pre-specified value in each of these sub-ranges.

9.5.2.2 Sub-Division Procedure

We will focus on the EDF model of §9.3.2 in this section. The same treatment is applicable to the Irving model of §9.3.1. The data from EDF is provided in the form of read-out charts relating the parameter values T_h, T_n, T_g, τ to the operating power θ. This data was reproduced in Table 9.2. The intermediate values are obtained by linear interpolation.

To begin with, the model parameters at 33 different power levels were interpolated based on the provided data. The power levels chosen were the following (all in %): 3.2, 3.5, 3.9, 4.1, 4.3, 4.6, 5, 5.8, 6.6, 7.4, 9.5, 10, 11.5, 12, 13, 13.5, 14.5, 15, 15.5, 16, 16.5, 17.25, 17.5, 18, 19, 20, 22, 23, 24.2, 26.5, 30 and $50 - 100$. Though the number

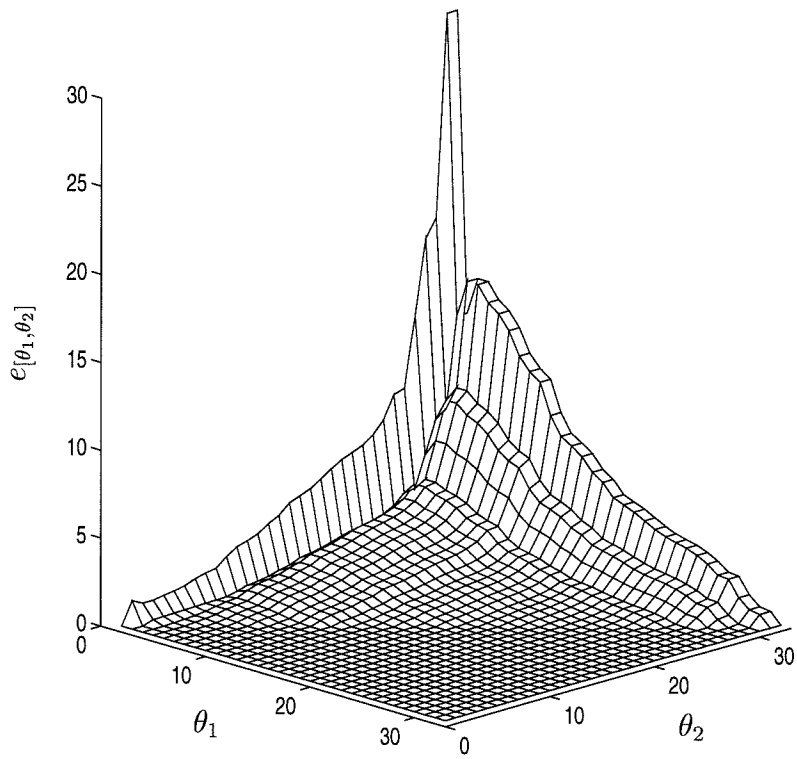

Figure 9.8: Model error $e_{[\theta_1,\theta_2]}$ as a function of θ_1 and θ_2.

of points chosen is arbitrary, their distribution over the operating power range is not arbitrary.

Due to significant variation of the model parameters in the low power range, almost all the chosen points are distributed in the power range $3.2 - 26.5\%$. Due to almost no parameter variation in the power range $50 - 100\%$, just one point suffices here. The linear models at the 33 chosen operating points constitute what we call the original model family.

From this family, $\frac{33\times32}{2}$ (all possible combinations from 33 models, taken two at a time) subranges can be generated. Next, we compute the model error $e_{[\theta_1,\theta_2]}$, $\theta_1 \leq \theta_2$ for these $\frac{33\times32}{2}$ subranges using the definition (9.21). Figure 9.8 shows this error as a function of the upper and lower power limits θ_1 and θ_2 of a given sub-range $[\theta_1, \theta_2]$.

We would like to choose contiguous sub-ranges covering the entire operating power

range such that the error in each of these sub-ranges is equal. This set of sub-ranges is obtained by simply plotting the contours of equal error. Such contour plots for errors ranging from 0.2 to 5 are shown in Figure 9.9.

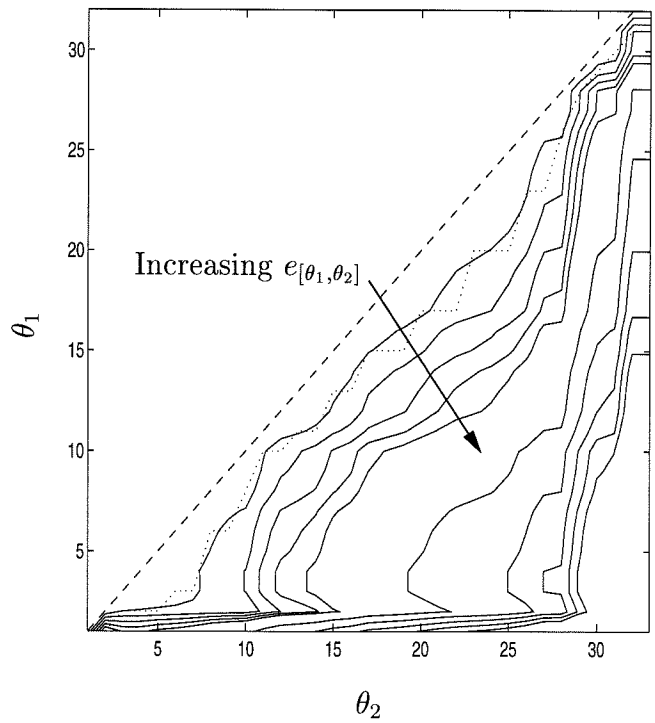

Figure 9.9: Contour plot for $e_{[\theta_1,\theta_2]}$ in the range 0.2 to 5. The dotted line denotes the chosen sub-division.

The appropriate sub-division for a given allowable error within each sub-range is now straightforward: for a given upper power limit of a sub-range, simply read-off the lower limit of that sub-range from the contour plot corresponding to the given allowable error. Thus, for an error level of 0.2, starting from a power of 30%, the next lower power level θ_1 such that $e_{[\theta_1,30]} = 0.2$ is 26.5%. We continue this process to arrive at the sub-division shown in Table 9.3. Note that since we have only used discrete points to generate the contour plots shown in Figure 9.9, the actual errors $e_{[\theta_1,\theta_2]}$ as given in Table 9.3 are somewhat different from 0.2. Note also that the difference is significant at the lowest power range ($[\theta_1, \theta_2] = [3.2, 3.5]$) because the contour plots are very closely spaced in this region, as can be seen from Figure 9.9.

From the contour plots shown in Figure 9.9, it should be clear that the larger the allowable model error in each sub-range, the less is the number of sub-ranges required to cover the entire operating range. On the other hand, as the model error specification goes to zero, we get a continuous model family.

θ_1	θ_2	$e_{[\theta_1,\theta_2]}$
30.0	50.0	0.5999
26.5	30.0	0.0570
24.2	26.5	0.3008
23.0	24.2	0.4000
20.0	23.0	0.1688
17.5	20.0	0.1910
16.0	17.5	0.1650
14.5	16.0	0.1612
13.0	14.5	0.1897
11.5	13.0	0.1681
9.5	11.5	0.1725
7.4	9.5	0.1810
5.8	7.4	0.1022
4.6	5.8	0.1671
3.9	4.6	0.0920
3.5	3.9	0.2000
3.2	3.5	1.2616

Table 9.3: Operating range subdivision ensuring a model error of about 0.2.

9.5.3 Prediction and Estimation with a Varying Model

When the system is operating in the power range $[\theta_1, \theta_2]$, it is described by (9.20)

$$\begin{aligned} x(k+1) &= \bar{A}(\theta)x(k) + \bar{B}(\theta)u(k) + \bar{B}_d(\theta)d(k) + n_1(k) \\ y(k) &= Cx(k) + n_2(k). \end{aligned} \tag{9.20'}$$

Here, $\bar{A}(\theta), \bar{B}(\theta), \bar{B}_d(\theta)$ is an appropriate discrete-time model for some $\theta \in [\theta_1, \theta_2]$, chosen based on the model family and the power sub-division procedure described in §9.5.2.2.

We will be assuming that we do not have a priori knowledge of how the power

is going to vary in the future. In this case, the model corresponding to the current operating point $\theta(k)$ is the best model we can use to *predict* the future behavior of the plant. It should therefore be clear that the prediction equation at time k, with operating power θ, is the following (compare with (9.16)):

$$\begin{aligned} x(k|k-1) &= \bar{A}(\theta)x(k-1|k-1) + \bar{B}(\theta)u(k-1|k-1) \\ y(k|k-1) &= Cx(k|k-1). \end{aligned} \tag{9.22}$$

Again, as in (9.16), a measured disturbance such as $d(k)$ for the steam generator, can be used for feed-forward control. Also, prediction for more than one step ahead is obtained by applying the above equations recursively.

Thus, in contrast to the LTI prediction model described by (9.16), although this prediction model remains the same over the prediction horizon p, it changes at each sampling time depending on the prevalent operating power at that sampling time.

Correspondingly, the estimator in MPC must also be modified to take into account this parameter varying linear model of the UTSG. The correction to the plant state, based on the measurement $\hat{y}(k) = y(k|k)$, is the following:

$$\hat{x}(k) = x(k|k) = x(k|k-1) + K(k)(\hat{y}(k) - y(k|k-1)). \tag{9.23}$$

As shown in [92, §6.5], the time-varying filter gain $K(k)$ is obtained from the following equation (compare with (9.17) and (9.18)):

$$K(k) = Q(k)C^T(CQ(k)C^T + V(k-1))^{-1}, \tag{9.24}$$

where $Q(k) > 0,\ k > 0$ is obtained from the following recursion:

$$Q(i+1) = \bar{A}(i)Q(i)(I - K(i)C)^T\bar{A}(i)^T + W(i) \tag{9.25}$$

with initial conditions $Q(0) = Q_0 > 0, K(0) = Q_0C^T[C(0)Q_0C^T + V(0)]^{-1}$. Note that here we have allowed the covariance matrices $V(i) > 0$ and $W(i)$ of the state

excitation noise n_1 and the measurement noise n_2 (both assumed to be uncorrelated white noises) to be varying with time.

Q_0 has the interpretation of being the variance of the error in the initial state estimate $x(0) - \hat{x}(0)$, assuming that the initial state $\hat{x}(0)$ of the filter is set equal to the expectation value of $x(0)$. Generally, this stochastic interpretation of the filter is not directly applied. Instead, Q_0 is considered as a design parameter to be tuned to get good estimation characteristics.

Although this development assumes the same sampling times for the estimator and the controller, it is also possible to make the estimator run faster than the controller. For example, since it is more likely that measurements can be obtained at a higher sampling rate than the rate at which the control move can be implemented, it is conceivable that the filter update can be carried out at a faster sampling rate than the control law computation. This would mean that the $\bar{A}(\theta), \bar{B}(\theta)$ matrices in the filter update equations (9.23), (9.24), (9.25) would be different from those used in the prediction equation (9.22) since they would be obtained from the continuous-time matrices $A(\theta), B(\theta)$ using different discretization times.

9.5.4 Effect of Model Switching on the Estimator

It is of fundamental importance that the state estimator functions properly during model switching. In this section, we will discuss the implications of model switching for the estimator by considering a simple system.

Figure 9.10 is a schematic one-dimensional representation of the true state trajectory $\hat{x}(k)$ of the system, with the two trajectories $x_I(k)$, $x_{II}(k)$ corresponding to linear approximations of the system around the steady states x_{0I} and x_{0II}. For this configuration, the relation between the true state and the linearized states can be expressed through the following relations:

$$\begin{aligned} \hat{x}(k) &= x_I(k) + x_{0I} + \epsilon_I(k) \\ &= x_{II}(k) + x_{0II} + \epsilon_{II}(k) \end{aligned} \tag{9.26}$$

where $\epsilon_I(k)$ and $\epsilon_{II}(k)$ represent respectively the model errors at time k associated with the linearizations around x_{0I} and x_{0II}.

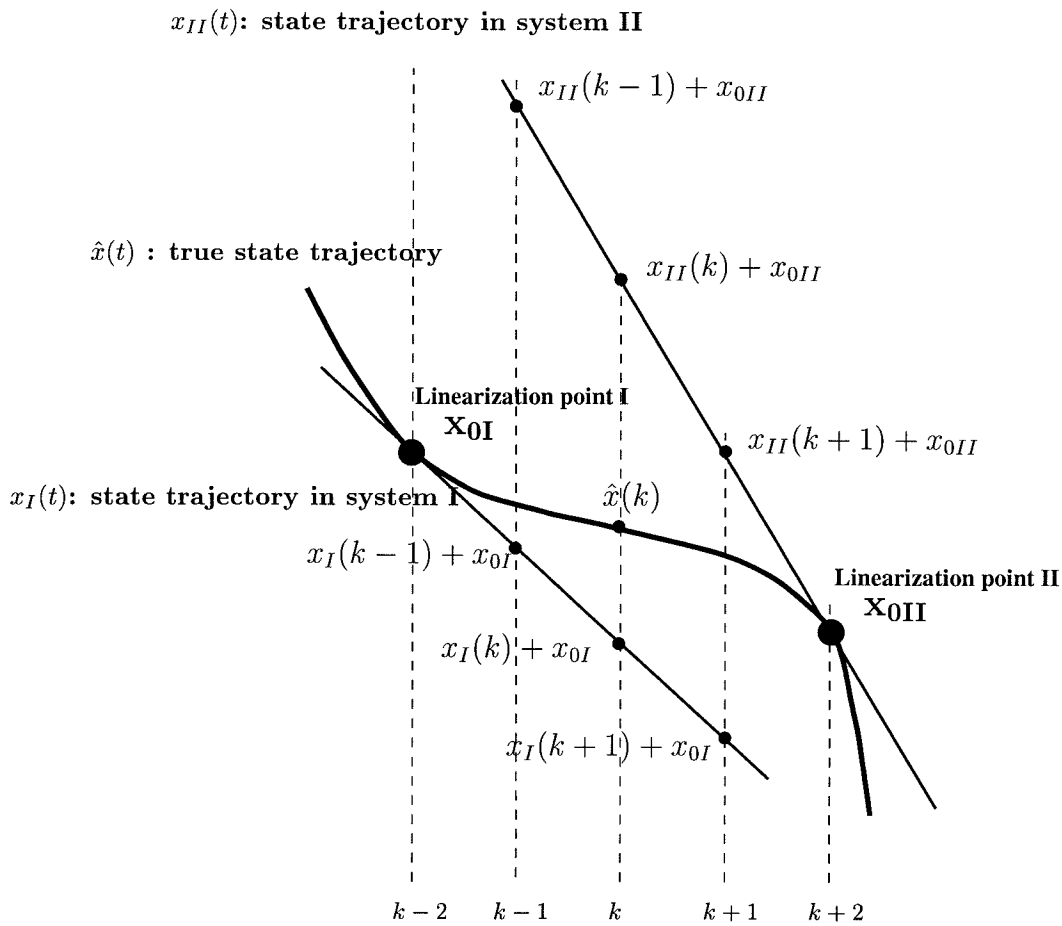

Figure 9.10: Model switching at the state level.

Now, let us assume that a model switch from the linear model around x_{0I} to that around x_{0II} takes place between the sampling times $k-1$ and k. This switch is motivated because at time k the model error $\epsilon_I(k)$, introduced by the linearization around x_{0I}, would be larger than the model error $\epsilon_{II}(k)$ introduced by the linearization around x_{0II}.

The key question that needs to be addressed here is how to initialize the new prediction model and the new estimator corresponding to the linear model at x_{0II}. Clearly, in order to use model II to predict the state trajectory, we first need to transform the system state from the x_I co-ordinates around the steady state x_{0I} to

the x_{II} co-ordinates around the steady state x_{0II}. This transformation can be derived from (9.26) as follows:

$$x_{II}(k) = x_I(k) + x_{0I} - x_{0II} + \epsilon_I(k) - \epsilon_{II}(k). \tag{9.27}$$

Note that in (9.27), only x_{0I} and x_{0II} are known and can be used as correction terms.

The LPV MPC estimator works with the state differences $\Delta x_I(k-1)$ and $\Delta x_{II}(k-1)$. In this case, if at time step k, we want to use model II to compute $\Delta x_{II}(k)$, we first need to transform $\Delta x_I(k-1)$ to $\Delta x_{II}(k-1)$. Since $\Delta x_I(k-1)$ is defined as $x_I(k-1) - x_I(k-2)$, to obtain $\Delta x_{II}(k)$, both $x_I(k-1)$ and $x_I(k-2)$ have to be transformed to the co-ordinate system around the steady state x_{0II}. Again, this transformation can be derived from (9.26) and (9.27) as follows:

$$\begin{aligned}
\Delta x_{II}(k-1) &= x_I(k-1) + x_{0I} - x_{0II} + \epsilon_I(k-1) - \epsilon_{II}(k-1) \\
&\quad -[x_I(k-2) + x_{0I} - x_{0II} + \epsilon_I(k-2) - \epsilon_{II}(k-2)] \\
&= x_I(k-1) - x_I(k-2) + \epsilon_I(k-1) - \epsilon_I(k-2) \\
&\quad -[\epsilon_{II}(k-1) - \epsilon_{II}(k-2)] \\
&= \Delta x_I(k-1) + \Delta\epsilon_I(k-1) - \Delta\epsilon_{II}(k-1).
\end{aligned} \tag{9.28}$$

In this case, we see that no correction can be made as $\Delta\epsilon_I(k-1)$ and $\Delta\epsilon_{II}(k-1)$ cannot be evaluated. Instead, we choose to use the approximation

$$\Delta x_{II}(k-1) \approx \Delta x_I(k-1). \tag{9.29}$$

This approximate initialization of the state-estimator and the prediction model is the best we can do and is justified if $\Delta\epsilon_I(k-1) - \Delta\epsilon_{II}(k-1)$ is small. This is the case when the two linearizations are close to being parallel, the value of the steady state being the main factor distinguishing the two linearizations. This can be achieved, for example, when the model error specification used for the operating range subdivision is small enough.

However, when $\Delta\epsilon_I(k-1) - \Delta\epsilon_{II}(k-1)$ is not small, the error introduced by (9.29)

can be considered as an estimation error which is to be corrected by an appropriate design of the estimator gain.

9.6 Simulations

The simulations are organized around two different power transients:

- a ramp-down in power from 30% to 5%; and
- a stair-up in power from 5% to 40% in steps of 5% power.

The model family used in these simulations is based on data supplied by EDF (see §9.3.2). It consists of 17 models for 17 sub-ranges as listed in Table 9.3. This choice of the model family ensures a model error of 0.2 in each sub-range, as we discussed in §9.5.2. The following issues will be illustrated in this section:

1. overall performance of the LPV MPC controller compared to the conventional MPC controller with a fixed internal model;
2. sensitivity to the choice of tuning parameters;
3. robustness against structural model change;
4. sensitivity to operating range subdivision and choice of model error specification;
5. sensitivity to measurement noise;
6. influence of estimator design;
7. comparison with existing gain-scheduled controllers at EDF.

9.6.1 Overall Performance

Figure 9.11 shows the system response to a ramp-down in power from 30% to 5%. All variables have been normalized and expressed as percent of their maximum values.

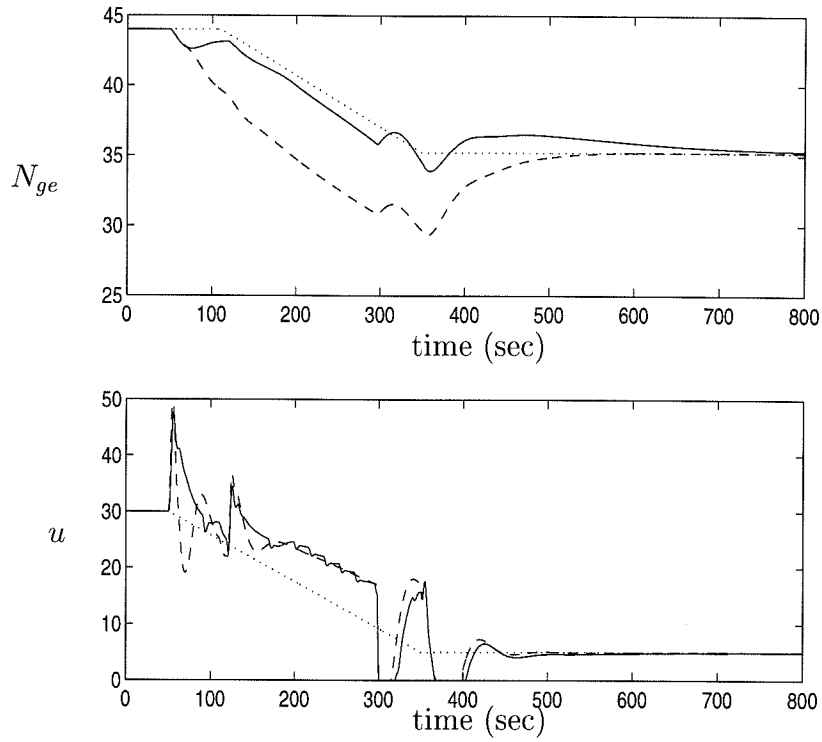

Figure 9.11: Responses to power ramp-down from 30% to 5% with a conservative choice of tuning parameters ($\Gamma_y = 1$, $\Gamma_u = 0$, $\Gamma_{\Delta u} = 0.1$, $p = 50$, $m = 2$); solid – LPV MPC; dashed – LTI MPC; dotted – desired N_{ge} set-point (upper plot), steam demand (lower plot).

A sampling time of 1 sec was used. The controller parameters were: $\Gamma_y = 1$, $\Gamma_u = 0$, $\Gamma_{\Delta u} = 0.1$, $p = 50$, $m = 2$. The estimator was designed using steady state versions of (9.24), (9.25) with $V(i) = 0.5I$, $W = 0.0001$ to obtain the model varying filter gain K. The improvement of model varying MPC over conventional linear MPC which uses a fixed internal model corresponding to the power level 5% is significant.

Similar improvement in controller performance is achieved when the power is increased in steps from 5% to 40%, as shown in Figure 9.12 for the water level response and in Figure 9.13 for the corresponding control action. Note that, as mentioned in §9.4.1, the set-point for N_{ge} is a function of the operating power, as denoted by the dotted curve in all the N_{ge} plots.

9.6.2 Sensitivity to Choice of Tuning Parameters

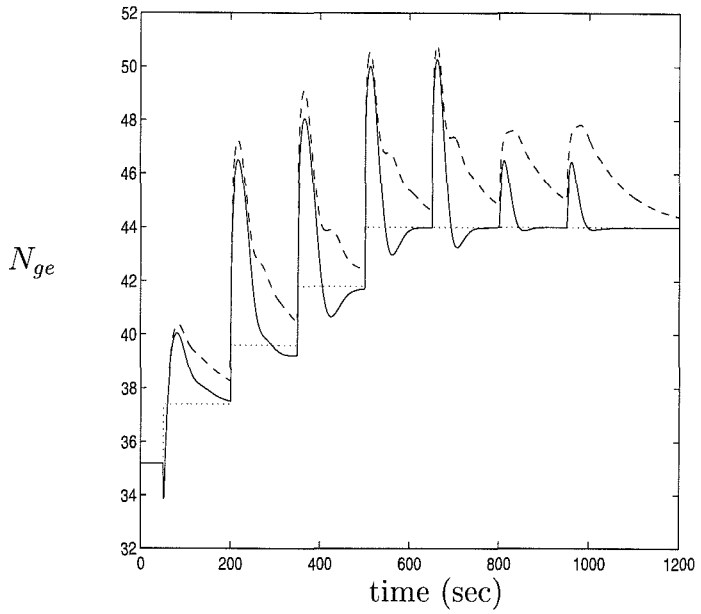

Figure 9.12: Water level response to step-wise power increase from 5% to 40% with a conservative choice of tuning parameters ($\Gamma_y = 1$, $\Gamma_u = 0$, $\Gamma_{\Delta u} = 0.1$, $p = 50$, $m = 2$); solid – LPV MPC; dashed – LTI MPC; dotted – desired set-point N_{ge}.

The simulation results in the last section were achieved with a conservative tuning scheme, detuned to allow the conventional fixed internal model MPC to work properly over the ranges of the simulated power transients. If the length of the control horizon is now changed to a more aggressive setting from $m = 2$ to $m = 10$ and at the same time the weight on Δu, $\Gamma_{\Delta u}$, is increased from 0.1 to 0.5 to contain this aggressive control action, then, for the same simulations as in the previous section, the conventional MPC controller is not only less effective than the LPV MPC controller, but its control action reaches the limit of instability. This can be observed in Figures 9.14, 9.15 and 9.16. Note that the estimator design is the same as in §9.6.1.

This is an important result as it also indicates that the LPV MPC controller is not very sensitive to the choice of tuning parameters, which can be interpreted as a robustness to changes in tuning parameters.

9.6.3 Robustness to Structural Model Change

To check if the LPV MPC controller is robust to structural model changes, the con-

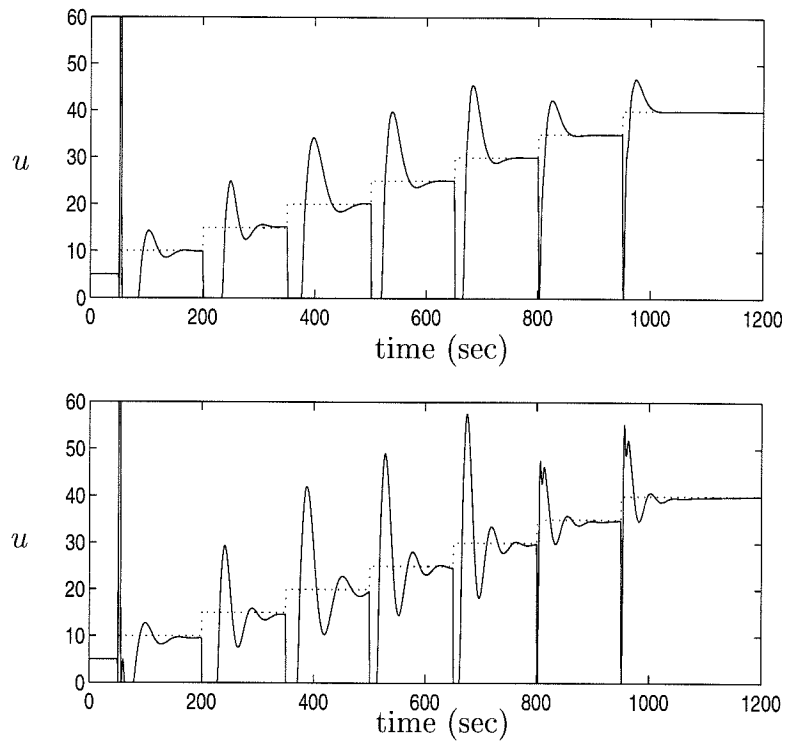

Figure 9.13: Feed-water response to step-wise power increase from 5% to 40% with a conservative choice of tuning parameters ($\Gamma_y = 1$, $\Gamma_u = 0$, $\Gamma_{\Delta u} = 0.1$, $p = 50$, $m = 2$); top – LPV MPC; bottom – LTI MPC; dotted – steam demand Q_v.

troller was implemented on a slightly different steam generator model. The feed-water dynamics were augmented with a non-minimum phase term, which gave an inverse response behavior to the feed-water system. This is an important check because as mentioned in §9.3.2, the inverse response behavior was neglected in the feed-water system dynamics.

The augmented system dynamics are given by the following equations: (compare with the model equations (9.10) and (9.11) which were used to derive the controller)

$$y_1(s) = \frac{1}{T_n s}\left(\frac{1+\frac{\beta_1}{\beta_0}s}{(1+\tau s)(1+T_h s)}u(s) - \frac{1-F_g T_g s}{1+T_g s}d(s)\right) \tag{9.30}$$

$$y_2(s) = \frac{1}{T_{int}s}(u(s)-d(s)). \tag{9.9'}$$

The parameters β_0, β_1 have been provided by EDF as functions of the operating power and are listed in Table 9.4.

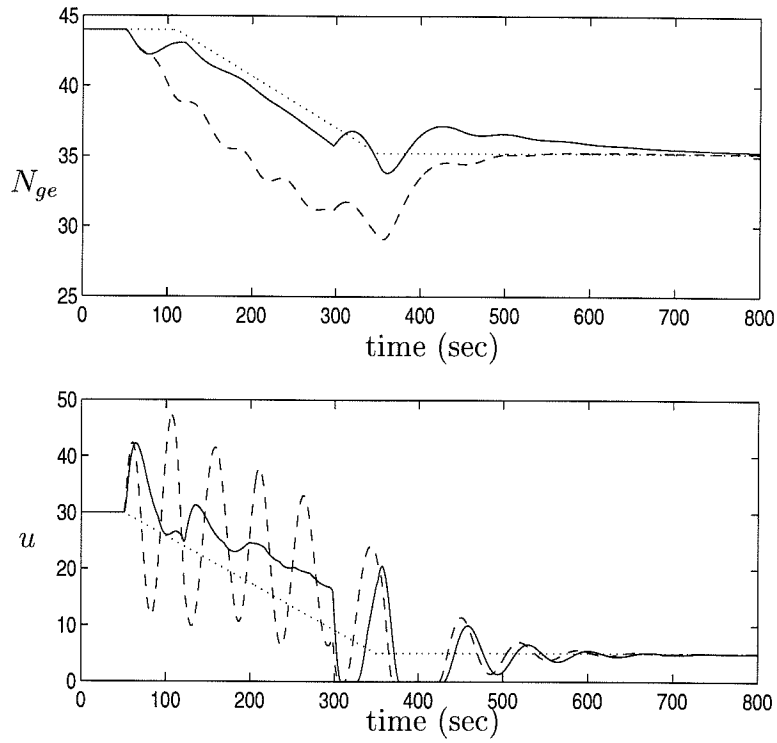

Figure 9.14: Responses to power ramp-down from 30% to 5% with a more aggressive choice of tuning parameters ($\Gamma_y = 1,\ \Gamma_u = 0,\ \Gamma_{\Delta u} = 0.5,\ p = 50,\ m = 10$); solid – LPV MPC; dashed – LTI MPC; dotted – desired N_{ge} set-point (upper plot), steam demand (lower plot).

Power (%)	5	7	9	11	13	18	25	30	50	100
β_0	-0.0030	-0.0036	-0.0042	-0.0050	-0.0063	-0.0113	-0.0198	-0.0256	-0.0403	-0.0412
β_1	0.0253	0.0240	0.0236	0.0240	0.0251	0.0292	0.0345	0.0368	0.0369	0.0370

Table 9.4: Parameter values for the augmented feed-water dynamics.

Figure 9.17 shows the power ramp-down simulation for this augmented plant. We can see that the performance is not strongly affected by the presence of the feed-water inverse response; only a slight oscillation is visible in the control action and water level response.

Next we investigate how the controller performance is influenced by various factors such as the model error specification for the original model family, measurement noise and choice of the MPC filter parameters.

9.6.4 Sensitivity to Model Error Specification

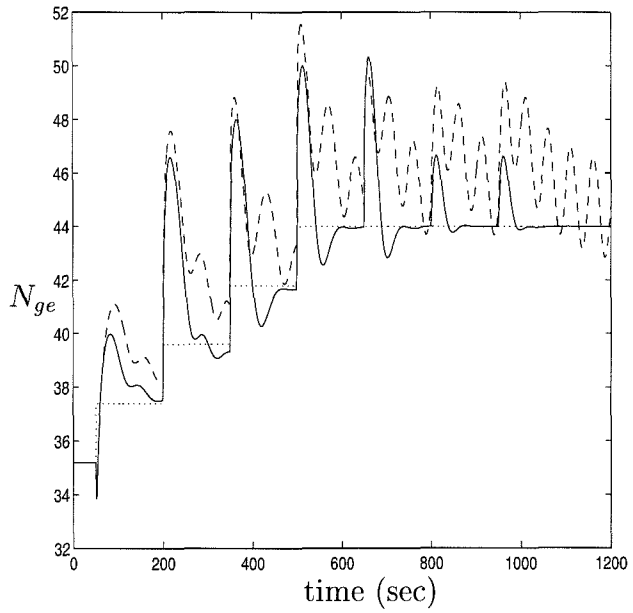

Figure 9.15: Water level response to step-wise power increase from 5% to 40% with a more aggressive choice of tuning parameters ($\Gamma_y = 1$, $\Gamma_u = 0$, $\Gamma_{\Delta u} = 0.5$, $p = 50$, $m = 10$); solid – LPV MPC; dashed – LTI MPC; dotted – desired set-point N_{ge}.

Figure 9.18 shows the water level response obtained with the parameter varying MPC scheme for different choices of the model families used to describe the steam generator. These model families differ in the value of the error specification used to generate these families from the EDF model data, as discussed in §9.5.2. Figure 9.19 shows the corresponding feed-water flow-rates. The circles in Figure 9.19 denote the points where the prediction model in the MPC algorithm switches to a new model based on the change in the operating point.

It is intuitively to be expected that when the model error specification is high, the overall control performance will be poor. This is seen from the greater undershoot of the water level response in Figure 9.18. From Figure 9.19, we also observe that there are greater discontinuities in the control action with increasing model error specification, as can be seen at the points at which the prediction and estimation model switches.

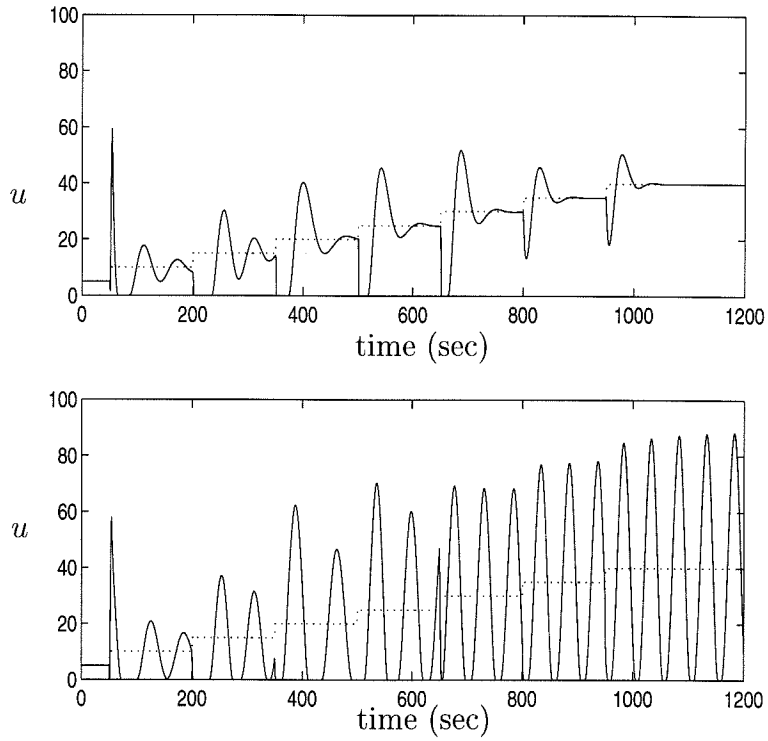

Figure 9.16: Feed-water response to step-wise power increase from 5% to 40% with a more aggressive choice of tuning parameters ($\Gamma_y = 1$, $\Gamma_u = 0$, $\Gamma_{\Delta u} = 0.5$, $p = 50$, $m = 10$); top – LPV MPC; bottom – LTI MPC; dashed – steam demand Q_v.

9.6.5 Sensitivity to Measurement Noise

Figures 9.20 and 9.21 show the effect of measurement noise (white noise) affecting, respectively, the steam flow and the narrow range level measurements. The estimator design is kept constant for all these simulations. We clearly see a stronger sensitivity to level measurement noise (Figure 9.21). The effect is much less pronounced for steam measurement noise, leading to a slightly higher overshoot and longer settling time (Figure 9.20). Note that the estimator is the same as the one in §9.6.1.

9.6.6 Sensitivity to Estimator Design

However, the degradation of performance due to level measurement noise can be significantly reduced by appropriately choosing the variance of the applied noise as a design parameter in the estimator design (**Step 3** in the LPV MPC algorithm

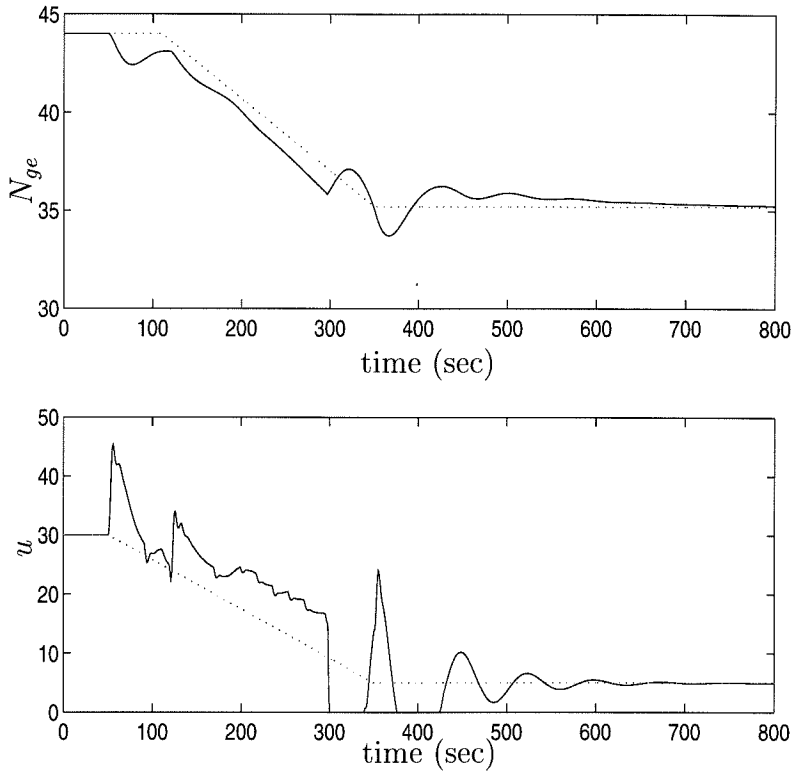

Figure 9.17: Power ramp-down simulation on plant extended with an inverse response behavior in the feed-water system; dotted – set-point for N_{ge} in the top plot and steam demand Q_v in the lower plot.

described in §9.5.1). The result of this change of the estimator is shown in Figure 9.22. Note that in this case, we have designed the estimator as in §9.6.1 but with the appropriate choices of V and W to reflect our knowledge of the noise characteristics.

9.6.7 Comparison with Controllers from EDF

Figure 9.23 shows the power ramp down simulation for the gain scheduled PID controller from EDF. For comparison, the responses using the LPV MPC controller are also given. The performance improvement using the LPV MPC controller (dashed curve) is significant. It is interesting to note the difference between the control actions for the two control schemes, in particular at the critical points corresponding to the beginning and end of the steam demand ramp-change. It is also interesting to note the full exploitation of the available control bandwith by the LPV MPC controller which can be seen between the simulation times of 300 sec and 400 sec. The gain

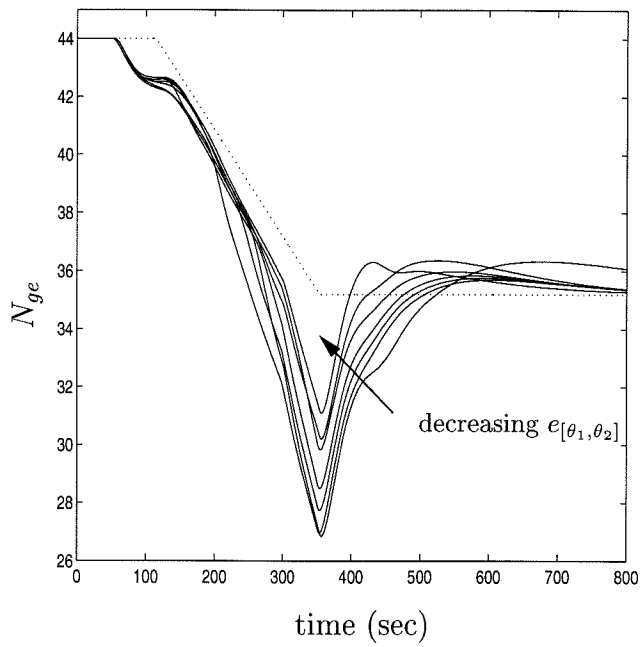

Figure 9.18: Water level responses for different model error specifications $e_{[\theta_1,\theta_2]}$; dotted – set-point for N_{ge}.

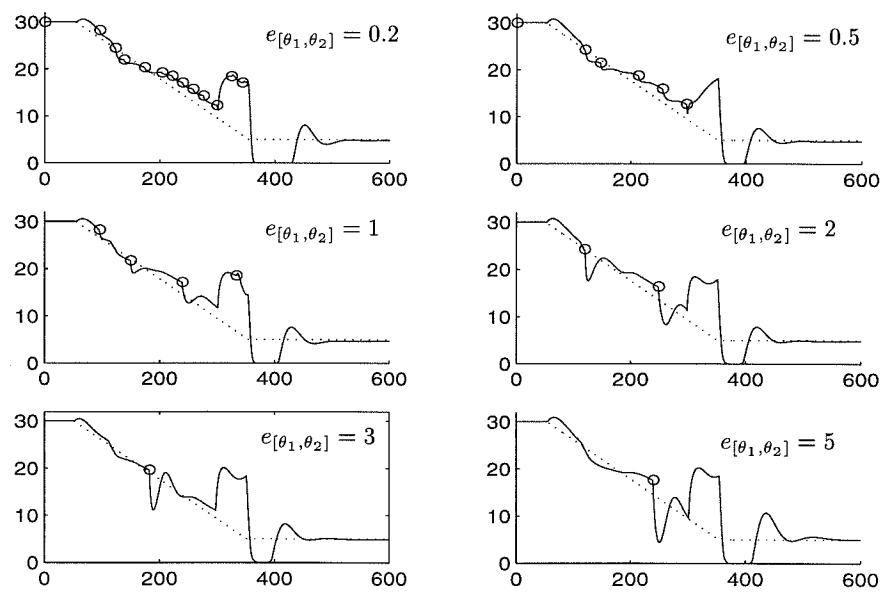

Figure 9.19: Feed-water responses for different model error specification $e_{[\theta_1,\theta_2]}$ in the power range sub-division procedure. For all plots, x-axis is time (sec), y-axis is N_{ge} (normalized %), circles are points where there is a model switch; dotted curve is steam demand Q_v.

scheduled PID controller from EDF was clearly tuned in a conservative manner as the trajectories of the manipulated variable show.

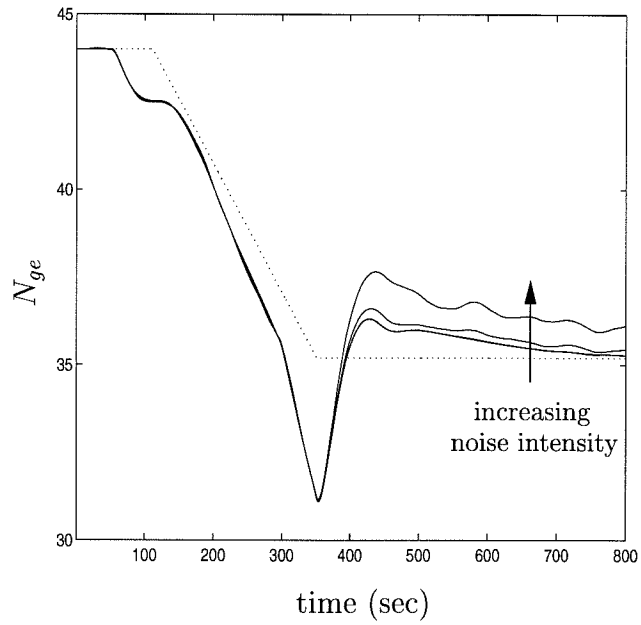

Figure 9.20: Sensitivity to steam flow measurement noise, for noise intensities 0.001, 0.01, 0.1, 0.5. The dotted curve is the N_{ge} set-point.

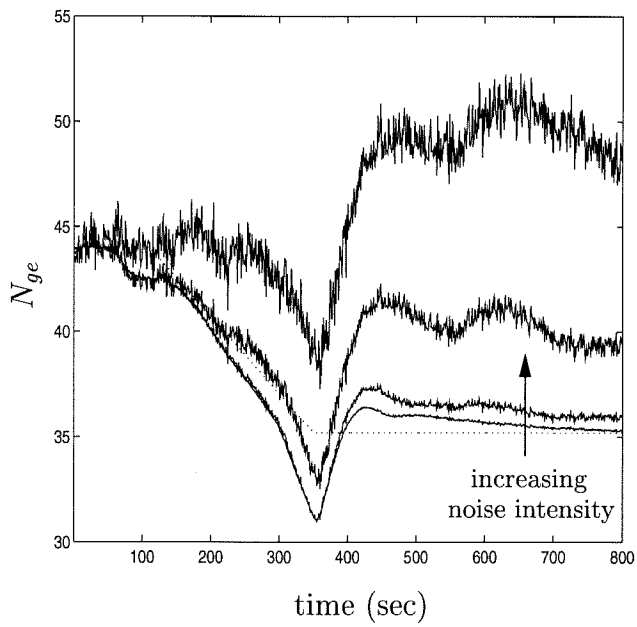

Figure 9.21: Sensitivity to N_{ge} level measurement noise, for noise intensities 0.001, 0.01, 0.1, 0.5. The dotted curve is the N_{ge} set-point.

9.7 Conclusions

In this chapter, we presented a general framework for systematically studying the UTSG level control problem over its entire operating power range using MPC tech-

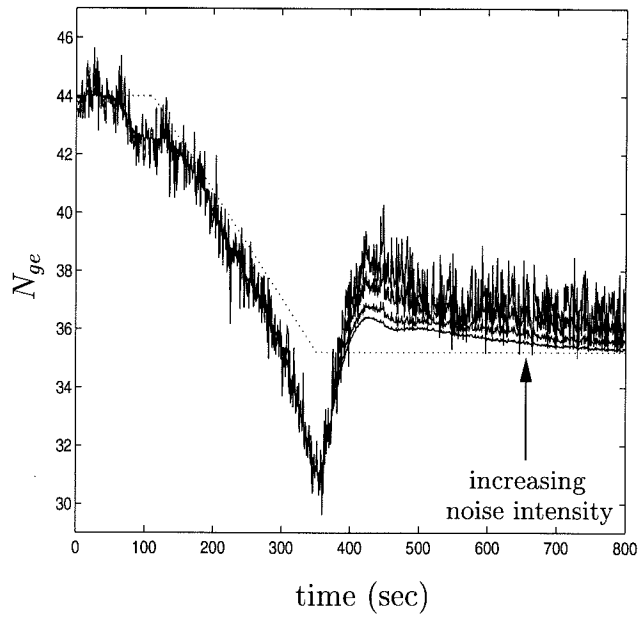

Figure 9.22: Sensitivity to N_{ge} measurement noise, for noise intensities 0.001, 0.01, 0.1, 0.5, with optimal estimator. The dotted curve is the N_{ge} set-point.

niques. The framework allows consideration of a discrete family of linear models which is derived from a LPV model of the plant using a model error criterion. The LPV model can be obtained from practical identification experiments. The basic control strategy involves updating the linear model in the MPC formulation. Issues such as constraints on the manipulated and controlled variables, use of feed-forward control, tracking of varying water level set-points and state estimation in the presence of noisy measurements can all be handled in this setting.

Acknowledgment

Partial financial support for this project from Direction des Etudes et Recherches, Electricité de France, Paris, France, is gratefully acknowledged.

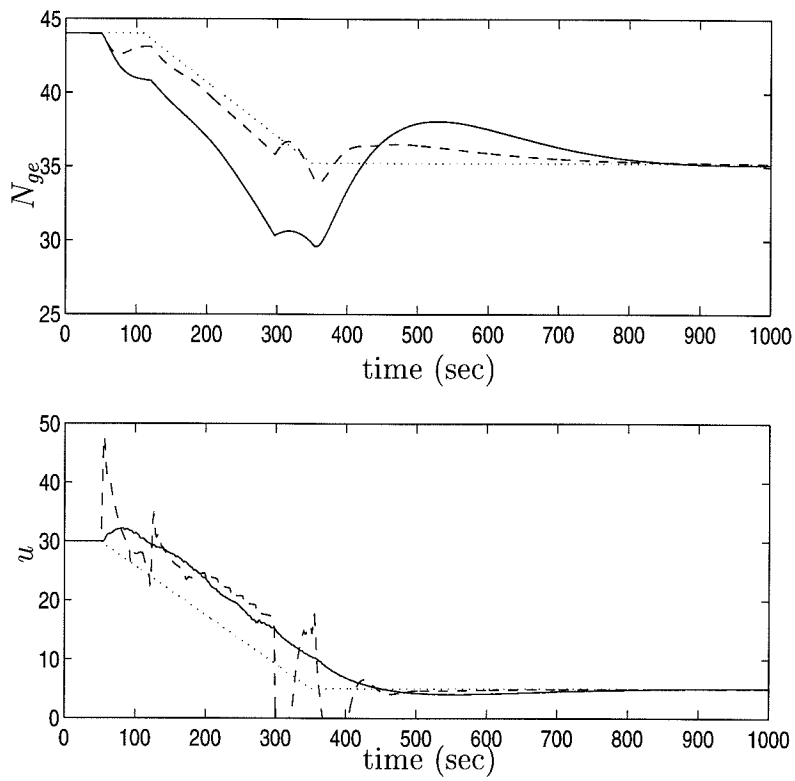

Figure 9.23: Water level and feed-water response obtained for the EDF gain scheduled PID controller (solid) and the LPV MPC controller (dashed). The dotted curve denotes the N_{ge} set-point and the steam demand Q_v in the upper and lower plots respectively.

Chapter 10 Conclusions

10.1 Summary of Contributions

This thesis focused on the problem of controlling systems with constraints. Two approaches to addressing the constrained control problem for linear systems were studied.

Anti-Windup Bumpless Transfer (AWBT)

This approach involved the development of a truly general unifying framework for the analysis and synthesis of AWBT control systems. The generality of the framework allowed consideration of any control system structure, including feed-forward, feedback and cascade, which are subject to control input nonlinearities. The theoretical development was based on the classical two-step AWBT paradigm of first designing the linear controller ignoring the input nonlinearities and then adding AWBT compensation to minimize the adverse effects of control input nonlinearities. In this sense, the essential structure inherent in AWBT schemes was captured in the framework. Not surprisingly, the framework was shown to unify numerous existing LTI AWBT schemes in terms of a co-prime factorization of the original linear controller. One particular scheme which was considered in detail was a novel anti-windup implementation of Internal Model Control (IMC).

The problem of AWBT analysis was carried out in the framework of the passivity theorem with appropriate choices of multipliers. The basic premise of this analysis was to cover the input nonlinearity by a class of sector bounded memoryless structured nonlinearities and then apply concepts from absolute stability theory to develop sufficient conditions guaranteeing stability for all nonlinearities in the specified class. This has been the predominant approach to analyzing stability properties of AWBT control systems reported in the literature. Once again, the resulting sufficient con-

ditions for stability were shown to generalize several previously reported attempts to analyze stability of AWBT control systems. These previously reported conditions were based on seemingly diverse techniques such as the Popov, Circle and Off-Axis Circle criteria, the optimally scaled small-gain theorem (generalized μ upper bounds) and describing functions. The general conditions developed in the AWBT analysis were shown to be less conservative than the existing conditions available in the literature.

An outline of the AWBT synthesis problem based on recent results on multi-objective controller synthesis was presented. Several promising lines of research, using a one-step AWBT compensation and dynamic AWBT compensation, were discussed to arrive at a suitable AWBT controller design.

Robust Model Predictive Control

The second approach to addressing the constrained control problem for linear systems involved model predictive control (MPC) techniques. A novel and complete framework for robust MPC synthesis was developed using techniques from the theory LMIs. The problem formulation allowed incorporation of two classes of very general and commonly encountered uncertainty descriptions. The on-line optimization involved the solution of an LMI-based linear objective minimization. The resulting time-varying state-feedback control law minimizes, at each time-step, an upper bound on the robust performance objective, subject to input and output constraints. The feasible receding horizon control algorithm was shown to robustly asymptotically stabilize the set of uncertain plants under consideration. A number of standard extensions to this state-feedback formulation such as constant set-point tracking, reference trajectory tracking, disturbance rejection, application to systems with time delays and the output feedback case with an appropriate observer design completed the theoretical development. We believe this was one of the first attempts to develop a truly general framework for robust MPC in the state-space formulation for a fairly broad class of realistic model uncertainty descriptions.

Model Varying Predictive Control

A case study involving application of model predictive control with a varying internal model was carried out for the steam generator level control problem in a nuclear power plant. The control technique involved an extension of standard MPC techniques to linear parameter varying systems. The improvement in the performance of the level control system was demonstrated by extensive simulation studies.

10.2 Suggestions for Future Work

A number of issues remain open, particularly in the area of AWBT controller synthesis. We will briefly discuss these issues.

Dynamic AWBT controller design Although promising lines for obtaining the AWBT controller using dynamic output feedback were outlined in Chapter 7, many of the details need to be worked out. In particular, the issue of obtaining good "recovery of linear performance," especially after the system comes out of saturation, needs to be addressed carefully. This is not a serious issue in the classical static AWBT compensation techniques, but with dynamics involved in the AWBT compensation, more care is required.

One-step AWBT controller design As with the dynamic AWBT controller design, the details of the controller synthesis in this one-step setting need to be worked out. Additionally, here, we suffer from the disadvantage that the final AWBT controller is of the same order as the plant to be controlled. In this sense, the controller order may be unnecessarily increased in this one-step synthesis. Note that this was not an issue in the classical "two-step" paradigm of AWBT compensation, where the original linear controller could be any low order system such as a PI controller, and the AWBT compensation would only "retrofit" this original controller. Techniques to allow design of fixed order AWBT controllers need to be explored. These might involve generalizations of the multi-objective

controller synthesis results presented in Chapter 7 to controllers of arbitrary prespecified orders as reported in Scherer (1995) [118].

Comparative studies Studies to compare the advantages and disadvantages of the numerous possibilities available to synthesize the AWBT controller (classical static two-step, dynamic and one-step) need to be done to evaluate which is the most feasible alternative. The final test would clearly be the ease in implementing the controller (controller order) and the achieved closed-loop performance in the presence of input constraints.

Comparison with MPC An important test of the AWBT schemes would be to compare their performance with that of MPC which *explicitly* incorporates both input and output constraints. In particular, guidelines to decide when to use MPC based on the severity of constraints, and when to apply the computationally cheaper alternative of AWBT compensation need to be developed.

Case studies The previous comparisons need to be supplemented with case studies on realistic plant conditions.

Beyond these issues, there needs to be greater focus on constrained control of nonlinear systems, an area which is just beginning to receive attention. We saw in Chapter 3 how the linear anti-windup IMC scheme could be extended to a class of input-output linearizable plants. Similarly, we saw in Chapter 8 that the robust MPC algorithm which we developed could also be applied to a class of nonlinear systems whose Jacobians lie in a polytope. Such extensions of ideas from linear control to the nonlinear case should be explored in their entirety before addressing the truly general nonlinear constrained control problem.

Bibliography

[1] F. Alizadeh, J.-P. A. Haeberly, and M. L. Overton. A new primal-dual interior-point method for semidefinite programming. In *Proceedings of the Fifth SIAM Conference on Applied Linear Algebra, Snowbird, Utah*, June 1994.

[2] J.C. Allwright and G.C. Papavasiliou. On linear programming and robust model-predictive control using impulse-responses. *Systems & Control Letters*, 18:159–164, 1992.

[3] P. Ambos, G. Duc, and C-M. Falinower. The application of $\mathcal{H}_2$ control design with disturbance feedforward to steam generator level in EDF PWR units. In *Proceedings of the Symposium on Control, Optimization and Supervision: Multiconference on "Computational Engineering in Systems Applications"*, pages 1299–1304, Lille, France, July 9-12, 1996.

[4] B. D. O. Anderson and S. Vongpanitlerd. *Network Analysis and Synthesis: A Modern Systems Theory Approach.* Prentice-Hall, Inc., Englewood Cliffs, NJ, 1973.

[5] K. J. Åström and T. Hägglund. *Automatic Tuning of PID Controllers.* Instrument Society of America, Research Triangle Park, NC, 1988.

[6] K. J. Åström and L. Rundqwist. Integrator windup and how to avoid it. In *Proceedings of the 1989 American Control Conference*, pages 1693–1698, 1989.

[7] K. J. Åström and B. Wittenmark. *Computer Controlled Systems Theory and Design.* Prentice-Hall, Inc., Englewood Cliffs, NJ, 1984.

[8] T. A. Badgwell. Robust stability constraints for model predictive control: A unifying review and some new results. In *AICHE Anual Meeting*, Chicago, IL, 1996.

[9] V. Balakrishnan. Construction of Lyapunov functions for robustness analysis with multipliers. In *Proceedings of the* 33^{rd} *IEEE Conference on Decision and Control*, pages 2021–2025, Orlando, FL, December 1994.

[10] V. Balakrishnan. Linear matrix inequalities in robustness analysis with multipliers. *Systems & Control Letters*, 25(4):265–272, July 1995.

[11] V. Balakrishnan, Y. Huang, A. Packard, and J. Doyle. Linear matrix inequalities in analysis with multipliers. In *Proceedings of the 1994 American Control Conference*, pages 1228–1232, Baltimore, MD, June 1994.

[12] V. Balakrishnan, Z. Zheng, and M. Morari. Constrained stabilization of discrete-time systems. In David Clarke, editor, *Advances in Model-Based Predictive Control*, pages 205–216. Oxford University Press, 1994.

[13] P. Bendotti and B. Bodenheimer. Identification and $\mathcal{H}_\infty$ control design for a pressurized water reactor. In *Proceedings of the* 33^{rd} *IEEE Conference on Decision and Control*, pages 1072–1077, Orlando, FL, December 1994.

[14] P. Bendotti, C-M. Falinower, M. V. Kothare, B. Mettler, and M. Morari. μ-analysis and $\mathcal{H}_\infty$ controller synthesis for the steam generator water level. In 2^{nd} *IFAC Workshop on Robust Control*, Budapest, June 1997 (submitted).

[15] P. Bendotti and E. Irving. Design of an $\mathcal{H}_2$ controller for a pressurized water reactor. In *Proceedings of the IFAC Symposium on Robust Control Design*, pages 382–387, Rio, Brazil, September 1994.

[16] D. S. Bernstein and A. N. Michel. A chronological bibliography on saturating actuators. *International Journal of Robust and Nonlinear Control*, 5(5):375–380, August 1995. Special issue: **Saturating Actuators**, Guest editors: D. S. Bernstein and A. N. Michel.

[17] J. Bernussou, P. L. D. Peres, and J. C. Geromel. A linear progamming oriented procedure for quadratic stabilization of uncertain systems. *Systems & Control Letters*, 13:65–72, 1989.

[18] R. R. Bitmead, M. Gevers, and V. Wertz. *Adaptive Optimal Control.* Prentice Hall, Englewood Cliffs, NJ, 1990.

[19] B. Bodenheimer and P. Bendotti. Optimal linear parameter-varying control design for a pressurized water reactor. In *Proceedings of the* 34^{th} *IEEE Conference on Decision and Control*, pages 182–187, New Orleans, LO, December 1995.

[20] S. Boyd and L. El Ghaoui. Method of centers for minimizing generalized eigenvalues. *Linear Algebra and Applications, special issue on Numerical Linear Algebra Methods in Control, Signals and Systems*, 188:63–111, July 1993.

[21] S. Boyd, L. El Ghaoui, E. Feron, and V. Balakrishnan. *Linear Matrix Inequalities in System and Control Theory*, volume 15 of *Studies in Applied Mathematics.* SIAM, Philadelphia, PA, June 1994.

[22] R. W. Brockett and J. L. Willems. Frequency domain stability criteria-Parts I and II. *IEEE Trans. Auto. Cont.*, 10(3,4):255–261, 407–412, 1965.

[23] P. S. Buckley. Designing overide and feedforward controls. *Control Engineering*, 18(8):48–51, 1971.

[24] P. J. Campo. *Studies in Robust Control of Systems Subject to Constraints.* PhD thesis, California Institute of Technology, Pasadena, CA, 1990.

[25] P. J. Campo and M. Morari. ∞-norm formulation of model predictive control problems. In *Proceedings of the 1986 American Control Conference*, pages 339–343, Seattle, Washington, 1986.

[26] P. J. Campo and M. Morari. Robust model predictive control. In *Proceedings of the 1987 American Control Conference*, pages 1021–1026, 1987.

[27] P. J. Campo and M. Morari. Robust control of processes subject to saturation nonlinearities. *Computers & Chemical Engineering*, 14(4/5):343–358, 1990.

[28] P. J. Campo, M. Morari, and C. N. Nett. Multivariable anti-windup and bumpless transfer: A general theory. In *Proceedings of the 1989 American Control Conference*, 1989.

[29] C-Y. Chen and M-H. Perng. An optimal anti-windup scheme for saturating MIMO systems. In *Proceedings of the* 35^{th} *IEEE Conference on Decision and Control*, pages 2832–2837, Kobe, Japan, December 1996.

[30] X. Chen and J. T. Wen. Robustness analysis of LTI systems with structured incrementally sector bounded nonlinearities. In *Proceedings of the 1995 American Control Conference*, pages 3883–3887, July 1995.

[31] Y.-S. Cho and K. S. Narendra. An off-axis circle criterion for the stability of feedback systems with a monotonic nonlinearity. *IEEE Trans. Auto. Cont.*, 13:413–416, August 1968.

[32] J. I. Choi, J. E. Meyer, and D. D. Lanning. Automatic controller for SG water level during low power operation. *Nuclear Engineering and Design*, 117:263–274, 1989.

[33] D. W. Clarke and C. Mohtadi. Properties of Generalized Predictive Control. *Automatica*, 25(6):859–875, 1989.

[34] D. W. Clarke, C. Mohtadi, and P. S. Tuffs. Generalized predictive control–II. Extensions and interpretations. *Automatica*, 23:149–160, 1987.

[35] I. Cohen, R. Hanus, and J. P. Vanbergen. The impact of the control structure on the closed loop efficiency. *journal A*, 26(1):18–25, 1985.

[36] E. Coulibaly, S. Maiti, and C. Brosilow. Internal Model Predictive Control (IMPC). *Automatica*, 31(10):1471–1482, October 1995.

[37] S. L. De Oliveira. *Model Predictive Control (MPC) for Constrained Nonlinear Systems.* PhD thesis, California Institute of Technology, Pasadena, CA, March 1996.

[38] S. L. De Oliveira and M. Morari. Robust model predictive control for nonlinear systems. In *Proceedings of the* 33^{rd} *IEEE Conference on Decision and Control*, pages 3561–3567, Orlando, FL, 1994.

[39] J. Debelle. A control structure based upon process models. *journal A*, 20(2):71–81, 1979.

[40] L. Del Re, J. Chapuis, and V. Nevistić. Predictive control with embedded feedback linearization for bilinear plants with input constraints. In *Proceedings of the* 32^{nd} *IEEE Conference on Decision and Control*, pages 2984–2989, San Antonio, TX, 1993.

[41] C. A. Desoer and M. Vidyasagar. *Feedback Systems: Input-Output Properties.* Academic Press, New York, 1975.

[42] J. C. Doyle and A. Packard. Uncertain multivariable systems from a state space perspective. In *Proceedings of the 1987 American Control Conference*, pages 2147–2152, Minneapolis, MN, 1987.

[43] J. C. Doyle, R. S. Smith, and D. F. Enns. Control of plants with input saturation nonlinearities. In *Proceedings of the 1987 American Control Conference*, pages 1034–1039, Minneapolis, MN, 1987.

[44] F. J. Doyle-III. An anti-windup input-output linearization scheme for SISO systems. *Automatica (submitted)*, June 1996.

[45] E. Feron, V. Balakrishnan, and S. Boyd. Design of stabilizing state feedback for delay systems via convex optimization. In *Proceedings of the* 31^{st} *IEEE Conference on Decision and Control*, volume 1, pages 147–148, Tucson, AZ, December 1992.

[46] H. A. Fertik and C. W. Ross. Direct digital control algorithm with anti-windup feature. *ISA Transactions*, 6(4):317–328, 1967.

[47] R. E. Fitts. Two counterexamples to Aizerman's conjecture. *IEEE Trans. Auto. Cont*, 11(3):553–556, 1966.

[48] P. Gahinet, A. Nemirovski, A. J. Laub, and M. Chilali. *LMI Control Toolbox: For use with MATLAB.* The Mathworks, Inc., Natick, MA, May 1995.

[49] C. E. García and M. Morari. Internal model control 1. A unifying review and some new results. *Ind. Eng. Chem. Process Des. & Dev.*, 21:308–232, 1982.

[50] C. E. García and M. Morari. Internal model control 2. Design procedure for multivariable systems. *Ind. Eng. Chem. Process Des. & Dev.*, 24:472–484, 1985.

[51] C. E. García and M. Morari. Internal model control 3. Multivariable control law computation and tuning guidelines. *Ind. Eng. Chem. Process Des. & Dev.*, 24:484–494, 1985.

[52] C. E. García, D. M. Prett, and M. Morari. Model predictive control: Theory and practice – A survey. *Automatica*, 25(3):335–348, May 1989.

[53] H. Genceli and M. Nikolaou. Robust stability analysis of constrained L_1-norm model predictive control. *AIChE Journal*, 39(12):1954–1965, 1993.

[54] J. C. Geromel, P. L. D. Peres, and J. Bernussou. On a convex parameter space method for linear control design of uncertain systems. *SIAM J. Control and Optimization*, 29(2):381–402, March 1991.

[55] L. El Ghaoui and J. P. Folcher. Multiobjective robust control of LTI systems subject to unstructured perturbations. *Systems & Control Letters*, 28(1):23–30, June 1996.

[56] Elmer G. Gilbert. Linear control systems with pointwise-in-time constraints. What do we do about them? Plenary lecture at the *1992 American Control Conference*, Chicago, IL, June 1992.

[57] A. H. Glattfelder and W. Schaufelberger. Stability analysis of single-loop control systems with saturation and antireset-windup circuits. *IEEE Trans. Auto. Cont.*, 28(12):1074–1081, December 1983.

[58] A. H. Glattfelder and W. Schaufelberger. Stability of discrete override and cascade-limiter single-loop control systems. *IEEE Trans. Auto. Cont.*, 33(6):532–540, June 1988.

[59] A. H. Glattfelder, W. Schaufelberger, and H. P. Fassler. Stability of override control systems. *Int. J. Control*, 37(5):1023–1037, 1983.

[60] G. C. Goodwin, S. E. Graebe, and W. S. Levine. Internal Model Control of linear systems with saturating actuators. In *Proceedings of the 1993 European Control Conference*, pages 1072–1077, 1993.

[61] D. Guo and W. J. Rugh. An approach to gain scheduling on fast variables. In *Proceedings of the 31st Conference on Decision and Control*, volume 1, pages 759–763, December 1992.

[62] R. Hanus and M. Kinnaert. Control of constrained multivariable systems using the conditioning technique. In *Proceedings of the 1989 American Control Conference*, pages 1711–1718, 1989.

[63] R. Hanus, M. Kinnaert, and J. L. Henrotte. Conditioning technique, a general anti-windup and bumpless transfer method. *Automatica*, 23(6):729–739, 1987.

[64] R. Hanus and Y. Peng. Conditioning technique for controllers with time delays. *IEEE Trans. Auto. Cont.*, 37(5):689–692, May 1992.

[65] J. O. Hill and R. E. Paris. Upgrading SG level control instrumentation at Prairie Island. *Nuclear Engineering International*, 35(429):24–26, April 1990.

[66] A. Höld. UTSG-2 - A theoretical model describing the transient behavior of a pressurized water reactor natural-circulation U-tube steam generator. *Nuclear Technology*, 90:98–118, April 1990.

[67] E. Irving, C. Miossec, and J. Tassart. Towards efficient full automatic operation of the PWR steam generator with water level adaptive control. In *Proceedings of the International Conference on Boiler Dynamics and Control in Nuclear Power Stations*, pages 309–329. British Nuclear Energy Society, London, 1980.

[68] A. Isidori. *Nonlinear Control Systems.* Springer-Verlag, 1989.

[69] P. Kapasouris and M. Athans. Multivariable control systems with saturating actuators, antireset windup strategies. In *Proceedings of the 1985 American Control Conference*, pages 1579–1584, 1985.

[70] P. Kapasouris and M. Athans. Control systems with rate and magnitude saturation for neutrally stable open loop systems. In *Proceedings of the* 29^{th} *IEEE Conference on Decision and Control*, pages 3404–3409, Honolulu, HI, December 1990.

[71] P. Kapasouris, M. Athans, and G. Stein. Design of feedback control systems for stable plants with saturating actuators. In *Proceedings of the* 27^{th} *IEEE Conference on Decision and Control*, pages 469–479, Austin, TX, December 1988.

[72] N. Kapoor, P. Daoutidis, and A. R. Teel. Anti-windup with guaranteed stability for linear systems with input constraints. In *Extended Abstracts, 1995 AICHE Annual Meeting, Miami, FL, paper no. 178g*, page 409 (paper no. 178g), 1995.

[73] N. Kapoor, A. R. Teel, and P. Daoutidis. An anti-windup design for linear systems. *Automatica (submitted)*, December 1995.

[74] T. A. Kendi and F. J. Doyle-III. An anti-windup scheme for multivariable nonlinear systems. *Journal of Process Control (submitted)*, 1996.

[75] H. K. Khalil. *Nonlinear Systems.* Prentice Hall, Inc., Upper Saddle River, NJ, second edition, 1996.

[76] J. Khanderia and W. L. Luyben. Experimental evaluation of digital algorithms for anti-reset windup. *Ind. & Engg. Chem., Proc. Des. and Dev.*, 15:278–285, 1976.

[77] P. P. Khargonekar and M. A. Rotea. Mixed $\mathcal{H}_2/\mathcal{H}_\infty$ control: A convex optimization approach. *IEEE Trans. Aut. Control*, 36(7):824–837, July 1991.

[78] K. K. Kim, J. E. Meyer, D. D. Lanning, and J. A. Bernard. Design and evaluation of model-based compensators for the control of steam generator level. In *Proceedings of the 1993 American Control Conference*, pages 2055–2060, San Francisco, CA, June 1993.

[79] M. V. Kothare, V. Balakrishnan, and M. Morari. Robust constrained model predictive control using linear matrix inequalities. In *Proceedings of the 1994 American Control Conference*, pages 440–444, Baltimore, June 1994.

[80] M. V. Kothare, V. Balakrishnan, and M. Morari. Robust constrained model predictive control using linear matrix inequalities. *Automatica*, 32(10):1361–1379, October 1996.

[81] M. V. Kothare, P. J. Campo, M. Morari, and C. N. Nett. A unified framework for the study of anti-windup designs. *Automatica*, 30(12):1869–1883, 1994. Also presented at the *1993 AIChE Annual Meeting*, MO.

[82] M. V. Kothare, B. Mettler, M. Morari, P. Bendotti, and C.-M. Falinower. Level control in the steam generator of a nuclear power plant. In *Proceedings of the* 35^{th} *IEEE Conference on Decision and Control*, Kobe, Japan, December 1996.

[83] M. V. Kothare, B. Mettler, M. Morari, P. Bendotti, and C.-M. Falinower. Level control in the steam generator of a nuclear power plant. In *The 1996 AICHE Annual Meeting*, Chicago, IL, November 1996.

[84] M. V. Kothare, B. Mettler, M. Morari, P. Bendotti, and C.-M. Falinower. Linear parameter varying model predictive control for steam generator level control. In *Proceedings of the European Symposium on Computer Aided Process*

Engineering-7 (ESCAPE-7)/Process Systems Engineering'97 (PSE'97) (jointly organized), Trondheim, Norway, 1997.

[85] M. V. Kothare and M. Morari. Multiplier theory for stability analysis of anti-windup control systems. In *Proceedings of the* 34^{th} *IEEE Conference on Decision and Control*, pages 3767–3772, New Orleans, LO, December 1995.

[86] M. V. Kothare and M. Morari. Stability analysis of constrained linear time-invariant systems. In *Proceedings of the Symposium on Control, Optimization and Supervision, Multiconference on "Computational Engineering in Systems Applications"*, pages 1032–1037, Lille, France, July 9-12, 1996.

[87] M. V. Kothare and M. Morari. Invited session: Control of Systems Subject to Input and Output Constraints. In *1997 American Control Conference*, Albuquerque, NM, June 1997. Organizer and chair: M. V. Kothare, co-chair: M. Morari.

[88] M. V. Kothare and M. Morari. Multivariable anti-windup controller synthesis using multi-objective optimization. In *Proceedings of the 1997 American Control Conference*, 1997.

[89] M. V. Kothare, V. Nevistić, and M. Morari. Robust constrained model predictive control for nonlinear systems: A comparative study. In *Proceedings of the* 34^{th} *IEEE Conference on Decision and Control*, pages 2884–2885, New Orleans, LO, December 1995.

[90] M. V. Kothare, V. Nevistić, and M. Morari. Robust control of nonlinear systems: A comparative study. In *1995 AICHE Annual Meeting (paper no. 180e)*, Miami, FL, November 1995.

[91] N. J. Krikelis. State feedback integral control with intelligent integrators. *Int. J. Control*, 32(3):465–473, 1980.

[92] H. Kwakernaak and R. Sivan. *Linear Optimal Control Systems.* Wiley-Interscience, New York, 1972.

[93] R. W. Liu. Convergent systems. *IEEE Trans. Aut. Control*, 13(4):384–391, August 1968.

[94] A. I. Lur'e. *Some nonlinear problems in the theory of automatic control.* Her Majesty's Stationery Office, London, 1957. In Russian, 1951.

[95] V. R. Marcopoli and S. M. Phillips. Analysis and synthesis tools for a class of actuator-limited multivariable control systems: A Linear Matrix Inequality approach. *International Journal of Robust and Nonlinear Control*, 6:1045–1063, 1996. Special Issue on Linear Matrix Inequalities and their applications.

[96] D. Q. Mayne. Optimization in model based control. In J. B. Rawlings, editor, 4^{th} *IFAC Symposium on Dynamics and Control of Chemical Reactors, Distillation Columns, and Batch Processes (DYCORD+ '95)*, pages 229–242. Danish Automation Society, June 1995.

[97] D. Q. Mayne. Plenary lecture. In *CPC V*, Lake Tahoe, CA, 1996.

[98] S. K. Menon and A. G. Parlos. Gain-scheduled nonlinear control of U-tube steam generator water level. *Nuclear Science and Engineering*, 111:294–308, 1992.

[99] S. Miyamoto and G. Vinnicombe. Robust control of plants with saturation nonlinearity based on coprime factor representations. In *Proceedings of the* 35^{th} *IEEE Conference on Decision and Control*, pages 2838–2840, Kobe, Japan, December 1996.

[100] M. Morari, C. E. Garcia, J. H. Lee, and D. M. Prett. *Model Predictive Control.* Prentice-Hall Inc., Englewood Cliffs, NJ (in preparation), 1997.

[101] M. Morari and E. Zafiriou. *Robust Process Control.* Prentice-Hall, Inc., Englewood Cliffs, NJ, 1989.

[102] K. R. Muske and J. B. Rawlings. Model predictive control with linear models. *AICHE Journal*, 39(2):262–287, February 1993.

[103] M. G. Na. Design of a steam generator water level controller via the estimation of the flow errors. *Annals of Nuclear Energy*, 22(6):367–376, 1995.

[104] M. G. Na and H. C. No. Design of an adaptive observer-based controller for the water level of steam generators. *Nuclear Engineering and Design*, 135:379–394, 1992.

[105] Yu. Nesterov and A. Nemirovsky. *Interior-point polynomial methods in convex programming*, volume 13 of *Studies in Applied Mathematics*. SIAM, Philadelphia, PA, 1994.

[106] V. Nevistić and L. Del Re. Feasible suboptimal model predictive control for linear plants with state dependent constraints. In *Proceedings of the 1994 American Control Conference*, pages 2862–2866, Baltimore, MD, June 1994.

[107] A. Packard. Gain scheduling via linear fractional transformations. *Systems & Control Letters*, 22:79–92, 1994.

[108] A. Packard and J. Doyle. The complex structured singular value. *Automatica*, 29(1):71–109, 1993.

[109] J-K. Park and C-H Choi. Dynamic compensation method for multivariable control systems with saturating actuators. *IEEE Trans. Auto. Control*, 40(9):1635–1640, September 1995.

[110] A. Parry, J. F. Petetrot, and M. J. Vivier. Recent Progress in SG level control in French PWR plants. In *Proceedings of the International Conference on Boiler Dynamics and Control in Nuclear Power Stations*, pages 81–88. British Nuclear Energy Society, London, 1985.

[111] E. Polak and T. H. Yang. Moving horizon control of linear systems with input saturation and plant uncertainty–Part 1. Robustness. *International Journal of Control*, 58(3):613–638, 1993.

[112] E. Polak and T. H. Yang. Moving horizon control of linear systems with input saturation and plant uncertainty–Part 2: Disturbance rejection and tracking. *International Journal of Control*, 58(3):639–663, 1993.

[113] V. M. Popov. Absolute stability of nonlinear systems of automatic control. *Automatic Remote Control*, 22(8):857–875, 1961.

[114] J. B. Rawlings and K. R. Muske. The stability of constrained receding horizon control. *IEEE Trans. Aut. Control*, 38(10):1512–1516, October 1993.

[115] W. J. Rugh. Analytical framework for gain scheduling. *IEEE Control Systems Magazine*, 11(1):79–84, January 1991.

[116] M. G. Safonov and G. Wyetzner. Computer-aided stability analysis renders Popov criterion obsolete. *IEEE Trans. Auto. Cont.*, 32(12):1128–1131, December 1987.

[117] I. W. Sandberg. On the $\mathcal{L}_2$-boundedness of solutions of nonlinear functional equations. *Bell Syst. Tech. J.*, 43(4):1581–1589, 1964.

[118] C. Scherer. Mixed $\mathcal{H}_2/\mathcal{H}_\infty$ control. In A. Isidori, editor, *Trends in Control: A European Perspective*, pages 173–216. Springer-Verlag London Limited, 1995.

[119] C. W. Scherer. From LMI Analysis to Multichannel MIxed LMI synthesis: A General Procedure. *Systems & Control Letters*, 1996 (submitted).

[120] C. W. Scherer, P. Gahinet, and M. Chilali. Multi-objective output-feedback control via LMI optimization. *IEEE Trans. Aut. Control*, 1995 (submitted).

[121] W. G. Schneider and J. T. Boyd. Steam generator level controllability. In *Proceedings of the International Conference on Boiler Dynamics and Control in Nuclear Power Stations*, pages 97–117. British Nuclear Energy Society, London, 1985.

[122] E.D. Sontag and H. J. Sussmann. Nonlinear output feedback design for linear systems with saturating controls. In *Proceedings of the* 29^{th} *IEEE Conference on Decision and Control*, pages 3414–3416, 1990.

[123] G. Stein. Respect the unstable–Bode lecture for being recipient of the 1989 Bode prize of the IEEE Control Systems Society. In 28^{th} *IEEE Conference on Decision and Control*, Tampa, FL, 1989.

[124] A. A. Stoorvogel and A. Saberi. Control problem with constraints. *International Journal of Robust and Nonlinear Control*, 1997 (to appear). Special issue: Guest editors: A. A. Stoorvogel and A. Saberi.

[125] H. J. Sussmann, E. D. Sontag, and Y. Yang. A general result on the stabilization of linear systems using bounded controls. *IEEE Trans. Auto. Control*, 39:2411–2425, 1994.

[126] A. R. Teel and N. Kapoor. The $\mathcal{L}_2$ anti-windup problem: Its definition and solution. In *Proceedings of the 1997 European Control Conference (ECC)*, Brussels, Belgium, May 1997.

[127] A.R. Teel. Global stabilization and restricted tracking for multiple integrators with bounded controls. *Systems & Control Letters*, 18:165–171, 1992.

[128] A. G. Tsirukis and M. Morari. Controller design with actuators constraints. In *Proceedings of the* 31^{st} *Conference on Decision and Control*, pages 2623–2628, Tucson, AZ, December 1992.

[129] F. Tyan and D. S. Bernstein. Anti-windup compensator synthesis for systems with saturation actuators. *International Journal of Robust and Nonlinear Control*, 5(5):521–537, August 1995.

[130] L. Vandenberghe and S. Boyd. A Primal-dual potential reduction method for problems involving linear matrix inequalities. *Mathematical Programming*, 69(1):205–236, July 1995.

[131] K. S. Walgama, S. Rönnbäck, and J. Sternby. Generalization of conditioning technique for anti-windup compensators. *IEE Proceedings-D*, 139(2):109–118, March 1992.

[132] K. S. Walgama and J. Sternby. Inherent observer property in a class of anti-windup compensators. *Int. J. Control*, 52(3):705–724, 1990.

[133] B. Wie and D. S. Bernstein. Benchmark problems for robust control design. *Journal of Guidance, Control, and Dynamics*, 15(5):1057–1059, 1992.

[134] V. A. Yakubovich. Nonconvex optimization problem: The infinite-horizon linear-quadratic control problem with quadratic constraints. *Systems & Control Letters*, 19:13–22, 1992.

[135] M. R. Yeung and P. L. Chan. Development and validation of a steam generator simulation model. *Nuclear Technology*, 92:309–314, December 1990.

[136] E. Zafiriou. Robust model predictive control of processes with hard constraints. *Computers & Chemical Engineering*, 14(4/5):359–371, 1990.

[137] E. Zafiriou and A. Marchal. Stability of SISO quadratic dynamic matrix control with hard output constraints. *AIChE Journal*, 37(10):1550–1560, 1991.

[138] G. Zames. On the input-output stability of time varying nonlinear feedback systems — Part I: Conditions derived using concepts of loop gain, conicity, and positivity. *IEEE Trans. Auto. Cont.*, 11(2):228–238, April 1966.

[139] G. Zames. On the input-output stability of time varying nonlinear feedback systems — Part II: Conditions involving circles in the frequency plane and sector nonlinearities. *IEEE Trans. Auto. Cont.*, 11(3):465–476, July 1966.

[140] G. Zames. Stability of systems with sector nonlinearities: A comparison of various inequalities. *IEEE Trans. Auto. Cont.*, 13(6):709–711, December 1968.

[141] G. Zames and P. L. Falb. Stability conditions for systems with monotone and slope-restricted nonlinearities. *SIAM J.*, 6(1):89–108, 1968.

[142] A. Zheng, V. Balakrishnan, and M. Morari. Constrained stabilization of discrete-time systems. *International Journal of Robust and Nonlinear Control*, 5(5):461–485, August 1995.

[143] A. Zheng, M. V. Kothare, and M. Morari. Anti-windup design for internal model control. *International Journal of Control*, 60(5):1015–1024, 1994. Also presented at the *1993 AIChE Annual Meeting*, MO.

[144] Z. Q. Zheng. *Robust Control of Systems Subject to Constraints.* PhD thesis, California Institute of Technology, Pasadena, CA, 1995.

[145] Z. Q. Zheng and M. Morari. Robust stability of constrained model predictive control. In *Proceedings of the 1993 American Control Conference*, volume 1, pages 379–383, San Francisco, CA, June 1993.

[146] Z. Q. Zheng and M. Morari. Stability of model predictive control with mixed constraints. *IEEE Trans. Aut. Control*, 40(10):1818–1823, October 1995.

[147] K. Zhou, J. C. Doyle, and K. Glover. *Robust and Optimal Control.* Prentice Hall Inc., New Jersey, 1996.